Nat.Lab. Unclassified Report NL-UR 2002/806

Date of issue: March 2005

Model derivation of Mextram 504

The physics behind the model

J.C.J. Paasschens, W.J. Kloosterman, and R. v.d. Toorn

Unclassified report
©Koninklijke Philips Electronics N.V. 2005

Authors' address data: R. v.d. Toorn WAY41; Ramses.van.der.Toorn@philips.com
J.C.J. Paasschens DB1.051; Jeroen.Paasschens@philips.com
W.J. Kloosterman M0.576; Willy.Kloosterman@philips.com

©Koninklijke Philips Electronics N.V. 2005
All rights are reserved. Reproduction in whole or in part is
prohibited without the written consent of the copyright owner.

Unclassified Report: NL-UR 2002/806

Title: Model derivation of Mextram 504
The physics behind the model

Author(s): J.C.J. Paasschens, W.J. Kloosterman, and R. v.d. Toorn

Part of project: Compact modelling

Customer: Semiconductors

Keywords: Mextram, spice, equivalent circuits, analogue simulation, semiconductor device models, semiconductor device noise, nonlinear distortion, heterojunction bipolar transistors, bipolar transistors, integrated circuit modelling, semiconductor technology

Abstract: Mextram 504 is the new version of the Philips compact model for bipolar transistors. This document contains the derivation of all the equations that are part of the model. This includes the description of the equivalent circuit of Mextram, the equations for the currents and the charges, the temperature-scaling model, the way self-heating is handled, and the noise model. We then discuss some small-signal approximations and the basis of geometric scaling.

The formal model definition needed for implementation is given in another report NL-UR 2000/811 [1], parameter extraction is discussed in the report NL-UR 2001/801 [2]. These reports and the source code can be found on our web-site [3].

©Koninklijke Philips Electronics N.V. 2005

Preface

October 2004 The Mextram bipolar transistor model has been put in the public domain in Januari 1994. At that time level 503, version 1 of Mextram was used within Koninklijke Philips Electronics N.V. In June 1995 version 503.2 was released which contained some improvements.

Mextram level 504 contains a complete review of the Mextram model. This document gives its physical background. This document was first released in March 2002. The current document corresponds to the October 2004 model definition.

October 2004, J.P.

March 2005 In the fall of 2004, Mextram was elected as a world standard transistor model by the *Compact Model Council (CMC)*, a consortium of representatives from over 20 major semiconductor manufacturers.

The current document corresponds to the model definition of March 2005.

RvdT.

History of model and documentation

June 2000 : Release of Mextram level 504 (preliminary version)
Complete review of the model compared to Mextram level 503

April 2001 : Release of Mextram 504, version 0 (504.0)
Small fixes:
– Parameters $\mathsf{R_{th}}$ and $\mathsf{C_{th}}$ added to MULT-scaling
– Expression for α in operating point information fixed
Changes w.r.t. June 2000 version:
– Addition of overlap capacitances $\mathsf{C_{BEO}}$ and $\mathsf{C_{BCO}}$
– Change in temperature scaling of diffusion voltages
– Change in neutral base recombination current
– Addition of numerical examples with self-heating

September 2001 : Release of Mextram 504, version 1 (504.1)
Lower bound on $\mathsf{R_{th}}$ is now 0°C/W
Small changes in $F_{\rm ex}$ and $Q_{B_1B_2}$ to enhance robustness

March 2002 : Release of Mextram 504, version 2 (504.2)
Numerical stability improvement of $x_i/W_{\rm epi}$ at small $\mathcal{V}_{\rm C_1C_2}$
Numerical stability improvement of p_0^*

October 2003 : Release of Mextram 504, version 3 (504.3)
MULT has been moved in list of parameters
Lower clipping value of $\mathsf{T_{ref}}$ changed to −273°C
Added I_C, I_B and $\beta_{\rm dc}$ to operating point information

 ©Koninklijke Philips Electronics N.V. 2005

April 2004	: Release of Mextram 504, version 4 (504.4) Noise of collector epilayer has been removed.
October 2004	: Release of Mextram 504, version 5 (504.5) Addition of temperature dependence of thermal resistance Addition of noise due to avalanche current
March 2005	: Release of Mextram 504, version 6 (504.6) Added parameter $\mathsf{dA}_{\mathsf{I_s}}$ for fine tuning of temp. dep. of I_{sT}; eqn. (7.24b) "$G_{EM} = 0$", in reverse and fully saturated operation Upper clipping value 1.0 of $\mathsf{K}_{\mathsf{avl}}$ introduced

©Koninklijke Philips Electronics N.V. 2005

 ©Koninklijke Philips Electronics N.V. 2005

Contents

Contents **vii**

1 Introduction **1**

1.1 Explanation of the equivalent circuit 1

1.1.1 General nature of the equivalent model 1

1.1.2 Intrinsic transistor and resistances 3

1.1.3 Extrinsic transistor and parasitics 4

1.1.4 Extended modelling 6

1.2 Overview of parameters 6

1.3 Physical basis 10

1.3.1 Basic semiconductor physics equations 10

1.3.2 PN-junctions 11

1.3.3 Gummel’s charge control relation 12

1.3.4 Charges, capacitances and transit times 15

2 The intrinsic transistor **17**

2.1 Main current 17

2.2 Depletion charges 18

2.2.1 General expression for depletion charges 18

2.2.2 Substrate depletion charge 18

2.2.3 Emitter depletion charge 19

2.2.4 Collector depletion charges 19

2.3 Early effect 20

2.3.1 Punch-through 21

2.3.2 Base width 21

2.4 Base diffusion charges 21

2.4.1 Short derivation 22

2.4.2 Not so short derivation 24

2.4.3 The Early effect on the diffusion charges 28

2.4.4 Extended modelling of excess phase shift 29

2.5 Emitter diffusion charge 30

2.6 Base currents 31

2.6.1 Ideal forward base current 31
2.6.2 Non-ideal forward base current 31
2.6.3 Non-ideal reverse base current 32
2.6.4 Extrinsic base current 32
2.7 Substrate currents 33
2.7.1 Substrate current 33
2.7.2 Substrate failure current 33

3 The collector epilayer model **34**
3.1 Introduction 34
3.2 Some qualitative remarks on the description of the epilayer 35
3.3 The epilayer current 42
3.3.1 The Kull model (without velocity saturation) 42
3.3.2 The Mextram model without velocity saturation 45
3.3.3 The Mextram model with velocity saturation 47
3.3.4 Current spreading 50
3.3.5 Reverse behaviour 51
3.3.6 The transition into hard saturation and into reverse 51
3.4 The epilayer diffusion charge 53
3.5 The intrinsic base-collector depletion charge 54
3.6 Avalanche 58
3.6.1 Normal avalanche modelling 60
3.6.2 Limiting the avalanche current 62
3.6.3 Extended avalanche modelling 63

4 Extrinsic regions **66**
4.1 Resistances 66
4.2 Overlap capacitance 66
4.3 Extrinsic currents 66
4.4 Extrinsic charges 66
4.5 Extended modelling of reverse current gain; extrinsic region 67
4.5.1 Charges 67
4.5.2 Currents 68
4.5.3 Modulation of the extrinsic reverse current 69

 ©Koninklijke Philips Electronics N.V. 2005

5 Current crowding **71**

5.1 DC current crowding: the variable base resistance 71

5.1.1 Determination of the small voltage resistance from the sheet resistance 75

5.1.2 DC current crowding in a circular geometry 76

5.1.3 DC current crowding in a rectangular geometry 76

5.2 AC current crowding 76

6 Heterojunction features **79**

6.1 Gradient in the Ge-profile 79

6.2 Early effect on the forward base current 83

7 Temperature modelling **85**

7.1 Notation 85

7.2 Definitions 85

7.3 General quantities 86

7.4 Depletion capacitances and diffusion voltages 86

7.5 Resistances 88

7.6 Currents 89

7.7 Early voltages 92

7.8 Transit times 92

7.9 Avalanche constant 94

7.10 Heterojunction features 94

7.11 Thermal resistance 94

8 Self-heating and mutual heating **95**

8.1 Dissipated power 95

8.2 Relation between power and increase of temperature 95

8.3 Implementation 96

8.4 Mutual heating 97

9 Noise model **98**

9.1 Introduction 98

9.2 Basic noise types 99

9.2.1 Thermal noise 99

©Koninklijke Philips Electronics N.V. 2005

9.2.2 Shot noise 99
9.2.3 Thermal noise and shot noise as one concept 100
9.2.4 Flicker or $1/f$-noise 101
9.3 Noise due to avalanche 101
9.4 Noise expressions in Mextram 103

10 Small-signal approximations in the operating-point 105
10.1 Small-signal model 105
10.1.1 Mextram implementation 108
10.1.2 The hybrid-pi model 109
10.1.3 Simple case 110
10.1.4 The reverse hybrid-pi model 111
10.2 Calculation of f_T 111
10.2.1 Mextram implementation 115
10.2.2 Possible simplified implementation 116

11 Geometric scaling 118
11.1 High current parameters 118
11.2 Self-heating 119

A General compact model formulations 121
A.1 Smooth minimum and maximum-like functions 121
A.1.1 Hyperboles 121
A.1.2 Exponents 121
A.1.3 The linear function with a maximum 122
A.2 Depletion capacitances 123
A.2.1 Spice-Gummel-Poon 124
A.2.2 De Graaff and Klaassen 124
A.2.3 Earlier versions of Mextram 125
A.2.4 Modern compact models 125

B Analytical calculation of the critical current 128
B.1 Derivation 128
B.2 The Mextram expression 130
B.3 The critical current in limiting cases 131

 ©Koninklijke Philips Electronics N.V. 2005

C The Kull-model around zero current **133**

D Current crowding at small currents **135**

D.1 Derivation 135

D.2 Recipe 136

D.3 Examples 137

E Crosslinks of variables and parameters **139**

F Expression of parameters in physical quantities **141**

G Full equivalent circuit **142**

References **143**

Index **151**

©Koninklijke Philips Electronics N.V. 2005

 ©Koninklijke Philips Electronics N.V. 2005

1 Introduction

Mextram [3] is a compact model for vertical bipolar transistors. A compact transistor model tries to describe the I-V characteristics of a transistor in a compact way, such that the model equations can be implemented in a circuit simulator. In principle Mextram is the same kind of model as the well known Ebers-Moll [4] and (Spice)-Gummel-Poon [5] models, described for instance in the texts about general semiconductor physics, Refs. [6, 7], or in the texts dedicated to compact device modelling [8, 9, 10] or high-frequency bipolar transistors [11]. These two models are, however, not capable of describing many of the features of modern down-scaled transistors. Therefore one has extended these models to include more effects. One of these more extended models is Mextram, which in its earlier versions has already been discussed in for instance Refs. [9, 12].

The complete model definition of Mextram, level 504, can be found on the web-site [3], for instance in the report [1]. In that report, however, only a small introduction is given into the physical basics of all the equations. This report tries to give a more complete description of the physics behind the Mextram model. In our description we will try to keep as close as possible to the notation and description of Ref. [1]. We will, however, try to explain all the equations in a logical order. Since the bipolar transistor model of Gummel and Poon [5] (or its Spice-implementation) is so well-known, we will start with those equations of the Mextram model that are closest to the Gummel-Poon model and work our way from there.

This report discusses the equations of Mextram, level 504. Now and then we will refer to the previous version, level 503, for which documentation can be found in Refs. [3, 13, 14, 15]. A large part of the physical background of Mextram, and of some other models, has also been published in the books by Berkner [10] (in German) and Reisch [11].

1.1 Explanation of the equivalent circuit

1.1.1 General nature of the equivalent model

The description of a compact bipolar transistor model is based on the physics of a bipolar transistor. An important part of this is realizing that a bipolar transistor contains various regions, all with different doping levels. Schematically this is shown in Fig. 1. (In this report we will base our description on a NPN transistor. It might be clear that the same model can be used for PNP transistors, using equivalent formulations.) One can discern the emitter, the base, collector and substrate regions, as well as an intrinsic part and an extrinsic part of the transistor.

One of the steps in developing a compact model of a bipolar transistor is the creation of an equivalent circuit. In such a circuit the different regions of the transistor are modelled with their own elements. In Fig. 1 we have shown a simplified version of the Mextram equivalent circuit, in which we only show the intrinsic part of the transistor, as well as the resistances to the contacts. This simplified circuit is comparable to the Gummel-Poon equivalent circuit.

©Koninklijke Philips Electronics N.V. 2005

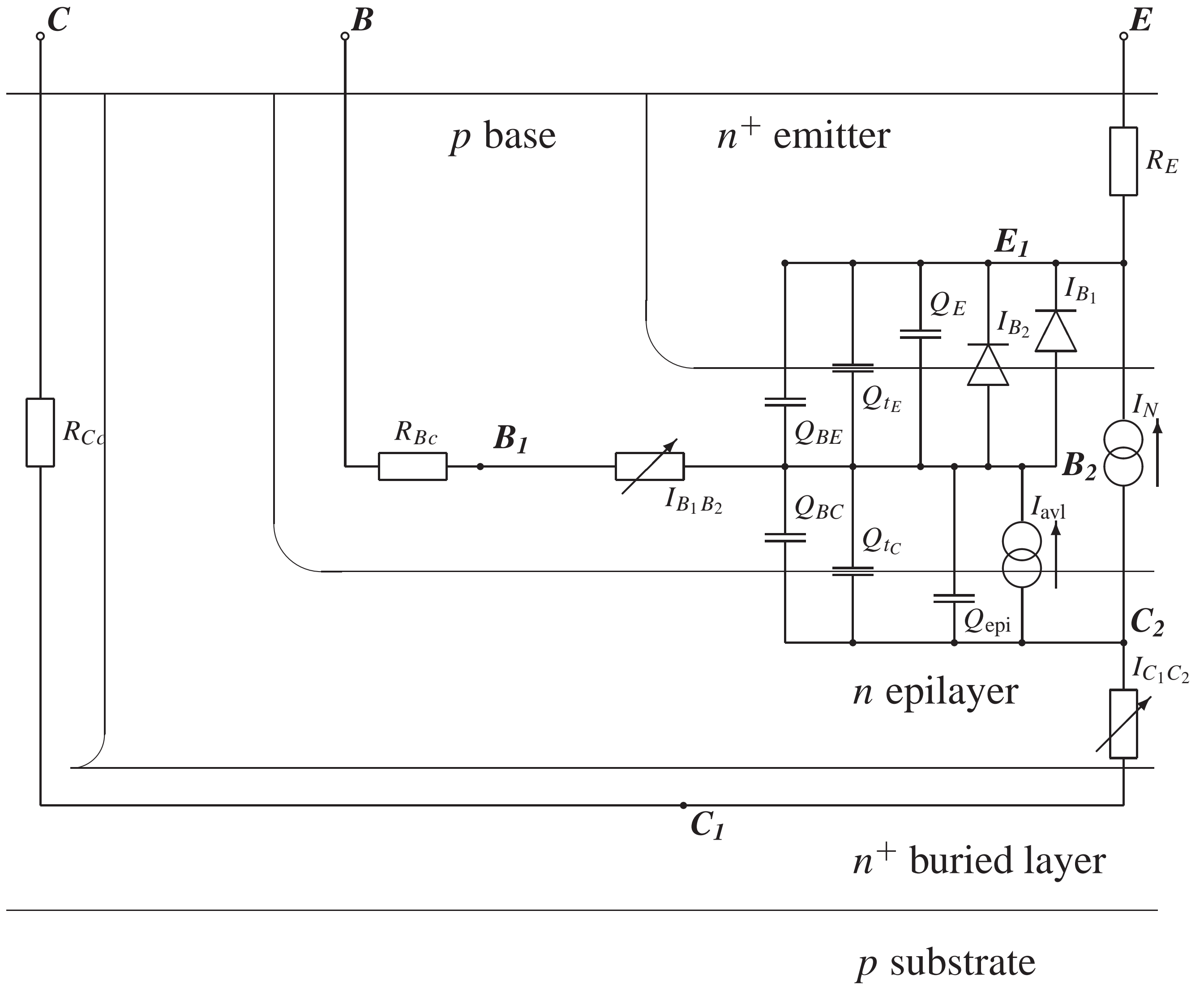

Figure 1: *A schematic cross-section of a bipolar transistor is shown, consisting of the emitter, base, collector and substrate. Over this cross-section we have given a simplified equivalent circuit representation of the Mextram model, which doesn't have the parasitics like the parasitic PNP, the base-emitter sidewall components, and the overlap capacitances. We did show the resistances from the intrinsic transistor to the external contacts. The current* $I_{B_1B_2}$ *describes the variable base resistance and is therefore sometimes called* R_{Bv}. *The current* $I_{C_1C_2}$ *describes the variable collector resistance (or epilayer resistance) and is therefore sometimes called* R_{Cv}. *This equivalent circuit is similar to that of the Gummel-Poon model, although we have split the base and collector resistance into two parts.*

 ©Koninklijke Philips Electronics N.V. 2005

The circuit has a number of internal nodes and some external nodes. The external nodes are the points where the transistor is connected to the rest of the world. In our case these are the collector node C, the base node B and the emitter node E. The substrate node S is not shown yet since it is only connected to the intrinsic transistor via parasitics which we will discuss later. Also five internal nodes are shown. These internal nodes are used to define the internal state of the transistor, via the local biases. The various elements that connect the internal and external nodes can then describe the currents and charges in the corresponding regions. These elements are shown as resistances, capacitances, diodes and current sources. It is, however, important to note that most of these elementary elements are not the normal linear elements one is used to. In a compact model they describe in general non-linear resistances, non-linear charges and non-linear current sources (diodes are of course non-linear also). Furthermore, elements can depend on voltages on other nodes than those to which they are connected.

For the description of all the elements we use equations. Together all these equations give a set of non-linear equations which will be solved by the simulator. In the equations a number of parameters are used. The value of these parameters will depend on the specific transistor being modelled. The equations are the same for all transistors. We will give an overview of these parameters in the next section. For a compact model it is important that these parameters can be extracted from measurements on real transistors. For Mextram 504 this is described in a separate report [2]. This means that the number of parameters can not be too large. On the other hand, many parameters are needed to describe the many different transistors in all regimes of operation.

1.1.2 Intrinsic transistor and resistances

Let us now discuss the various elements in the simplified circuit. The precise expressions will be given in the following chapters. Here we will only give a basic idea of the various elements in the Mextram model. Let us start with the resistances. Node E_1 corresponds to the emitter of the intrinsic transistor. It is connected to the external emitter node via the emitter resistor R_E. Both the collector node C and the base node B are connected to their respective internal nodes B_2 and C_2 via two resistances. For the base these are the constant resistor R_{Bc} and the variable resistor R_{Bv}. This latter resistor, or rather this non-linear current source, describes DC current crowding under the emitter. Between these two base resistors an extra internal node is present: B_1. The collector also has a constant resistor R_{Cc} connected to the external collector node C. Furthermore, since the epilayer is lightly doped it has its own 'resistance'. For low currents this resistance is R_{Cv}. For higher currents many extra effects take place in the epilayer. In Mextram the epilayer is modelled by a controlled current source $I_{C_1C_2}$.

Next we discuss the currents present in the model. First of all the main current I_N gives the basic transistor current. In Mextram the description of this current is based on the Gummel's charge control relation (see Section 1.3.3). This means that the deviations from an ideal transistor current are given in terms of the charges in the intrinsic transistor. The main current depends (even in the ideal case) on the voltages of the internal nodes E_1, B_2 and C_2.

Apart from the main current we also have base currents. In the forward mode these are the ideal base current I_{B_1} and the non-ideal base current I_{B_2}. Since these base currents are basically diode currents they are represented by a diode in the equivalent circuit.

In reverse mode Mextram also has an ideal and a non-ideal base current. However, these are mainly determined by the extrinsic base-collector pn-junction. Hence they are not included in the intrinsic transistor. The last current source in the intrinsic transistor is the avalanche current. This current describes the generation of electrons and holes in the collector epi-layer due to impact ionisation, and is therefore proportional to the current $I_{C_1C_2}$. We only take weak avalanche into account.

At last the intrinsic transistor shows some charges. These are represented in the circuit by capacitances. The charges Q_{t_E} and Q_{t_C} are almost ideal depletion charges resulting from the base-emitter and base-collector pn-junctions. The extrinsic regions will have similar depletion capacitances. The two diffusion charges Q_{BE} and Q_{BC} are related to the built-up of charge in the base due to the main current: the main current consists of mainly electrons traversing the base and hence adding to the total charge. Q_{BE} is related to forward operation and Q_{BC} to reverse operation. In hard saturation both are present. The charge Q_E is related to the built-up of holes in the emitter. Its bias dependence is similar to that of Q_{BE}. The charge Q_{epi} describes the built-up of charge in the collector epilayer.

1.1.3 Extrinsic transistor and parasitics

After the description of the intrinsic transistor we now turn to the extrinsic PNP-region and the parasitics. In Fig. 2 we have added some extra elements: a base-emitter side-wall parasitic, the extrinsic base-collector regions, the substrate and the overlap capacitances. Note that Mextram has a few flags that turn a part of the modelling on or off. In Fig. 34 on page 142, where it is easily found for reference, the full Mextram equivalent circuit is shown which also includes elements only present when all the extended modelling is used.

Let us start with the base-emitter sidewall parasitic. Since the pn-junction between base and emitter is not only present in the intrinsic region below the emitter, a part of the ideal base current will flow through the sidewall. This part is given by $I^S_{B_1}$. Similarly, the sidewall has a depletion capacitance given by the charge $Q^S_{t_E}$.

The extrinsic base-collector region has the same elements as the intrinsic transistor. We already mentioned the base currents. For the base-collector region these are the ideal base current I_{ex} and the non-ideal base current I_{B_3}. Directly connected to these currents is the diffusion charge Q_{ex}. The depletion capacitance between the base and the collector is split up in three parts. We have already seen the charge Q_{t_C} of the intrinsic transistor. The charge Q_{tex} is the junction charge between the base and the epilayer. Mextram models also the charge XQ_{tex} between the outer part of the base and the collector plug.

Then we have the substrate. The collector-substrate junction has, as any pn-junction, a depletion capacitance given by the charge Q_{t_S}. Furthermore, the base, collector and

 ©Koninklijke Philips Electronics N.V. 2005

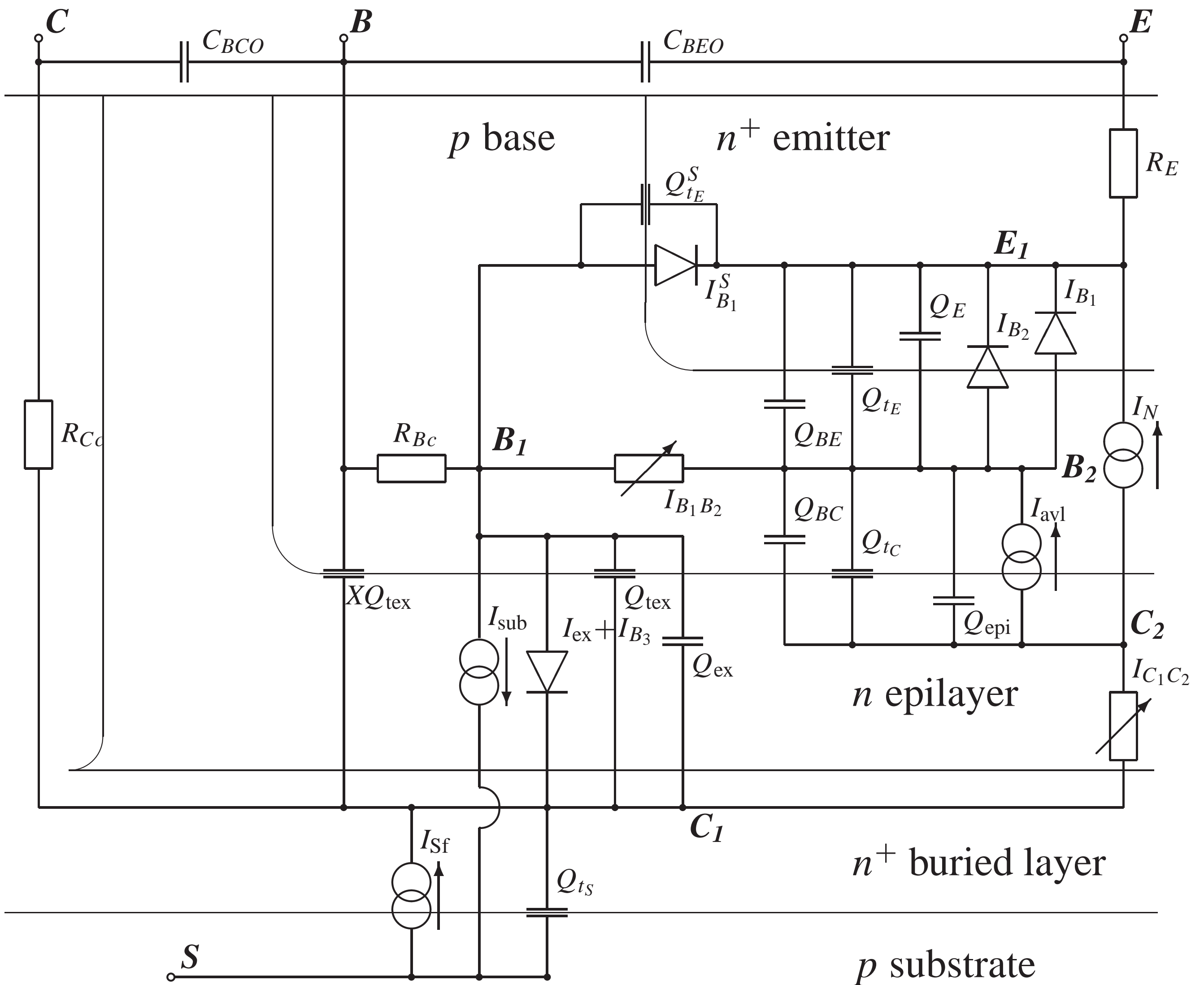

Figure 2: *Shown is the Mextram equivalent circuit for the vertical NPN transistor, without extra modelling (i.e.* EXMOD = 0 *and* EXPHI = 0*). As in Fig. 1 we have schematically shown the different regions of the physical transistor.*

©Koninklijke Philips Electronics N.V. 2005

substrate together form a parasitic PNP transistor. This transistor has a main current of itself, given by $I_{\rm sub}$. This current runs from the base to the substrate. The reverse mode of this parasitic transistor is not really modelled, since it is assumed that the potential of the substrate is the lowest in the whole circuit. However, to give a signal when this is no longer true a substrate failure current $I_{\rm Sf}$ is included that has no other function than to warn a designer that the substrate is at a wrong potential.

Finally the overlap capacitances C_{BEO} and C_{BCO} are shown that model the constant capacitances between base and emitter or base and collector, due to for instance overlapping metal layers (this should *not* include the interconnect capacitances).

1.1.4 Extended modelling

In Mextram two flags can introduce extra elements in the equivalent circuit (see Fig. 34 on page 142). When $\mathsf{EXPHI} = 1$ the charge due to AC-current crowding in the pinched base (i.e. under the emitter) is modelled with $Q_{B_1B_2}$. (Also another non-quasi-static effect, base-charge partitioning, is then modelled.) When $\mathsf{EXMOD} = 1$ the external region is modelled in some more detail (at the cost of some loss in the convergence properties in a circuit simulator). The currents $I_{\rm ex}$ and $I_{\rm sub}$ and the charge $Q_{\rm ex}$ are split in two parts, similar to the splitting of $Q_{\rm tex}$. The newly introduced elements are parallel to the charge $Q_{\rm tex}$.

1.2 Overview of parameters

In this section we will give an overview of the parameters used in Mextram. These parameters can be divided into different categories. In the formal description these parameters are given by a letter combination, e.g. IS. In equations however we will use a different notation for clarity, e.g. $\mathsf{I_S}$. Note that we used a sans-serif font for this. Using this notation it is always clear in an equation which quantities are parameters, and which are not. Many of the parameters are dependent on temperature. For this dependence the model contains som extra parameters. When the parameter is corrected for temperature it is denoted by an index T, e.g. $\mathsf{I_{ST}}$. In the formal documentation [3, 1] the difference between the parameter at reference temperature $\mathsf{I_S}$ and the parameter after temperature scaling $\mathsf{I_{ST}}$ is made in a very stringent way. In this report however we don't add the temperature subscript, unless it is needed.

First of all we have some general parameters. Flags are either 0 when the extra modelling is not used, or 1 when it is.

LEVEL	LEVEL	Model level, here always 504
EXMOD	EXMOD	Flag for EXtended MODelling of the external regions
EXPHI	EXPHI	Flag for extended modelling of distributed HF effects in transients
EXAVL	EXAVL	Flag for EXtended modelling of AVaLanche currents
MULT	MULT	Number of parallel transistors modelled together

 ©Koninklijke Philips Electronics N.V. 2005

As mentioned in the description of the equivalent circuit some currents and charges are split, e.g. in an intrinsic part and an extrinsic part. Such a splitting needs a parameter. There are 2 for the side-wall of the base-emitter junction. Then the collector-base region is split into 3 parts, using 2 parameters.

XI_{B_1}	XIBI	Fraction of the ideal base current that goes through the sidewall
XC_{j_E}	XCJE	Fraction of the emitter-base depletion capacitance that belongs to the sidewall
XC_{j_C}	XCJC	Fraction of the collector-base depletion capacitance that is under the emitter
X_{ext}	XEXT	Fraction of external charges/currents between B and C_1 instead of B_1 and C_1

A transistor model must in the first place describe the currents, and we use some parameters for this. The main currents of both the intrinsic and parasitic transistors are described by a saturation current and a high-injection knee current. We also have two Early voltages for the Early effect in the intrinsic transistor. The two ideal base currents are related to the main currents by a current gain factor. The non-ideal base currents are described by a saturation current and non-ideality factor or a cross-over voltage (due to a kind of high-injection effect). The avalanche current is described by three parameters.

I_s	IS	Saturation current for intrinsic transistor
I_k	IK	High-injection knee current for intrinsic transistor
I_{Ss}	ISS	Saturation current for parasitic PNP transistor
I_{ks}	IKS	High-injection knee current for parasitic PNP transistor
V_{ef}	VEF	Forward Early voltage of the intrinsic transistor
V_{er}	VER	Reverse Early voltage of the intrinsic transistor
β_f	BF	Current gain of ideal forward base current
β_{ri}	BRI	Current gain of ideal reverse base current
I_{Bf}	IBF	Saturation current of the non-ideal forward base current
m_{Lf}	MLF	Non-ideality factor of the non-ideal forward base current
I_{Br}	IBR	Saturation current of the non-ideal reverse base current
V_{Lr}	VLR	Cross-over voltage of the non-ideal reverse base current
W_{avl}	WAVL	Effective width of the epilayer for the avalanche current
V_{avl}	VAVL	Voltage describing the curvature of the avalanche current
S_{fh}	SFH	Spreading factor for the avalanche current

Mextram contains both constant and variable resistances. For variable resistances the resistance for low currents is used as a parameter. The epilayer resistance has two extra parameters related to velocity saturation and one smoothing parameter.

R_E	RE	Constant resistance at the external emitter
R_{Bc}	RBC	Constant resistance at the external base

©Koninklijke Philips Electronics N.V. 2005

R_{Bv}	RBV	Low current resistance of the pinched base (i.e. under the emitter)
R_{Cc}	RCC	Constant resistance at the external collector
R_{Cv}	RCV	Low current resistance of the epilayer
SCR_{Cv}	SCRCV	Space charge resistance of the epilayer
I_{hc}	IHC	Critical current for hot carriers in the epilayer
a_{xi}	AXI	Smoothing parameter for the epilayer model

All depletion capacitances are given in terms of the capacitance at zero bias, a built-in or diffusion voltage and a grading coefficient (typically between the theoretical values $1/2$ for an abrupt junction and $1/3$ for a graded junction). The collector depletion capacitance is limited by the width of the epilayer region. Its intrinsic part also has a current modulation parameter.

C_{j_E}	CJE	Depletion capacitance at zero bias for emitter-base junction
p_E	PE	Grading coefficient of the emitter-base depletion capacitance
V_{d_E}	VDE	Built-in diffusion voltage emitter-base
C_{j_C}	CJC	Depletion capacitance at zero bias for collector-base junction
p_C	PC	Grading coefficient of the collector-base depletion capacitance
V_{d_C}	VDC	Built-in diffusion voltage collector-base
X_p	XP	Fraction of the collector-base depletion capacitance that is constant
m_C	MC	Current modulation factor for the collector depletion charge
C_{j_S}	CJS	Depletion capacitance at zero bias for collector-substrate junction
p_S	PS	Grading coefficient of the collector-substrate depletion capacitance
V_{d_S}	VDS	Built-in diffusion voltage collector-substrate

New in Mextram 504 are two constant overlap capacitances.

C_{BEO}	CBEO	Base-emitter overlap capacitance
C_{BCO}	CBCO	Base-collector overlap capacitance

Most of the diffusion charges can be given in terms of the DC parameters. For accurate AC-modelling, however, it is better that DC effects and AC effects have their own parameters, which in this case are transit time parameters.

τ_E	TAUE	(Minimum) transit time of the emitter charge
m_τ	MTAU	Non-ideality factor of the emitter charge
τ_B	TAUB	Transit time of the base
τ_{epi}	TEPI	Transit time of the collector epilayer
τ_R	TAUR	Reverse transit time

©Koninklijke Philips Electronics N.V. 2005

Noise in the transistor is modelled by using only three extra parameters for flickernoise and one extra for the noise due to avalanche.

K_f	KF	Flicker-noise coefficient of the ideal base current
K_{fN}	KFN	Flicker-noise coefficient of the non-ideal base current
A_f	AF	Flicker-noise exponent
K_{avl}	KAVL	Switch for white noise contribution due to avalanche

Then we have the temperature parameters. First of all two parameters describe the temperature itself. Next we have some temperature coefficients, that are related to the mobility exponents in the various regions. We also need some band-gap voltages to describe the temperature dependence of some parameters.

T_{ref}	TREF	Reference temperature
dT_a	DTA	Difference between device and ambient temperatures
$A_{Q_{B0}}$	AQBO	Temperature coefficient of zero bias base charge
A_E	AE	Temperature coefficient of R_E
A_B	AB	Temperature coefficient of R_{Bv}
A_{epi}	AEPI	Temperature coefficient of R_{Cv}
A_{ex}	AEX	Temperature coefficient of R_{Bc}
A_C	AC	Temperature coefficient of R_{Cc}
A_S	AS	Temperature coefficient of the mobility related to the substrate currents
$dV_{g\beta f}$	DVGBF	Difference in band-gap voltage for forward current gain
$dV_{g\beta r}$	DVGBR	Difference in band-gap voltage for reverse current gain
V_{g_B}	VGB	Band-gap voltage of the base
V_{g_C}	VGC	Band-gap voltage of the collector
V_{g_S}	VGS	Band-gap voltage of the substrate
V_{g_j}	VGJ	Band-gap voltage of base-emitter junction recombination
$dV_{g\tau_E}$	DVGTE	Difference in band-gap voltage for emitter charge

New in Mextram 504 are two formulations that are dedicated to SiGe modelling. For a graded Ge content we have a bandgap difference. For recombination in the base we have another parameter.

dE_g	DEG	Bandgap difference over the base
X_{rec}	XREC	Pre-factor for the amount of base recombination

Also new in Mextram 504 is the description of self-heating, for which we have the two standard parameters and a temperature coefficient.

R_{th}	RTH	Thermal resistance
C_{th}	CTH	Thermal capacitance
A_{th}	ATH	Temperature coefficient of the thermal resistance

1.3 Physical basis

Mextram is a compact model that is based on a physical description of the different transistor regions. These descriptions are discussed in various texts, e.g. [6, 7, 8, 9, 10, 12]. It is therefore not our goal to repeat all of the derivations here. However, to understand some parts of Mextram it is necessary to review some general results from semiconductor physics.

1.3.1 Basic semiconductor physics equations

For the description of the main current and the base charges as well as the description of the epilayer in principle a 1-dimensional transistor model is used. In this model we describe the hole and electron densities (p and n), together with the currents. In general we can describe the densities in terms of quasi-Fermi levels φ_n and φ_p.

$$n = n_i \exp[(\psi - \varphi_n)/V_T], \tag{1.1a}$$
$$p = n_i \exp[(\varphi_p - \psi)/V_T]. \tag{1.1b}$$

The thermal voltage $V_T = kT/q$ is given in terms of the unit-charge q, the Boltzmann constant k and the absolute temperature T. Both densities depend on the intrinsic carrier density n_i and the electrostatic potential ψ.

The total charge density is given by

$$\rho = q(p - n + N_D - N_A), \tag{1.2}$$

where N_D is the density of (ionised) donor-impurities (in the emitter and collector) and N_A the density of (ionised) acceptor impurities (in the base). We will also use the notation N_{epi} for the donor density in the epilayer of the collector. Poisson's equation relates the electric field to the charge density

$$\frac{\mathrm{d}E}{\mathrm{d}x} = \frac{\rho}{\varepsilon}, \tag{1.3}$$

where ε is the dielectric constant of the medium. The electrostatic potential is directly related to the electric field

$$E = -\frac{\mathrm{d}\psi}{\mathrm{d}x}. \tag{1.4}$$

Apart from the carrier densities we will also need the electron and hole current densities. These consist of a drift current due to an applied electric field and a diffusion current due to a gradient in the density :

$$J_n = -q\mu_n n \frac{\mathrm{d}\varphi_n}{\mathrm{d}x} = q\mu_n n E + qD_n \frac{\mathrm{d}n}{\mathrm{d}x}, \tag{1.5a}$$
$$J_p = -q\mu_p p \frac{\mathrm{d}\varphi_p}{\mathrm{d}x} = q\mu_p p E - qD_p \frac{\mathrm{d}p}{\mathrm{d}x}. \tag{1.5b}$$

 ©Koninklijke Philips Electronics N.V. 2005

The diffusion coefficient D and the mobility μ are related by Einstein's relation (for both electrons and holes)

$$D = V_T\ \mu. \tag{1.6}$$

For a complete description one also needs the continuity equations

$$\frac{\partial n}{\partial t} = \frac{1}{q}\frac{\partial J_n}{\partial x} + \text{RG-terms}, \tag{1.7a}$$

$$\frac{\partial p}{\partial t} = -\frac{1}{q}\frac{\partial J_p}{\partial x} + \text{RG-terms}. \tag{1.7b}$$

With 'RG-terms' we mean recombination-generation terms. These equations will however not be directly used in the derivation of Mextram model equations.

At this point it is important to note that the quasi-Fermi levels are important in analytical models of a transistor. However, they are not always well defined without calculating a full solution based on the continuity equations. In practice we can say that at the points where the base, emitter and collector-voltages are applied the majority quasi-Fermi level equals the applied voltage.

1.3.2 PN-junctions

In a pn-junction we can distinguish three regions: a p-region, a depletion region and a n-region. Consider now the hole quasi-Fermi level. At the start of the p-region it has the value of the applied bias at that point (more or less by definition, since holes are majority over there). When the current density is not too large (i.e. when we can neglect resistive effects) the derivative of the hole quasi-Fermi level must be small, as long as the hole density is appreciable. This is in the whole p-region, but also in the depletion region. In the latter region the number of holes is much smaller than the background doping, but it is still much larger than in the n-region. For the same reason is the electron quasi-Fermi level nearly constant in the depletion region and in the n-region.

If we now look at the expressions for the electron and hole density, and when we multiply them, we get

$$np = n_i^2 \exp[(\varphi_p - \varphi_n)/V_T]. \tag{1.8}$$

We have seen that especially in the depletion region both quasi-Fermi levels are constant. Their difference equals the bias applied over the junction. Hence in, and on both sides of the depletion region, we have the very important relation

$$np = n_i^2\, e^{V/V_T}. \tag{1.9}$$

It is important to realise that in many places within compact models the potential V is used. In almost all cases the difference between quasi-Fermi levels is meant, $V = \varphi_p - \varphi_n$, and not the electrostatic potential ψ.

©Koninklijke Philips Electronics N.V. 2005

1.3.3 Gummel's charge control relation

Maybe the most important equation for the description of bipolar transistors is Gummel's charge control relation [16] for the main current[1]

$$I_N = \frac{q D_n n_{i0}^2 A_{\rm em}}{\int_{x_{E_1}}^{x_{C_2}} p(x) \mathrm{d}x} \left(e^{\mathcal{V}_{\rm B_2E_1}/V_T} - e^{\mathcal{V}_{\rm B_2C_2}/V_T} \right). \tag{1.10}$$

For low biases this is the same as the Moll-Ross relation [17]. Equation (1.10) is often called the Integral-Charge-Control Relation (ICCR) [18]. It is used in all modern bipolar compact models. Due to its importance we will repeat a derivation here.

For our derivation we will follow Ref. [12]. We can rewrite the equation for the electron current (1.5) as

$$e^{[\varphi_p(x_B)-\varphi_n(x)]/V_T} \mathrm{d}\varphi_n = -\frac{J_n(x)}{q\mu_n(x) n_i(x)} e^{[\varphi_p(x_B)-\psi(x)]/V_T} \, \mathrm{d}x, \tag{1.11}$$

where we multiplied by $\exp[\varphi_p(x_B)/V_T]$. The first assumption now is that the hole quasi-Fermi level is constant in the region of interest, where the hole charge is non-negligible (i.e. the base and possibly the epilayer). This assumption is based on the fact that the hole current is small. Looking at the hole current density in Eq. (1.5) we see that for a small hole current and a large hole density (i.e. in the base and possibly in a part of the epilayer) the derivative of the hole quasi-Fermi level must be negligibly small. A constant hole quasi-Fermi level is confirmed by device simulations [19]. The hole quasi-Fermi level equals the base potential $\mathcal{V}_{\rm B_2}$. Using Eq. (1.1) we can then express the exponent of the electrostatic potential in terms of the hole density $p(x)$. We integrate from position $x = x_1$ to $x = x_2$ and find

$$e^{[\mathcal{V}_{\rm B_2}-\varphi_n(x_2)]/V_T} - e^{[\mathcal{V}_{\rm B_2}-\varphi_n(x_1)]/V_T} = \int_{x_1}^{x_2} \frac{J_n(x) p(x)}{q D_n(x) n_i^2(x)} \, \mathrm{d}x, \tag{1.12}$$

where we used the Einstein relation. The boundaries x_1 and x_2 used in Eq. (1.12) are still arbitrary. For use in a compact model we must make a choice.

First we consider the case of low injection. The main contribution to the integral in Eq. (1.12) will come from the region where the hole density is appreciable. This means the neutral base. When we choose x_1 and x_2 outside this neutral base, it is no longer important where they are exactly. We will choose $x_1 = x_{E_1}$, the position of the internal emitter node, and $x_2 = x_{C_2}$, the position of the internal collector node. Both of these can be considered to be at the actual junctions, which, under normal forward operation, will lie in the depletion region. The electron quasi-Fermi level at the points E_1 and C_2 are equal to the corresponding node voltage.

[1] Here we already use the fact that in Mextram the intrinsic transistor is connected to the nodes B_2, E_1 and C_2. In this way we will not get confused as to which exact node potential has to be used.

 ©Koninklijke Philips Electronics N.V. 2005

Under high-injection conditions holes will also be present in the emitter or in the epilayer. We will not change the position of x_1 and x_2 depending on the injection level. The epilayer model (both current and charge description) will take care of the high-injection effects for $x > x_2$ (see below), and Eq. (1.12) will be used to calculate the charge. In a sense, the epilayer model will take care that the node potential $\mathcal{V}_{\mathrm{C}_2}$ gets the correct value, once the external collector potential V_C (or V_{C_1} for that matter) is given.

The charge in the emitter is also part of Mextram. This charge, however, does not influence the current model, but is kept independent. The node voltage at E_1 is determined by the ohmic voltage drop in the emitter.

The next assumption in the derivation is that there is no recombination in the regions where $p(x)$ is appreciable, so the electron current density is constant. Since we take the positive x-direction from emitter to collector the current density is negative for the normal forward mode of operation. Hence we define the main current as

$$I_N = -A_{\mathrm{em}} J_n, \tag{1.13}$$

where A_{em} is the surface of the emitter. Taking all terms together we find

$$e^{\mathcal{V}_{\mathrm{B_2E_1}}/V_T} - e^{\mathcal{V}_{\mathrm{B_2C_2}}/V_T} = \frac{I_N}{q A_{\mathrm{em}} n_{i0}^2} \int_{x_{E_1}}^{x_{C_2}} \frac{p(x) n_{i0}^2}{D_n(x) n_i^2(x)}\, \mathrm{d}x \equiv \frac{I_N}{q A_{\mathrm{em}} n_{i0}^2}\, G_B. \tag{1.14}$$

The last part defines the base Gummel number G_B.

In Mextram we now assume that the diffusion constant and the intrinsic carrier density are constant. (For SiGe transistors this is no longer true, see Chapter 6.) The Gummel number is then proportional to the total base charge

$$Q_B = q A_{\mathrm{em}} \int_{x_{E_1}}^{x_{C_2}} p(x)\, \mathrm{d}x. \tag{1.15}$$

The expression for the main current then becomes

$$I_N = \frac{q^2 D_n n_{i0}^2 A_{\mathrm{em}}^2}{Q_B} \left(e^{\mathcal{V}_{\mathrm{B_2E_1}}/V_T} - e^{\mathcal{V}_{\mathrm{B_2C_2}}/V_T} \right). \tag{1.16}$$

The reason why the main current is inversely proportional to the base charge can be explained as follows. First of all, as is generally known, the current through a diffusive region is inversely proportional to the width of this region. In the base this width is the distance between the two depletion regions. For low injection this width is directly proportional to the charge Q_B, which is a sum of the base charge at zero bias Q_{B0} and the extra charge due to the change in depletion region width (see also Section 2.3). These two extra charges at the emitter side and at the collector side are given by the two depletion charges Q_{t_E} and Q_{t_C}. The variation of the current due to this variation in base width is called the Early effect.

For higher injection not only the width is important, but also the number of carriers, in this case electrons. The more carriers, the lower the resistance. The electron density is proportional to n_i^2/p, see Eq. (1.9). The resistance is then proportional to p/n_i^2 and also to D_n^{-1}. For a varying density of holes, we need to take the integral over the whole base width to determine the total resistance. The current is then proportional to the inverse of the resistance, or the inverse of the Gummel number (or base charge). Since the number of electrons is also inversely proportional to the exponent of the electron quasi-Fermi level, we get the equation for the main current as above.

When high-injection effects play a role, the hole density in the epilayer will no longer be negligible. We can follow the same line of reasoning as above, but now using $x_1 = x_{C_2}$ and $x_2 = x_{C_1}$. We then get the relation between the charge Q_{epi} and the current $I_{C_1C_2}$ in the epilayer

$$I_{C_1C_2} = \frac{q^2 D_n n_{i0}^2 A_{\text{em}}^2}{Q_{\text{epi}}} \left(e^{\mathcal{V}_{\text{B}_2\text{C}_2}/V_T} - e^{\mathcal{V}_{\text{B}_2\text{C}_1}/V_T} \right). \tag{1.17}$$

Implicitly we have made the assumption that the diffusion constant in the epilayer equals that in the base. When the doping levels are very different this is no longer true. Therefore, when we use Eq. (1.17) to calculate the charge Q_{epi}, we will introduce a parameter as prefactor that can take the difference of diffusion constant into account. At the same time a difference in intrinsic carrier concentration between base and epilayer (e.g. due to Ge in the base) can be taken into account.

We mentioned before that x_{C_2} is at the physical base-collector junction and that $\mathcal{V}_{\text{C}_2}$ equals the electron quasi-Fermi level at $x = x_{C_2}$. It is important to realise that under high-injection conditions the electron and hole concentrations do not vary as abruptly as in our model. This means that it is not possible to define in the same way as in the model where the base ends and where the epilayer starts: the position x_{C_2} becomes somewhat undefined. The value $\mathcal{V}_{\text{C}_2}$ will, therefore, not necessarily be equal to the quasi-Fermi level at the exact physical junction.

In Mextram we will use Eq. (1.16) to determine the main current in terms of charges, whereas Eq. (1.17) is used to determine Q_{epi} in terms of the current through the epilayer.

From Eqs. (1.16) and (1.17) it seems logical to make a description where the main current is given in terms of the biases $\mathcal{V}_{\text{B}_2\text{E}_1}$ and $\mathcal{V}_{\text{B}_2\text{C}_1}$ and the total hole charge $Q_B + Q_{\text{epi}}$. There are three reasons why we prefer not to do this. First, we now have a current model independent of the epilayer charge model. This means that the parameter τ_{epi} can be used freely to get a better description of the cut-off frequency, without influencing the DC behaviour. Second, Eqs. (1.16) and (1.17) hold for a one-dimensional transistor. They do not include current spreading effects, which can be very important in the epilayer. By having a parameter available for the epilayer charge that has no influence on the currents we can keep these effects separated. Third, by describing the base and the collector epilayer separately, we have a more natural description of SiGe-base/Si-collector transistors. We do not need to include extra charge enhancement factors [20] to be able to use an equation like Eq. (1.16) simultaneously in the base and in the epilayer. Instead, we use it twice, once for each region, with separated parameters.

 ©Koninklijke Philips Electronics N.V. 2005

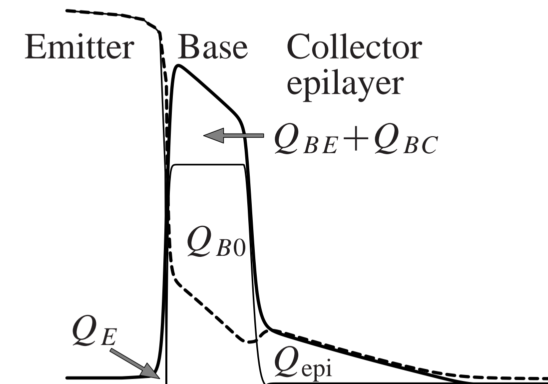

Figure 3: *A schematic cross-section of the intrinsic transistor, under high-injection conditions, showing the doping levels (thin), the hole density (thick) and the electron density (dashed). The various contributions to the hole charge Q_B are shown. Note that $Q_{BE} + Q_{BC}$ is equal to the electron charge in the base layer, and that the hole charge in the epilayer is almost equal to the electron charge in the epilayer.*

1.3.4 Charges, capacitances and transit times

We have seen above that the charges play an important role in the description of the main DC current. The charges also have to be modelled to be able to describe the currents as function of time or frequency. We will now discuss the charges in a bit more detail.

The total base charge Q_B has different contributions. Schematically this is shown in Fig. 3, for high injection conditions, neglecting the depletion charges. All of the charges we will describe are given in terms of the holes present. We now briefly describe where all the charge contributions are located. For zero bias the amount of holes in the base is given by the quantity Q_{B0}. This charge equals the integral over the dope $N_A(x)$ in the base from the base-emitter depletion region to the base-collector depletion region. When the bias over one of these junctions increases, the depletion layer thickness becomes smaller. This means that in the region which has become un-depleted an amount of holes is gathered. This charge is the depletion charge. Note that on the other side of the junction an equal amount of electron charge will be added. (We will see in Section 3.5 that the depletion charge of the base-epilayer junction can best be calculated by considering the change in electron charge in the epilayer).

When the bias of a normal pn-junction is changed three (hole) charges will change. We have already seen that the depletion charge is one of them. From the p-region (say the base) holes will be injected into the n-region (say the emitter). In the emitter these holes will either recombine somewhere with electrons (creating the ideal base current) or remain fixed in a stationary distribution. We assume neutrality in the emitter so the number of electrons must also increase. These, however, we do not model directly. The hole-charge in the neutral emitter is denoted by Q_E. The equivalent charge in the epilayer is denoted by $Q_{\rm epi}$. This last charge is mainly a high-injection charge. The third charge present is due to the current. In the p-region (the base) an electron current will flow. These electrons have a total charge basically given by the transit time times the current. Due to neutrality

©Koninklijke Philips Electronics N.V. 2005

also an extra number of holes must be present. These are again stationary. This total diffusion charge is split up between a part depending on the base-emitter voltage Q_{BE} and a part depending on the base-collector voltage Q_{BC}.

In our compact model the charges are shown as capacitances between two nodes in the equivalent circuit. Most of the charges are expressed as function of the applied voltages. Sometimes, however, the charge depends also on the current running through that specific part of the transistor. In the first case we associate the charge with a capacitance C (e.g. $Q = CV$). In the second case we associate it with a transit time τ (e.g. $Q = \tau I$). We can then write for an infinitesimal increment of a charge $Q = Q(V, I)$:

$$\mathrm{d}Q = C\mathrm{d}V + \tau\mathrm{d}I, \tag{1.18}$$

where the capacitance and the transit time are given by

$$C = \left(\frac{\partial Q}{\partial V}\right)_I; \qquad \tau = \left(\frac{\partial Q}{\partial I}\right)_V. \tag{1.19}$$

The distinction between a capacitive part and a transit time part of a charge is rather arbitrary. In a compact model the currents are again a function of bias. Hence in all cases the charges are ultimately a function of bias. In Mextram we therefore prefer to express most charges directly as function of the biases.

 ©Koninklijke Philips Electronics N.V. 2005

2 The intrinsic transistor

In this chapter we will give the model equations of Mextram for those elements that can be readily understood, without many extra derivations. Those elements that need some extra explanation are handled in the next chapters. In all chapters we use the convention that when a certain quantity is mentioned in the margin (like next to the equation below), then this quantity can be found in the equivalent circuit, and its corresponding equation is also given in the model definition of Mextram [1]. In other words, the quantities in the margin give the places where the actually implemented equations are given, and not just preliminary results.

2.1 Main current

The description of the main current is based on the ICCR (1.16). In Mextram it is given by[2]

$\mathbf{I_N}$

$$I_f = \mathsf{I_S}\ \exp(\mathcal{V}_{B_2E_1}/V_T), \tag{2.1a}$$
$$I_r = \mathsf{I_S}\ \exp(\mathcal{V}_{B_2C_2}/V_T), \tag{2.1b}$$
$$I_N = \frac{I_f - I_r}{q_B}. \tag{2.1c}$$

The parameter we introduced is $\mathsf{I_S}$, the saturation current of the main transistor. The base charge Q_B, normalised to the base charge at zero bias Q_{B0} is denoted by q_B[3]. From the ICCR (1.16) we see that the product of the saturation current and the zero bias base charge is

$$\mathsf{I_S}\ Q_{B0} = q^2 D_n A_{\mathrm{em}}^2 n_i^2. \tag{2.2}$$

(In Appendix F we show a list of parameters and model quantities like Q_{B0}, and give their relation to basic physical quantities.) As discussed in Section 1.3 the total base charge has a number of contributions. In principle these contributions for a one-dimensional transistor are:

$$Q_B = Q_{B0} + Q_{t_E} + Q_{t_C} + Q_{BE} + Q_{BC}. \tag{2.3}$$

Note that, as discussed in Section 1.3.3, we do not include the emitter charge and epilayer charge in the description of the main current. We will now discuss the various charge contributions.

[2]Note that in the official documentation $V^*_{B_2C_2}$ is used, instead of $\mathcal{V}_{B_2C_2}$. The difference between the two is not important here, but will be discussed in Chapter 3.

[3]When heterojunction effects play a role, one might need to distinguish between q_B as needed in current formulations and q_B as needed in charge formulations. This will be discussed in Chapter 6.

2.2 Depletion charges

2.2.1 General expression for depletion charges

The depletion charges are directly related to the well-known junction capacitances. The basic model for these capacitances [6, 7, 8] is

$$C = \frac{C_0}{(1 - V/V_d)^p}, \tag{2.4}$$

with V the applied bias, V_d the diffusion voltage, p the grading coefficient. The grading coefficient has a theoretical value of $1/2$ for an abrupt junction and $1/3$ for a graded junction. In practice the parameter may have other values after parameter extraction. The pre-factor in the capacitance formula is the capacitance for zero bias: $C_0 = C(V{=}0)$.

The charge, corresponding to the ideal depletion capacitance is

$$Q = \frac{C_0 V_d}{1 - p}\left[1 - (1 - V/V_d)^{1-p}\right], \tag{2.5}$$

where we added a constant term such that $Q(V{=}0) = 0$. The latter is needed to make sure that at zero bias we have indeed $Q_B = Q_{B0}$ in Eq. (2.3).

Clearly, the ideal capacitance has a singularity for $V = V_d$. This makes the formula inappropriate to use in a compact model. We need a continuous and smooth equation. (Smooth means that the first and higher order derivatives are continuous.) How this is done is discussed in Appendix A. The result is that we write the depletion charge as

$$Q = C_0 \cdot V_{\text{depletion}}(V|V_d, p|a). \tag{2.6}$$

Here $V_{\text{depletion}}$ is a function with the following properties

$$V_{\text{depletion}}(V|V_d, p|a) \simeq V, \quad \text{for small } |V|, \tag{2.7a}$$

$$C = \frac{\mathrm{d}Q}{\mathrm{d}V} \simeq \frac{C_0}{(1 - V/V_d)^p}, \quad \text{for } V \lesssim V_d, \tag{2.7b}$$

$$C = \frac{\mathrm{d}Q}{\mathrm{d}V} \simeq a\,C_0, \quad \text{for } V \gtrsim V_d. \tag{2.7c}$$

The quantity a is a Mextram constant, different for each of the depletion capacitances: $a_{j_E} = 3$, $a_{j_C} = 2$, and $a_{j_S} = 2$. In Fig. 4 we show an example of a depletion capacitance.

2.2.2 Substrate depletion charge

Q_{t_S}

The total depletion charge Q_{t_S} between collector and substrate is given using the parameters $\mathsf{C_{jS}}$, $\mathsf{p_S}$ and $\mathsf{V_{dS}}$ and the potential $\mathcal{V}_{SC_1}$:

$$Q_{t_S} = \mathsf{C_{jS}}\; V_{\text{depletion}}(\mathcal{V}_{SC_1}|\mathsf{V_{dS}}, \mathsf{p_S}|a_{j_S}). \tag{2.8}$$

 ©Koninklijke Philips Electronics N.V. 2005

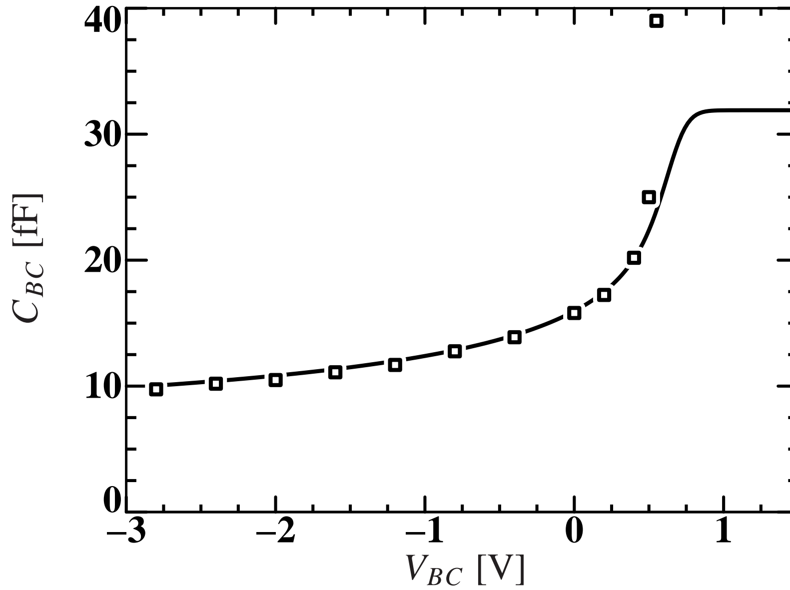

Figure 4: *An example of the capacitance formula. The markers are measurements. The lines is the model. When the junction is in forward, the diffusion capacitance dominates the depletion capacitance and we can safely make the depletion capacitance constant.*

2.2.3 Emitter depletion charge

The depletion charge between base and emitter is split into two parts, an intrinsic one and one belonging to the side-wall. Both are given using the parameters $\mathsf{C_{jE}}$, $\mathsf{p_E}$, $\mathsf{V_{d_E}}$ and $\mathsf{XC_{jE}}$ and the potentials $\mathcal{V}_{\mathrm{B_2E_1}}$, resp. $\mathcal{V}_{\mathrm{B_1E_1}}$: **$Q_{t_E}$** **$Q^S_{t_E}$**

$$Q_{t_E} = (1-\mathsf{XC_{jE}})\,\mathsf{C_{jE}}\;V_{\mathrm{depletion}}(\mathcal{V}_{\mathrm{B_2E_1}}|\mathsf{V_{d_E}},\mathsf{p_E}|a_{jE}), \tag{2.9a}$$

$$Q^S_{t_E} = \mathsf{XC_{jE}}\;\mathsf{C_{jE}}\;V_{\mathrm{depletion}}(\mathcal{V}_{\mathrm{B_1E_1}}|\mathsf{V_{d_E}},\mathsf{p_E}|a_{jE}). \tag{2.9b}$$

2.2.4 Collector depletion charges

The basic formula for the total collector depletion charge is that of a junction given above. However, we will split the total charge into three parts. First we have the intrinsic charge Q_{t_C}, which is beneath the emitter and hence between the nodes B_2 and C_2. This charge is important in for instance the Early effect. The external charges are split in a part (Q_{tex}, fraction $1-\mathsf{X_{ext}}$) between the nodes B_1 and C_1, and a part (XQ_{tex}, fraction $\mathsf{X_{ext}}$) between the nodes B and C_1. The fraction of the total capacitance below the emitter is given by $\mathsf{XC_{jC}}$.

For all three of these capacitances we must take the finite thickness of the epilayer into account. For zero junction voltage the capacitance equals in principle $C_{j0} = \varepsilon_{\mathrm{Si}}/x_{d0}$ (per unit surface). Here x_{d0} is the width of the depletion region in the epilayer at zero bias (assuming a negligible width in the base). When the junction becomes strongly reverse biased the depletion layer will be wider than the epilayer. Since the buried layer has a much larger doping, the width of the depletion layer will not increase much beyond

the width of the epilayer $W_{\rm epi}$ (reach-through). From there on, the capacitance will be approximately constant, with a value of in principle $\varepsilon_{\rm Si}/W_{\rm epi}$. We will approximate this behaviour by taking the sum of a constant part and a junction part. The parameter we use is given by $\mathsf{X_p} = x_{d0}/W_{\rm epi}$.

Qtex
XQtex

The extrinsic collector depletion charges are now given by

$$Q_{\rm tex} = (1-\mathsf{X_{ext}})\,(1-\mathsf{XC_{jc}})\,\mathsf{C_{jc}}\left[(1-\mathsf{X_p})V_{\rm depletion}(\mathcal{V}_{\rm B_1C_1}|\mathsf{V_{d_C}},\mathsf{p_C}|b_{jC}) + \mathsf{X_p}\mathcal{V}_{\rm B_1C_1}\right], \tag{2.10a}$$

$$XQ_{\rm tex} = \mathsf{X_{ext}}\,(1-\mathsf{XC_{jc}})\,\mathsf{C_{jc}}\left[(1-\mathsf{X_p})V_{\rm depletion}(\mathcal{V}_{\rm B\,C_1}|\mathsf{V_{d_C}},\mathsf{p_C}|b_{jC}) + \mathsf{X_p}\mathcal{V}_{\rm B\,C_1}\right]. \tag{2.10b}$$

Instead of a_{jC} we used b_{jC}, defined by

$$b_{jC} = \frac{a_{jC} - \mathsf{X_p}}{1-\mathsf{X_p}}. \tag{2.11}$$

This makes sure that for junction voltages above the diffusion voltage the capacitance of both the variable part and the constant part add up to a_{jC} times the zero-bias capacitance.

If we take the complement of the extrinsic collector depletion charges, we would arrive at the following expression for the charge of the intrinsic collector:

$$Q_{tC} \simeq \mathsf{XC_{jc}}\,\mathsf{C_{jc}}\left[(1-\mathsf{X_p})V_{\rm depletion}(\mathcal{V}_{\rm B_2C_1}|\mathsf{V_{d_C}},\mathsf{p_C}|b_{jC}) + \mathsf{X_p}\mathcal{V}_{\rm B_2C_1}\right] \quad \text{(incomplete!)} \tag{2.12}$$

However, the epilayer makes the model more complex, because the charge becomes dependent on the current. Equation 2.12 is only the low-current limit of the base-collector depletion charge, and therefore the expression above is incomplete. We will discuss Q_{tC} in Section 3.5.

2.3 Early effect

The Early effect is the effect that the main current gets modulated due to a variation in effective base width. This effective base width changes due to the fact that the depletion regions vary in thickness as function of the bias over the junction (both on the base-emitter side and on the base-collector side).

In Mextram (and in other modern bipolar compact transistor models) the Early effect is modelled using Eqs. (2.1) and (2.3). We neglect for the moment the diffusion charges. The normalised base charge (now called q_0) is then given by

$$q_0 = \frac{Q_B}{Q_{B0}} = 1 + \frac{Q_{t_E}}{Q_{B0}} + \frac{Q_{t_C}}{Q_{B0}}. \tag{2.13}$$

Referring to Eq. (2.9) we see that we can write for the second term in Eq. (2.13)

$$\frac{Q_{t_E}}{Q_{B0}} = \frac{(1-\mathsf{XC_{jE}})\,\mathsf{C_{jE}}}{Q_{B0}}\,V_{\rm depletion}(\mathcal{V}_{\rm B_2E_1}|\mathsf{V_{d_E}},\mathsf{p_E}|a_{jE}). \tag{2.14}$$

 ©Koninklijke Philips Electronics N.V. 2005

Now we introduce a new parameter, the reverse Early voltage $\mathsf{V_{er}} = Q_{B0}/(1-\mathsf{XC_{jE}})\,\mathsf{C_{jE}}$, which is the inverse of the pre-factor in the last equation. In the same way we can define the forward Early voltage $\mathsf{V_{ef}} = Q_{B0}/\mathsf{XC_{jC}}\,\mathsf{C_{jC}}$. Using the definitions

$$V_{t_E} = \frac{Q_{t_E}}{(1-\mathsf{XC_{jE}})\,\mathsf{C_{jE}}}, \qquad \Big(= V_{\text{depletion}}(\mathcal{V}_{\mathrm{B_2E_1}}|\mathsf{V_{d_E}}, \mathsf{p_E}|a_{j_E})\Big), \tag{2.15a}$$

$$V_{t_C} = \frac{Q_{t_C}}{\mathsf{XC_{jC}}\,\mathsf{C_{jC}}}. \tag{2.15b}$$

we arrive at the Early-effect term

$$q_0 = 1 + \frac{V_{t_E}}{\mathsf{V_{er}}} + \frac{V_{t_C}}{\mathsf{V_{ef}}}. \tag{2.16}$$

2.3.1 Punch-through

When both the base-emitter and the base-collector junctions are very much reverse biased, the depletion layers could touch each other. This is the effect of punch-through. Mextram is not meant to describe this effect correctly. In the case of punch-through the term q_0 becomes zero. Since we will divide by it to get the main current, we must make sure that it cannot become zero. We use, therefore,

$$q_1 = \tfrac{1}{2}\left(q_0 + \sqrt{q_0^2 + 0.01}\right), \tag{2.17}$$

instead of q_0 directly.

2.3.2 Base width

It is interesting to note that using the depletion capacitances we actually can calculate the effective base width, i.e. the distance between the two depletion regions. This width is approximately given by

$$W_{\text{eff}} \simeq W_B \frac{Q_{B0} + Q_{t_E} + Q_{t_C}}{Q_{B0}} \rightarrow W_B\, q_1. \tag{2.18}$$

(This is only completely true for a flat doping profile.)

2.4 Base diffusion charges

As we have seen in Eq. (2.1) the main current is defined in terms of both the depletion and the diffusion charges. Here we will describe the diffusion charges. To describe them we need to consider the neutral part of the base, i.e. the part where

$$p(x) = n(x) + N_A(x). \tag{2.19}$$

This region is bounded by the positions x_E and x_C that mark the boundaries of the depletion regions. The width is given by $W_B = x_C - x_E$. For the moment we will consider a constant base width.

Most of our derivations will be based on a constant doping profile. The results can also be used for other doping profiles, as will be discussed in Section 2.4.2. But first we will give a short derivation that gives the physical basics of our expressions. Note that most of our results can be found, in some way or another, in other basic texts as well.

2.4.1 Short derivation

To calculate the diffusion charges we need to know the electron density profile. (Recall that the hole density profile is given by Eq. (2.19).) Both in high-injection and for a constant base doping profile the electron density will be linear:

$$n(x) = n(0)\ (1 - x/W_B) + n(W_B)\ x/W_B. \tag{2.20}$$

The total electron charge is therefore

$$Q_{B,\mathrm{elec}} = \tfrac{1}{2} q A_{\mathrm{em}} W_B\ n(0) + \tfrac{1}{2} q A_{\mathrm{em}} W_B\ n(W_B). \tag{2.21}$$

As one can see the charge has a contribution from the electron density $n(0)$ at the base-emitter edge, and a contribution from the electron density $n(W_B)$ at the base-collector edge. The first is related to forward operation, and depends on the base-emitter bias $\mathcal{V}_{\mathrm{B_2E_1}}$. We will call this part Q_{BE}. The latter is related to reverse operation, and depends on the bias-collector bias $\mathcal{V}_{\mathrm{B_2C_2}}$.We will call this part Q_{BC}. We therefore get

$$Q_{BE} = \tfrac{1}{2} Q_{B0}\ n_0, \tag{2.22a}$$

$$Q_{BC} = \tfrac{1}{2} Q_{B0}\ n_B, \tag{2.22b}$$

where $Q_{B0} = q A_{\mathrm{em}} W_B N_A$, $n_0 = n(0)/N_A$ and $n_B = n(W_B)/N_A$. As we see, the diffusion charges are expressed in terms of the (normalised) electron densities at the edges of the neutral base region, and in terms of the zero bias base charge. So now we need expressions for these.

We have found (as discussed in the end of Section 2.4.2) that in normal forward operation the effective base transit time is almost constant. This means that the base-emitter diffusion charge can be expressed as $Q_{BE} = \tau_{\mathrm{B}}\ I$. Combining this with the ICCR (1.16) we get [5]

$$I = \frac{\mathsf{I_s}\ e^{\mathcal{V}_{\mathrm{B_2E_1}}/V_T}}{1 + \tau_{\mathrm{B}}\ I/Q_{B0}}. \tag{2.23}$$

This equation can be solved for I, and we get

$$I = \frac{2\,\mathsf{I_s}\ e^{\mathcal{V}_{\mathrm{B_2E_1}}/V_T}}{1 + \sqrt{1 + \dfrac{4\mathsf{I_s}}{\mathsf{I_k}}\ e^{\mathcal{V}_{\mathrm{B_2E_1}}/V_T}}}. \tag{2.24}$$

 ©Koninklijke Philips Electronics N.V. 2005

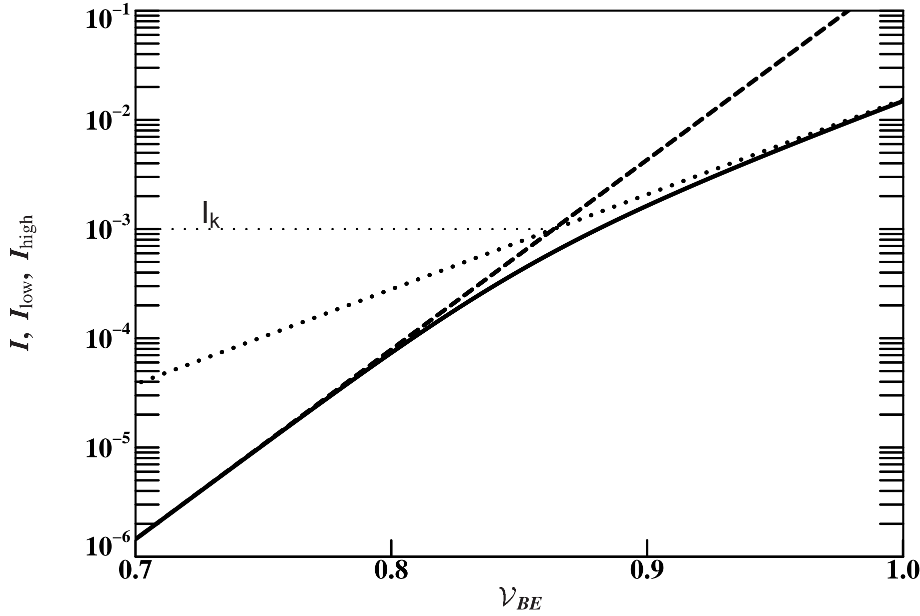

Figure 5: *The current I from Eq. (2.24) as function of bias, together with its asymptotes I_{low} (dashed) and I_{high} (dotted) from Eq. (2.25).*

Here we used $Q_{B0} = \tau_{\mathsf{B}}\,\mathsf{I_k}$, with $\mathsf{I_k}$ the knee current, as will become clear below. Let us look at the two asymptotes of the equation for the current, also shown in Fig. 5. For low currents, (i.e. small $\mathcal{V}_{\mathrm{B_2E_1}}$) we have

$$I_{\mathrm{low}} = \mathsf{I_s}\; e^{\mathcal{V}_{\mathrm{B_2E_1}}/V_T}, \tag{2.25a}$$

as can be expected. For high currents we get

$$I_{\mathrm{high}} = \sqrt{\mathsf{I_s}\;\mathsf{I_k}}\; e^{\mathcal{V}_{\mathrm{B_2E_1}}/2V_T}. \tag{2.25b}$$

We can calculate the point where both asymptotes cross:

$$I_{\mathrm{low}} = I_{\mathrm{high}} \Rightarrow I = \mathsf{I_k}. \tag{2.26}$$

Hence the 'knee' of the current, as shown in Fig. 5, is indeed at the knee current $\mathsf{I_k}$. Hence its name.

Now we only need an expression for the electron density. From Eq. (2.22) we find $n_0 = 2Q_{BE}/Q_{B0} = 2\tau_{\mathsf{B}} I/Q_{B0} = 2I/\mathsf{I_k}$. Hence

$$f_1 = \frac{4\,\mathsf{I_s}}{\mathsf{I_k}}\; e^{\mathcal{V}_{\mathrm{B_2E_1}}/V_T}, \tag{2.27a}$$

$$n_0 = \frac{f_1}{1+\sqrt{1+f_1}}. \tag{2.27b}$$

©Koninklijke Philips Electronics N.V. 2005

We do the same for reverse, and find

$$f_2 = \frac{4\,\mathsf{I_s}}{\mathsf{I_k}}\,e^{\mathcal{V}_{B_2C_2}/V_T}, \tag{2.28a}$$

$$n_B = \frac{f_2}{1+\sqrt{1+f_2}}. \tag{2.28b}$$

We now have an expression for the (normalised) electron densities n_0 and n_B as function of the respective junction biases. The diffusion charges are then given in terms of these electron biases and the zero bias base charge $Q_{B0} = \tau_\mathsf{B}\,\mathsf{I_k}$. It is also important to realise that the normalised base charge (called q_2 when we neglect the Early effect), given by

$$q_2 = 1 + \tfrac{1}{2}n_0 + \tfrac{1}{2}n_B, \tag{2.29}$$

is *independent* of the base time transit parameter τ_B. This means that this parameter does not influence the current description of our model. The knee current, of course, does influence the current description.

2.4.2 Not so short derivation

Next we give a more thorough derivation. This will also give us a chance to express the model parameters in terms of physical quantities.

To find the diffusion charges we have to solve the current density equations together with the continuity equations. (We assume all equations from Section 1.3 known and will not refer to them.) We assume that recombination in the base can be neglected. The hole current then vanishes: $J_p = 0$. This is of course only true when $\beta \gg 1$ such that the base current can be neglected. Using the expression for J_p we can find the electric field in the base: $E = V_T\,p^{-1}\mathrm{d}p/\mathrm{d}x$. Since the electric field is known, the expression for the electron current density $J_n = -I/A_\mathrm{em}$ gives a differential equation for the electron density:

$$I = -q\,D_n A_\mathrm{em}\left(\frac{2n+N_A}{n+N_A}\,\frac{\mathrm{d}n}{\mathrm{d}x} + \frac{n}{n+N_A}\,\frac{\mathrm{d}N_A}{\mathrm{d}x}\right). \tag{2.30}$$

This equation is the basic equation that can be used in any neutral region without recombination. For the moment, we will assume a constant base doping. The second term between parenthesis can then be neglected. Although an exact formulation solution is possible, we will start with the low and high injection limits.

As before we will give the solution in terms of the electron densities at the edges of the neutral base region. These can be given using the boundary conditions, see Eq. (1.9),

$$n_0\,(n_0+1) = \frac{n_i^2}{N_A^2}\,e^{\mathcal{V}_{B_2E_1}/V_T}, \tag{2.31a}$$

$$n_B\,(n_B+1) = \frac{n_i^2}{N_A^2}\,e^{\mathcal{V}_{B_2C_2}/V_T}. \tag{2.31b}$$

 ©Koninklijke Philips Electronics N.V. 2005

Since Eq. (2.30) is a first order differential equation, one would normally only need one boundary condition. Here, however, the second boundary condition is needed to determine I.

Constant base doping profile under low injection conditions. In the low injection regime we assume that $n \ll N_A$. Equation (2.30) then reduces to the simple differential equation

$$I = -q D_n A_{\mathrm{em}} \frac{\mathrm{d}n}{\mathrm{d}x}. \tag{2.32}$$

This implies that $n(x)$ is linear. The electron density is given as

$$n(x) = N_A\big[(1 - x/W_B)n_0 + (x/W_B)n_B\big]. \tag{2.33}$$

The electron charge is given as

$$Q_{B,\mathrm{elec}} = \tfrac{1}{2}\, q A_{\mathrm{em}} W_B N_A\ (n_0 + n_B) = \tfrac{1}{2} Q_{B0}(n_0 + n_B). \tag{2.34}$$

From this we see that for low injection we can write $Q_{BE} = \frac{1}{2} Q_{B0}\, n_0$ and $Q_{BC} = \frac{1}{2} Q_{B0}\, n_B$, just as before.

Of course we can also calculate the current:

$$I = \frac{q D_n A_{\mathrm{em}} N_A}{W_B}(n_0 - n_B). \tag{2.35}$$

We want to write this in the same way as Eq. (1.16). To this end we can write for low injection, see Eq. (2.31), $n_0 \simeq (n_i^2/N_A^2) e^{\mathcal{V}_{\mathrm{B_2E_1}}/V_T}$ and equivalently for n_B. Re-expressing I gives

$$I = \frac{q D_n A_{\mathrm{em}} n_i^2}{N_A W_B} \left(e^{\mathcal{V}_{\mathrm{B_2E_1}}/V_T} - e^{\mathcal{V}_{\mathrm{B_2C_2}}/V_T}\right). \tag{2.36}$$

This is the expression for I at small injection and without the Early effect. The pre-factor is the saturation current parameter $\mathsf{I_S}$.

We can now also calculate the effective forward transit time (calculated assuming $n_B = 0$)

$$\tau_f = \frac{\mathrm{d}Q_{BE}}{\mathrm{d}I} = \frac{W_B^2}{2\, D_n}. \tag{2.37}$$

The reverse transit time (of the intrinsic transistor) is the same.

©Koninklijke Philips Electronics N.V. 2005

Constant base doping profile under high injection conditions. Next we consider the high injection limit, $n \gg N_A$. In this limit the electron and hole densities are almost equal: $n \simeq p$. The differential equation for the electron density now reads

$$I = -2q D_n A_{\mathrm{em}} \frac{\mathrm{d}n}{\mathrm{d}x}, \tag{2.38}$$

and is the same as before, apart from a factor 2. This implies that the expressions for the charges above do not change. For the expression for the current we need, again from Eq. (2.31), $n_0 \simeq (n_i/N_A) e^{\mathcal{V}_{\mathrm{B_2E_1}}/2V_T}$. This leads to

$$I = \frac{2q D_n A_{\mathrm{em}} N_A}{W_B}(n_0 - n_B) = \mathsf{I_s}\,\frac{2N_A}{n_i}\left(e^{\mathcal{V}_{\mathrm{B_2E_1}}/2V_T} - e^{\mathcal{V}_{\mathrm{B_2C_2}}/2V_T}\right). \tag{2.39}$$

As we can see, we need a new parameter, that describes the ratio between N_A and n_i. This parameter is again the knee current. It is defined using the high injection asymptote, which we can write as

$$I = \sqrt{\mathsf{I_s}\,\mathsf{I_k}}\left(e^{\mathcal{V}_{\mathrm{B_2E_1}}/2V_T} - e^{\mathcal{V}_{\mathrm{B_2C_2}}/2V_T}\right). \tag{2.40}$$

For a constant base doping profile we therefore find

$$\mathsf{I_k} = \mathsf{I_s}(2N_A/n_i)^2 = \frac{4q D_n A_{\mathrm{em}} N_A}{W_B}. \tag{2.41}$$

The (forward) transit time is now

$$\tau_f = \frac{\mathrm{d}Q_{BE}}{\mathrm{d}I} = \frac{W_B^2}{4\,D_n}. \tag{2.42}$$

As we can see, this transit time has been reduced by a factor of 2 from its low-injection value (for a constant base doping).

Constant base doping profile under general injection conditions. Next we need to consider the interpolation between the low and high-current regimes. We have seen that the electron density is linear, both for low and for high injection conditions. When we assume that it is linear for all injection conditions we can find a simple expression for the current. For a linear density, we can express the diffusion charge in terms of the electron densities at the boundaries as in Eq. (2.22). The electron densities at the boundaries follow from the boundary conditions (2.31). Using Eq. (2.1) with $q_B = q_2$ given in Eq. (2.29), we can write

$$I = \mathsf{I_s}\left(e^{\mathcal{V}_{\mathrm{B_2E_1}}/V_T} - e^{\mathcal{V}_{\mathrm{B_2C_2}}/V_T}\right)/q_2. \tag{2.43}$$

 ©Koninklijke Philips Electronics N.V. 2005

For future reference we give this solution for the current expressed solely in terms of n_0 and n_B:

$$I = \tfrac{1}{4}\mathsf{I_k}\frac{n_0(n_0+1) - n_B(n_B+1)}{1+\frac{1}{2}n_0+\frac{1}{2}n_B} = \tfrac{1}{4}\mathsf{I_k}\,\frac{n_0 - n_B}{1+\frac{1}{2}n_0+\frac{1}{2}n_B}\,(n_0+n_B+1)\,. \qquad (2.44)$$

We can clearly see the transition from low to high injection. For low injection we find $I = \frac{1}{4}\mathsf{I_k}\ (n_0 - n_B)$ and for high injection $I = \frac{1}{2}\mathsf{I_k}\ (n_0 - n_B)$. The transit changes from $W_B^2/2D_n$ to $W_B^2/4D_n$, as function of bias.

Equation (2.43) is not what is implemented in Mextram, as we discuss in the paragraph about non-constant base doping below.

Exact solution in the case of a constant base doping profile. We mentioned before that also the exact solution of Eq. (2.30) can be given for a constant base doping profile. We will give it here for completeness sake. Using the definition of $\mathsf{I_k}$ we can write

$$I\ \mathrm{d}x/W_B = -\tfrac{1}{4}\mathsf{I_k}\left(2 - \frac{N_A}{n+N_A}\right)\mathrm{d}n/N_A. \qquad (2.45)$$

Integration from $x = 0$ to $x = W_B$ gives the exact result

$$I = \tfrac{1}{4}\mathsf{I_k}\left(2n_0 - 2n_B - \log\frac{1+n_0}{1+n_B}\right). \qquad (2.46)$$

We will see expressions like these again when we consider the epilayer. They form the basis of the Kull-model [19]. After some algebra we can re-express Eq. (2.46), such that we can compare it with Eq. (2.44):

$$I = \tfrac{1}{4}\mathsf{I_k}\ \frac{n_0 - n_B}{1+\frac{1}{2}n_0+\frac{1}{2}n_B}\left[n_0+n_B+2-\left(\frac{2+n_0+n_B}{n_0-n_B}\,\mathrm{artanh}\,\frac{n_0-n_B}{2+n_0+n_B}\right)\right].(2.47)$$

The approximation we made in the previous paragraph (assuming a linear electron density for all injection levels) is equivalent to replacing, in the equation above, the expression between parenthesis by 1. For low injection this is the correct limit. But also for high injection this term will remain of the order 1. Since for high injection $n_0 \gg 1$ or $n_B \gg 1$ the term between parenthesis is not important. It can be shown that the approximate solution of Eq. (2.44) differs nowhere more than 5% from the exact solution.

Non-constant base doping profile. In practice the doping profile is not constant. For that reason, in earlier versions of Mextram [21] a formulation was used based on an exponential doping profile profile:

$$N_A(x) = N_{A0}\ e^{-\eta x/W_B}. \qquad (2.48)$$

©Koninklijke Philips Electronics N.V. 2005

The reason for using this profile is that it is reasonable realistic but still leads to analytic results. The parameter η is sometimes called the built-in field parameter, since at low injection the electric field is given as $E = V_T N_A^{-1} \mathrm{d}N_A/\mathrm{d}x = -\eta V_T / W_B$. Typical values of η are 3 or 4.

Using such a doping profile one can find the low and high current limits, and one can find interpolation formulas [21, 14]. We will not repeat all of the results here, but only note that the high-current limit is always independent of the actual base doping profile.

One of the results is that the low-injection forwards transit time depends on the doping profile. In practice, for values around $\eta = 3$ or 4, the transit time is nearly constant, and equal to the high-injection limit of $W_B^2/4D_n$. For this reason we chose to take a injection-independent base transit time. This also simplifies the formulations considerably. Hence we now use the expressions, already given in Section 2.4.1. Note that this also implies that we take the (intrinsic) reverse transit time to be constant. This is not so much of a problem, since there are a lot of other parameters (especially the transit time of the epilayer τ_{epi}) that can be used to model the charges in (quasi) saturation.

Another advantage is that we don't need η as a parameter anymore. Many years of experience with Mextram showed that the parameter η had a very limited influence on the characteristics. This can be explained as follows. As has been shown in Fig. 5 at some point the current starts to deviate from the ideal exponential behaviour. There used to be two parameters to model this: the built-in field parameter η and the knee current $\mathsf{I_k}$. The latter should also be used for the asymptote at higher currents. This asymptote, however, is never reached due to other high-current effects (resistances, quasi-saturation). Hence the knee current is by itself enough to model the initial deviation from the ideal exponential behaviour. Since the asymptote is never reached, the parameter $\mathsf{I_k}$ is in practice not very well defined. After parameter extraction it does not always have a value close to the estimate based on the doping profile. One needs to take this into account when doing parameter extraction.

2.4.3 The Early effect on the diffusion charges

Up to now we have assumed a constant base width $W_B = x_C - x_E$. In reality this width changes as function of bias since the depletion regions change with bias. This has its effect on the main current and is called the Early effect (see Section 2.3). It also has its influence on the diffusion charges. We have seen that these charges are proportional to the base charge Q_{B0} when we do not take the Early effect into account. The Early effect is then simply modelled by using $Q_{B0} + Q_{t_E} + Q_{t_C}$ instead of Q_{B0}, via q_1. The expressions for the base diffusion charges therefore become

$\mathbf{Q}_{BE}$
$\mathbf{Q}_{BC}$

$$Q_{BE} = \tfrac{1}{2}\, q_1 Q_{B0}\, n_0, \tag{2.49a}$$
$$Q_{BC} = \tfrac{1}{2}\, q_1 Q_{B0}\, n_B, \tag{2.49b}$$

where $Q_{B0} = \tau_{\mathsf{B}}\, \mathsf{I_k}$. The normalised base charge used in Eq. (2.1) then is

$$q_B = q_1\; (1 + \tfrac{1}{2} n_0 + \tfrac{1}{2} n_B). \tag{2.50}$$

 ©Koninklijke Philips Electronics N.V. 2005

2.4.4 Extended modelling of excess phase shift

It is possible to model distributed high frequency effects in the intrinsic base. These are modelled, in first order approximation, both in lateral direction (current crowding, to be discussed in Section 5.2) and in vertical direction (excess phase-shift). The distributed effects are an optional part of the Mextram model and can be switched on and off by flag EXPHI (on: $\mathsf{EXPHI} = 1$ and off: $\mathsf{EXPHI} = 0$)

In vertical direction (excess phase-shift) base-charge-partitioning [12, 22] is used. Base charge partitioning means that the charge Q_{BE} is assigned not only to the base-emitter junction, but partly also to the base-collector junction. The reason is that, for instance in the case of an AC-signal, a part of this charge is not supplied through the emitter contact, but through the collector contact. This will lead to an extra phase shift in the transconductance.

The general way to find the partitioning is by writing [22]

$$Q_{BE} = q A_{\mathrm{em}} \int_0^{W_B} n(x)\ (1 - x/W_B)\mathrm{d}x, \tag{2.51a}$$

$$Q_{BC} = q A_{\mathrm{em}} \int_0^{W_B} n(x)\ x/W_B\ \mathrm{d}x. \tag{2.51b}$$

For the simple case of a linear electron density $n(x) = n(0)(1 - x/W_B)$ we find $Q_{BE} = \frac{2}{3} Q_{\mathrm{tot}}$ and $Q_{BC} = \frac{1}{2} Q_{\mathrm{tot}}$, where $Q_{\mathrm{tot}} = \frac{1}{2} Q_{B0} n_0$.

There is another way of looking at it, that might give some insight. Let us solve the diffusion equation for electrons $J = q D_n \partial n/\partial x$, together with the continuity equation $\partial J/\partial x + q \partial n/\partial t = 0$, for an AC signal with frequency ω. The equation to solve is then

$$D_n \frac{\partial^2 n}{\partial x^2} = -j\omega n. \tag{2.52}$$

Introducing the complex quantity $\lambda^2 = j\omega W_B^2/D_n$ $(= 2j\omega\tau_f$ at low injections) the solution is given by

$$n(x) = n(0)\ \sinh[\lambda(1 - x/W_B)]/\sinh\lambda. \tag{2.53}$$

From the electron density we can find the electron current density and hence the electron current, which is now not a constant, but depends on position. The current that goes to the emitter is $I(0)$, whereas the current that goes to the collector is $I(W_B)$. In the low-frequency limit they are given by

$$I(0) = I_{DC} + j\omega \tfrac{2}{3} Q_{\mathrm{tot}} = I_{DC} + \frac{\mathrm{d}(\frac{2}{3} Q_{\mathrm{tot}})}{\mathrm{d}t}, \tag{2.54a}$$

$$I(W_B) = I_{DC} - j\omega \tfrac{1}{3} Q_{\mathrm{tot}} = I_{DC} - \frac{\mathrm{d}(\frac{1}{3} Q_{\mathrm{tot}})}{\mathrm{d}t}. \tag{2.54b}$$

Here I_{DC} is the DC current. Again we see that only two-thirds of the variation of the charge belongs to the emitter side.

The derivations given above implicitly assume a constant base doping profile. For non-constant base doping profiles the derivation becomes more difficult [23, 24] (see also the report [25]). Of course then the pre-factors $2/3$ and $1/3$ also depend on the doping profile, or rather the actual electron density. We have seen that for high-injection, the situation where these charges are important, the electron density is indeed linear. For low injection it might be different, but we have no parameter (like η) to make the partitioning bias dependent. Hence we stick with the partitioning factors as derived above. For simplicity reasons we only implemented base charge partitioning for the forward base charge (Q_{BE})

Q_{BE}
Q_{BC}

So, when $\mathsf{EXPHI} = 1$, Q_{BE} and Q_{BC} (Eq. 2.49) are redefined according to

$$Q_{BC} \rightarrow \tfrac{1}{3}\, Q_{BE} + Q_{BC}, \tag{2.55a}$$

$$Q_{BE} \rightarrow \tfrac{2}{3}\, Q_{BE}. \tag{2.55b}$$

2.5 Emitter diffusion charge

The emitter diffusion charge models the hole charge on the emitter side of the neutral base edge. This means the hole charge both in the neutral emitter, as well as the hole charge in the depletion region not related to the depletion charge. The hole density giving rise to the latter charge is that part of the hole charge in the depletion region that is locally compensated for by an electron density. It is therefore sometimes called the neutral charge of the depletion region [26].

Since the charge is in the emitter region, which has normally a much higher doping than the base, we do not need to take high-injection effects into account: the charge does not have a 'knee'. We do allow for a non-ideality factor and therefore write

Q_E

$$Q_E = Q_{E0}\,\left(e^{\mathcal{V}_{B_2E_1}/\mathsf{m}_\tau V_T} - 1\right), \tag{2.56}$$

with m_τ normally between 1 and 2.

Next we need to express the pre-factor Q_{E0} in terms of the transit time parameter τ_E. Let us therefore calculate the effective transit time of Q_E. For low injection, where the current is given by Eq. (2.25a), we find

$$Q_E \simeq Q_{E0}\,\left(\frac{I}{\mathsf{I_s}}\right)^{1/\mathsf{m}_\tau} \quad\Rightarrow\quad \tau_{Q_E} \simeq \frac{\mathrm{d}Q_E}{\mathrm{d}I} = \frac{Q_{E0}}{\mathsf{m}_\tau\ \mathsf{I_s}}\,\left(\frac{I}{\mathsf{I_s}}\right)^{1/\mathsf{m}_\tau - 1}. \tag{2.57}$$

This transit time decreases with current when $\mathsf{m}_\tau > 1$. For high injection, where the current is given by Eq. (2.25b), we find

$$Q_E \simeq Q_{E0}\,\left(\frac{I}{\sqrt{\mathsf{I_s\,I_k}}}\right)^{2/\mathsf{m}_\tau} \quad\Rightarrow\quad \tau_{Q_E} \simeq \frac{2\,Q_{E0}}{\mathsf{m}_\tau\ \sqrt{\mathsf{I_s\,I_k}}}\,\left(\frac{I}{\sqrt{\mathsf{I_s\,I_k}}}\right)^{2/\mathsf{m}_\tau - 1}. \tag{2.58}$$

 ©Koninklijke Philips Electronics N.V. 2005

This transit time increases with current. Hence, when $\mathsf{m}_\tau > 1$, the effective transit time τ_{Q_E} has a minimum.

We must now ask ourselves, which of these possible effective transit times do we take to be the parameter τ_E? Preferably, we need both parameters τ_E and m_τ to be as independent as possible. This means that for instance τ_E should not change very much, when we change m_τ. (Note that the charge depends exponentially on m_τ.) Since τ_E will be determined around the top of f_T, it is best to take the minimum of τ_{Q_E} as the independent parameter τ_E. The minimum occurs approximately at the knee in the current. We will not use the exact minimum, because this depends on the exact expression for I itself, including all extra effects. We just take Eq. (2.57) at $I = \mathsf{I_k}$ and find $\tau_\mathsf{E} = \tau_{Q_E} \simeq Q_{E0}\ (\mathsf{I_k}/\mathsf{I_s})^{1/\mathsf{m}_\tau}/\mathsf{I_k}$. For the pre-factor we therefore take

$$Q_{E0} = \tau_\mathsf{E}\ \mathsf{I_k}\ \left(\frac{\mathsf{I_s}}{\mathsf{I_k}}\right)^{1/\mathsf{m}_\tau}. \tag{2.59}$$

Note that for $\mathsf{m}_\tau = 1$ we get the simple expression

$$Q_E = \tau_\mathsf{E}\ \mathsf{I_s}\ e^{\mathcal{V}_{\mathrm{B_2E_1}}/V_T} = \tau_\mathsf{E}\ I_{\mathrm{low}}. \tag{2.60}$$

For other values of m_τ we have made sure that the minimum of the effective emitter charge transit time, which is around the top of f_T, is almost independent of m_τ and of the order of τ_E. For lower or higher currents the effective transit time can differ very much from the parameter value.

2.6 Base currents

2.6.1 Ideal forward base current

The total ideal base current is separated into a bulk and a side-wall current (the latter has a fraction $\mathsf{XI_{B_1}}$). Both depend on separate voltages. As in the basic Ebers-Moll and Gummel-Poon models we use the (forward) current gain β_f as a parameter that gives the ratio between the main saturation current and base saturation current. We get

$\mathbf{I_{B_1}}$

$\mathbf{I^S_{B_1}}$

$$I_{B_1} = (1 - \mathsf{XI_{B_1}})\frac{\mathsf{I_s}}{\beta_\mathsf{f}}\Big(\exp(\mathcal{V}_{\mathrm{B_2E_1}}/V_T) - 1\Big), \tag{2.61a}$$

$$I^S_{B_1} = \mathsf{XI_{B_1}}\frac{\mathsf{I_s}}{\beta_\mathsf{f}}\Big(\exp(\mathcal{V}_{\mathrm{B_1E_1}}/V_T) - 1\Big). \tag{2.61b}$$

Note that the expression for the ideal base current changes when one of the heterojunction features is used (see Chapter 6).

2.6.2 Non-ideal forward base current

The non-ideal forward base current is given by

$\mathbf{I_{B_2}}$

$$I_{B_2} = \mathsf{I_{Bf}} \left(e^{\mathcal{V}_{B_2E_1}/\mathsf{m_{Lf}} V_T} - 1 \right), \tag{2.62}$$

and is simply a diode current with a non-ideality factor $\mathsf{m_{Lf}}$.

2.6.3 Non-ideal reverse base current

$\mathbf{I_{B_3}}$

The non-ideal reverse base current is given by

$$I_{B_3} = \mathsf{I_{Br}} \frac{\exp(\mathcal{V}_{B_1C_1}/V_T) - 1}{\exp(\mathcal{V}_{B_1C_1}/2V_T) + \exp(\mathsf{V_{Lr}}/2V_T)}. \tag{2.63}$$

This expression is basically an approximation to the Shockley-Read-Hall recombination. The recombination takes place in the depletion layers. It is well known that for small junction voltages this current goes exponentially with $\exp(\mathcal{V}_{B_1C_1}/V_T)$. For higher voltages this changes into $\exp(\mathcal{V}_{B_1C_1}/2V_T)$. The model above introduces a cross-over voltage to describe the effective behaviour of the recombination current. In practice, however, the ideal part of this current can often not be measured due to the low cross-over voltage.

2.6.4 Extrinsic base current

The modelling of the extrinsic base current is rather analogous to the ideal forward base current I_{B_1} and the reverse current I_r/q_B. (The real intrinsic reverse current is more complicated due to avalanche and epilayer contributions). As we did for the main current (or rather for the diffusion charges) we use an interpolation between low injection and high injection. Here we use an interpolate function directly for the current. It is again expressed in terms of the electron density, in this case n_{Bex} at the end of the extrinsic base:

$$g_1 = \frac{4\,\mathsf{I_s}}{\mathsf{I_k}} \exp(\mathcal{V}_{B_1C_1}/V_T), \tag{2.64a}$$

$$n_{Bex} = \frac{g_1}{1 + \sqrt{1 + g_1}}. \tag{2.64b}$$

The expression for the electron density n_{Bex} is the same as that of n_B in Eq. (2.28), but now it depends on $\mathcal{V}_{B_1C_1}$ instead of $\mathcal{V}_{B_2C_2}$. The expression for the current must now be something like

$$I_{ex} \simeq \frac{1}{\beta_{\mathsf{ri}}} \frac{\mathsf{I_s} \exp(\mathcal{V}_{B_1C_1}/V_T)}{1 + \frac{1}{2} n_{Bex}}, \tag{2.65}$$

which includes the high-injection behaviour and is similar to the main current Eq. (2.1) without Early effect ($q_B \simeq q_2$) and where q_2 from Eq. (2.29) contains only one charge contribution. Since here the current depends on only one voltage (there is no ‘reverse’, or rather ‘forward’, term here) we can simplify it to

$\mathbf{I_{ex}}$

 ©Koninklijke Philips Electronics N.V. 2005

$$I_{\text{ex}} = \frac{1}{\beta_{\text{ri}}} \left(\tfrac{1}{2} \mathsf{I_k}\, n_{B\text{ex}} - \mathsf{I_s} \right). \tag{2.66}$$

The saturation current $\mathsf{I_s}$ is added to make sure that there is no current at zero bias.

2.7 Substrate currents

2.7.1 Substrate current

The substrate current includes high-injection and is given by [cf. Eq. (2.24)] **$\mathbf{I}_{\text{sub}}$**

$$I_{\text{sub}} = \frac{2\, \mathsf{I_{Ss}} \Big(\exp(\mathcal{V}_{\text{B}_1\text{C}_1}/V_T) - 1 \Big)}{1 + \sqrt{1 + 4 \dfrac{\mathsf{I_s}}{\mathsf{I_{ks}}} \exp(\mathcal{V}_{\text{B}_1\text{C}_1}/V_T)}}. \tag{2.67}$$

Here $\mathsf{I_{ks}}$ is the knee-current. This knee-current is given with respect to $\mathsf{I_s}$ instead of to $\mathsf{I_{Ss}}$ since this is easier for extraction. The formulation of this current is basically the same as that which we found for the main currents (see Section 2.4.1) under the assumption of a flat doping profile in the epilayer (which is the base of the parasitic PNP).

2.7.2 Substrate failure current

The substrate-collector junction should always be reverse biased. Hence we don't need to model the reverse behaviour of the parasitic PNP. To give a designer a warning that the junction is biased wrong, we included a substrate 'failure' current, simply given as **$\mathbf{I}_{\text{Sf}}$**

$$I_{\text{Sf}} = \mathsf{I_{Ss}} \Big(\exp(\mathcal{V}_{\text{SC}_1}/V_T) - 1 \Big). \tag{2.68}$$

This current has no physical meaning.

©Koninklijke Philips Electronics N.V. 2005

3 The collector epilayer model

3.1 Introduction

The epilayer of a bipolar transistor is the most difficult part to model. The reason for this is that a number of effects play a role and act together. We will restrict ourselves to modelling the epilayer in as far as it is part of the intrinsic transistor. The current I_{epi} through the epilayer[4] is for low current densities mainly determined by the main current I_N. Hence the epilayer is a part of the transistor that is current driven. Since the dope concentration in the epilayer is in general small, high injection effects are important. In that case the epilayer will be (partly) flooded by holes and electrons. Even though then the main current and the epilayer current depend on each other and their equations become coupled, we will still consider the epilayer to be current driven, i.e. our model will have I_{epi} as a starting quantity. The regions where no injection takes place can either be ohmic, which implies charge neutral, or depleted. In depletion regions the electric field is large and the electrons will therefore move with the saturation velocity. These electrons can be called hot carriers. The electrons will contribute to the charge. In case of large currents this moving charge becomes comparable to the dope, the net charge decreases, or even changes sign. The net charge has its influence on the electric field, which in its turn determines the velocity of the electrons: for low electric fields we have ohmic behaviour, for large electric fields the velocity of the electrons will be saturated.

All these effects determine the effective resistance of the epilayer. As is well known, the potential drop over the collector region can cause quasi-saturation. In that case the external base-collector bias is in reverse, which is normal in forward operation, but the internal junction is forward biased. Injection of holes into the epilayer then takes place. The charge in the epilayer and in the base-collector region depends on the carrier concentrations in the epilayer, and will increase significantly in the case of quasi-saturation.

The electric field in the epilayer is directly related to the base-collector depletion capacitance. As we will see in Section 3.6 the avalanche current is determined by the same electric field, and in particular by its maximum. Hence our description of the epilayer must also include a correct description of the electric field.

For modern small transistors we must take current spreading into account. This means that the electrons that come from the emitter, through the base, go to a region of the collector with a surface larger than the emitter area A_{em}. This spreading effect decreases the resistance of the epilayer and also the maximum electric field, and hence the avalanche current.

Extensive literature about the physics of the epilayer is available, e.g. [8, 9, 10, 19, 27, 28, 29, 30, 31, 32, 33, 34, 35, 36]. The basis of the Mextram epilayer model was given by Kull et al. [19]. Their model has become known as the Kull model. Their paper also discusses the approximations made. This model has been incorporated and extended in

[4] In this chapter we will consequently write I_{epi} for the current through the epilayer because this is more clear, especially in those intermediate expressions in which the current is not necessarily equal to the $I_{C_1C_2}$ that is really implemented, see Eq. (3.26). Only when discussing the real implementation we use $I_{C_1C_2}$.

 ©Koninklijke Philips Electronics N.V. 2005

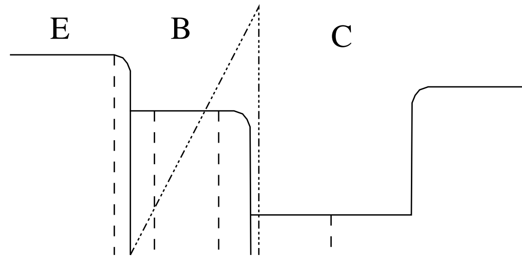

Figure 6: *Schematic representation of the doping profile of a one-dimensional bipolar transistor. One can observe the emitter, the base, the collector epilayer and the (buried) collector. Constant doping profiles are assumed in many of the derivations. The collector epilayer is in this chapter located between $x = 0$ and $x = W_{\rm epi}$ and has a dope of $N_{\rm epi}$. We have also shown where the various nodes E_1, B_2, C_2 and C_1 of the intrinsic transistor are located approximately.*

Mextram. For Mextram 503 these extensions have been published in Ref. [33], at least for current-voltage relations. In Ref. [37] a thorough description of all parts of the epilayer model is given, that was implemented in Mextram 503. The report includes the charge model, as well as the description of the avalanche current. Another way of describing it was given in Ref. [14].

In this chapter we give the description of the same material, based on Refs. [36, 38], leading to the Mextram 504 implementation, in order to clarify the physics behind the model, as well as the approximations made.

In Section 3.2 we give a qualitative description of the various effects that play a role in the epilayer. The actual derivation of the collector current and the internal base-collector bias is given in Section 3.3. The diffusion charge in the epilayer $Q_{\rm epi}$ is discussed in Section 3.4. In Section 3.5 we describe the depletion charge Q_{t_C}. Finally the avalanche model is given in Section 3.6.

3.2 Some qualitative remarks on the description of the epilayer

Let us now concentrate on a one-dimensional model of the lightly doped epilayer. In this chapter we assume the epilayer to be along the x-axis from $x = 0$ to $x = W_{\rm epi}$, as has been schematically shown in Fig. 6. (Note that in the description of the main current I_N we used another offset for the x-axis.) The base is then located at $x < 0$, while the highly doped collector region, the buried layer, is situated at $x > W_{\rm epi}$. We assume a flat dope in the epilayer and an abrupt epi-collector junction for the derivation of our equations. In the final description of the model we will generalise some factors to account for non-ideal profiles. (For instance the depletion charge has a parameter for the grading coefficient). For the same reason most of the parameters will have an effective value. This is even more so when current spreading is taken into account, see Section 3.3.4.

We assume that the potential of the buried layer, at the interface with the epilayer, is given by the node potential $\mathcal{V}_{\rm C_1}$. The resistance in the buried layer and further away at the

©Koninklijke Philips Electronics N.V. 2005

collector contact are modelled by the resistance $\mathsf{R_{Cc}}$ and will not be discussed here.

We assume that the doping concentration in the base is much higher than that in the epilayer. In that case the depletion region will be located almost only in the epilayer (i.e. we have a one-sided pn-junction). The potential of the internal base (i.e. the base potential while neglecting the base resistance) is given by $\mathcal{V}_{\mathrm{B_2}}$.

The nodes of the equivalent circuit In the Mextram model, as well as in many other compact models, there is an intrinsic collector node, in our case C_2. The potential at this node is the electron quasi-Fermi level at the base-collector interface. This potential plays an important role in the description of the effects in the collector epilayer, both for low currents where it determines the depletion capacitance and for high currents where it is important for the description of quasi-saturation.

For high injection the potential difference $\mathcal{V}_{\mathrm{B_2C_2}}$ determines the (reverse) main current I_r and the directly related diffusion charge Q_{BC}, as we have seen in Chapter 2, Eqs. (2.1), (2.22) and (2.28). So for high injection, including reverse operation and (quasi) saturation, the bias $\mathcal{V}_{\mathrm{B_2C_2}}$ must be such that it describes correctly the electron and hole concentration at the base-collector interface. In Mextram we need for instance n_B, the electron concentration at the base-side of this junction, and p_0, the hole concentration at the collector side. In formula, the potential difference $\mathcal{V}_{\mathrm{B_2C_2}}$ must fulfil Eq. (1.8), repeated here for convenience:

$$n(0)\,p(0) = n_i^2 e^{\mathcal{V}_{\mathrm{B_2C_2}}/V_T}. \tag{3.1}$$

For low currents the precise value of the electron concentration at the base-epilayer junction is of minor importance. In this regime the value of the potential $\mathcal{V}_{\mathrm{C_2}}$ is used to describe the depletion capacitance correctly, using a formula similar to Eq. (2.12).

Hence the intrinsic collector node voltage has a double function, one for low currents, one for high injection. When we also demand that the model is not only continuous but also smooth, this double function can no longer be achieved by a single node potential.

In Mextram 504 we therefore make a distinction between three biases. In Mextram 503 all three of them are given by the bias $\mathcal{V}_{\mathrm{B_2C_2}}$ as it comes from the circuit simulator. In Mextram 504 we have instead

$\mathcal{V}_{\mathrm{B_2C_2}}$: The bias as it is given by the circuit simulator. This bias is used to calculate the current $I_{C_1C_2}$ through the epilayer, using the previously mentioned Kull model. It is however not used to calculate other quantities. It is therefore only a first step in the calculation and acts as a help variable. No physical meaning should be attached to it in forward mode.

$V^*_{B_2C_2}$: This bias is the bias that is in some sense the most physical one, since the effect of quasi-saturation is taken into account. It is calculated using the external base-collector bias $\mathcal{V}_{\mathrm{B_2C_1}}$ and the current $I_{C_1C_2}$. This makes it possible to make sure that $V^*_{B_2C_2}$ behaves smoothly over bias and current. It will be used to calculate other quantities like I_r, Q_{BC} and Q_{epi}.

 ©Koninklijke Philips Electronics N.V. 2005

$V_{\rm junc}$: This is the bias that is used to calculate the intrinsic base-collector depletion capacitance. It is also calculated using the external base-collector bias $\mathcal{V}_{\rm B_2C_1}$ and the current $I_{C_1C_2}$, but is does *not* include quasi-saturation. In this way we do not need the charge $\Delta Q_{\rm sat}$ that was introduced in Mextram 503 as a bug fix [39] (see also the report [14]). The difference between the three biases will become more clear as we go along.

Velocity saturation The drift velocity of carriers is given by the product of the mobility and the electric field. The mobility of the electrons itself, however, also depends on the electric field. It has a low field value μ_{n0}, such that the low-field drift velocity equals $v = \mu_{n0}\,E$. At high electric fields, however, this velocity saturates. the maximum value given by the saturation velocity $v_{\rm sat}$. A simple equation that can be used to describe this effect is

$$\mu_n = \frac{\mu_{n0}}{1+\mu_{n0}E/v_{\rm sat}}; \qquad v = \mu_n E = \frac{\mu_{n0}E}{1+\mu_{n0}E/v_{\rm sat}}. \tag{3.2}$$

As one can see there is a cross-over from $v = \mu_{n0}E$ for small electric fields to $v = v_{\rm sat}$ for large electric fields. This cross-over happens at the critical electric field defined by

$$E_c = \frac{v_{\rm sat}}{\mu_{n0}}. \tag{3.3}$$

Typical vales for Si are $v_{\rm sat} = 1.07 \cdot 10^7\,{\rm cm/s}$, $\mu_{n0} = 1.0 \cdot 10^3\,{\rm cm^2/Vs}$ and $E_c = 7 \cdot 10^3\,{\rm V/cm}$.

The current In normal forward mode electrons move from base to collector, i.e. in positive x-direction. The current density $J_{\rm epi}$ is then negative, due to the negative charge of electrons. The current $I_{\rm epi}$ itself, however, is generally defined as going from collector to emitter, via the base, and is positive in forward mode. We therefore write

$$I_{\rm epi} = -A_{\rm em}\,J_{\rm epi} \tag{3.4}$$

just as we did for the main current through the base in Chapter 2.

The electric field As mentioned before, the electric field in the epilayer is important. The basic description of the electric field is the same as that in a simple pn-junction. In the epilayer (of an NPN) it is negative (which means we must be careful with some minus-signs). According to general pn-junction theory, the integral of the electric field from node B_2 to node C_1 equals the applied voltage $\mathcal{V}_{\rm C_1B_2}$ plus the built-in voltage $\mathsf{V_{dC}}$:

$$-\int_{B_2}^{C_1} E(x){\rm d}x = -\int_0^{W_{\rm epi}} E(x){\rm d}x = \mathcal{V}_{\rm C_1B_2} + \mathsf{V_{dC}}. \tag{3.5}$$

Here we assumed that the electric field in the base and in the highly doped collector drops very fast to zero, such that the contribution to the integral only comes from the region $0 < x < W_{\mathrm{epi}}$.

Equation (3.5) is an important limitation on the electric field. It is in itself not enough to find the electric field. To this end we need Gauss' law

$$\frac{\mathrm{d}E}{\mathrm{d}x} = \frac{\rho}{\varepsilon}. \tag{3.6}$$

Here ρ is the total charge density, given by

$$\rho = q(N_{\mathrm{epi}} - n + p). \tag{3.7}$$

Consider now the electric field in an ohmic region. It is constant and has the value

$$E = \frac{J_{\mathrm{epi}}}{\sigma} = -\frac{I_{\mathrm{epi}}}{\sigma A_{\mathrm{em}}}. \tag{3.8}$$

Here σ is the conductivity. The electric field is negative, as mentioned before. In ohmic regions the electric field is low enough to prevent velocity saturation. The net charge is zero and the number of electrons equals the dope N_{epi}. A negligible number of holes are present. The ohmic resistance of the epilayer can then be calculated and is given by the parameter $\mathsf{R}_{\mathsf{Cv}} = W_{\mathrm{epi}}/q\mu_n A_{\mathrm{em}} N_{\mathrm{epi}}$.

Next we consider the depletion regions. In these regions the electric field will be high. Hence we can assume that the velocity of electrons is saturated. There will be no holes in these regions either. The electron density however depends on the current density. Since the electron velocity is constant we have $n = |J_{\mathrm{epi}}|/v_{\mathrm{sat}}$. The total net charge is then given by a sum of the dope and the charge density resulting from the current: $\rho = qN_{\mathrm{epi}} - |J_{\mathrm{epi}}|/v_{\mathrm{sat}}$. For the charge density it does not matter whether the current moves forth or back. This gives us

$$\frac{\mathrm{d}E}{\mathrm{d}x} = \frac{qN_{\mathrm{epi}}}{\varepsilon}\left(1 - \frac{I_{\mathrm{epi}}}{\mathsf{I}_{\mathsf{hc}}}\right), \tag{3.9}$$

where we defined the hot-carrier current $\mathsf{I}_{\mathsf{hc}} = qN_{\mathrm{epi}}A_{\mathrm{em}}v_{\mathrm{sat}}$. When the epi-layer current equals the hot-carrier current the total charge in that part of the epilayer will vanish. We still call these regions depleted, since the electrons still move with v_{sat}, in contrast to the ohmic regions.

For currents larger than the hot-carrier current the derivative of the electric field will be negative. There will still be a voltage drop over the epilayer. This voltage drop, however, is no longer ohmic, but space-charge limited. The corresponding resistance of the epilayer is now given by the Space-Charge Resistance $\mathsf{SCR}_{\mathsf{Cv}}$. We will discuss this in more detail below.

Let us consider the current dependence of the electric field distribution in some more detail, for both cases discussed above. At low current density (i.e. before quasi-saturation

 ©Koninklijke Philips Electronics N.V. 2005

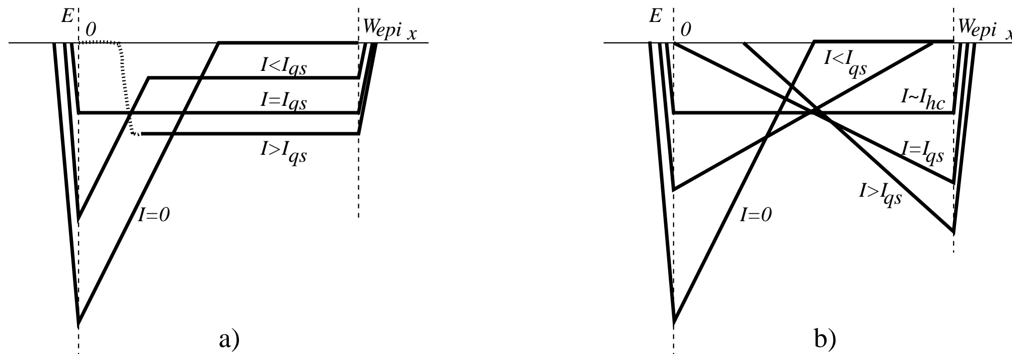

Figure 7: *Figure describing the electric field in the epilayer as function of current. In a) the width of the depletion layer decreases because ohmic voltage drop is the dominant effect. In b) the width of the depletion layer increases because velocity saturation is dominant (Kirk effect). At* $I = I_{qs}$ *quasi-saturation starts (see text).*

defined below) the electric field in the epilayer is similar to that of a diode in reverse bias. Next to the base we have a depletion region. This region is followed by an ohmic region. When the current increases the width of the depletion layer changes. There are two competing effects that make that this width either increases or decreases. The precise dependence of the thickness of the depletion layer on the current is given in Eq. (3.68), but here we will discuss both effects quantitatively.

We know that the bias over the depletion region itself is given by the bias $\mathcal{V}_{\mathrm{C_1B_2}}$ minus the ohmic potential drop. Hence when the ohmic region is large the intrinsic junction potential will decrease with current, and so will the depletion region width. This is schematically shown in Fig. 7a). At some point the depletion layer thickness vanishes, and the whole electric field is used for the ohmic voltage drop. Since at higher currents we still need to fulfil Eq. (3.5) the electric field becomes smaller close to the base. This is possible because holes get injected into the epilayer, which reduces the resistance in the region next to the base. This effect, quasi-saturation, will be discussed in more detail later.

The other effect that has an influence on the width of the electric field is velocity saturation. As can be seen from Eq. (3.9), the slope of the electric field decreases with increasing current. This means that to keep the total integral over the electric field constant, as in Eq. (3.5), the width of the depletion layer must increase. This is schematically shown in Fig. 7b). With increasing current the depletion width will continue to increase, until it reaches the highly doped collector. For even higher currents the total epilayer will be depleted. The slope of the electric field still decreases and can change sign. At some level of current the value of the electric field at the base-epilayer junction drops beneath the critical field E_c for velocity saturation and holes get injected into the epilayer. As before, at this point high injection effects in the epilayer start to play a role. This is again the regime of quasi-saturation. When quasi-saturation is due to a voltage drop as a result of the reversal of the slope of the electric field, the effect is better known as the Kirk effect.

Note that in both cases described above a situation occurs where the electric field is (approximately) flat over the whole epilayer, as shown in Fig. 7. In the ohmic case this will

©Koninklijke Philips Electronics N.V. 2005

happen at much smaller electric field (and therefore collector-base bias) than in the case of space charge dominated resistance (Kirk effect).

Quasi-saturation Consider the normal forward operating regime. The (external) base collector bias will be negative: $\mathcal{V}_{\mathrm{B_2C_1}} < 0$. The epilayer, however, has some resistance, which can either be ohmic, or space charge limited, as discussed above. As a result the internal base-collector bias, in our model given by $V^*_{B_2C_2}$, is less negative than the external bias. For large enough currents, it even becomes forward biased. This also means that the carrier densities at the base-collector interface increase. At some point, to be more precise when $V^*_{B_2C_2} \simeq \mathsf{V_{dC}}$, these carrier densities become comparable to the background doping. From there on high-injection effects in the epilayer become important. This is the regime of quasi-saturation. Note that we use the term quasi-saturation when the voltage drop is due to an ohmic resistance, but also when it is due to a space-charge limited resistance, in which case the effect is also known as Kirk effect.

For our description the current at which quasi-saturation starts, I_{qs}, is very important. So let us consider it in more detail. As mentioned before, quasi-saturation starts when $V^*_{B_2C_2} = \mathsf{V_{dC}}$. In that case we can express the integral over the electric field in terms of V_{qs}, the potential drop over the epilayer, using Eq. (3.5):

$$V_{qs} = \mathsf{V_{dC}} - \mathcal{V}_{\mathrm{B_2C_1}} = -\int_0^{W_{\mathrm{epi}}} E(x)\mathrm{d}x. \tag{3.10}$$

So, at the onset of quasi-saturation the integral over the electric field is fixed by the external base-collector bias, and does no longer depend on the current. We can then use the relation between the electric field and the current to determine the current I_{qs}. In the ohmic case the electric field is constant over the epilayer. The voltage drop is simply the ohmic voltage drop and we can write

$$I_{qs} = V_{qs}/\mathsf{R_{Cv}}. \tag{3.11}$$

For higher currents the electric field is no longer constant, due to the net charge present in the epilayer. Its derivative is given by Eq. (3.9) and depends on the current. The current at onset of quasi-saturation can still be given as V_{qs} over some effective resistance:

$$I_{qs} = V_{qs}/\mathsf{SCR_{Cv}}, \tag{3.12}$$

as will be shown in Section 3.3.3. The effective resistance $\mathsf{SCR_{Cv}}$ is the space-charge resistance introduced above.

When the (internal) base-collector is forward biased, as in quasi-saturation, holes from the base will be injected in the epilayer. Charge neutrality is maintained in this injection layer, so also the electron density will increase. As we noted already in the description of the main current, at high injection the hole and electron densities will have a linear profile. This linear profile in the base is now continued into the epilayer. The width of the base has effectively become wider, from the base-emitter junction to the end of the injection

 ©Koninklijke Philips Electronics N.V. 2005

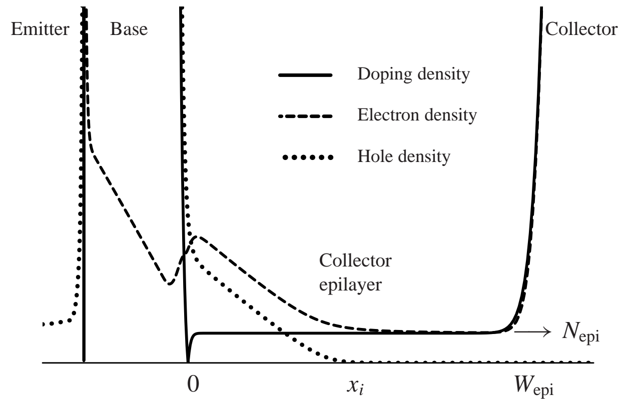

Figure 8: *Schematic view of the doping, electron and hole densities in the base-collector region (on an arbitrary linear scale), in the case of base push-out/quasi-saturation. It also shows the thickness of the epilayer* W_{epi} *and the injection layer* x_i*. From Refs. [36, 38].*

region in the epilayer. This is known as base push-out and is shown in Fig. 8. It decreases transistor performance considerably. As an example we show the output characteristics in Fig. 9. Note that in the Spice-Gummel-Poon model quasi-saturation is not modelled. The reduction of the current as modelled by Mextram shows the effect.

It is important to note that although the hole density profile and the electron density profile are similar, only the electrons carry current. The electric field and the density gradient work together to move the electrons. However for the holes they act opposite and create an equilibrium. This equilibrium will be used to determine the electric field (which will be considerably below the critical electric field E_c), as is being done in the Kull model. Also the electron current in the injection region will in Mextram be described by the Kull model.

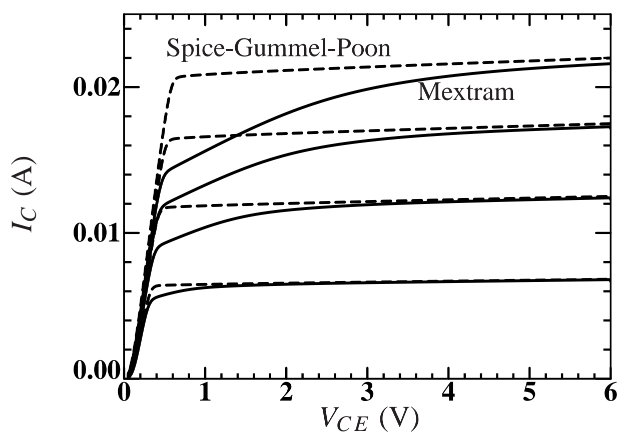

Figure 9: *The output characteristics for both the Spice-Gummel-Poon model and the Mextram model. From Refs. [36, 38].*

©Koninklijke Philips Electronics N.V. 2005

3.3 The epilayer current

We start with the description of the epilayer current $I_{\rm epi}$. We do this for a one-dimensional transistor. First we describe the Kull model, which in Mextram is used to calculate $I_{C_1C_2}(= I_{\rm epi})$ from the node voltage $\mathcal{V}_{\rm B_2C_2}$. As discussed before, $\mathcal{V}_{\rm B_2C_2}$ is not the physical quantity we can use for further calculations. We therefore need to calculate $V^*_{B_2C_2}$, which is more physical, from the current. We start with the ohmic case and after that introduce velocity saturation. Then we consider the reverse behaviour and the situation around $I_{\rm epi} = 0$. Finally we consider what happens in a real transistor where current spreading plays a role.

3.3.1 The Kull model (without velocity saturation)

The Kull model [19] is an important part of our epilayer model. The model can be used in those parts of the epilayer that have a neutral charge (we will discuss velocity saturation of the Kull model later):

$$n = N_{\rm epi} + p. \tag{3.13}$$

This means that it can be used in the injection regions and in the ohmic regions. It is important to realise that this assumption is only valid as long as the electric field, or rather its derivative, is small enough. In device simulations (even without velocity saturation) small deviations from neutrality can be observed. Here we will neglect this.

Following Kull we assume that there is no recombination and therefore no hole current in the epilayer:

$$J_p = 0 \tag{3.14}$$

Hence the hole quasi-Fermi level φ_p is constant. It equals the base potential $\mathcal{V}_{\rm B_2}$. That it is indeed constant has been checked by numerical simulation by Kull [19]. The product of hole and electron density in the epilayer is then given by the local collector potential $\mathcal{V}_{\rm C_x}$, which we take equal to the local electron quasi-Fermi level $\varphi_n(x)$. We can then write

$$p(x)\, n(x) = n_i^2 \exp[-(V_{C_x} - \mathcal{V}_{\rm B_2})/V_T]. \tag{3.15}$$

For our calculations we need a parameter that describes the epilayer doping $N_{\rm epi}$, or rather the ratio $N_{\rm epi}/n_i$. For this purpose we will use

$$\mathsf{V}_{\mathsf{dC}} = V_T \ln \frac{N_{\rm epi}^2}{n_i^2}. \tag{3.16}$$

This same voltage is also used in the calculations for the depletion charges, where it acts as the built-in voltage. Normally one would write for this built-in voltage $V_{\rm bi}$ =

 ©Koninklijke Philips Electronics N.V. 2005

$V_T \ln(N_{\rm epi} N_A / n_i^2)$, where N_A is the dope of the base close to the epilayer. This effective base doping is often not known. Furthermore, for the calculation of the depletion charges the relative small difference between $V_{\rm bi}$ and $\mathsf{V}_{\mathsf{d_C}}$ can be neglected. Hence we can suffice with only one parameter: $\mathsf{V}_{\mathsf{d_C}}$.

Next we normalise the hole charge densities to the doping level and write

$$p_x = \frac{p(x)}{N_{\rm epi}}, \qquad n_x = \frac{n(x)}{N_{\rm epi}}. \tag{3.17}$$

Since we assumed quasi-neutrality we can write $n_x = p_x + 1$.

Using Eq. (3.16) we can now express the hole charge densities p_0 and p_W at both ends of the epilayer in terms of the node voltages

$$p_0(p_0 + 1) = \exp[(\mathcal{V}_{\rm B_2C_2} - \mathsf{V}_{\mathsf{d_C}})/V_T], \tag{3.18a}$$
$$p_W(p_W + 1) = \exp[(\mathcal{V}_{\rm B_2C_1} - \mathsf{V}_{\mathsf{d_C}})/V_T]. \tag{3.18b}$$

Following Kull, we introduce

$$K_x = \sqrt{1 + 4\exp[(V_{B_2C_x} - \mathsf{V}_{\mathsf{d_C}})/V_T]} = 2p_x + 1. \tag{3.19}$$

This gives us also the values K_0 and K_W at the base-epilayer junction and at the interface with the buried layer.

The derivation of the Kull model [19] is now simple. We start with the basic equations (1.5) for the electron and hole current:

$$J_n = q\mu_n \left(nE(x) + V_T \frac{\mathrm{d}n}{\mathrm{d}x} \right), \tag{3.20a}$$
$$J_p = q\mu_p \left(pE(x) - V_T \frac{\mathrm{d}p}{\mathrm{d}x} \right), \tag{3.20b}$$

where we already used the Einstein relation. From Eqs. (3.14) and (3.20b) we see that the hole density in the epilayer must be such that there is an equilibrium between the diffusion term and the drift term. This gives a relation for the electric field:

$$E(x) = V_T \, \frac{1}{p} \, \frac{\mathrm{d}p}{\mathrm{d}x}. \tag{3.21}$$

Using this electric field in the expression for the electron current and using charge neutrality we get an equation for the electron current density in terms of the hole density:

$$J_n = q\mu_n V_T \left(\frac{n}{p} \, \frac{\mathrm{d}p}{\mathrm{d}x} + \frac{\mathrm{d}n}{\mathrm{d}x} \right) = q\mu_n V_T \left(2 + \frac{N_{\rm epi}}{p} \right) \, \frac{\mathrm{d}p}{\mathrm{d}x}. \tag{3.22}$$

The current density in our one-dimensional model is constant. As mentioned before it is given by $J_n = -I_{\rm epi}/A_{\rm em}$. We can simply integrate the equation for J_n from $x = x_1$ to $x = x_2$ and find

$$I_{\rm epi} = \frac{q\mu_{n0} V_T N_{\rm epi} A_{\rm em}}{x_2 - x_1}\left(2p_{x_1} - 2p_{x_2} + \ln\frac{p_{x_1}}{p_{x_2}}\right), \tag{3.23}$$

where we used that for the low fields we consider here $\mu_n = \mu_{n0}$. Next we can use that

$$2p_x = K_x - 1 = \frac{K_x^2 - 1}{K_x + 1} = \frac{4\exp[(V_{B_2C_x} - \mathsf{V_{dC}})/V_T]}{K_x + 1}. \tag{3.24}$$

The collector current can then be rewritten to

$$I_{\rm epi} = \frac{W_{\rm epi}}{x_2 - x_1}\frac{E_{x_2x_1} + V_{x_2x_1}}{\mathsf{R_{Cv}}}, \tag{3.25a}$$

$$E_{x_2x_1} = V_T\left(K_{x_1} - K_{x_2} - \ln\frac{K_{x_1} + 1}{K_{x_2} + 1}\right), \tag{3.25b}$$

where we defined the resistance of the epilayer $\mathsf{R_{Cv}} = W_{\rm epi}/q\mu_{n0}N_{\rm epi}A_{\rm em}$. This result is very general in the sense that it holds for all x_1 and x_2 (in the neutral region). Substituting $x_1 = 0$, which is at the location of node C_2, and $x_2 = W_{\rm epi}$ at node C_1, we get Kull's result (without velocity saturation):

$\mathbf{I_{C_1C_2}}$

$$I_{C_1C_2} = I_{\rm epi} = \frac{E_C + \mathcal{V}_{\rm C_1C_2}}{\mathsf{R_{Cv}}}, \tag{3.26a}$$

$$E_C = V_T\left(K_0 - K_W - \ln\frac{K_0 + 1}{K_W + 1}\right). \tag{3.26b}$$

When no high injection effects occur, K_0 and K_W are very close to 1, E_C is very small and the epilayer current is given by $I_{\rm epi} = \mathcal{V}_{\rm C_1C_2}/\mathsf{R_{Cv}}$. This is just ohmic behaviour with a resistance given by the parameter $\mathsf{R_{Cv}}$.

Equation (3.26) for the collector current is used in Mextram for the calculation of the current as function of the node potential $\mathcal{V}_{\rm B_2C_2}$ (and $\mathcal{V}_{\rm B_2C_1}$), both in forward and in reverse. The rest of the model, at least in forward mode, is expressed in terms of this current (and again $\mathcal{V}_{\rm B_2C_1}$). For the forward mode of operation we could have taken any other expression to calculate the current from $\mathcal{V}_{\rm B_2C_2}$. The Kull model is used because we use it in reverse, which simplifies the implementation.

Note that later on the Kull model Eq. (3.25) between $x_1 = 0$ and $x_2 = x_i$, the end of the injection layer, will be used again to calculate the hole concentration p_0^* at the base-collector junction.

The thickness of the injection region in the Kull model Before we discuss the Mextram formulation, let us first analyse the Kull model somewhat more. In Fig. 8 we have

 ©Koninklijke Philips Electronics N.V. 2005

already shown on a linear scale the electron and hole densities in the collector epilayer, in the case of quasi-saturation. We can see that the epilayer consists of two parts. The first part, between $x = 0$ and x_i, is the injection region where the hole density is comparable to the electron density. The second part, between $x = x_i$ and W_{epi}, is the ohmic region where the hole density is negligible. At the point $x = x_i$, the difference between hole and electron quasi-Fermi levels is approximately $\mathcal{V}_{\mathrm{B_2C_{x_i}}} \simeq \mathsf{V_{dC}}$. We will use this observation in the following.

Within the framework of the Kull model we can calculate the thickness of the injection region x_i. Since the voltage drop over the injection region is small, the voltage drop over the ohmic region is almost equal to the total voltage drop. For a constant doping profile the resistance of the non-injected region is proportional to its length, and we can write

$$\mathcal{V}_{\mathrm{C_1C_2}} = \mathcal{V}_{\mathrm{B_2C_2}} - \mathcal{V}_{\mathrm{B_2C_1}} = I_{\mathrm{epi}}\ \mathsf{R_{Cv}}\ \left(1 - x_i/W_{\mathrm{epi}}\right). \tag{3.27}$$

By using $\mathcal{V}_{\mathrm{B_2C_2}}$ here instead of $\mathsf{V_{dC}}$ the relation also holds for low current densities ($x_i \rightarrow 0$). We show x_i/W_{epi} as function of current in Fig. 10 (dashed line).

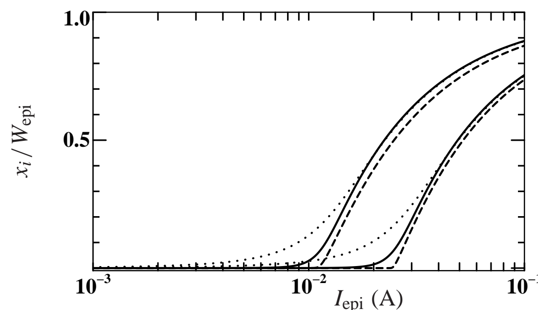

Figure 10: *The normalised thickness of the injection region x_i/W_{epi} as function of the current I_{epi} for $\mathcal{V}_{\mathrm{B_2C_1}} = -1,\ -3\,\mathrm{V}$. Dashed line: Kull model Eq. (3.28). Solid line ($\mathsf{a_{xi}} = 0.1$) and dotted line ($\mathsf{a_{xi}} = 0.3$): our model Eq. (3.31). From Refs. [36, 38].*

From Fig. 10 we observe that the Kull model has an abrupt onset of injection (this is the point where x_i/W_{epi} starts to rise). This abrupt transition between the two operating regimes leads to poor modelling of the higher derivatives of the current. This can, for instance, be observed in low-frequency distortion analysis. Hence in Mextram we take another approach, discussed below, in which the injection thickness is calculated using the current I_{epi}, and not using the potential $\mathcal{V}_{\mathrm{B_2C_2}}$.

3.3.2 The Mextram model without velocity saturation

We consider two parts in the epilayer: the injection region and the non-injected region. Since by far most of the voltage drop is in the second region, we can use the equations for the electric field to determine how wide it is, thereby calculating the thickness of the injection region x_i. Then, using a slight modification of the Kull model, we can calculate the intrinsic junction bias $V^*_{B_2C_2}$ from this thickness.

The thickness of the injection region First we calculate x_i, the thickness of the injection region. When there is injection ($x_i > 0$) we can express this thickness as

$$\frac{x_i}{W_{\text{epi}}} = 1 - \frac{\mathsf{V_{d_C}} - \mathcal{V}_{\text{B}_2\text{C}_1}}{I_{\text{epi}}\ \mathsf{R_{Cv}}}. \tag{3.28}$$

We can use this equation to determine the current I_{qs} discussed before, at which quasi-saturation starts, by simply putting $x_i = 0$. This results in

$$I_{qs} = \frac{\mathsf{V_{d_C}} - \mathcal{V}_{\text{B}_2\text{C}_1}}{\mathsf{R_{Cv}}}. \tag{3.29}$$

We can now express the thickness of the injection region as function of current and this I_{qs} as

$$\frac{x_i}{W_{\text{epi}}} = \begin{cases} 1 - I_{qs}/I_{\text{epi}}, & \text{for } I_{\text{epi}} > I_{qs}, \\ 0, & \text{for } I_{\text{epi}} < I_{qs}. \end{cases} \tag{3.30}$$

For our compact model we must of course create a smooth transition between both cases. To do this we replace Eq. (3.30) by

$$\frac{x_i}{W_{\text{epi}}} = 1 - \frac{I_{qs}}{\tilde{I}_{\text{epi}}}, \tag{3.31}$$

where

$$\tilde{I}_{\text{epi}} = I_{qs}\ \frac{1 + \mathsf{a_{xi}}\ \ln\{1 + \exp[(I_{\text{epi}}/I_{qs} - 1)/\mathsf{a_{xi}}]\}}{1 + \mathsf{a_{xi}}\ \ln\{1 + \exp[-1/\mathsf{a_{xi}}]\}}. \tag{3.32}$$

Note that $\tilde{I}_{\text{epi}}$ is always larger than I_{qs}, unless $I_{\text{epi}} = 0$ in which case $\tilde{I}_{\text{epi}} = I_{qs}$. This assures a non-negative x_i. When $I_{\text{epi}} \gg I_{qs}$ we have approximately $\tilde{I}_{\text{epi}} \simeq I_{\text{epi}}$, as desired. The parameter $\mathsf{a_{xi}}$ has a smoothing purpose. From Eqs. (3.29) and (3.31) we have

$$\tilde{I}_{\text{epi}} = \frac{\mathsf{V_{d_C}} - \mathcal{V}_{\text{B}_2\text{C}_1}}{\mathsf{R_{Cv}}\ (1 - x_i/W_{\text{epi}})}, \tag{3.33}$$

a relation we state here for later reference.

The internal base-collector bias Next we need to calculate the internal base-collector bias via the hole density p_0. To prevent ambiguity, we denote the hole density calculated using the current and the thickness of the injection layer as p_0^*, in contrast to p_0 as calculated from Eq. (3.18). In this way p_0 is directly related to $\mathcal{V}_{\text{B}_2\text{C}_2}$, which we will not use anymore, whereas p_0^* is in exactly the same way related to $V^*_{B_2C_2}$.

To calculate p_0^* we need a description of the collector epilayer between $x = 0$ and $x = x_i$. In this injection region the electric field is low, and we do not need to take velocity

 ©Koninklijke Philips Electronics N.V. 2005

saturation into account. Hence we can suffice with the expression used in the Kull model, Section 3.3.1. We combine Eqs. (3.26) and (3.27) to get

$$\frac{x_i}{W_{\text{epi}}}\, I_{\text{epi}}\, \mathsf{R}_{\mathsf{Cv}} = E_C = V_T\left[2p_0^* - 2p_W - \ln\left(\frac{1+p_0^*}{1+p_W}\right)\right], \tag{3.34}$$

where the right-hand side is E_C expressed in terms of the hole densities p_0^* and p_W. From this equation we can not calculate p_0^* directly, since the equation does not yield an explicit expression for p_0^*. We therefore approximate the equation above with

$$\frac{x_i}{W_{\text{epi}}}\, I_{\text{epi}}\, \mathsf{R}_{\mathsf{Cv}} = 2\, V_T\, (p_0^* - p_W)\, \frac{p_0^* + p_W + 1}{p_0^* + p_W + 2}. \tag{3.35}$$

The approximation for E_C we just made does not differ more than 5% from the original equation for E_C over the whole range of p_0^* and p_W values. Using the second order equation (3.35) we can now calculate p_0^* from p_W, I_{epi} and x_i/W_{epi}. The internal base-collector bias can be found from Eq. (3.18):

$$V^*_{B_2C_2} = \mathsf{V}_{\mathsf{dC}} + V_T \ln[p_0^*\,(p_0^* + 1)]. \tag{3.36}$$

3.3.3 The Mextram model with velocity saturation

The equations we presented above hold only when velocity saturation in the epilayer does not play a role. We will now include this in our description. As mentioned before, for low electric field the drift velocity of the electrons is proportional to the electric field: $v = \mu_n\, E$. For higher electric fields the velocity saturates and has as a maximum the saturated drift velocity v_{sat}. We can estimate the currents for which velocity saturation becomes important by considering the ohmic region (which has a constant electric field), and calculating when the the drift velocity becomes equal to the saturated drift velocity. The current that we find is the hot-carrier current introduced before:

$$\mathsf{I}_{\mathsf{hc}} = q N_{\text{epi}} A_{\text{em}} v_{\text{sat}}. \tag{3.37}$$

For epilayer currents of the order of I_{hc} or higher velocity saturation effects need to be included.

In the original Kull model [19] velocity saturation is included, under the assumption, however, that the epilayer is quasi-neutral throughout. When velocity saturation is important, this assumption does no longer hold, as we will show. Therefore the velocity saturation part of the Kull model is insufficient and therefore can not be used to describe velocity saturation effects, including the Kirk effect, which is important in many modern technologies.

At a current I_{hc} the amount of electrons needed to sustain this current, assuming they are travelling at v_{sat}, is equal to the doping level. For even higher currents (or lower effective velocity) the electron concentration is even higher. These electrons have a negative

charge, whereas the doping atoms provide a positive background charge. The net charge will be no longer negligible. With increasing current the net charge will become negative. This has an effect on the electric field: it will not be constant anymore. Consequently, once velocity saturation needs to be taken into account ($I_{epi} \gtrsim \mathsf{I_{hc}}$), the assumption of quasi-neutrality (and of a constant electric field) no longer holds. The net charge in the epilayer will eventually lead to the Kirk effect (also a form of quasi-saturation).

The thickness of the injection region To include velocity saturation in our description we will start with considering a very high current. Our approach is based on the same principles as those of Ref. [33]. As before we consider the region without injection to calculate the thickness of the injection layer. We start with Eqs. (3.9) and (3.10), which we repeat for clarity:

$$\frac{\mathrm{d}E}{\mathrm{d}x} = \frac{q N_{epi}}{\varepsilon} \left(1 - \frac{I_{epi}}{\mathsf{I_{hc}}}\right), \tag{3.38a}$$

$$\int_{x_i}^{W_{epi}} E \, \mathrm{d}x = \mathcal{V}_{B_2C_1} - \mathsf{V_{dC}}. \tag{3.38b}$$

Because of the high carrier concentration and hence the low resistance, the electric field in the injection region can be neglected. As a boundary condition we therefore use that the electric field at the end of the injection region is just the critical electric field, see Eq. (3.3), needed for velocity saturation:

$$E(x_i) = -v_{sat}/\mu_{n0} = -\mathsf{I_{hc}}\, \mathsf{R_{Cv}}/W_{epi}, \tag{3.39}$$

where we used the low-field mobility. After a double integration of Eq. (3.38a) and using Eq. (3.38b) we get

$$\mathsf{V_{dC}} - \mathcal{V}_{B_2C_1} = \mathsf{I_{hc}}\, \mathsf{R_{Cv}} \left(1 - \frac{x_i}{W_{epi}}\right) + (I_{epi} - \mathsf{I_{hc}})\, \mathsf{SCR_{Cv}} \left(1 - \frac{x_i}{W_{epi}}\right)^2. \tag{3.40}$$

Here $\mathsf{SCR_{Cv}} = W_{epi}^2/2\varepsilon v_{sat} A_{em}$ is the space-charge resistance of the epilayer, i.e. the effective resistance of a region dominated by a current whose charge is not compensated by a background charge.

Equation (3.40) is similar to Eq. (3.27) (of course with $\mathcal{V}_{B_2C_2} \to \mathsf{V_{dC}}$) for the ohmic case. Now, however, we have described quasi-saturation due to the Kirk effect instead of due to an ohmic voltage drop. In both cases we have a similar base-widening ($x_i > 0$) and injection of holes into the epilayer.

Interpolation between the two cases We have to find an interpolation between the two cases of ohmic resistance and space charge resistance. We can use the same interpolation that has been used in Ref. [33, Eq. (19)]. When we look at Eqs. (3.27) and (3.40) we

 ©Koninklijke Philips Electronics N.V. 2005

see that the latter transforms into the former when we let $\mathsf{I_{hc}} \to I_{\mathrm{epi}}$. So we find our interpolation by replacing $\mathsf{I_{hc}}$ in Eq. (3.40) by

$$I_{\mathrm{low}} = \frac{\mathsf{I_{hc}}\, I_{\Omega}}{\mathsf{I_{hc}} + I_{\Omega}}, \tag{3.41}$$

where we defined, conform Eq. (3.33), the current that would be running in the ohmic case:

$$I_{\Omega} = \frac{\mathsf{V_{dC}} - \mathcal{V}_{\mathrm{B_2C_1}}}{\mathsf{R_{Cv}}\,(1 - x_i\,/\,W_{\mathrm{epi}})}. \tag{3.42}$$

The current I_{low} will go to I_{epi} for low voltages over the epilayer. For high voltages over the epilayer I_{low} will go to $\mathsf{I_{hc}}$. The final result is found by substituting Eqs. (3.41) and (3.42) into Eq. (3.40) and solving for I_{epi}. It gives a relation between I_{epi} and $x_i\,/\,W_{\mathrm{epi}}$:

$$I_{\mathrm{epi}} = \frac{\mathsf{V_{dC}} - \mathcal{V}_{\mathrm{B_2C_1}}}{\mathsf{SCR_{Cv}}\; y_i^2}\; \frac{\mathsf{V_{dC}} - \mathcal{V}_{\mathrm{B_2C_1}} + \mathsf{I_{hc}}\;\mathsf{SCR_{Cv}}\; y_i^2}{\mathsf{V_{dC}} - \mathcal{V}_{\mathrm{B_2C_1}} + \mathsf{I_{hc}}\;\mathsf{R_{Cv}}\; y_i}, \tag{3.43}$$

where we abbreviated

$$y_i = \left(1 - \frac{x_i}{W_{\mathrm{epi}}}\right). \tag{3.44}$$

Equation (3.43) can, as before, only be used for epilayer currents larger than I_{qs}, the current at the onset of injection, because it assumes that the local bias at the junction reaches at least $\mathsf{V_{dC}}$. The current I_{qs} can be determined by putting $x_i = 0$ in the expression (3.43) above, which gives us

$$I_{qs} = \frac{\mathsf{V_{dC}} - \mathcal{V}_{\mathrm{B_2C_1}}}{\mathsf{SCR_{Cv}}}\; \frac{\mathsf{V_{dC}} - \mathcal{V}_{\mathrm{B_2C_1}} + \mathsf{I_{hc}}\;\mathsf{SCR_{Cv}}}{\mathsf{V_{dC}} - \mathcal{V}_{\mathrm{B_2C_1}} + \mathsf{I_{hc}}\;\mathsf{R_{Cv}}}. \tag{3.45}$$

In Fig. 11 we have shown I_{qs} as function of $V_{qs} = \mathsf{V_{dC}} - \mathcal{V}_{\mathrm{B_2C_1}}$. In Appendix B we compare our approximation with an analytical expression, which is too complicated to use, and see that both have a comparable behaviour.

Next we follow the same procedure as we did for the ohmic case. Now that we have I_{qs}, we use Eq. (3.32) again for the definition of the current $\tilde{I}_{\mathrm{epi}}$. We then replace I_{epi} in Eq. (3.43) by $\tilde{I}_{\mathrm{epi}}$. This leads to a third order equation for y_i. This equation can be solved and an explicit formula can be given. However, we have found that we can simplify it to a second order equation without loss of accuracy. This is much easier for the implementation in a circuit simulator. Finally we then find the following equation

$$\tilde{I}_{\mathrm{epi}} = \frac{\mathsf{V_{dC}} - \mathcal{V}_{\mathrm{B_2C_1}}}{\mathsf{SCR_{Cv}}\; y_i^2}\; \frac{\mathsf{V_{dC}} - \mathcal{V}_{\mathrm{B_2C_1}} + \mathsf{I_{hc}}\;\mathsf{SCR_{Cv}}\; y_i}{\mathsf{V_{dC}} - \mathcal{V}_{\mathrm{B_2C_1}} + \mathsf{I_{hc}}\;\mathsf{R_{Cv}}}. \tag{3.46}$$

©Koninklijke Philips Electronics N.V. 2005

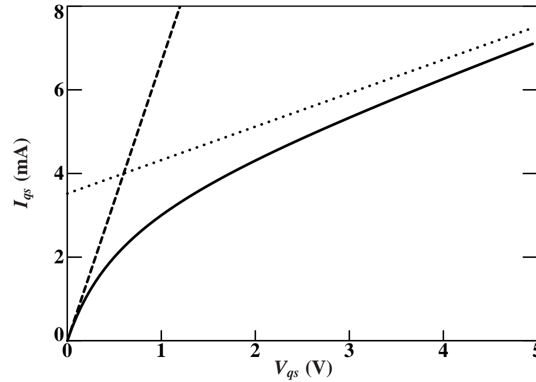

Figure 11: *The current at onset of injection as function of the applied voltage* $V_{qs} = \mathsf{V_{d_C}} - \mathcal{V}_{\mathrm{B_2C_1}}$ *for the default parameter set [1]. We have also shown the two limiting cases, that intersect exactly at* $\mathsf{I_{hc}}$*, which here equals* 4 mA.

From this equation we solve y_i (or x_i).

Note that in the limit $\mathsf{I_{hc}} \to \infty$ we get the ohmic result back from the previous section. In the other limit, $\mathsf{I_{hc}} \to 0$, we get $\tilde{I}_{\mathrm{epi}} = (\mathsf{V_{d_C}} - \mathcal{V}_{\mathrm{B_2C_1}})/[\mathsf{SCR_{Cv}}\ (1 - x_i/W_{\mathrm{epi}})^2]$. The relation between the current and the thickness of the injection region is now quadratic, instead of linear as in Eq. (3.33).

The internal base-collector bias Just as we did in our model without velocity saturation, Section 3.3.2, we now calculate the internal base-collector bias $V^*_{B_2C_2}$ from the description of the epilayer between $x = 0$ and $x = x_i$. As before we can suffice with the Kull model in this region, because in the injection region the electric field is low and we do not need to take velocity saturation into account. Hence, using the thickness x_i we calculate p_0 from Eq. (3.35) and the internal base-collector bias $V^*_{B_2C_2}$ from Eq. (3.36).

3.3.4 Current spreading

The derivation we have given above contains the same physics as the Kull model [19] for the ohmic case or the Mextram 503 model [33, 37] when including velocity saturation. Up to now it is a one-dimensional model. To take current spreading into account the most important change is due to the fact that the three high current parameters $\mathsf{R_{Cv}}$, $\mathsf{SCR_{Cv}}$ and $\mathsf{I_{hc}}$ no longer have their one-dimensional value. Instead they get an effective value. This effective value depends on the actual size of the emitter region in relation to the epilayer thickness. In Ref. [33] an example is given of the scaling of the high-current equations with geometry. We will discuss this again in Chapter 11.

The next concern is a change in current spreading as function of bias, or as function of the current through the epilayer. In principle this could be included. In [33, Eq. (27)] it was shown that this can be done by replacing $\mathsf{SCR_{Cv}}$ by $\mathsf{SCR_{Cv}}/(1 + S_F\, x_i/W_{\mathrm{epi}})$, with S_F a spreading parameter. We observed that in practice the current spreading as function of the epilayer current is of minor importance. Including it would mean solving a third

 ©Koninklijke Philips Electronics N.V. 2005

order equation for y_i, something which we do not want (for numerical reasons), if it can be prevented. We therefore did not include this extra feature in our model.

3.3.5 Reverse behaviour

The reverse behaviour is very simple. The current is given by Eq. (3.26). Since in reverse there are no velocity saturation effects we can safely take $V^*_{B_2C_2} = \mathcal{V}_{\mathrm{B_2C_2}}$. The expression for the thickness of the injection layer can be found by combining Eqs. (3.26) and (3.27) and is given by

$$\frac{x_i}{W_{\mathrm{epi}}} = \frac{E_c}{E_c + \mathcal{V}_{\mathrm{C_1C_2}}}. \tag{3.47}$$

3.3.6 The transition into hard saturation and into reverse

In the previous sections we have described the physics of the epilayer current model of Mextram 504. In this section we consider two subtle points that need to be taken care of. Both have to do with the transition from one working regime into the other.

The transition into hard saturation In a number of the equations of the (forward) epilayer model we see the expression $\mathsf{V_{dC}} - \mathcal{V}_{\mathrm{B_2C_1}}$. When the transistor goes into hard saturation this term can become negative. Hence we will replace it by V_{qs}, to be calculated below, which is always positive. The equations used in Mextram are then given by

$$I_{qs} = \frac{V_{qs}}{\mathsf{SCR_{Cv}}} \, \frac{V_{qs} + \mathsf{I_{hc}}\, \mathsf{SCR_{Cv}}}{V_{qs} + \mathsf{I_{hc}}\, \mathsf{R_{Cv}}}, \tag{3.48a}$$

$$\tilde{I}_{\mathrm{epi}} = \frac{V_{qs}}{\mathsf{SCR_{Cv}}\, y_i^2} \, \frac{V_{qs} + \mathsf{I_{hc}}\, \mathsf{SCR_{Cv}}\, y_i}{V_{qs} + \mathsf{I_{hc}}\, \mathsf{R_{Cv}}}. \tag{3.48b}$$

When the transistor goes into hard saturation the voltage V_{qs} must go to zero. When does this happen? We can say that this happens when $\mathcal{V}_{\mathrm{B_2C_1}} = \mathsf{V_{dC}}$, taking the same approach as in describing quasi-saturation which starts when $V^*_{B_2C_2} = \mathsf{V_{dC}}$. We found, however, that this is too early for high currents.

For high currents it is better to look at the internal junction bias $\mathcal{V}^*_{\mathrm{B_2C_2}}$ (given the current, but assuming still a reverse biased external bias $\mathcal{V}_{\mathrm{B_2C_1}}$) and saying that hard saturation starts when $\mathcal{V}_{\mathrm{B_2C_1}}$ equals this voltage. We can estimate this voltage by looking at Eq. (3.35) and taking $p_W \to 0$. Since we are talking about going into hard saturation at high currents we can take $x_i/W_{\mathrm{epi}} \to 1$ and $p_0^* \gg 1$. We then get $p_0^* \simeq I_{\mathrm{epi}}\mathsf{R_{Cv}}/(2V_T)$ and therefore

$$V^*_{B_2C_2} \simeq \mathsf{V_{dC}} + 2V_T \ln \frac{I_{\mathrm{epi}}\, \mathsf{R_{Cv}}}{2\, V_T}. \tag{3.49}$$

©Koninklijke Philips Electronics N.V. 2005

So at high currents we must have $V_{qs} \rightarrow 0$ when $\mathcal{V}_{B_2C_1}$ approaches this internal bias. Hence we can write

$$V_{qs} = \mathsf{V_{dC}} + 2V_T \ln \frac{I_{epi}\,\mathsf{R_{Cv}}}{2\,V_T} - \mathcal{V}_{B_2C_1}. \quad (3.50)$$

To make sure that we can use the same equation also for low currents, and to prevent V_{qs} to actually become zero, the Mextram model has

$$V_{qs}^{th} = \mathsf{V_{dC}} + 2V_T \ln\left(\frac{I_{epi}\,\mathsf{R_{Cv}}}{2\,V_T} + 1\right) - \mathcal{V}_{B_2C_1}, \quad (3.51a)$$

$$V_{qs} = \tfrac{1}{2}\left(V_{qs}^{th} + \sqrt{(V_{qs}^{th})^2 + 4\,(0.1\,\mathsf{V_{dC}})^2}\right). \quad (3.51b)$$

The situation around zero current Let us consider the situation that for given $\mathcal{V}_{B_2C_1}$ the current I_{epi} goes to zero. This is the situation where the forward and reverse models meet. Mextram is not continuous in all derivatives here. But we need to make sure that at least the effective resistance is continuous.

The effective resistance is found when we consider the relation between the current I_{epi} and $V = \mathcal{V}_{B_2C_2} - \mathcal{V}_{B_2C_1}$ in reverse, or $V = V_{B_2C_2^*} - \mathcal{V}_{B_2C_1}$ in forward. Let us first consider reverse. After some algebra it can be shown that

$$I_{epi}\,\mathsf{R_{Cv}} = (1 + p_W)\,V. \quad (3.52)$$

For forward mode we consider Eq. (3.35), which is being used to calculate p_0^* and hence $V_{B_2C_2}^*$. After again some algebra we get

$$\left(\frac{x_i}{W_{epi}}\right) I_{epi}\,\mathsf{R_{Cv}} = p_W V. \quad (3.53)$$

To have the same effective resistance V/I_{epi} both in forward as well as in reverse we must demand that

$$\left(\frac{x_i}{W_{epi}}\right)_{I_{epi}=0} = \frac{p_W}{1 + p_W}. \quad (3.54)$$

Note that this relation is true in the Kull model also. (In Appendix C we discuss the numerical behaviour of the Kull model around $\mathcal{V}_{C_1C_2} = 0$.)

How is x_i/W_{epi} calculated in Mextram? Well, first y_i is found from Eq. (3.48). When $I_{epi} = 0$ we have $\tilde{I}_{epi} = I_{qs}$ and hence $y_i = 1$. When we then simply use $x_i/W_{epi} = 1 - y_i$ we do not get the right answer for x_i/W_{epi}. In Mextram, therefore, we use

$$\frac{x_i}{W_{epi}} = 1 - \frac{y_i}{1 + p_W y_i}. \quad (3.55)$$

Now, when $I_{epi} \rightarrow 0$ and hence $y_i \rightarrow 1$ we do indeed find $x_i/W_{epi} \rightarrow p_W/(p_W + 1)$.

 ©Koninklijke Philips Electronics N.V. 2005

3.4 The epilayer diffusion charge

At this point it is convenient to discuss the epilayer diffusion charge. This is the charge of the holes in epilayer, and is therefore directly linked to the injection model discussed above. Note that these holes carry no net current, but that the diffusion current and the drift current exactly cancel.

For the calculation of the epilayer charge we use Eq. (1.17)

$$I_{\rm epi} = \frac{q^2 D_n n_{i0}^2 A_{\rm em}^2}{Q_{\rm epi}} \left(e^{V^*_{B_2C_2}/V_T} - e^{\mathcal{V}_{\rm B_2C_1}/V_T} \right), \tag{3.56}$$

where changed $\mathcal{V}_{\rm B_2C_2}$ into its more physical counterpart $V^*_{B_2C_2}$. The only thing we have to do is replace the various terms using expressions from the previous section. The current is re-expressed using Eq. (3.35) and the definition of $\mathsf{R_{Cv}}$, for the exponentials we use Eq. (3.18) taking $\mathsf{V_{d_C}}$ according to Eq. (3.16), and we use the Einstein relation $D_n = \mu_n V_T$. Taking it all together we get

$$\begin{aligned} \frac{W_{\rm epi}}{x_i} \frac{q\mu_n N_{\rm epi} A_{\rm em}}{W_{\rm epi}} \, 2\, V_T \, (p_0^* - p_W) \, \frac{p_0^* + p_W + 1}{p_0^* + p_W + 2} & \\ = \frac{q^2 D_n n_{i0}^2 A_{\rm em}^2}{Q_{\rm epi}} \left[p_0^*(p_0^*+1) - p_W(p_W+1) \right] \frac{N_{\rm epi}^2}{n_{i0}^2}. & \end{aligned} \tag{3.57}$$

Simplifying this equation gives us a very simple expression for the epilayer charge: **$Q_{\rm epi}$**

$$Q_{\rm epi} = \tfrac{1}{2} \, Q_{\rm epi0} \, \frac{x_i}{W_{\rm epi}} \, (p_0^* + p_W + 2), \tag{3.58}$$

where $Q_{\rm epi0} = q N_{\rm epi} A_{\rm em} W_{\rm epi}$ is the background charge of the epilayer. It is possible to express this charge in terms of other parameters of the epilayer and of the base. In parameter extraction [2] this is used in the initialisation to get a first estimate. In Mextram 503 this is also implicitly used because no separate parameter is available. In Mextram 504, however, we introduce an extra transit time parameter $\boldsymbol{\tau}_{\mathsf{epi}}$, which has physically the value $W_{\rm epi}^2/4D_n$. The background charge can then be expressed as

$$Q_{\rm epi0} = \frac{4\, \boldsymbol{\tau}_{\mathsf{epi}} \, V_T}{\mathsf{R_{Cv}}}. \tag{3.59}$$

Let us discuss the epilayer charge a little bit more. In the normal forward operating regime we can simplify the charge by taking $p_W = 0$. Using again Eq. (3.35) we get

$$Q_{\rm epi} \simeq \boldsymbol{\tau}_{\mathsf{epi}} \left(\frac{x_i}{W_{\rm epi}} \right)^2 I_{\rm epi}. \tag{3.60}$$

This equation was first given in Ref. [27] and is used in other compact models [35]. Rather than Eq. (3.60), we use the full expression (3.58) for the charge because it also describes

the charge in the case of hard saturation (where the current is small but the charge is not) as well as in reverse mode of operation.

It is also interesting to compare our charge model with that of the Kull model [19], since both basically describe the charge in the neutral injection region. Rewriting the Kull charge model into our terms we find

$$Q_{\rm Kull} \simeq \tfrac{1}{2}\, Q_{\rm epi0}\, (p_0 + p_W - 2n_i^2/N_{\rm epi}^2). \tag{3.61}$$

The last contribution is clearly negligible, but note that the factor $x_i/W_{\rm epi}$ is completely absent. The reason for this is that the Kull charge model is an approximation valid for low injection conditions (in which case the charge is negligible anyhow) and very high injection conditions (in which case $x_i/W_{\rm epi} \simeq 1$). A more complete expression for the charge is also given in Ref. [19]. The difference between this expression and ours (3.58) is due to our approximation (3.35). An other difference between the Kull charge model and ours is that we do not split the charge into two terms, one between nodes B_2 and C_2 and one between nodes B_2 and C_1, but keep it as one charge between nodes B_2 and C_2.

3.5 The intrinsic base-collector depletion charge

Next we will calculate the depletion charge Q_{t_C} of the intrinsic base-collector junction. It is basically the same as $Q_{\rm tex}$ but has one extra feature: it is current dependent. This current dependence comes into the description in three places. First of all, the depletion layer thickness changes due to the charge of the electrons moving at the saturated velocity in the epilayer, as discussed in the paragraph about the electric field in Section 3.2. This effect is modelled by the factor f_I given below. The second place where the current plays a role is in that the junction voltage to be used for the depletion charge must include the voltage drop over the epilayer. So instead of taking $\mathcal{V}_{\rm B_2C_1}$ as the voltage for calculating the depletion layer thickness, we use $V_{\rm junc}$, which equals $\mathcal{V}_{\rm B_2C_1} + I_{\rm epi}\,\mathsf{R_{Cv}}$ for low currents (see also the paragraph about the nodes of the equivalent circuit in Section 3.2). At last we must make sure that the transition into hard saturation does not give sudden changes in the capacitance and hence in the total transit time. For this reason we make V_{ch}, also discussed below, current dependent.

For the calculation of the charge we use Eq. (3.6): $\mathrm{d}E/\mathrm{d}x = \rho/\varepsilon$. The electric field has the form sketched in Fig. 12. Integrating the electric field from the base-collector junction, where $E = E_0 < 0$ to a position well into the buried layer where the electric field is negligible, we find the total (depletion) charge in the epilayer

$$Q = A_{\rm em} \int_0 \rho \mathrm{d}x = -\varepsilon A_{\rm em} E_0. \tag{3.62}$$

So for the calculation of the charge we need to find E_0.

Let us again use the basic equation of the electric field in the epilayer to calculate the thickness of the depletion layer. We start with the equation for the electric field in the

 ©Koninklijke Philips Electronics N.V. 2005

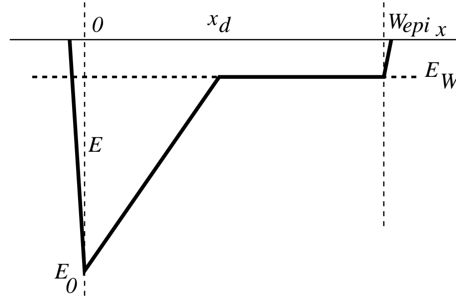

Figure 12: *Figure describing the electric field in the epilayer for the calculation of the depletion width x_d. For $x > x_d$ the electric field has the value $E_W = -I_{\rm epi}\mathsf{R_{Cv}}/W_{\rm epi}$.*

depletion layer.

$$\frac{\mathrm{d}E}{\mathrm{d}x} = \frac{qN_{\rm epi}}{\varepsilon}\left(1 - \frac{I_{\rm epi}}{\mathsf{I_{hc}}}\right). \tag{3.63}$$

The solution of the electric field is then given by

$$E(x) = E_0 + \frac{qN_{\rm epi}}{\varepsilon}\left(1 - \frac{I_{\rm epi}}{\mathsf{I_{hc}}}\right)x. \tag{3.64}$$

The depletion region ends at x_d. When $x_d < W_{\rm epi}$ the electric field in the region behind the depletion layer, $x > x_d$, will be constant. We assume for a moment that it is ohmic, and therefore write:

$$E_W = -I_{\rm epi}\mathsf{R_{Cv}}/W_{\rm epi}. \tag{3.65}$$

Of course the electric field must be continuous at $x = x_d$. This gives the relation

$$E_W = E_0 + \frac{qN_{\rm epi}}{\varepsilon}\left(1 - \frac{I_{\rm epi}}{\mathsf{I_{hc}}}\right)x_d. \tag{3.66}$$

Integrating the electric field over all x and using again Eq. (3.5) we find

$$\mathsf{V_{dC}} - \mathcal{V}_{\rm B_2C_1} = -E_W W_{\rm epi} + \tfrac{1}{2}(E_W - E_0)x_d, \tag{3.67}$$

or, using Eqs. (3.65) and (3.66)

$$\frac{qN_{\rm epi}}{2\varepsilon}\left(1 - \frac{I_{\rm epi}}{\mathsf{I_{hc}}}\right)x_d^2 = \mathsf{V_{dC}} - \mathcal{V}_{\rm B_2C_1} - I_{\rm epi}\mathsf{R_{Cv}}. \tag{3.68}$$

We see that x_d depends on the current due to two effects, as mentioned before. When we consider the right-hand-side, we see that instead of $\mathsf{V_{dC}} - \mathcal{V}_{\rm B_2C_1}$, the normal expression used when calculating depletion capacitances, the current becomes involved and we have

©Koninklijke Philips Electronics N.V. 2005

$V_{d_C} - V_{junc}$. We will discuss V_{junc} in more detail below. We also have an extra factor $(1 - I_{epi}/I_{hc})$. When we calculate the ideal depletion charge from the equation above, we find[5]

$$Q = 2\,V_{d_C}\,C_0\sqrt{1 - V_{junc}/V_{d_C}}\,\sqrt{1 - I_{epi}/I_{hc}}, \tag{3.69}$$

where $C_0 = \varepsilon A_{em}/x_{d0}$ is the zero-bias capacitance, in our case equal to $XC_{j_C}\,C_{j_C}$. We will denote the factor determining the current dependence of Q, in the equation above the last factor, by f_I. We must make sure that the argument of the square root of f_I can not become negative. We therefore replace I_{epi} by I_{cap}, the current as used in the capacitance model. It is defined as

$$I_{cap} = \frac{I_{hc}\,I_{epi}}{I_{hc} + I_{epi}}. \tag{3.70}$$

We also introduce a new parameter m_C to describe the current dependence of the capacitance and write

$$f_I = \left(1 - \frac{I_{cap}}{I_{hc}}\right)^{m_C}. \tag{3.71}$$

Q_{t_C} The capacitance is now given by

$$V_{C_V} = \frac{V_{d_C T}}{1 - p_C}\left[1 - f_I\,(1 - V_{jC}/V_{d_C T})^{1-p_C}\right] + f_I\,b_{jC}(V_{junc} - V_{jC}), \tag{3.72a}$$

$$V_{t_C} = (1 - X_{pT})\,V_{C_V} + X_{pT}\mathcal{V}_{B_2C_1}, \tag{3.72b}$$

$$Q_{t_C} = XC_{j_C}\,C_{j_C T}\,V_{t_C}. \tag{3.72c}$$

This equation is very similar to the incomplete expression (2.12) given before, but now an explicit expression is used instead of the function $V_{depletion}$, the current dependent junction bias V_{junc} is used for the variable part, and the current dependent factor f_I is introduced.

We still need to give V_{jC}, in a similar way as described in Appendix A:

$$V_{FC} = V_{d_C T}\left(1 - b_{jC}^{-1/p_C}\right), \tag{3.73a}$$

$$V_{jC} = V_{junc} - V_{ch}\ln\left\{1 + \exp[(V_{junc} - V_{FC})/V_{ch}]\right\}. \tag{3.73b}$$

Here, however, we do not use $V_{ch} = 0.1\,V_{d_C}$ in forward mode, because this will give a much too steep increase from the zero-bias value to a_{jC} times this value when due to quasi-saturation V_{junc} goes from negative values to values larger than the diffusion

[5] In the calculation of the charge a contribution $I_{C_1C_2}R_{Cv}/W_{epi}$ has not be taken into account. In the original derivation this was a mistake. However, since it only contributes a constant transit time, it can easily be compensated by other model parameters. Please note that this correction *is* needed to find a transit time contribution proportional to $C \cdot R_{Cv}(1 - x_d)$, instead of only $C \cdot R_{Cv}$.

 ©Koninklijke Philips Electronics N.V. 2005

voltage $\mathsf{V_{dC}}$. We therefore have to reduce this increase around quasi-saturation and do this by increasing V_{ch}, which describes the transition region:

$$V_{ch} = \mathsf{V_{dC}} \left(0.1 + \frac{2\,I_{\rm epi}}{I_{\rm epi} + I_{qs}}\right). \tag{3.74}$$

Note that we use the current I_{qs} to determine when quasi-saturation starts.

Calculating the junction bias $V_{\rm junc}$ As a last point we need to calculate $V_{\rm junc}$. We already mentioned that for small currents it must equal $\mathcal{V}_{\rm B_2C_1} + I_{\rm epi}\,\mathsf{R_{Cv}}$. Furthermore, the point where for the capacitance a vanishing depletion width results ($V_{\rm junc} \rightarrow \mathsf{V_{dC}}$), is physically equal to the onset of quasi-saturation. We need to make sure that the same happens in our model. Hence we need $V_{\rm junc} = \mathsf{V_{dC}}$, when $I_{\rm epi} = I_{qs}$. A logical choice would be to take $V_{\rm junc} = V^*_{B_2C_2}$. There is however a catch to this.

Let us consider the total transit time. One of the contributions is due to the RC-time of the base-collector depletion capacitance and the (differential) resistance of the epilayer. The capacitance is fairly constant as function of current. The resistance, however, becomes very small once the transistor goes into quasi-saturation. This means that the contribution of this RC-time vanishes when the transistor is in quasi-saturation. This is not unphysical, as device simulations show [40]. However, in real life the total transit time is still smooth because the total charge is a smooth function of the current. The decrease in transit time due to one component is automatically compensated by an increase in another component. (The distinction between the various components in device simulations is rather arbitrary anyhow.) In a compact model, however, all the different components are modelled separately and added afterwards. Since each of these components has its own parameters and bias or current dependence, we must make sure that each component itself behaves smooth, even when going into quasi-saturation.

Let us consider the corresponding transit time in some more detail. We consider the Kirk effect, just before quasi-saturation. The depletion width is then equal to the epilayer width and the capacitance is given by $C = \varepsilon A_{\rm em}/W_{\rm epi}$. The partial resistance of the epilayer equals $\mathsf{SCR_{Cv}}$. The contribution to the transit time is then

$$C \times \mathsf{SCR_{Cv}} = \frac{W_{\rm epi}}{2\,v_{\rm sat}}, \tag{3.75}$$

a well-known expression. The time needed to cross the epilayer is the width divided by the velocity. The extra factor of 2 is a result from the electric field distribution which is triangular instead of flat. The corresponding charge will be given by

$$Q \simeq \frac{I_{\rm epi}\,W_{\rm epi}}{2\,v_{\rm sat}}. \tag{3.76}$$

When injection starts, this charge will be modified. The effective space charge resistance will get an extra factor $(1 - x_i/W_{\rm epi})^2$. This means that the charge now becomes

$$Q \simeq \frac{I_{\rm epi}\,W_{\rm epi}}{2 v_{\rm sat}} \left(1 - \frac{x_i}{W_{\rm epi}}\right)^2. \tag{3.77}$$

In practice this means that the charge becomes nearly constant. The corresponding transit time, which is the derivative of the charge w.r.t. the current, then vanishes.

The only way to prevent this in our model is to make sure that the effective epilayer resistance, in as far as it is used in this capacitance model, does not vanish once the transistor goes into quasi-saturation. We therefore take an expression for V_{junc} that is allowed to keep steadily increasing with current, even when $V_{\mathrm{junc}} > \mathsf{V_{dC}}$. Furthermore, we want it as close to our epilayer model as possible.

We need to calculate the effective voltage drop over the epilayer. The derivation is basically the same as the derivation of the current at the onset of quasi-saturation I_{qs}. Now, however, we do not take V_{qs}, the voltage drop at the onset of quasi-saturation, but the real voltage drop V_{epi}. Similar to Eq. (3.48), we therefore write

$$I_{\mathrm{epi}} = \frac{V_{\mathrm{epi}}}{\mathsf{SCR_{Cv}}} \, \frac{V_{\mathrm{epi}} + \mathsf{I_{hc}} \, \mathsf{SCR_{Cv}}}{V_{\mathrm{epi}} + \mathsf{I_{hc}} \, \mathsf{R_{Cv}}}. \tag{3.78}$$

From this equation we calculate V_{epi} as function of I_{epi}. Since we use it also when $x_i > 0$, even though the equation only holds for $x_i \simeq 0$, we call it $V_{x_i=0}$. The solution is given by

$$B_1 = \tfrac{1}{2}\mathsf{SCR_{Cv}}(I_{\mathrm{epi}} - \mathsf{I_{hc}}), \tag{3.79a}$$

$$B_2 = \mathsf{SCR_{Cv}} \, \mathsf{R_{Cv}} \, \mathsf{I_{hc}} \, I_{\mathrm{epi}}, \tag{3.79b}$$

$$V_{x_i=0} = B_1 + \sqrt{B_1^2 + B_2}. \tag{3.79c}$$

The junction voltage is now the external voltage plus the voltage drop over the epilayer:

$$V_{\mathrm{junc}} = \mathcal{V}_{\mathrm{B_2C_1}} + V_{x_i=0}. \tag{3.80}$$

3.6 Avalanche

The last part of the epilayer model we need to discuss is the avalanche model, presented also in Ref. [41]. The avalanche current is a result of impact ionisation in the epilayer due to the high electric fields. Our model is based on Chynoweth's empirical law for the ionisation coefficient [42]

$$\alpha_n(E) = A_n \exp(-B_n/|E|), \tag{3.81}$$

where E is the electric field and A_n and B_n are material constants. These two constants also appear as constants in Mextram. They depend on the polarity of the transistor and are therefore different for NPN and PNP transistors. We use the Si values given by van Overstraeten and de Man [43]. Note that in practice these values can also be used for other materials, even thought then the parameters of the avalanche model will differ from their physical value.

As one can see the generation of electron-hole pairs is largest where the electric field is largest. Since this is mainly in the epilayer, we will consider only impact ionisation and

 ©Koninklijke Philips Electronics N.V. 2005

avalanche currents in the epilayer. To describe the electric field, we will not use the results of the previous section. To keep the avalanche model and the depletion capacitance model independent of each other, we have chosen for a formulation where the parameters are separate. For the avalanche model we will therefore use a simple depletion approximation, based again on the equations (3.5) and (3.9) for the electric field, given before. For low currents, our model is very similar to that of Ref. [44, 45]. The most important influence of the current is due to the change in the slope of the electric field. This effect was already incorporated in the model of Ref. [46]. In our model we also take the finite thickness of the epilayer into account, and the possibility that the maximum of the electric field moves to the interface witht the buried-layer.

The total avalanche current is the ionisation coefficient times the epilayer current, integrated over all positions where this ionisation takes place. This holds of course only in the weak avalanche regime, where the generated current does not generate extra avalanche itself.[6] We can then write

$$I_{\rm avl} = I_{\rm epi} \int_0^{W_{\rm eff}} \alpha_n[E(x)]\, {\rm d}x = G\ I_{\rm epi}, \tag{3.82}$$

where G is the generation factor we need to determine. The value $W_{\rm eff}$ in the integral is the effective width (non-injected region) of the epilayer, which in normal cases is equal to $W_{\rm epi}$. The case of quasi-saturation will be discussed in Section 3.6.3. The width of the epilayer is very important for determining the electric field. Therefore we use the parameter $\mathsf{W_{avl}}$ for this width in the avalanche model. When the epilayer current becomes negative, the epilayer will be flooded by electrons from the buried collector and the electric field is low. Hence we take $I_{\rm avl} = 0$ for negative currents.

The most important contribution to the integral is that for maximal electric field. For a general electric field distribution we can linearise around the maximum field E_M:

$$|E(x)| = E_M\ (1 - x/\lambda_D), \tag{3.83}$$

for some given λ_D. (Note that for the maximum of the electric field, as well as for its average discussed below, we will take absolute values.) We will approximate this by writing

$$|E(x)| \simeq \frac{E_M}{1 + x/\lambda_D}. \tag{3.84}$$

Performing the integral we find the value of the generation coefficient from the electric field

$$G_{\rm EM} = \frac{A_n}{B_n} \lambda_D E_M \left\{ \exp\left[-\frac{B_n}{E_M} \right] - \exp\left[-\frac{B_n}{E_M} \left(1 + \frac{W_{\rm eff}}{\lambda_D} \right) \right] \right\}. \tag{3.85}$$

We still need to determine λ_D and E_M, both of which depend on collector voltage and current.

[6] This is basically saying that 'avalanche' is a misnomer, since we explicitely do not take avalanching into account. We will keep the term since it is widely used.

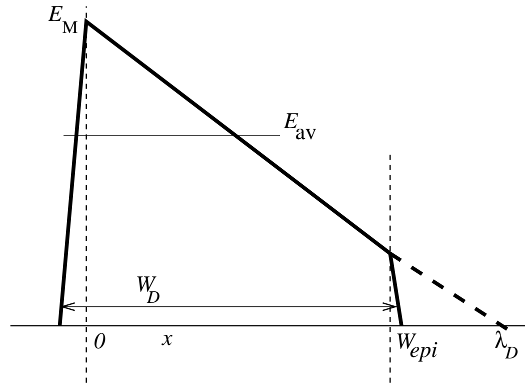

Figure 13: *Schematic representation of the* absolute *value of the electric field for use in the avalanche model.*

3.6.1 Normal avalanche modelling

In this section we will calculate the maximum of the electric field E_M and the extrapolation length λ_D for normal usage. In this case the Mextram flag called 'extended avalanche' has to be put to zero: $\mathsf{EXAVL} = 0$. Extended avalanche modelling ($\mathsf{EXAVL} = 1$) will be discussed in Section 3.6.3.

As mentioned before the electric field is important. We have given a schematic representation of the electric field in Fig. 13. We start with the average of the (absolute value) of the electric field over the depletion region, which is found from Eq. (3.5) to be

$$E_{\mathrm{av}} = \frac{\mathsf{V}_{\mathsf{dC}} - \mathcal{V}_{\mathrm{B_2C_1}}}{W_D}, \tag{3.86}$$

where W_D is the width of the depletion region, calculated below. From this expression we see that the average of the electric field becomes zero when $\mathcal{V}_{\mathrm{B_2C_1}} = \mathsf{V}_{\mathsf{dC}}$. In that case the base-collector junction is already far in forward and again the epilayer will be flooded with electrons and holes resulting in a low electric field. We therefore take $I_{\mathrm{avl}} = 0$ when $\mathcal{V}_{\mathrm{B_2C_1}} > \mathsf{V}_{\mathsf{dC}}$. Note that the expressions below are such that also the maximum of the electric field will go to zero when its average goes to zero. The expression (3.85) for the generation factor is such that at that point also G_{EM} will go to zero (including all its derivatives!).

Next we consider the derivative of the electric field. At zero current it is given by

$$dEdx_0 = \frac{q N_{\mathrm{epi}}}{\varepsilon} = \frac{2\,\mathsf{V}_{\mathsf{avl}}}{\mathsf{W}_{\mathsf{avl}}{}^2}. \tag{3.87}$$

Here we introduced our second parameter of the avalanche model, $\mathsf{V}_{\mathsf{avl}}$. This new parameter is therefore a measure for the derivative of the electric field, especially around the maximum electric field. For this simple and 1-dimensional model it should be equal to the punch-through voltage $\mathsf{I}_{\mathsf{hc}}\ \mathsf{SCR}_{\mathsf{Cv}}$. In practice the electric field does not really have a triangular shape. Especially due to non-local effects the effective electric field is much

 ©Koninklijke Philips Electronics N.V. 2005

broader around its maximum. This means that the value of $\mathsf{V_{avl}}$ can become small. The direct relation with the doping level is then also lost.

We can now calculate the electric field E_0 at the base-collector junction as (see also Fig. 13)

$$E_0 = E_{av} + \tfrac{1}{2} W_D \; dEdx_0 \left(1 - \frac{I_{cap}}{\mathsf{I_{hc}}}\right), \tag{3.88}$$

where we included the current dependence in the same way as for the capacitance model using I_{cap} instead of I_{epi} to prevent a negative value of E_0. In normal operating regimes the maximum of the electric field will be at the base-collector junction, and therefore we take

$$E_M = E_0. \tag{3.89}$$

If, due to the reversal of the slope of the electric field (Kirk effect), the maximum of the electric field moves to the epilayer-buried layer interface, the model becomes somewhat more complex and numerically more unstable. Mextram can describe these effects, as will be discussed in Section 3.6.3, but will only do so when $\mathsf{EXAVL} = 1$. Here we will discuss the basic model, used when $\mathsf{EXAVL} = 0$.

Next we need to calculate λ_D, representing the slope of the electric field. We could use Eq. (3.83) and write

$$\left|\frac{\mathrm{d}E}{\mathrm{d}x}\right| = \frac{E_M}{\lambda_D} = dEdx_0 \left(1 - \frac{I_{cap}}{\mathsf{I_{hc}}}\right). \tag{3.90}$$

We prefer, however, an expression which can be used also in Section 3.6.3, when we modify the expression for the maximum electric field. We can write for the electric field

$$|E(x)| = E_0 - \frac{2x}{W_D}(E_0 - E_{av}), \tag{3.91}$$

which is given in such a way that the electric field at $x = W_D/2$ equals the average electric field: $|E(W_D/2)| = E_{av}$. In the case discussed here we have $E_0 = E_M$. From the expression for the electric field, and from $|\mathrm{d}E/\mathrm{d}x| = E_M/\lambda_D$ we find the expression

$$\lambda_D = \frac{E_M W_D}{2(E_M - E_{av})}. \tag{3.92}$$

The same expression for λ_D can be found if the maximum of the electric field is at the epilayer-buried layer interface (to be discussed in Section 3.6.3), in which case the electric field is given by $|E(x)| = E_W + 2(x - W_D)(E_W - E_{av})/W_D$.

The last thing we need to do is calculating the thickness of the depletion layer. As mentioned before we use a very simple abrupt junction depletion model and find [see also Eq. (3.68)]

$$x_D = \sqrt{\frac{2}{dEdx_0}} \sqrt{\frac{\mathsf{V_{d_C}} - \mathcal{V}_{B_2C_1}}{1 - I_{cap}/\mathsf{I_{hc}}}}, \tag{3.93}$$

©Koninklijke Philips Electronics N.V. 2005

where $I_{\rm cap}$ is defined in Eq. (3.70). This formula can lead to depletion layers larger than the (effective) epilayer width $W_{\rm eff}$ (here taken to be equal to $\mathsf{W_{avl}}$). We therefore use for the thickness over which the electric field is important the expression

$$W_D = \frac{x_D\, W_{\rm eff}}{\sqrt{x_D^2 + W_{\rm eff}^2}}. \tag{3.94}$$

3.6.2 Limiting the avalanche current

The value of $G_{\rm em}$ can not be used directly to calculate the avalanche current, because it may become very large, for instance in the iteration process of a circuit simulator, thus destroying convergency. We will consider two upper bounds to prevent this

First of all, we demand that

$$G < 1. \tag{3.95}$$

This means that the avalanche current can never be larger than the epilayer current.

Next we need to consider the case that the collector voltage is very large, which means that the avalanche current is large. This large current might lead to a negative base current. The voltage drop over the base resistance then makes it possible for the internal base-emitter voltage $\mathcal{V}_{\rm B_2E_1}$ to be larger than the external base-emitter voltage. This in itself is not unphysical, but for convergence we demand that the internal base-emitter voltage increases when the current increases. Turning the argument around, for convergence we demand that the collector current increases when we increase the external base-emitter bias.

The external base-emitter voltage is given by

$$\mathcal{V}_{\rm BE} = \mathcal{V}_{\rm B_2E_1} + (I_N + I_{B_1})\mathsf{R_E} + (I_{B_1} - I_{\rm avl})R_B. \tag{3.96}$$

Here we neglect the reverse currents and the non-ideal base currents. The other quantities can be given as

$$I_N = \frac{I_f}{q_B^I}, \tag{3.97a}$$

$$I_f = \mathsf{I_s}(e^{\mathcal{V}_{\rm B_2E_1}/V_T} - 1), \tag{3.97b}$$

$$I_{B_1} = I_f/\beta_{\mathsf{f}}, \tag{3.97c}$$

$$I_{\rm avl} = G\, I_{\rm epi}, \tag{3.97d}$$

$$R_b = \mathsf{R_{Bc}} + R_{B2}. \tag{3.97e}$$

Note that R_{B2}, which will be defined in Eq. (5.14) is not equal to $\mathsf{R_{Bv}}$, but includes the high injection effects and current crowding. This will be discussed in Section 5.1. To make sure that the collector current increases when the external base-emitter voltage

 ©Koninklijke Philips Electronics N.V. 2005

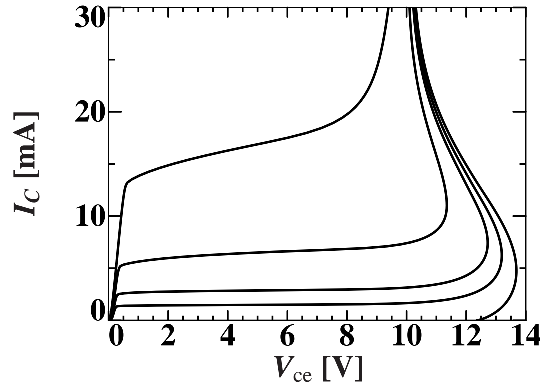

Figure 14: *The output characteristic of Mextram showing snap-back effects.*

increases we need $\partial\mathcal{V}_{\rm BE}/\partial\mathcal{V}_{\rm B_2E_1} > 0$. In doing this derivative we assume that q_B^I is constant, which is nearly true. Furthermore we assume that $I_{B_1} \ll I_N$. We find

$$V_T\,\frac{\partial\mathcal{V}_{\rm BE}}{\partial\mathcal{V}_{\rm B_2E_1}} \simeq V_T + I_N\,\mathsf{R_E} + (I_f/\beta_f - G\,I_{\rm epi})\,R_B > 0. \tag{3.98}$$

This leads to

$$G < G_{\rm max} = \frac{V_T}{I_{C_1C_2}\,(\mathsf{R_{Bc}} + R_{B2})} + \frac{q_B^I}{\beta_f} + \frac{\mathsf{R_E}}{\mathsf{R_{Bc}} + R_{B2}}, \tag{3.99}$$

where we assumed that $I_N \simeq I_{\rm epi}$.

Using these two upper bounds we finally find for the avalanche current **$I_{\rm avl}$**

$$I_{\rm avl} = I_{\rm epi}\;G = I_{C_1C_2}\,\frac{G_{\rm EM}\cdot G_{\rm max}\cdot 1}{G_{\rm EM}\cdot G_{\rm max} + G_{\rm EM}\cdot 1 + G_{\rm max}\cdot 1}. \tag{3.100}$$

It is obvious that G meets both requirements (3.95) and (3.99).

3.6.3 Extended avalanche modelling

Mextram contains an extended avalanche model, that can be switched on by setting $\mathsf{EXAVL} = 1$. Two extra effects are then taken into account: the decrease of the effective epilayer width due to base-widening and the effect that due to change in sign of the slope of the electric field the maximum of the electric field moves to the epilayer-buried layer interface. When these effects are included it is possible to describe snap-back effects at high currents, see Fig. 14. Although this describes a physical effect, it can lead to serious convergence problems (multiple solutions are possible). It is for this reason that this part of the model is optional. We will now discuss both effects.

As mentioned above, the effective width of the epilayer becomes smaller due to injection. Hence we can write

$$W_{\rm eff} = \mathsf{W_{avl}}\left(1 - \frac{x_i}{W_{\rm epi}}\right), \tag{3.101}$$

©Koninklijke Philips Electronics N.V. 2005

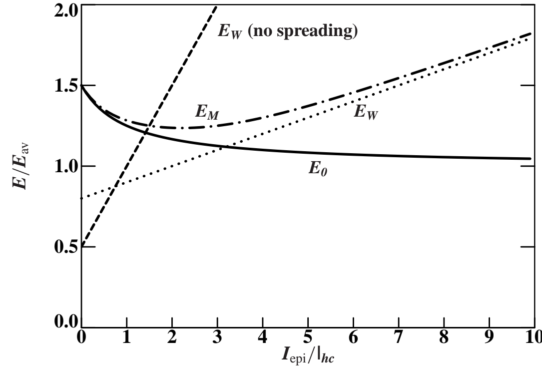

Figure 15: *The various extrema of the electric field normalised to the average electric field as function of the current. We have taken* $dEdx_0 = E_{av}/W_D$ *and* $\mathsf{S_{fh}} = 2$.

where x_i/W_{epi} is calculated in Section 3.3. Since this can lead to very small effective width, giving very large electric fields (E_{av} for instance), we modify the equation to be numerically more stable to

$$W_{eff} = \mathsf{W_{avl}} \left(1 - \frac{x_i}{2\,W_{epi}}\right)^2, \tag{3.102}$$

which gives the same result for small x_i.

For the description of the second effect, which is of course very much related to quasi-saturation and the Kirk effect, we must calculate the electric field E_W at the end of the epilayer. We could simply write

$$E_W = E_{av} - \tfrac{1}{2} W_D dEdx_0 \left(1 - \frac{I_{epi}}{\mathsf{I_{hc}}}\right). \tag{3.103}$$

Note that here we do not need to take I_{cap} instead of I_{epi}. We allow E_W to be below E_{av}, whereas we always have $E_0 > E_{av}$. For these high electric fields, however, current spreading needs to be taken into account. This lowers the maximum electric field somewhat as function of current. With one extra parameter $\mathsf{S_{fh}}$ we describe this somewhat empirically as (see also Ref. [41] and Fig. 15)

$$SH_W = 1 + 2\,\mathsf{S_{fh}} \left(1 + 2\,\frac{x_i}{W_{epi}}\right), \tag{3.104a}$$

$$E_{fi} = \frac{1 + \mathsf{S_{fh}}}{1 + 2\,\mathsf{S_{fh}}}, \tag{3.104b}$$

$$E_W = E_{av} - \tfrac{1}{2}\,W_D\;dEdx_0 \left(E_{fi} - \frac{I_{epi}}{\mathsf{I_{hc}}\;SH_W}\right). \tag{3.104c}$$

For the maximum of the electric we take an smoothing function that determines the maximum of E_0 and E_W:

$$E_M = \tfrac{1}{2}\left(E_W + E_0 + \sqrt{(E_W - E_0)^2 + 0.1\;E_{av}^2\;I_{cap}/\mathsf{I_{hc}}}\right). \tag{3.105}$$

 ©Koninklijke Philips Electronics N.V. 2005

Note that for $I_{\text{epi}} = 0$ the maximum of the electric field is at the base side: $E_M = E_0$.

Apart from the change in W_{eff} and E_M the extended avalanche model is the same as the normal model described in Section 3.6.1.

©Koninklijke Philips Electronics N.V. 2005

4 Extrinsic regions

4.1 Resistances

As mentioned already in Section 1.1 there are five basic resistances in our model. Three of these resistances are constant. They model the resistance from the emitter contact to the intrinsic transistor, from the collector contact to the buried layer and from the base contact to part of the base under the emitter. These three resistances have their own parameters, and we can write

$\mathbf{R_E}$
$\mathbf{R_{Cc}}$
$\mathbf{R_{Bc}}$

$$R_E = \mathsf{R_E}, \quad (4.1a)$$
$$R_{Bc} = \mathsf{R_{Bc}}, \quad (4.1b)$$
$$R_{Cc} = \mathsf{R_{Cc}}. \quad (4.1c)$$

Furthermore we have two variable resistances. The variable base resistance is described in Section 5.1. The variable collector resistance modelled by the current through the epilayer has already been described in Chapter 3.

4.2 Overlap capacitance

Apart from constant resistances Mextram also has two constant overlap capacitances, that can be used for parasitic, but constant capacitances in the transistor itself. The capacitances are simply given by

$\mathbf{C_{BEO}}$
$\mathbf{C_{BCO}}$

$$C_{BEO} = \mathsf{C_{BEO}}, \quad (4.2a)$$
$$C_{BCO} = \mathsf{C_{BCO}}. \quad (4.2b)$$

4.3 Extrinsic currents

The extrinsic base currents are already given in Section 2.6. The substrate currents are already given in Section 2.7.

4.4 Extrinsic charges

Now we will give the extrinsic charges, which, unlike the extrinsic currents, have not been given in Chapter 2, because the charges contain a contribution similar to the epilayer charge Q_{epi} discussed in the previous chapter. In the intrinsic transistor we have between the base node B_2 and the collector node C_1 an extra node C_2, located at say the metallurgical junction. In the extrinsic region we do not have such a node. Hence we can also make no difference between the charge concentration $p_{0\mathrm{ex}}$ and $p_{W\mathrm{ex}}$ as we did for p_0 and

 ©Koninklijke Philips Electronics N.V. 2005

p_W in the epilayer. Furthermore, the charge is only useful in reverse, when the whole epilayer is flooded, and effectively $x_i = W_{\mathrm{epi}}$. We therefore write, conform Eq (3.58):

$$Q_{\mathrm{ex,epi}} = a_\tau \, \tfrac{1}{2} \, Q_{\mathrm{epi0}} \, p_{W\mathrm{ex}}. \tag{4.3}$$

The extra pre-factor a_τ is a result from the differences in surface between the intrinsic and the extrinsic regions. We will discuss it below. The value of $p_{W\mathrm{ex}}$ is determined in the same way as for the intrinsic transistor, see Eq. (3.24),

$$g_2 = 4 \, e^{(\mathcal{V}_{\mathrm{B_1C_1}} - \mathsf{V_{dC}})/V_T}, \tag{4.4a}$$

$$p_{W\mathrm{ex}} = \frac{g_2}{1 + \sqrt{1 + g_2}}, \tag{4.4b}$$

apart from a factor of 2, but very equivalent to formulations used in Section 2.4 for n_0 and n_B, Eqs. (2.27) and (2.28).

The second contribution to Q_{ex} is similar to the diffusion charge Q_{BC}, given in Eq. (2.49). It is given by

$$Q_{\mathrm{ex,BC}} = a_\tau \, \tfrac{1}{2} \, Q_{B0} \, n_{B\mathrm{ex}}. \tag{4.5}$$

The value of the electron density at the base collector junction is given in Eq. (2.64).

The total extrinsic charge is now given by $Q_{\mathrm{ex}} = Q_{\mathrm{ex,epi}} + Q_{\mathrm{ex,BC}}$. For small reverse currents, this charge will approximately be equal to $a_\tau \, (\tau_{\mathsf{B}} + \tau_{\mathsf{epi}}) \, I_{\mathrm{intr}}$, a transit time times the intrinsic current. The total effective transit time of this charge has its own parameter τ_{R}, such that $\tau_{\mathsf{R}} = a_\tau \, (\tau_{\mathsf{B}} + \tau_{\mathsf{epi}})$. Taking everything together, we get **Q_{ex}**

$$Q_{\mathrm{ex}} = \frac{\tau_{\mathsf{R}}}{\tau_{\mathsf{B}} + \tau_{\mathsf{epi}}} \left(\tfrac{1}{2} \, Q_{B0} \, n_{B\mathrm{ex}} + \tfrac{1}{2} \, Q_{\mathrm{epi0}} \, p_{W\mathrm{ex}} \right). \tag{4.6}$$

4.5 Extended modelling of reverse current gain; extrinsic region

It is possible in Mextram to describe the extrinsic regions in some more detail. This is done when $\mathsf{EXMOD} = 1$. The charges and currents in the extrinsic base-collector region are split into two parts using $\mathsf{X_{ext}}$, just as we always, i.e. independent of EXMOD, do with the base-collector depletion capacitance, see Section 2.2.4. We start with the charges since these are related to what we mentioned in the previous section.

4.5.1 Charges

The extrinsic charge is split into two contributions, just as we did for the depletion charges. This means first of all that Q_{ex} is redefined as **Q_{ex}**

$$Q_{\mathrm{ex}} \to (1 - \mathsf{X_{ext}}) \, Q_{\mathrm{ex}}. \tag{4.7}$$

This notation means that the actual Q_{ex} that is being used in the equivalent circuit (the left-hand-side) is calculated as a factor times the previously calculated value of Q_{ex} (the right-hand-side). The other part of the charge, that between nodes B and C_1, becomes dependent on the voltage $\mathcal{V}_{\mathrm{BC}_1}$. Hence we get

XQ$_{\mathrm{ex}}$

$$
\begin{aligned}
Xg_2 &= 4\, e^{(\mathcal{V}_{\mathrm{BC}_1} - \mathsf{V}_{\mathsf{dC}})/V_T}, && (4.8a)\\
Xp_{W\mathrm{ex}} &= \frac{Xg_2}{1+\sqrt{1+Xg_2}}, && (4.8b)\\
XQ_{\mathrm{ex}} &= F_{\mathrm{ex}}\, \mathsf{X}_{\mathsf{ext}}\, \frac{\tau_{\mathsf{R}}}{\tau_{\mathsf{B}}+\tau_{\mathsf{epi}}} \left(\tfrac{1}{2}\, Q_{B0}\, Xn_{B\mathrm{ex}} + \tfrac{1}{2}\, Q_{\mathrm{epi0}}\, Xp_{W\mathrm{ex}}\right). && (4.8c)
\end{aligned}
$$

The value for $Xn_{B\mathrm{ex}}$ will be determine below, when we consider the currents. Also the extra factor F_{ex} will be discussed below.

4.5.2 Currents

Next we consider the currents. These are also split into two contributions. Hence we redefine:

I$_{\mathrm{ex}}$

I$_{\mathrm{sub}}$

$$
\begin{aligned}
I_{\mathrm{ex}} &\rightarrow (1-\mathsf{X}_{\mathsf{ext}})\, I_{\mathrm{ex}}, && (4.9a)\\
I_{\mathrm{sub}} &\rightarrow (1-\mathsf{X}_{\mathsf{ext}})\, I_{\mathrm{sub}}. && (4.9b)
\end{aligned}
$$

The other parts are again directly connected to the base terminal. We repeat the formulations for I_{sub} and I_{ex} from before, Eqs. (2.64)–(2.67), but with a different bias and get

$$
\begin{aligned}
XIM_{\mathrm{sub}} &= \mathsf{X}_{\mathsf{ext}}\, \frac{2\, \mathsf{I}_{\mathsf{Ss}}\Big(\exp(\mathcal{V}_{\mathrm{BC}_1}/V_T)-1\Big)}{1+\sqrt{1+4\dfrac{\mathsf{I}_{\mathsf{s}}}{\mathsf{I}_{\mathsf{ks}}}\exp(\mathcal{V}_{\mathrm{BC}_1}/V_T)}}, && (4.10a)\\
Xg_1 &= \frac{4\, \mathsf{I}_{\mathsf{s}}}{\mathsf{I}_{\mathsf{k}}}\, \exp(\mathcal{V}_{\mathrm{BC}_1}/V_T), && (4.10b)\\
Xn_{B\mathrm{ex}} &= \frac{Xg_1}{1+\sqrt{1+Xg_1}}, && (4.10c)\\
XIM_{\mathrm{ex}} &= \frac{\mathsf{X}_{\mathsf{ext}}}{\beta_{\mathsf{ri}}} \left(\tfrac{1}{2}\, \mathsf{I}_{\mathsf{k}}\, Xn_{B\mathrm{ex}} - \mathsf{I}_{\mathsf{s}}\right). && (4.10d)
\end{aligned}
$$

XI$_{\mathrm{sub}}$

XI$_{\mathrm{ex}}$

Then we find the currents themselves as

$$
\begin{aligned}
XI_{\mathrm{sub}} &= F_{\mathrm{ex}}\, XIM_{\mathrm{sub}}, && (4.11a)\\
XI_{\mathrm{ex}} &= F_{\mathrm{ex}}\, XIM_{\mathrm{ex}}. && (4.11b)
\end{aligned}
$$

Again we see the extra factor F_{ex}. We will explain this in the next subsection.

 ©Koninklijke Philips Electronics N.V. 2005

4.5.3 Modulation of the extrinsic reverse current

The reverse currents $XI_{\rm ex}$ and $XI_{\rm sub}$ we want to describe are basically diode currents between base and collector. For the $\rm BC_1$ diode there is, in Mextram, no resistance between the base contact and the diode. Two effects can take place. The first of these effects is a maximum in the external collector current. The second effect is a current-voltage characteristic which is not smooth, but has a wiggle. We will consider these effects separately, although the way to prevent them is the same.

Consider the case of normal operation at high collector current I_C. The voltage at node $\rm C_1$ is given by $\mathcal{V}_{\rm C_1} = \mathcal{V}_{\rm C} - I_C \mathsf{R_{Cc}}$. The voltage drop over the $\rm BC_1$-diode then is $\mathcal{V}_{\rm BC_1} = \mathcal{V}_{\rm B} - \mathcal{V}_{\rm C} + I_C \mathsf{R_{Cc}}$. In the normal working regime the collector voltage is higher than the base voltage, which means that the diode is reverse biased. Under high current conditions however (strong quasi-saturation) the diode can be forward biased. When the forward bias reaches the diffusion voltage $\mathsf{V_{d_C}}$ all extra intrinsic collector current will flow from the extrinsic base into the collector and from there to the intrinsic transistor. This means that the external collector current is limited to about $(\mathcal{V}_{\rm CB} + \mathsf{V_{d_C}})/\mathsf{R_{Cc}}$. This causes problems in circuit simulators. Furthermore it is hardly physical reality.

Next we consider the total reverse current between base and collector. As mentioned before, it consists of two parts. Basically these are two diode currents over the junctions $\rm B_1C_1$ and $\rm BC_1$. The former has a larger saturation current and will therefore dominate at low currents. For larger currents however it has an extra resistance R_{Bc} compared to the second diode. Consequently, at some point the current-voltage characteristic will become less steep. For even higher voltages the second diode becomes dominating, making the characteristic again exponentially, until this second current will be limited by the resistance $\mathsf{R_{Cc}}$. This combination then results in a non-smooth current voltage characteristic.

The solution to both problems is adding an extra base node and an extra resistance in the base, directly connected to base contact. However, an extra node leads to extra calculational time and was found to be an inferior solution. Instead the $\rm BC_1$ diode itself was replaced by the diode in series with a resistance $\mathsf{R_{Cc}}$. To overcome the problem of an extra node, the combination of diode and resistor will be approximated by an analytical formula. The current through the diode-resistor will then be limited due to the resistor.

Our goal is then to describe with a simple formula the combination of a diode (saturation current I_{s_d}) and a resistor (R) in series. Let the total voltage be given by $V = V_D + V_R$, the voltage across the diode plus the voltage across the resistor. The current is given by (neglecting the -1 in the diode part)

$$I = \frac{V_R}{R} = I_{s_d} e^{V_D/V_T}. \tag{4.12}$$

This leads to the equation

$$I = I_{s_d} \exp[(V - IR)/V_T]. \tag{4.13}$$

This non-linear equation cannot be solved analytically in terms of elementary functions. Therefore we construct an approximate solution. For small voltages the diode will dom-

©Koninklijke Philips Electronics N.V. 2005

inate the behaviour. For large voltages the voltage drop across the diode will be rather constant and the current is given by the resistance. Let us estimate the cross-over point. The resistor has a conductance $\mathrm{d}I/\mathrm{d}V_R = 1/R$. For some voltage $V_{d_{gm}}$ the diode has the same conductance. This voltage is given by

$$V_{d_{gm}} = V_T \ln \frac{V_T}{I_{s_d} R}. \tag{4.14}$$

This voltage will also be approximately the voltage across the diode for high currents. In that case, the voltage across the resistor equals $V_R = V - V_{d_{gm}}$ and the current is given by $I_{\max} = V_R/R$. For low voltages the current is given by the diode current $I_d = I_{s_d} e^{V/V_T}$. We need an interpolation between the two regimes. This interpolation will be given by

$$I = \frac{I_{\max}}{I_d + I_{\max}}\, I_d \equiv F_{\mathrm{ex}} I_d. \tag{4.15}$$

Here we see the factor F_{ex} appear. The current $I_{\max} = (V - V_{d_{gm}})/R$ as defined before can become negative for small voltages. We need it to be not only positive, but also (much) larger than the diode current (at small voltages). To this end we define

$$I_{\max} = \frac{V - V_{d_{gm}} + \sqrt{(V - V_{d_{gm}})^2 + k}}{2R}. \tag{4.16}$$

Now $I_{\max}$ has the correct behaviour for large voltages and is large enough for small voltages. In the intermediate regime the cross-over is determined by k. Taking this parameter too small or too large results in a non-smooth current I, i.e. a current which has kink-like behaviour in second and third order derivatives. A good value is $k = 0.01$. We can get an even better behaviour when we add $2V_T$ to $V_{d_{gm}}$, and increase k slightly to 0.0121.

For the implementation in Mextram we must determine the saturation current. It is a sum of two components (a reverse base current part and a substrate part). The diode current to be used is $I_d = XIM_{\mathrm{sub}} + XIM_{\mathrm{ex}}$. The complete Mextram expression now reads

$$I_{s_d} = \mathsf{X}_{\mathsf{ext}}\,(\mathsf{I_s}/\beta_{\mathsf{ri}} + \mathsf{I_{Ss}}), \tag{4.17a}$$

$$V_{d_{gm}} = V_T \left(2 - \ln \frac{I_{s_d}\,\mathsf{R_{Cc}}}{V_T} \right), \tag{4.17b}$$

$$VB_{\mathrm{ex}} = \tfrac{1}{2} \left(\mathcal{V}_{\mathrm{BC}_1} - V_{d_{gm}} + \sqrt{(\mathcal{V}_{\mathrm{BC}_1} - V_{d_{gm}})^2 + 0.0121} \right), \tag{4.17c}$$

$$F_{\mathrm{ex}} = \frac{VB_{\mathrm{ex}}}{\mathsf{R_{Cc}}\,(XIM_{\mathrm{sub}} + XIM_{\mathrm{ex}} + I_{s_d}) + VB_{\mathrm{ex}}}, \tag{4.17d}$$

(hence $I_{\max} = VB_{\mathrm{ex}}/\mathsf{R_{Cc}}$). The term I_{s_d} is added in F_{ex} to prevent the current part in the denominator to become negative, which would mean a value of F_{ex} larger than 1.

This factor F_{ex} is derived based on the DC currents. We also use it to modulate the diffusion charges. This is of course not completely correct. However for the case of diffusion charges where $Q \sim \tau\ I$ it should be a reasonable approximation.

 ©Koninklijke Philips Electronics N.V. 2005

5 Current crowding

The variable base resistance in Mextram is the resistance between the nodes B_1 and B_2. It is intended to describe the (effective) resistance of the part of the base under the emitter. This part of the base is in general thin. Hence a material parameter is the sheet resistance $\rho_\square$. With this quantity one should be able to calculate the base resistance. One should however bear in mind that the base current does not need to traverse the whole part of the base under the emitter. A part of the base current already enters the emitter at its boundary closest to the external base contact. Only a very small part will traverse to the part of the emitter furthest away from the base connection. The effective resistance thus depends on the geometry. It will be a (dimensionless) constant times the sheet resistance. We will determine this factor in Section 5.1.1.

There is also another effect which takes place in the part of the base discussed above. Due the current flowing through the base there will be a potential drop across this base region. For large currents this drop can be appreciable. The local voltage determines the local part of the main current. A voltage drop means that the main current is not everywhere under the emitter the same, but will be more or less concentrated at the position where the base current enters the region under the emitter. This effect is called current crowding. In Mextram this is taken into account by a variable base resistance, discussed in the next section. For the AC currents also an extra capacitance is introduced. This will be discussed in Section 5.2. Crowding also has an effect on the (thermal) noise, see Chapter 9, and is discussed in detail in Ref. [25].

In this chapter we consider only the most relevant geometries, that of a rectangular and of a circular emitter. Generalisations to more arbitrary geometries (but including also the two specific geometries) have been published in Ref. [47].

5.1 DC current crowding: the variable base resistance

To study DC current crowding [47, 48, 49] in the pinched base (under the emitter) we assume an emitter of length L_{em} and a width H_{em}. The emitter surface is $A_{\mathrm{em}} = H_{\mathrm{em}} L_{\mathrm{em}}$. We assume an effectively one-dimensional system, such that the coordinate along L_{em} is irrelevant. What we try to study is schematically shown in Fig. 16. We have two independent variables. One is the current $I(x)$, going from left to right through the resistive base. The other is the local potential $\mathcal{V}_{\mathrm{B}}(x)$. DC current crowding can be calculated using the equations

$$\frac{\mathrm{d}I}{\mathrm{d}x} = -\frac{J_s L_{\mathrm{em}}}{\boldsymbol{\beta}_{\mathsf{f}}} e^{(\mathcal{V}_{\mathrm{B}}(x)-\mathcal{V}_{\mathrm{E}_1})/V_T}, \tag{5.1a}$$

$$\frac{\mathrm{d}\mathcal{V}_{\mathrm{B}}}{\mathrm{d}x} = -\frac{\rho_\square}{L_{\mathrm{em}}} I(x). \tag{5.1b}$$

Here $\rho_\square$ is the pinch resistance of the base, $\boldsymbol{\beta}_{\mathsf{f}}$ is the forward current gain, and $J_s = \mathsf{I_S}/A_{\mathrm{em}}$ is the saturation current density. We neglect all non-ideal base currents. As schematically

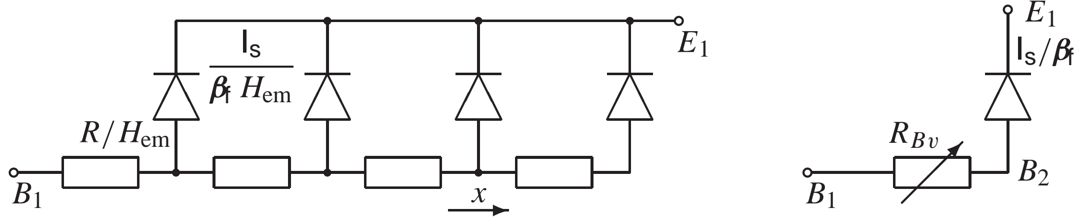

Figure 16: *On the left a circuit showing a simplified mode of the equations we try to solve for current crowding. On the right is the effective circuit, which is part of the Mextram equivalent circuit. For the diodes we have shown the corresponding saturation current.*

shown in Fig. 16, we assume a base connection at only one side. The boundary conditions are given by $I(x{=}0) = I_B$ and $I(x{=}H_{\rm em}) = 0$.

In Mextram the distributed system is modelled by the circuit shown in the right of Fig. 16. We just need to find an equation for the current from B_1 to B_2. The connection between the extrinsic base and the pinched (distributed) base is the node B_1. Hence we have $\mathcal{V}_{\rm B}(x{=}0) = \mathcal{V}_{\rm B_1}$. In Mextram we also have an expression for the base current, which goes from B_2 to E_1:

$$I_B = \frac{J_s L_{\rm em} H_{\rm em}}{\beta_{\rm f}} e^{\mathcal{V}_{\rm B_2E_1}/V_T}. \tag{5.2}$$

In this expression the node potential $\mathcal{V}_{\rm B_2}$ appears. Using the equations and the boundary conditions we need to find an expression for the base current between nodes B_1 and B_2, i.e. we need to give I_B as function of $\mathcal{V}_{\rm B_1B_2}$. For small values of $\mathcal{V}_{\rm B_1B_2}$ the current I_B will be proportional to this voltage difference. The parameter $\mathsf{R_{Bv}}$ will be chosen to reflect this ohmic behaviour for low voltages: $\mathcal{V}_{\rm B_1B_2} = I_B\, \mathsf{R_{Bv}}$.

To find the exact solution to the differential equations above, it is useful to refer all voltages to $\mathcal{V}_{\rm B_2}$, which is a kind of average over $\mathcal{V}_{\rm B}(x)$. (This also means that $\mathcal{V}_{\rm B_2}$ is not directly related to a certain position.) We therefore introduce

$$V(x) = \mathcal{V}_{\rm B}(x) - \mathcal{V}_{\rm B_2}, \tag{5.3}$$

and express the differential equations (5.1) in terms of this voltage difference:

$$\frac{\mathrm{d}I}{\mathrm{d}x} = -\frac{I_B}{H_{\rm em}} e^{V/V_T}, \tag{5.4a}$$

$$\frac{\mathrm{d}V}{\mathrm{d}x} = -\frac{\rho_\square}{L_{\rm em}} I. \tag{5.4b}$$

Note that there is no longer a reference to the saturation current or the current gain. This means that the expressions we find will be independent of the parameters belonging to the diode part! Combining the two equations in (5.4) we get

$$\frac{\mathrm{d}^2 I}{\mathrm{d}x^2} = -\frac{I_B}{H_{\rm em} V_T} e^{V/V_T} \frac{\mathrm{d}V}{\mathrm{d}x} = \cdots = \frac{\rho_\square}{2 L_{\rm em} V_T} \frac{\mathrm{d}I^2}{\mathrm{d}x}. \tag{5.5}$$

 ©Koninklijke Philips Electronics N.V. 2005

The solution to this equation can be given by [48]

$$I(x) = \frac{2V_T L_{\rm em}}{\rho_\square H_{\rm em}} \, Z \tan[Z(1 - x/H_{\rm em})]. \tag{5.6}$$

This solution is already such that $I(x{=}H_{\rm em}) = 0$. There is still one integration constant, Z, that can be found from the boundary condition at $x = 0$:

$$I_B = \frac{2V_T L_{\rm em}}{\rho_\square H_{\rm em}} \, Z \tan Z. \tag{5.7}$$

We can also find the voltage, by using again Eq. (5.4) and the solution for I:

$$e^{V/V_T} = \frac{Z}{\tan Z \;\cos^2[Z(1 - x/H_{\rm em})]}. \tag{5.8}$$

From this we find the voltage difference $\mathcal{V}_{\rm B_1B_2} = V(0)$ as

$$e^{\mathcal{V}_{\rm B_1B_2}/V_T} = \frac{Z}{\sin Z \;\cos Z}. \tag{5.9}$$

We see that Z plays an important role. From Z we can find both the current I_B and the voltage $\mathcal{V}_{\rm B_1B_2}$. Since the solution is only given in an implicit way, we need an approximate formula. We will do this, following Groendijk [49], by first looking at two limits.

Low current limit In the low current limit Z will be small and we can approximate Eqs. (5.7) and (5.9) by $I_B \simeq (2V_T L_{\rm em}/\rho_\square H_{\rm em})\, Z^2$ and $e^{\mathcal{V}_{\rm B_1B_2}/V_T} \simeq 1 + \frac{2}{3} Z^2$. This gives us

$$\frac{\mathcal{V}_{\rm B_1B_2}}{I_B} = \frac{\rho_\square H_{\rm em}}{3\, L_{\rm em}} = \mathsf{R_{Bv}}. \tag{5.10}$$

This gives us a definition of the parameter $\mathsf{R_{Bv}}$ in terms of the sheet resistance. (We will discuss this in some more detail in Section 5.1.1).

High current limit In the high current limit we have $Z \to \pi/2$. For the voltage difference we can then write

$$e^{\mathcal{V}_{\rm B_1B_2}/V_T} = \frac{Z \tan Z}{\sin^2 Z} \to Z \tan Z = I_B \frac{\rho_\square H_{\rm em}}{2V_T L_{\rm em}}. \tag{5.11}$$

This gives us

$$I_B = \frac{2V_T}{3\,\mathsf{R_{Bv}}} \, e^{\mathcal{V}_{\rm B_1B_2}/V_T}. \tag{5.12}$$

©Koninklijke Philips Electronics N.V. 2005

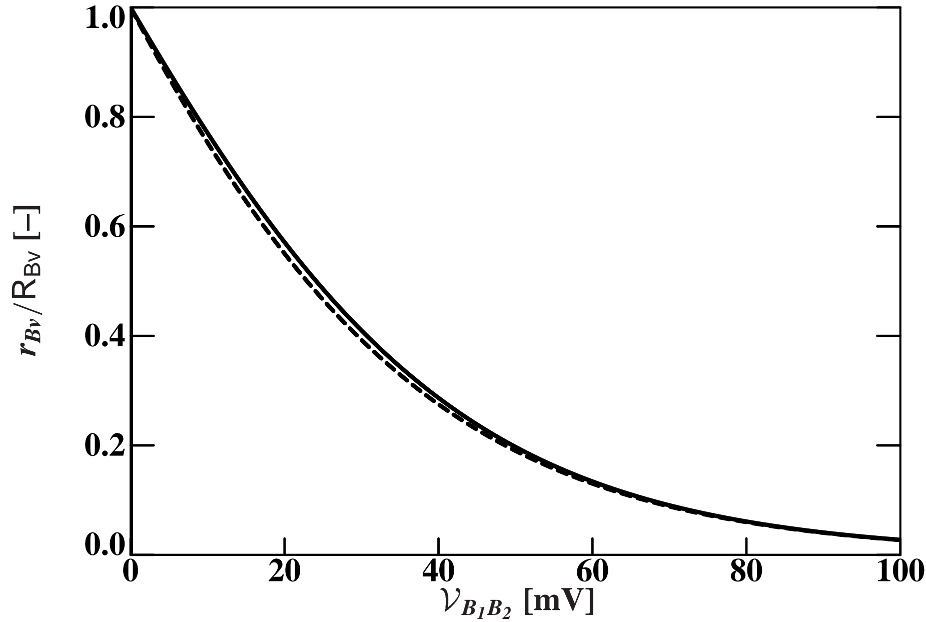

Figure 17: *The differential resistance* $\mathrm{d}\mathcal{V}_{\mathrm{B_1B_2}}/\mathrm{d}I_B$ *normalised on* $\mathsf{R_{Bv}}$*, both for the exact solution from Eqs. (5.7) and (5.9) (solid) and from the interpolation (5.14) (dashed).*

Interpolation We can now give an interpolation [49] between the low and the high current limits:

$$I_B = \frac{1}{3\,\mathsf{R_{Bv}}}\left[2V_T\left(e^{\mathcal{V}_{\mathrm{B_1B_2}}/V_T}-1\right)+\mathcal{V}_{\mathrm{B_1B_2}}\right]. \tag{5.13}$$

This interpolation is correct within 4% for $\mathcal{V}_{\mathrm{B_1B_2}} > 0$ and within 10% for $\mathcal{V}_{\mathrm{B_1B_2}} < 0$. The expression has the correct limits for $|V| \ll V_T$ and for $|V| \gg V_T$.

It is this interpolation that is used in Mextram. The full expression also includes a modulation of the pinch resistance due to the Early effect and high injection, when more charge[7] is present. This is similar to the discussion about the 'resistance' seen by the main current, as discussed below Eq. (1.16) in Chapter 1. We write

$\mathbf{I_{B_1B_2}}$

$$R_{B2} = \frac{3\,\mathsf{R_{Bv}}}{q_B}, \tag{5.14a}$$

$$I_{B_1B_2} = \frac{1}{R_{B2}}\left[2V_T\left(e^{\mathcal{V}_{\mathrm{B_1B_2}}/V_T}-1\right)+\mathcal{V}_{\mathrm{B_1B_2}}\right]. \tag{5.14b}$$

In Fig. 17 we have shown the differential resistance of both the exact solution and the interpolation formula. The correspondence is quite good.

Large negative base current We already mentioned that the interpolation can also be used for negative currents. This can be important when a transistor is used in normal

[7] Due to the fact that the hole charge is important, we use q_B^Q and not q_B^I in the formal model definition. See Chapter 6.

 ©Koninklijke Philips Electronics N.V. 2005

forward operation, but with a voltage on the collector larger than BV_{ceo}. The net base current (forward base current minus avalanche current) will then be negative. Also in this case current crowding can appear. But now, the part furthest away from the base contact will get the largest current. This means that the current, on average, must pass through more of the base resistance. The effective resistance will then increase from $\mathsf{R_{Bv}}$ to $3\,\mathsf{R_{Bv}} = \rho_{\Box} H_{em}/L_{em}$, i.e. the total resistance under the emitter.

We can also show this from the exact solution. For finding negative base currents we need to make Z imaginary. We therefore write $Z = j\xi$. This leads to a base current given by $I_B = -(2V_T L_{em}/\rho_{\Box} H_{em})\xi \tanh\xi$, and to $e^{\mathcal{V}_{B_1B_2}/V_T} = \xi/\sinh\xi\cosh\xi$. For very large ξ we then find

$$\mathcal{V}_{B_1B_2} = \frac{\rho H_{em}}{L_{em}} I_B = 3\,\mathsf{R_{Bv}} I_B. \tag{5.15}$$

In the situation of a large negative base current the transistor can collapse due to instabilities [50, 51]. Mextram does not model these instabilities, because the generation factor of the avalanche current is limited by G_{max}, see Section 3.6.1. For a total emitter current pinch-in (current crowding at the centre of the emitter) a model for the base resistance is needed in which the resistance goes to infinity for large negative base currents. The expression given below for a circular geometry, Eq. (5.19), is one such expression.

5.1.1 Determination of the small voltage resistance from the sheet resistance

In the previous subsection we have seen that we can calculate the parameter $\mathsf{R_{Bv}}$ from the pinch resistance $\rho_{\Box}$ and the geometry of the base. For the case of an emitter L_{em} long and H_{em} wide we found

$$\mathsf{R_{Bv}} = \tfrac{1}{3}\rho_{\Box} \frac{H_{em}}{L_{em}}. \tag{5.16}$$

The ratio H_{em}/L_{em} follows directly from Ohms law. The pre-factor however is dependent on the geometry and the number of base contacts. For a rectangular emitter and only a single base contact this pre-factor is $1/3$. When the base has a contact on either side, we can use symmetry and the previous result to find the pre-factor as $1/12$. (One factor of 2 comes from the fact that the current only needs to go half the distance. Then however the length is twice the effective width, which gives another factor of 2.) The same factor $1/12$ holds when a long rectangular base $L_{em} \gg H_{em}$ is contacted on all four sides.

In Appendix D we will give a method to calculate this pre-factor also in other geometries. Here we will only present two more results. For a square emitter ($H_{em} = L_{em}$) contacted at all sides the pre-factor is approximately $1/28.45$. For a circular emitter we find $\mathsf{R_{Bv}} = \rho_{\Box}/8\pi \simeq \rho_{\Box}/25.1$.

5.1.2 DC current crowding in a circular geometry

In practice the base is not always a rectangle contacted at two sides. For small emitters the base is often effectively contacted at all sides. It is not possible to give an exact solution of current crowding in that case. However, in the case of a pinched base in the shape of a disc, a solution is possible [52]. In the equations above, we have to replace L_{em} by the circumference $2\pi r$ at a distance r from the centre. The area is given by $A_{\mathrm{em}} = \pi R^2$, with R the radius of the pinched base. The equations then become

$$\frac{\mathrm{d}I}{\mathrm{d}r} = 2\pi r \frac{I_B}{A_{\mathrm{em}}} e^{V/V_T}, \tag{5.17a}$$

$$\frac{\mathrm{d}V}{\mathrm{d}r} = \frac{\rho_\square}{2\pi r} I. \tag{5.17b}$$

(The fact that r decreases when going from the boundary at R to the centre gives an extra minus sign.) These equations can be solved exactly:

$$I(r) = I_B \, \frac{r^2}{R^2 + (R^2 - r^2)\,\frac{\rho_\square I_B}{8\pi V_T}}. \tag{5.18}$$

With this solution we find, after some algebra similar to the case above, that the current through the pinched base is simply given by

$$I_B = \frac{V_T}{\mathsf{R_{Bv}}} \left(e^{\mathcal{V}_{\mathrm{B_1B_2}}/V_T} - 1 \right), \tag{5.19}$$

where $\mathsf{R_{Bv}} = \rho_\square / 8\pi$, as above.

5.1.3 DC current crowding in a rectangular geometry

No exact solution exists for current crowding in a square geometry, with contacts on all sides. An approximate expression was given in Ref. [53], and was found to be the same as Eq. (5.19), with a value of $\mathsf{R_{Bv}} = \rho_\square/32$. The exact low bias value of the resistance is given in Appendix D and is close to $\rho_\square/28.45$.

For rectangular geometries contacted on all sides a similar expression can be used [54], $I_B = g V_T/\mathsf{R_{Bv}} \times [\exp(\mathcal{V}_{\mathrm{B_1B_2}}/g V_T) - 1]$, where g is a geometry dependent factor of order 1, such that one obtains a good fit to the exact result for not too large crowding. Obviously it does not give the correct results in the limit of large $\mathcal{V}_{\mathrm{B_1B_2}}$ and in reverse.

5.2 AC current crowding

To describe AC current crowding [55] we first start with the case of small currents (no DC-crowding) and consider the capacitance. The circuit we want to approximate and the approximate circuit are both given in Fig. 18.

 ©Koninklijke Philips Electronics N.V. 2005

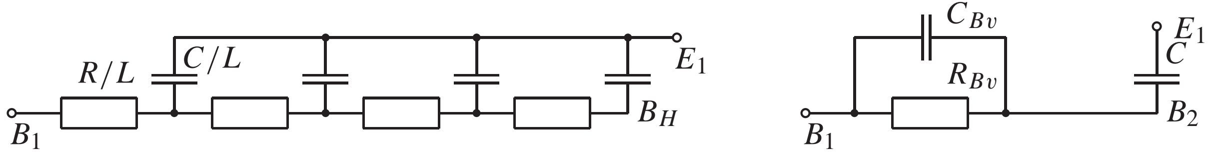

Figure 18: *On the left a circuit showing a kind of transmission line between base and emitter. On the right an effective circuit, as used in Mextram.*

The circuit consisting of the transmission line can be described using the differential equations

$$\frac{d\mathcal{V}_B}{dx} = -\frac{IR}{H_{em}}, \tag{5.20a}$$

$$\frac{dI}{dx} = -(\mathcal{V}_B - \mathcal{V}_{E_1})\frac{j\omega C}{H_{em}} = -(\mathcal{V}_B - \mathcal{V}_{E_1})\frac{z^2}{H_{em}R}, \tag{5.20b}$$

where we defined $z^2 = j\omega CR$. The resistance R and the capacitance C are the total resistance c.q. capacitance present. The solution is given by

$$\mathcal{V}_B(x) = \mathcal{V}_{E_1} + \frac{\mathcal{V}_{B_1E_1}\left(e^{z(1-\frac{x}{H_{em}})} - e^{-z(1-\frac{x}{H_{em}})}\right) + \mathcal{V}_{B_HE_1}\left(e^{\frac{zx}{H_{em}}} - e^{-\frac{zx}{H_{em}}}\right)}{e^z - e^{-z}}. \tag{5.21}$$

Using the same boundary condition $I(H_{em}) = 0$ as before, we find

$$\mathcal{V}_{B_HE_1} = \mathcal{V}_{B_1E_1} / \cosh z, \tag{5.22}$$

and consequently

$$I_B = I(0) = \frac{\mathcal{V}_{B_1E_1}}{R} z \tanh z. \tag{5.23}$$

From this we find that the voltage over the base-part is given by

$$\mathcal{V}_{B_1B_2} = \mathcal{V}_{B_1E_1} - I_B \times j\omega C = I_B R\, \frac{z \coth z - 1}{z^2}. \tag{5.24}$$

This means that we can write the current in terms of voltage as

$$I_B = \mathcal{V}_{B_1B_2}\frac{z^2}{R}\frac{1}{z\coth z - 1} \simeq \mathcal{V}_{B_1B_2}\left(\frac{3}{R} + \frac{z^2}{5R}\right) = \mathcal{V}_{B_1B_2}(3R^{-1} + \tfrac{1}{5}j\omega C). \tag{5.25}$$

This implies a parallel circuit containing a resistance and a capacity [55]

$$R_{Bv} = R/3, \tag{5.26a}$$

$$C_{Bv} = C/5. \tag{5.26b}$$

©Koninklijke Philips Electronics N.V. 2005

The factor $1/3$ we have seen before, calculating dc-current crowding for small currents. The capacitance is new. Of course one can also calculate higher order corrections, and try to find a more general fit to the exact result. We will not do this. Neither will we consider an expression including both high-currents (DC-crowding) and AC-crowding at the same time.

As discussed in Section 2.4.4, only when $\mathsf{EXPHI} = 1$ this capacitance model is used in Mextram. AC-current crowding is then modelled as a capacitance C_{Bv}, equal to the capacitance of the base-emitter junction divided by 5, parallel to the variable base resistance.

$\mathbf{Q_{B_1B_2}}$

$$C_{Bv} = \tfrac{1}{5}\left(\frac{\mathrm{d}Q_{t_E}}{\mathrm{d}\mathcal{V}_{\mathrm{B_2E_1}}} + \tfrac{1}{2}\,Q_{B0}\,q_1^Q\,\frac{\mathrm{d}n_0}{\mathrm{d}\mathcal{V}_{\mathrm{B_2E_1}}} + \frac{\mathrm{d}Q_E}{\mathrm{d}\mathcal{V}_{\mathrm{B_2E_1}}}\right), \tag{5.27a}$$

$$Q_{B_1B_2} = C_{Bv}\,\mathcal{V}_{\mathrm{B_1B_2}}. \tag{5.27b}$$

The total capacitance is taken as the derivative of the charge $Q_{t_E} + Q_{BE} + Q_E$ between the base and emitter junctions. Instead of taking the total derivative of Q_{BE}, we have taken $\frac{1}{2}Q_{B0}\,q_1^Q\mathrm{d}n/\mathrm{d}\mathcal{V}_{\mathrm{B_2E_1}}$, neglecting the derivatives of q_1^Q. This has only a very limited influence on the characteristics, but is simplifies the implementation a lot.

 ©Koninklijke Philips Electronics N.V. 2005

6 Heterojunction features

The model formulations presented in the previous chapters are satisfactory for describing standard Si transistors. Modern processes involve processes which have a part Ge in the base-region. These SiGe processes can, in many cases, be described using the same formulations as pure Si processes. The parameters will have different values of course, now directly related to, for instance, the bandgap narrowing in the base.

In a few cases, however, either the Ge that is present or the change in the doping profile result in effects that can not be modelled by the formulations given before. In these cases Mextram 504 offers two formulations [56], each with one extra parameter, to describe the effects.

6.1 Gradient in the Ge-profile

Let us start with recalling the description we use for the Early effect. We have seen that Gummel's charge control relation forms the basis of modern compact models. An important quantity is the total hole charge in the base Q_B. We have seen that when we neglect high injection effects, this base charge is a sum of Q_{B0}, the charge at zero bias, and the depletion charges Q_{t_E} and Q_{t_C}. We can write

$$Q_B = Q_{B0} + Q_{t_E} + Q_{t_C} = q A_{\text{em}} \int_{x_E}^{x_C} p(x)\, \mathrm{d}x. \tag{6.1}$$

Since we do not take high injection effects into account we can write $p(x) = N_A(x)$, the doping in the base. The limits of the integral are the boundaries of the neutral base region. At zero bias we define $x_E = 0$ and $x_C = W_{B0}$, and therefore have

$$Q_{B0} = q A_{\text{em}} \int_0^{W_{B0}} N_A(x)\, \mathrm{d}x. \tag{6.2}$$

When we assume a constant doping profile, we get even simpler equations:

$$Q_{B0} = q A_{\text{em}} N_A W_{B0}; \qquad Q_B = q A_{\text{em}} N_A (x_C - x_E). \tag{6.3}$$

This gives us directly the link between the variation in the depletion thicknesses and the depletion charges:

$$Q_{t_E} = q A_{\text{em}} N_A (0 - x_E); \qquad Q_{t_C} = q A_{\text{em}} N_A (x_C - W_{B0}). \tag{6.4}$$

If we now recall that in Mextram we do model the Early effect via the factor $q_0 = Q_B/Q_{B0}$ (see Section 2.3), we arrive at the following equations for the depletion thicknesses (again under the assumption of a constant base dope):

$$(0 - x_E) = \frac{V_{t_E}}{\mathsf{V_{er}}}; \qquad (x_C - W_{B0}) = \frac{V_{t_C}}{\mathsf{V_{ef}}}. \tag{6.5}$$

©Koninklijke Philips Electronics N.V. 2005

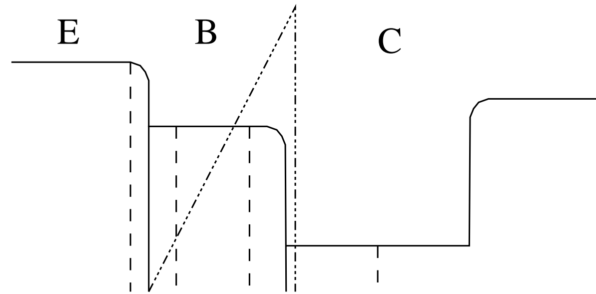

Figure 19: *Schematic doping profile for the case of a SiGe transistor which has a graded Ge content. The depletion layers are schematically shown with dashed lines. The triangular Ge-profile is shown with a dash-dotted line.*

Derivation The expressions we gave above are capable of modelling pure Si transistors, as well as SiGe transistors with a reasonably constant Ge profile. In some cases, however, the profile looks more like the one shown in Fig. 19: the Ge content is low at the emitter side and high at the collector side. This has a large influence on the description of the Early effect [57, 58, 59].

If one carefully looks at the derivation of Gummel's charge control relation [16, 60, 20], one sees that the current is not really determined by the base charge, but rather by the base Gummel number, defined, similar to Eq. (1.14), by

$$G_B = \int_{x_E}^{x_C} \frac{N_A(x)}{D_n(x)} \frac{n_{i0}^2}{n_i^2(x)} \, \mathrm{d}x, \tag{6.6}$$

where n_{i0} is a reference intrinsic carrier concentration (e.g. that of un-doped Si). This integral contains not only the variation of the doping profile, but also the variation of the diffusion constant and the intrinsic carrier concentration. For a pure Si transistor it suffices to take an average over the latter two quantities. The Gummel number then becomes

$$G_B = \overline{n_{i0}^2/n_i^2 D_n} \int_{x_E}^{x_C} N_A(x) \mathrm{d}x, \tag{6.7}$$

and therefore becomes proportional to the base charge Q_B.

In a SiGe transistor with a gradient in the Ge-content this is no longer allowed. The variation of the intrinsic carrier concentration is too large to just work with an average. For instance, at the collector side the Ge content is high, and therefore so is the intrinsic carrier concentration. That part of the base then has only a small contribution to the total Gummel number. A variation in the depletion layer edge is then also of minor importance. This means [61] that the forward Early effect is small (large effective forward Early voltage). The most important contribution to the Gummel number comes from the region where there is not much Ge: at the emitter edge. Any variation here of the depletion width has a large influence on the current: the reverse Early voltage is small. Even worse, the effective reverse Early voltage depends very much on whether the transistor is forward biased or reverse biased [56]. This variation of the Early voltage can not be

 ©Koninklijke Philips Electronics N.V. 2005

modelled by the formulation of the Early effect we have given before. Hence we need a new formulation.

To get an analytical formulation we will assume that the intrinsic carrier concentration can be written as

$$n_i^2 \propto \exp\left(\frac{x}{W_{B0}}\,\frac{\Delta\mathsf{E_g}}{kT}\right). \tag{6.8}$$

What we basically assume here is that the bandgap will decrease linearly: $E_g = E_{g0} - \Delta\mathsf{E_g}\, x/W_{B0}$, as was done in Ref. [62]. The major part of this bandgap grading will be due to the Ge, but part might also be a result of bandgap narrowing due to doping. The new parameter $\Delta\mathsf{E_g}$ is the difference in bandgap between the neutral edges of the base, at zero bias. It can therefore be estimated using process knowledge.

Since the variation of the intrinsic carrier concentration is dominant, we will, as before, assume a constant doping profile and diffusion constant. (It is maybe even better to say that any variation in doping profile and diffusion constant will effectively be taken into account by giving $\Delta\mathsf{E_g}$ an effective value.) The Gummel number can now be calculated as

$$\begin{aligned} G_B &= \overline{N_A n_{i0}^2/D_n}\int_{x_E}^{x_C}\exp\left(-\frac{x}{W_{B0}}\,\frac{\Delta\mathsf{E_g}}{kT}\right)\mathrm{d}x \\ &= \overline{N_A n_{i0}^2/D_n}\,\frac{kT\,W_{B0}}{\Delta\mathsf{E_g}}\left[\exp\left(-\frac{x_E}{W_{B0}}\,\frac{\Delta\mathsf{E_g}}{kT}\right) - \exp\left(-\frac{x_C}{W_{B0}}\,\frac{\Delta\mathsf{E_g}}{kT}\right)\right]. \end{aligned} \tag{6.9}$$

We can also find the Gummel number at zero bias:

$$G_{B0} = \overline{N_A n_{i0}^2/D_n}\,\frac{kT\,W_{B0}}{\Delta\mathsf{E_g}}\left[1 - \exp\left(-\frac{\Delta\mathsf{E_g}}{kT}\right)\right]. \tag{6.10}$$

Using furthermore the relations in Eq. (6.5) that give expressions for the depletion edges, we find for the ratio of the Gummel number and the Gummel number at zero bias:

$$\frac{G_B}{G_{B0}} = \frac{\exp\left(\left[\frac{V_{t_E}}{\mathsf{V_{er}}}+1\right]\frac{\Delta\mathsf{E_g}}{kT}\right) - \exp\left(\frac{-V_{t_C}}{\mathsf{V_{ef}}}\,\frac{\Delta\mathsf{E_g}}{kT}\right)}{\exp\left(\frac{\Delta\mathsf{E_g}}{kT}\right) - 1}. \tag{6.11}$$

It is important to realise that in the limit of $\Delta\mathsf{E_g} \to 0$ we get back our old relation

$$\frac{G_B}{G_{B0}} = 1 + \frac{V_{t_E}}{\mathsf{V_{er}}} + \frac{V_{t_C}}{\mathsf{V_{ef}}}. \tag{6.12}$$

©Koninklijke Philips Electronics N.V. 2005

Implementation We have seen that for the current we must not use the base charge, but rather the Gummel number. For the charge description, as well as for the base resistance of the pinched region, we still need the base charge. Both are modelled by a factor q_0, but now we make a distinction between a q_0 for current (I) and one for charges (Q):

$$q_0^Q = \frac{Q_B}{Q_{B0}} = 1 + \frac{V_{t_E}}{\mathsf{V_{er}}} + \frac{V_{t_C}}{\mathsf{V_{ef}}}, \tag{6.13a}$$

$$q_0^I = \frac{G_B}{G_{B0}} = \frac{\exp\left(\left[1 + \frac{V_{t_E}}{\mathsf{V_{er}}}\right]\frac{\Delta\mathsf{E_g}}{kT}\right) - \exp\left(\frac{-V_{t_C}}{\mathsf{V_{ef}}}\frac{\Delta\mathsf{E_g}}{kT}\right)}{\exp\left(\frac{\Delta\mathsf{E_g}}{kT}\right) - 1}. \tag{6.13b}$$

The normalised charge q_0^I (and also q_1^I, see Section 2.3.1) is now used in the expression for q_B^I, Eq. (2.50), that is used for the main current Eq. (2.1). The normalised charges q_0^Q and q_1^Q are used in the Early effect in the diffusion charges, Eq. (2.49), as well as in the expression for q_B^Q that is used in $I_{B_1B_2}$, Eq. (5.14). In the formal model definition [3, 1] we have used the superscripts in a consistent way, and never used the ambiguous expressions q_0, q_1 and q_B.

Effective Early voltages It can be useful to look at the effective Early voltages, and how they depend on the parameter $\Delta\mathsf{E_g}$. For simplicity we will consider the zero bias situation. The absolute values of the currents will be low, but the expressions for the effective Early voltages become quite simple. For these low biases we can approximate $V_{t_E} \simeq \mathcal{V}_{\rm BE}$ and $V_{t_C} \simeq \mathcal{V}_{\rm BC}$.

The forward Early voltage is normally found using the derivative of the current w.r.t. the collector voltage. We can write (see also Ref. [2])

$$V_{\textit{effective forward Early}} = I_C \left(\frac{\partial I_C}{\partial \mathcal{V}_{\rm CB}}\right)^{-1}. \tag{6.14}$$

Since the only collector voltage dependence (in normal forward operation) is in q_0 ($I_c \propto 1/q_0$), we can find the effective Early voltages using the derivative of $1/q_0$. The same holds for the reverse Early voltage. For the Early effect on the charges, as well as for the case of pure Si, we find (at zero bias)

$$V_{\textit{effective forward Early, charge}} = \left(\frac{\partial (q_0^Q)^{-1}}{\partial \mathcal{V}_{\rm CB}}\right)^{-1} = \mathsf{V_{ef}}, \tag{6.15a}$$

$$V_{\textit{effective reverse Early, charge}} = \left(\frac{\partial (q_0^Q)^{-1}}{\partial \mathcal{V}_{\rm EB}}\right)^{-1} = \mathsf{V_{er}}. \tag{6.15b}$$

We see here that in the case of pure Si the Early voltage parameters give the effective Early voltages at zero bias. The effective Early voltages at normal operating biases can differ from the parameters.

 ©Koninklijke Philips Electronics N.V. 2005

For the current in a SiGe transistor with a graded Ge content, we need to take the derivative of q_0^I. We then find

$$V_{\textit{effective forward Early, current}} = \left(\frac{\partial (q_0^I)^{-1}}{\partial \mathcal{V}_{\rm CB}}\right)^{-1} = \mathsf{V}_{\mathsf{ef}}\, \frac{e^{\Delta \mathsf{E}_\mathsf{g}/kT} - 1}{\Delta \mathsf{E}_\mathsf{g}/kT}, \tag{6.16a}$$

$$V_{\textit{effective reverse Early, current}} = \left(\frac{\partial (q_0^I)^{-1}}{\partial \mathcal{V}_{\rm EB}}\right)^{-1} = \mathsf{V}_{\mathsf{er}}\, \frac{1 - e^{-\Delta \mathsf{E}_\mathsf{g}/kT}}{\Delta \mathsf{E}_\mathsf{g}/kT}. \tag{6.16b}$$

In a typical case where $\Delta \mathsf{E}_\mathsf{g} \simeq 100\,\mathrm{eV} \simeq 4kT$, we find that the effective forward Early voltage has become $\simeq 13\,\mathsf{V}_{\mathsf{ef}}$, whereas the effective reverse Early voltage has become $\simeq 0.24\,\mathsf{V}_{\mathsf{er}}$. As mentioned in the introduction we indeed see a large forward Early voltage, and a small reverse Early voltage.

It is also important to realise that the Early voltage *parameters*, V_{er} and V_{ef}, have a value that corresponds to a pure Si transistor with the same doping as that of the SiGe transistor. In other words, the Early voltage parameters describe the Early voltages of the charges. The Early voltages of the currents are determined by the combination of the Early voltage parameters and $\Delta \mathsf{E}_\mathsf{g}$.

6.2 Early effect on the forward base current

Not all SiGe processes have a doping profile that can schematically be represented as in Fig. 19. Some transistors have a doping profile more similar to that in Fig. 20. Although the Ge-content now does not give rise to the need of an extra formulation, the very high base doping can cause extra recombination (e.g. Auger recombination) in the base. This means that neutral base recombination can become a significant part of the total base current. Auger recombination is a three particle process. In a normal NPN transistor its contribution of the base current scales with the integral of $p^2 n$, where the hole density p is equal to the base doping level since due to the high doping high injection effects in the base do not occur. This means that the recombination base current depends on the electron concentration n and, just as the collector current, on the width of the base. The base current therefore becomes collector voltage dependent: there is an Early effect on the base current.

In Mextram 504 we model this very empirically by writing for the ideal forward base current

$$I_{B_1} = \frac{\mathsf{I}_\mathsf{s}}{\beta_\mathsf{f}} \left(e^{\mathcal{V}_{\rm B_2E_1}/V_T} - 1\right)\left(1 + \mathsf{X}_{\mathsf{rec}}\, \frac{V_{t_C}}{\mathsf{V}_{\mathsf{ef}}}\right). \tag{6.17}$$

Note the similarity of the last term and the expression for the forward Early effect in the collector current, which is given by the factor q_0 of Eq. (2.16). The new parameter $\mathsf{X}_{\mathsf{rec}}$ determines the amount of the base current that is due to neutral base recombination (as opposed to hole injection into the emitter). The effective Early voltage of the base current

©Koninklijke Philips Electronics N.V. 2005

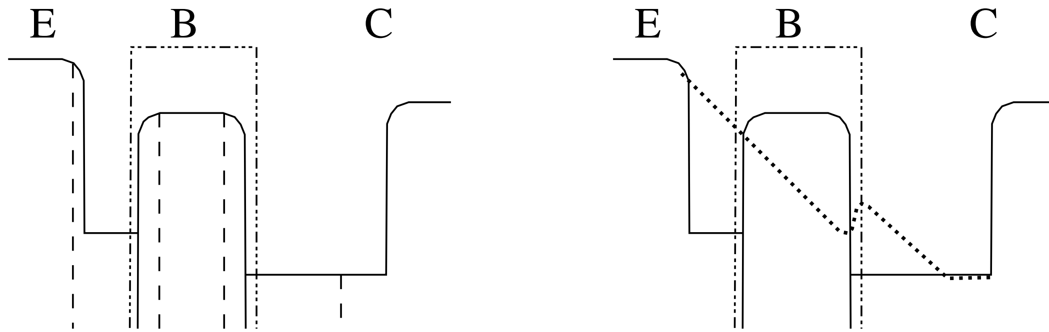

Figure 20: *Schematic doping profile for the case of a SiGe transistor which has a large base doping, an emitter cap and a constant Ge content. The Ge-profile is shown with a dash-dotted line. in the left figure the depletion layers are schematically shown with dashed lines. In the right figure we have added schematically the electron concentration (dotted) in case of high injection.*

is $\mathsf{V_{ef}}/\mathsf{X_{rec}}$. This formulation should suffice to model the collector-bias dependence of the forward base currents at not too high base-emitter biases.

It is important to realise that this formulation can also be used when the Early effect of the base current is not due to neutral base recombination, but due to other effects, like recombination at the SiGe-Si interface.

High injection effects We have mentioned before that the neutral base recombination current depends on the electron concentration in the base. It is well known that in the case of base widening (quasi-saturation, Kirk effect) the electron concentration at the collector side of the base increases very much, as schematically shown in Fig. 20. We need to take this into account in our formulation.

The base current contains two contributions: a part corresponding to the hole injection into the emitter, which scales with $\exp(\mathcal{V}_{\mathrm{B_2E_1}}/V_T)$, and a part corresponding to the neutral base recombination current. The latter contains the Early effect term, as well as a term for the increases in the electron density at the collector edge, which goes with $\exp(V^*_{B_2C_2}/V_T)$. The final formulation is then

$\mathbf{I_{B_1}}$

$$I_{B_1} \;\rightarrow\; \frac{\mathsf{I_{sT}}}{\beta_{\mathsf{fT}}}(1-\mathsf{XI_{B_1}})\Big[(1-\mathsf{X_{rec}})\;\left(e^{\mathcal{V}_{\mathrm{B_2E_1}}/V_T}-1\right) + \mathsf{X_{rec}}\left(e^{\mathcal{V}_{\mathrm{B_2E_1}}/V_T}+e^{V^*_{B_2C_2}/V_T}-2\right)\left(1+\frac{V_{t_C}}{\mathsf{V_{efT}}}\right)\Big]. \quad (6.18)$$

We also included the factor for splitting the base current between the intrinsic part and the extrinsic part $I^S_{B_1}$.

 ©Koninklijke Philips Electronics N.V. 2005

7 Temperature modelling

In this chapter we discuss the temperature model of Mextram. Many of the model parameters describe physical quantities that are dependent on the temperature. Since most parameters are effective parameters, rather than exact calculable quantities, also the temperature dependence should have some free fitting parameters. Since in practice it is difficult to determine the temperature parameters, we have chosen not to have too many parameters that describe the temperature behaviour. Instead, some electrical parameters share the same temperature parameter.

In Table 1 we have given the parameters that are independent of temperature. The rest of the parameters will be discussed below.

Table 1: *Temperature independent parameters. Not included are the temperature parameters themselves.*

LEVEL	$\mathsf{XI_{B_1}}$	$\mathsf{m_{Lf}}$	$\mathsf{SCR_{Cv}}$	$\mathsf{p_E}$	$\mathsf{C_{BEO}}$	$\mathsf{K_f}$
EXMOD	$\mathsf{XC_{j_E}}$	$\mathsf{V_{Lr}}$	$\mathsf{I_{hc}}$	$\mathsf{p_C}$	$\mathsf{C_{BCO}}$	$\mathsf{K_{fN}}$
EXPHI	$\mathsf{XC_{j_C}}$	$\mathsf{W_{avl}}$	$\mathsf{a_{xi}}$	$\mathsf{p_S}$	$\mathsf{R_{th}}$	$\mathsf{A_f}$
EXAVL	$\mathsf{X_{ext}}$	$\mathsf{V_{avl}}$	$\mathsf{m_\tau}$	$\mathsf{m_C}$	$\mathsf{C_{th}}$	
MULT	$\mathsf{X_{rec}}$	$\mathsf{S_{fh}}$				

7.1 Notation

It is convenient to mention something about notation. In the rest of this report, we give all parameters in a special font, e.g. $\mathsf{I_s}$. When we do this we implicitly mean the temperature corrected quantity. In this section however we need to distinguish between the given parameter $\mathsf{I_s}$ and the temperature corrected parameter $\mathsf{I_{sT}}$. So we add a subscript T when we mean a temperature corrected parameter.

7.2 Definitions

To describe the temperature effects we first need a few general definitions involving the temperature. We define for instance

$$T = \mathrm{TEMP} + \mathsf{dT_a} + 273.15 + \mathcal{V}_{\mathrm{dT}}, \tag{7.1a}$$

$$T_{\mathrm{ref}} = \mathsf{T_{ref}} + 273.15, \tag{7.1b}$$

$$t_N \equiv \frac{T}{T_{\mathrm{ref}}}, \tag{7.1c}$$

where $\mathcal{V}_{\mathrm{dT}}$ is the increase in temperature ΔT due to self-heating (see Chapter 8). We also need the difference in thermal voltage

$$\frac{1}{V_{\Delta T}} \equiv \frac{1}{V_T} - \frac{1}{V_{T_{\mathrm{ref}}}} = \frac{q}{k}\left(\frac{1}{T} - \frac{1}{T_{\mathrm{ref}}}\right). \tag{7.2}$$

©Koninklijke Philips Electronics N.V. 2005

7.3 General quantities

Let us start with the intrinsic carrier density. It is given by

$$n_i^2 = N_C N_V e^{-V_g/V_T}, \tag{7.3}$$

where V_g is the energy gap. Both N_C and N_V are proportional to $T^{3/2}$. Hence we can write

$$n_i^2 = n_{i,\mathrm{ref}}^2 \cdot t_N^3 \; e^{-V_g/V_{\Delta T}}. \tag{7.4}$$

To describe the resistances and some other quantities we need the mobility of various parts. The mobility depends on the dope and on the temperature. Furthermore it is different for a minority carrier and for a majority carrier, as well as different for holes and electrons. In principle, we therefore have 4 functions: $\mu_{p,\mathrm{maj}}$, $\mu_{p,\mathrm{min}}$, $\mu_{n,\mathrm{maj}}$, and $\mu_{n,\mathrm{min}}$. For a certain region, say the base in a NPN transistor, we need both $\mu_{p,\mathrm{maj}}$ and $\mu_{n,\mathrm{min}}$. Both depend on the same dope level. Although it is possible to give expressions that give these mobilities in terms of the doping level [63, 64], we will take a simplified approach and write

$$\mu \propto t_N^{-\mathsf{A}}, \tag{7.5}$$

where the parameter A takes the temperature dependence into account.

7.4 Depletion capacitances and diffusion voltages

The general formula for a diffusion voltage is given by

$$\begin{aligned} V_{d\mathrm{T}} &= V_T \ln \frac{N_A N_D}{n_i^2} = \frac{kT}{q} \ln \frac{N_A N_D}{n_{i,\mathrm{ref}}^2 \cdot t_N^3 e^{-V_g/V_{\Delta T}}} \\ &= t_N \, V_d - 3 V_T \ln t_N + V_g (1 - t_N), \end{aligned} \tag{7.6}$$

with at the reference temperature $V_d = V_T \ln(N_A N_D / n_{i,\mathrm{ref}}^2)$. For increasing temperatures this diffusion voltage will decrease. It might even go negative. This is not physical, but due to the fact that in the equation above it is assumed that the majority carrier concentration equals the doping concentration. For very high temperatures, however, the material will become intrinsic again. Once this happens, the formulations in our compact model, like those of the capacitances, are no longer valid. It is therefore not very useful to look for a physical formulation [65] of V_d which does not go through zero. Since, however, in some places in our formulations we divide by the diffusion voltage, we do need a way to prevent the diffusion voltage to become zero. We take a lower limit of $V_{\mathrm{d,low}} = 50\,\mathrm{mV}$ (a

 ©Koninklijke Philips Electronics N.V. 2005

model constant). For the three diffusion voltages in Mextram, we then get

$$U_{d_ET} = -3\,V_T\;\ln t_N + \mathsf{V}_{\mathsf{d_E}}\;t_N + (1-t_N)\;\mathsf{V}_{\mathsf{g_B}}, \tag{7.7a}$$
$$\mathsf{V}_{\mathsf{d_ET}} = U_{d_ET} + V_T\ln\{1+\exp[(V_{\mathrm{d,low}} - U_{d_ET})/V_T]\}, \tag{7.7b}$$
$$U_{d_CT} = -3\,V_T\;\ln t_N + \mathsf{V}_{\mathsf{d_C}}\;t_N + (1-t_N)\;\mathsf{V}_{\mathsf{g_C}}, \tag{7.7c}$$
$$\mathsf{V}_{\mathsf{d_CT}} = U_{d_CT} + V_T\ln\{1+\exp[(V_{\mathrm{d,low}} - U_{d_CT})/V_T]\}, \tag{7.7d}$$
$$U_{d_ST} = -3\,V_T\;\ln t_N + \mathsf{V}_{\mathsf{d_S}}\;t_N + (1-t_N)\;\mathsf{V}_{\mathsf{g_S}}, \tag{7.7e}$$
$$\mathsf{V}_{\mathsf{d_ST}} = U_{d_ST} + V_T\ln\{1+\exp[(V_{\mathrm{d,low}} - U_{d_ST})/V_T]\}. \tag{7.7f}$$

A depletion capacitance is in general given by

$$C_j = \frac{\varepsilon A}{x_d}, \tag{7.8}$$

where x_d is the thickness of the depletion region, A the surface, and ε the dielectric constant. For zero voltage and for grading coefficient p we have

$$x_{d0} \propto (V_d)^p. \tag{7.9}$$

This means that the temperature dependence of the capacity at zero voltage is given by

$$C_{j\mathrm{T}} = C_j\left(\frac{V_d}{V_{d\mathrm{T}}}\right)^p. \tag{7.10}$$

We can use this directly for the emitter-base and collector-substrate junctions:

$$\mathsf{C_{j_ET}} = \mathsf{C_{j_E}}\left(\frac{\mathsf{V_{d_E}}}{\mathsf{V_{d_ET}}}\right)^{\mathsf{p_E}}, \tag{7.11a}$$
$$\mathsf{C_{j_ST}} = \mathsf{C_{j_S}}\left(\frac{\mathsf{V_{d_S}}}{\mathsf{V_{d_ST}}}\right)^{\mathsf{p_S}}. \tag{7.11b}$$

For the base-collector depletion capacitance $\mathsf{C_{j_C}}$ we need some more work, since it consists of a constant part and a variable part (see Section 2.2.4). We can write, with $\mathsf{X_p} = \varepsilon A_{\mathrm{base}}/W_{\mathrm{epi}}$,

$$C(V) = \frac{\varepsilon A_{\mathrm{base}}}{x_{d0}}\left(\frac{1 - x_{d0}/W_{\mathrm{epi}}}{(1-V/V_d)^p} + \frac{x_{d0}}{W_{\mathrm{epi}}}\right). \tag{7.12}$$

From this we find

$$C_{j_0} = \frac{\varepsilon A_{\mathrm{base}}}{x_{d0}}; \qquad \mathsf{X_p} = \frac{x_{d0}}{W_{\mathrm{epi}}}. \tag{7.13}$$

Since both ε and $W_{\rm epi}$ are temperature independent, so is $C_{j_0}\,\mathsf{X_p}$. Hence we have in all cases

$$\mathsf{X_{pT}} = \mathsf{X_p}\,\frac{\mathsf{C_{j_C}}}{\mathsf{C_{j_C T}}}. \tag{7.14}$$

If we assume that around zero bias there is only a real depletion capacitance (no effect of the finite epilayer thickness), we also have

$$\mathsf{C_{j_C T}} = \mathsf{C_{j_C}}\left(\frac{\mathsf{V_{d_C}}}{\mathsf{V_{d_C T}}}\right)^{\mathsf{p_C}}. \tag{7.15}$$

This latter formula is however not the one implemented in Mextram. The reason for this is as follows. The model for C_j is an approximation to a model which has a normal dependence for $V > -V_c$ and which is constant for $V < -V_c$, for some critical V_c. The constant part is of course given by $\mathsf{C_{j_C}}\,\mathsf{X_p}$. The variable part is given by $\mathsf{C_{j_C}}/(1 - V/\mathsf{V_{d_C}})^q$, where q is the realistic grading coefficient. It should be this q that is used in the temperature dependence of $\mathsf{C_{j_C}}$. How do we determine this q? This can be done by demanding that the derivative of C_j at $V = 0$ is the same for both this model as well as the model that is implemented in Mextram. We then find $q = \mathsf{p_C}(1 - \mathsf{X_p})$. Hence we write

$$\mathsf{C_{j_C T}} = \mathsf{C_{j_C}}\left(\frac{\mathsf{V_{d_C}}}{\mathsf{V_{d_C T}}}\right)^{\mathsf{p_C}(1-\mathsf{X_p})}. \tag{7.16}$$

The capacitance increases less strongly than with only the power $\mathsf{p_C}$. In Mextram this smaller increase is modelled as

$$\mathsf{C_{j_C T}} = \mathsf{C_{j_C}}\left[(1-\mathsf{X_p})\left(\frac{\mathsf{V_{d_C}}}{\mathsf{V_{d_C T}}}\right)^{\mathsf{p_C}} + \mathsf{X_p}\right]. \tag{7.17}$$

This expression is appealing, since it is similar to the expression for the capacitance itself. The reason for this choice is arbitrary and historical. Note that around $\mathsf{V_{d_C}} = \mathsf{V_{d_C T}}$ both expressions give the same result. Since the difference between the two expressions is not too large, we chose not to change the expression used in Mextram 503 and keep with Eq. (7.17).

7.5 Resistances

In Mextram all temperature dependencies of the resistances are modelled with a power law. These resistances are directly linked to the mobilities. This means that the corresponding temperature parameters will also influence other quantities that depend on these mobilities, like saturation currents and gain factors. The general formula for the temperature dependence of a mobility becomes

$$\mu \sim t_N^{-\mathsf{A}}, \tag{7.18}$$

 ©Koninklijke Philips Electronics N.V. 2005

with parameter A depending on the local doping, and therefore on the region of the transistor.

The temperature dependence of the resistances is then

$$\mathsf{R}_{\mathsf{ET}} = \mathsf{R}_{\mathsf{E}}\, t_N^{\mathsf{A}_{\mathsf{E}}}, \tag{7.19a}$$

$$\mathsf{R}_{\mathsf{BcT}} = \mathsf{R}_{\mathsf{Bc}}\, t_N^{\mathsf{A}_{\mathsf{ex}}}, \tag{7.19b}$$

$$\mathsf{R}_{\mathsf{CcT}} = \mathsf{R}_{\mathsf{Cc}}\, t_N^{\mathsf{A}_{\mathsf{C}}}, \tag{7.19c}$$

$$\mathsf{R}_{\mathsf{CvT}} = \mathsf{R}_{\mathsf{Cv}}\, t_N^{\mathsf{A}_{\mathsf{epi}}}, \tag{7.19d}$$

with parameters A_{E}, A_{ex}, A_{C}, $\mathsf{A}_{\mathsf{epi}}$.

For the sheet-resistance of the base we can write

$$\rho_{\square} = \frac{A_{\mathrm{em}}}{\mu_{p,B}\, Q_{B0}}. \tag{7.20}$$

It is important to realise that Q_{B0} also depends on temperature. This is due to the change in depletion layer width as function of temperature (a variation of the base width), and a little on the change in ionisation factor. For our model we must model the temperature dependence of Q_{B0}, even though it is not a parameter. For simplicity we write:

$$\frac{Q_{B0\mathrm{T}}}{Q_{B0}} = t_N^{\mathsf{A}_{\mathsf{Q_{B0}}}}. \tag{7.21}$$

The temperature dependence of the intrinsic base resistance now becomes

$$\mathsf{R}_{\mathsf{BvT}} = \mathsf{R}_{\mathsf{Bv}}\, t_N^{\mathsf{A}_{\mathsf{B}}-\mathsf{A}_{\mathsf{Q_{B0}}}}. \tag{7.22}$$

7.6 Currents

Let us consider the saturation current,

$$I_s = \frac{q^2 D_n A_{\mathrm{em}}^2 n_i^2}{Q_{B0}}. \tag{7.23}$$

The diffusion constant $D_n = \mu_n\, V_T$ depends on the mobility of the intrinsic base, whose temperature dependence is modelled by A_{B}, multiplied by the temperature via $V_T \propto T$. The intrinsic carrier concentration is proportional to T^3, and contains an exponential dependence on the bandgap. As we have seen, Q_{B0} also depends on temperature with parameter $\mathsf{A}_{\mathsf{Q_{B0}}}$. This means that we could write

$$\mathsf{I}_{\mathsf{sT}} = \mathsf{I}_{\mathsf{s}}\, t_N^{4-\mathsf{A}_{\mathsf{B}}-\mathsf{A}_{\mathsf{Q_{B0}}}}\ \exp[-\mathsf{V}_{\mathsf{g_B}}/V_{\Delta T}]. \tag{7.24a}$$

According to this scaling rule, the temperature dependence of the collector saturation current I_{sT} is expressed in terms of parameters that are shared with the temperature scaling rules for the emitter-base diffusion voltage (7.7a), the zero bias base charge (7.21) and the intrinsic base resistance (7.22). Such a sharing of parameters usually reduces the burden of parameter extraction and is therefore generally considered as an advantage of the model. Upto and including version 504.5, the rule (7.24a) was the temperature scaling rule for the collector saturation current in Mextram. To provide more flexibility however, in Mextram 504.6, the independent parameter $\mathsf{dA}_{\mathsf{I_s}}$, having a default value 0, was added:

$$\mathsf{I}_{\mathsf{sT}} = \mathsf{I}_{\mathsf{s}}\, t_N^{4-\mathsf{A}_\mathsf{B}-\mathsf{A}_{\mathsf{Q_{B0}}}+\mathsf{dA}_{\mathsf{I_s}}} \;\exp[-\mathsf{V}_{\mathsf{g_B}}/V_{\Delta T}]\ . \tag{7.24b}$$

The current gain can be expressed as

$$\beta_\mathsf{f} = \frac{G_E}{G_B}. \tag{7.25}$$

The temperature dependence of the base Gummel number can be related to that of the saturation current, since $I_s = qn_{i0}^2/G_B$. Here n_{i0} is the value of the intrinsic carrier concentration at the reference temperature. The temperature dependence of the emitter Gummel number can be given as

$$G_E \propto \frac{1}{D_p n_{ie}^2} \propto \frac{1}{T\mu_p n_{ie}^2} \propto \mu_p^{-1} T^{-4} e^{V_{gE}/V_{\Delta T}}. \tag{7.26}$$

Note that there is no temperature dependent charge-component like Q_{B0} in the emitter. This leads to a temperature dependence of the current gain

$$\beta_{\mathsf{fT}} = \beta_\mathsf{f}\, t_N^{\mathsf{A}_\mathsf{E}-\mathsf{A}_\mathsf{B}-\mathsf{A}_{\mathsf{Q_{B0}}}} \;\exp[-\mathsf{dV}_{\mathsf{g}\beta\mathsf{f}}/V_{\Delta T}]. \tag{7.27}$$

Here $\mathsf{dV}_{\mathsf{g}\beta\mathsf{f}} = \mathsf{V}_{\mathsf{g_B}} - V_{gE}$ is the difference between the bandgap in the base and in the emitter. Normally it is positive, but for a SiGe-base it might be negative. In the same way, we write for the reverse current gain:

$$\beta_{\mathsf{riT}} = \beta_{\mathsf{ri}} \;\exp[-\mathsf{dV}_{\mathsf{g}\beta\mathsf{r}}/V_{\Delta T}], \tag{7.28}$$

where β_{ri} is the the difference between the bandgap in the base and in the collector.

We also have the recombination current, the non-ideal base current. At high injection this current can be given by

$$I_{B_2} = \frac{q A_{\mathrm{em}} L_{\mathrm{eff}}\, n_i}{\tau_0}\; e^{\mathcal{V}_{\mathrm{B_2E_1}}/2\,V_T}. \tag{7.29}$$

Here L_{eff} is some effective length not incorporated in Mextram. The inverse of the mean free collision time τ_0^{-1} scales with the thermal velocity $v_{\mathrm{th}} \propto T^{1/2}$. This means that the pre-factor scales with n_i/τ_0 or, in the case $\mathsf{m}_{\mathsf{Lf}} = 2$:

$$\mathsf{I}_{\mathsf{BfT}} = \mathsf{I}_{\mathsf{Bf}}\, t_N^2 \;\exp[-\mathsf{V}_{\mathsf{g_j}}/2\,V_{\Delta T}]. \tag{7.30}$$

 ©Koninklijke Philips Electronics N.V. 2005

This non-ideal base current has its own bandgap $\mathsf{V_{g_j}}$, which should be the bandgap of the region with the most recombination.

When $\mathsf{m_{Lf}}$ becomes smaller, and close to 1, the non-ideal base current I_{B_2} is almost ideal (it no longer models recombination). This must be reflected in the temperature dependence, such that the temperature behaviour becomes similar as that of $I_{B_1} \propto \mathsf{I_s}/\beta_\mathsf{f}$ (where we will neglect $\mathsf{A_E}$). Hence we need a pre-factor t_N^4, when $\mathsf{m_{Lf}} \to 1$. We interpolate between the two cases and get

$$\mathsf{I_{BfT}} = \mathsf{I_{Bf}}\; t_N^{(6-2\mathsf{m_{Lf}})}\; \exp[-\mathsf{V_{g_j}}/\mathsf{m_{Lf}}\; V_{\Delta T}]. \tag{7.31}$$

For the reverse non-ideal base current we do not need the extra precaution and write (without extra parameter)

$$\mathsf{I_{BrT}} = \mathsf{I_{Br}}\; t_N^2\; \exp[-\mathsf{V_{gC}}/2\; V_{\Delta T}]. \tag{7.32}$$

Next we consider the knee currents, given by

$$\mathsf{I_k} = \frac{4\, D_n}{W_B^2} Q_{B0}. \tag{7.33}$$

The temperature dependence of D_n and Q_{B0} is known. For the width we will take the simplifying approximation $W_B^2 \propto Q_{B0}$, such that the Q_{B0}-dependence is not in $\mathsf{I_k}$:

$$\mathsf{I_{kT}} = \mathsf{I_k}\; t_N^{1-\mathsf{A_B}}. \tag{7.34}$$

The expressions for the substrate current are now rather straightforward. We assume that the effective thickness of the base of the parasitic PNP (i.e. the collector buried layer) does not vary with temperature, or at least that this variation is negligible. The temperature rules for the substrate currents are then given by the accordingly simplified counterpart of Eq. (7.24a) and a modified version of Eq. (7.34):

$$\mathsf{I_{SsT}} = \mathsf{I_{Ss}}\; t_N^{4-\mathsf{A_S}}\; \exp[-\mathsf{V_{gS}}/\, V_{\Delta T}], \tag{7.35a}$$

$$\mathsf{I_{ksT}} = \mathsf{I_{ks}}\; t_N^{1-\mathsf{A_S}}\; \frac{\mathsf{I_{sT}}}{\mathsf{I_s}}\, \frac{\mathsf{I_{Ss}}}{\mathsf{I_{SsT}}}. \tag{7.35b}$$

For the substrate knee current we have to take into account that in the expression for the substrate current we actually use $\mathsf{I_s}/\mathsf{I_{ks}}$, instead of $\mathsf{I_{Ss}}/\mathsf{I_{ks}}$. This is reflected in the temperature rule.

For the mobility we use the parameter $\mathsf{A_S}$, which must be related to the mobility of the n-region most important for the Gummel number of the substrate current. We must make a distinction between two kinds of buried layers. A closed buried layer is a layer beneath all of the base region and closed in by some form of isolation (e.g. pn-isolation or deep trench isolation). There is no current path from base to substrate that does not go through the buried layer. The n-region that determines the Gummel number of the substrate current

is the highly doped buried layer, and therefore $\mathsf{A_S} = \mathsf{A_C}$. An open buried layer, present in older processes, is not beneath all of the base layer. Hence there is a current path from base to substrate, without going through the buried layer. The n-region that determines the Gummel number of the substrate current is now the epilayer, and $\mathsf{A_S} = \mathsf{A_{epi}}$.

7.7 Early voltages

The temperature rule for the Early voltages follows from the relations $\mathsf{V_{er}} = Q_{B0}/(1 - \mathsf{XC_{j_E}})\,\mathsf{C_{j_E}}$ and $\mathsf{V_{ef}} = Q_{B0}/\mathsf{XC_{j_C}}\,\mathsf{C_{j_C}}$, given in Section 2.3. Hence

$$\mathsf{V_{efT}} = \mathsf{V_{ef}}\, t_N^{\mathsf{A_{Q_{B0}}}} \left[(1 - \mathsf{X_p}) \left(\frac{\mathsf{V_{d_C}}}{\mathsf{V_{d_CT}}} \right)^{\mathsf{p_C}} + \mathsf{X_p} \right]^{-1}, \tag{7.36a}$$

$$\mathsf{V_{erT}} = \mathsf{V_{er}}\, t_N^{\mathsf{A_{Q_{B0}}}} \left(\frac{\mathsf{V_{d_E}}}{\mathsf{V_{d_ET}}} \right)^{-\mathsf{p_E}}. \tag{7.36b}$$

Note that these Early parameters are independent of the Ge-content, see Chapter 6.

7.8 Transit times

The transit time of the base is physically given by $\tau_{\mathsf{B}} = W_B^2/4D_n$. Assuming again, as we did for the very closely related knee current, that $W_B^2 \propto Q_{B0}$, we get

$$\tau_{\mathsf{BT}} = \tau_{\mathsf{B}}\, t_N^{\mathsf{A_{Q_{B0}}} + \mathsf{A_B} - 1}, \tag{7.37}$$

where we used the Einstein relation $D_n = \mu_n\, V_T$ to describe the temperature dependence of the diffusion constant D_n in the base.

The transit time of the epilayer is, similar to the base transit time, given by $\tau_{\mathsf{epi}} = W_{\mathsf{epi}}^2/4D_n$. The epilayer thickness is assumed constant, and the diffusion constant now belongs to the epilayer. Hence we get

$$\tau_{\mathsf{epiT}} = \tau_{\mathsf{epi}}\, t_N^{\mathsf{A_{epi}} - 1}. \tag{7.38}$$

The reverse transit time is simply the sum of the base and epilayer transit times, multiplied by an area ratio independent of temperature. The temperature rule of the reverse transit time is then simply

$$\tau_{\mathsf{RT}} = \tau_{\mathsf{R}}\, \frac{\tau_{\mathsf{BT}} + \tau_{\mathsf{epiT}}}{\tau_{\mathsf{B}} + \tau_{\mathsf{epi}}}. \tag{7.39}$$

The temperature dependence of the emitter transit time takes some more effort. The best physical basis is given when we assume that the emitter charge is the neutral charge in the base-emitter depletion region [26]. It is then given by

$$Q_E = 2\, V_T\, C_{\mathrm{depl}}\, e^{(\mathcal{V}_{\mathrm{B_2E_1}} - \mathsf{V_{d_E}})/2\, V_T}. \tag{7.40}$$

 ©Koninklijke Philips Electronics N.V. 2005

Here C_{depl} is the depletion capacitance, which we here assume to be constant, both as function of bias and temperature (its variation is small anyhow). Furthermore, we can use that $e^{-\mathsf{V}_{\mathsf{d}_\mathsf{E}}/2\,V_T} = n_i/N_E$, where N_E is the doping in the emitter. This gives us then the temperature dependence of Q_E.

The expression for the charge, given in Eq. (7.40), implies $\mathsf{m}_\tau = 2$. The expression for the charge, in Mextram terms, is then

$$Q_E = \tau_\mathsf{E}\sqrt{\mathsf{I_s}\,\mathsf{I_k}}\;\; e^{\mathcal{V}_{\mathrm{B_2E_1}}/2\,V_T}. \tag{7.41}$$

We are interested in the temperature dependence of the transit time parameter. We know already the temperature dependence of all the parameters used in Eq. (7.41), except τ_E, as well as that of Q_E, as discussed above. Combining these temperature dependences, we get

$$\tau_\mathsf{E} \propto \frac{t_N \cdot t_N^{3/2}\, e^{-V_{g_E}/2\,V_T}}{t_N^{2-\mathsf{A_B}/2}\, e^{-V_{g_B}/2\,V_T} \cdot t_N^{1/2-\mathsf{A_B}/2}} \propto t_N^{\mathsf{A_B}}\;\exp[-(V_{g_E} - V_{g_B})/2\,V_T]. \tag{7.42}$$

For simplicity we neglected the temperature dependence of Q_{B0}.

In alternative cases, Q_E just describes the hole charge due to the hole current (the base current) in the emitter. The corresponding charge will go as

$$Q_E = \frac{q\,A_{\text{em}} W_E n_i^2}{N_E}\; e^{\mathcal{V}_{\mathrm{B_2E_1}}/V_T}. \tag{7.43}$$

In Mextram terms, with $\mathsf{m}_\tau = 1$, we have

$$Q_E = \tau_\mathsf{E}\,\mathsf{I_s}\, e^{\mathcal{V}_{\mathrm{B_2E_1}}/V_T}. \tag{7.44}$$

For the transit time parameter we thus get

$$\tau_\mathsf{E} \propto t_N^{(\mathsf{A_B}-1)}\;\exp[-(V_{g_E} - V_{g_B})/V_T]. \tag{7.45}$$

Interpolating between the two expressions, we get

$$\tau_{\mathsf{E}\mathrm{T}} = \tau_\mathsf{E}\; t_N^{(\mathsf{A_B}-2+\mathsf{m}_\tau)}\;\exp[-(V_{g_E} - V_{g_B})/\mathsf{m}_\tau\,V_T]. \tag{7.46}$$

To keep closer to the Mextram 503 formulation, and to make the temperature dependence of τ_E independent of m_τ we take for the temperature parameter in Mextram 504:

$$\tau_{\mathsf{E}\mathrm{T}} = \tau_\mathsf{E}\; t_N^{(\mathsf{A_B}-2)}\;\exp[-\mathsf{dV}_{\mathsf{g}\tau_\mathsf{E}}/V_{\Delta T}]. \tag{7.47}$$

where the new parameter is physically given by $\mathsf{dV}_{\mathsf{g}\tau_\mathsf{E}} = (V_{g_E} - V_{g_B})/\mathsf{m}_\tau\,V_T$.

7.9 Avalanche constant

The Mextram parameters for avalanche are temperature independent. However, the material constant B_n used in the avalanche model *is* taken temperature dependent. Its dependence is based on the work of Ref. [44, 45], and given by

$$B_{n\mathrm{T}} = B_n\ [1 + 7.2 \cdot 10^{-4}\ (T_K - 300) - 1.6 \cdot 10^{-6}\ (T_K - 300)^2]. \tag{7.48}$$

Note that this temperature rule is independent of $\mathsf{T}_{\mathsf{ref}}$ since B_n is a material constant.

7.10 Heterojunction features

The parameter $\mathsf{dE_g}$ is the difference between the bandgap at the two ends of the neutral region. Hence, for a constant gradient in the bandgap, the parameter scales with the neutral base width W_B, or with Q_{B0}. We then get simply

$$\mathsf{dE}_{\mathsf{g}\mathrm{T}} = \mathsf{dE_g}\ t_N^{\mathsf{A}_{\mathsf{Q_{B0}}}}. \tag{7.49}$$

7.11 Thermal resistance

Since the thermal conductance decreases with temperature, the thermal resistance increases with temperature. This is modelled as

$$\mathsf{R_{th,Tamb}} = \mathsf{R_{th}} \cdot \left(\frac{T_{\mathrm{amb}}}{T_{RK}}\right)^{\mathsf{A_{th}}}. \tag{7.50}$$

Please note that this temperature depedence is given in terms of the ambient temperature

$$T_{\mathrm{amb}} = \mathrm{TEMP} + \mathsf{DTA} + 273.15, \tag{7.51}$$

and not in terms of the junction temperature T_K. For a more detailed discussion see Ref. [66] or the report [67].

 ©Koninklijke Philips Electronics N.V. 2005

8 Self-heating and mutual heating

In general a transistor will dissipate power. The generated power has an influence on the temperature of the device and its surroundings. Hence, due to the power dissipation the device will get warmer. This is called self-heating. To describe self-heating we need to consider two things: what is the dissipated power and what is the relation between the dissipated power and the increase in temperature. A more detailed discussion of the usage of self-heating is given in Ref. [67].

8.1 Dissipated power

The power that flows into a device can be calculated as a sum over currents times voltage drops. For instance for a three-terminal bipolar transistor we can write

$$P = I_C \, \mathcal{V}_{\mathrm{CE}} + I_B \, \mathcal{V}_{\mathrm{BE}}. \tag{8.1}$$

Since normally the collector current is larger than the base current and the collector voltage is larger than the base voltage, the first term is usually dominant.

Not all the power that flows into a transistor will be dissipated. Part of it will be stored as the energy on a capacitor. This part can be released later on. So to calculate the *dissipated* power, we need to add all the contributions of the dissipated elements, i.e., all the DC currents times their voltage drops. In Mextram we then get

$$\begin{aligned} P_{\mathrm{diss}} \;=\; & I_N \, (\mathcal{V}_{\mathrm{B_2E_1}} - V^*_{B_2C_2}) + I_{C_1C_2} \, (V^*_{B_2C_2} - \mathcal{V}_{\mathrm{B_2C_1}}) - I_{\mathrm{avl}} \, V^*_{B_2C_2} \\ & + \mathcal{V}^2_{\mathrm{EE_1}}/\mathsf{R_E} + \mathcal{V}^2_{\mathrm{CC_1}}/\mathsf{R_{Cc}} + \mathcal{V}^2_{\mathrm{BB_1}}/\mathsf{R_{Bc}} \\ & + I_{B_1B_2} \, \mathcal{V}_{\mathrm{B_1B_2}} + (I_{B_1} + I_{B_2})\mathcal{V}_{\mathrm{B_2E_1}} + I^S_{B_1} \, \mathcal{V}_{\mathrm{B_1E_1}} \\ & + (I_{\mathrm{ex}} + I_{B_3} + I_{\mathrm{sub}}) \, \mathcal{V}_{\mathrm{B_1C_1}} + (XI_{\mathrm{ex}} + XI_{\mathrm{sub}}) \, \mathcal{V}_{\mathrm{BC_1}} \\ & + (XI_{\mathrm{sub}} + I_{\mathrm{sub}} - I_{\mathrm{Sf}}) \, \mathcal{V}_{\mathrm{C_1S}}. \end{aligned} \tag{8.2}$$

The difference between the power flow into the transistor and the dissipated power, as calculated above, must then be stored in the capacitances. In Mextram, as in other compact models, the capacitances are not ideal. Instead they can depend on more than one voltage. In that case it is no longer true that the capacitance (or rather the charge) does not dissipate. One can show that under certain periodic bias conditions the charges actually do dissipate a little. The amount of dissipation depends on the precise bias conditions, as function of time. Since this effect is only due to our limited way of modelling charges, we will not (and can not) take this dissipation into account.

8.2 Relation between power and increase of temperature

Next we need a relation between the dissipated power and the rise in temperature. In a DC case we can assume a linear relation: $\Delta T = \mathsf{R_{th}} \; P_{\mathrm{diss}}$, where the coefficient $\mathsf{R_{th}}$ is

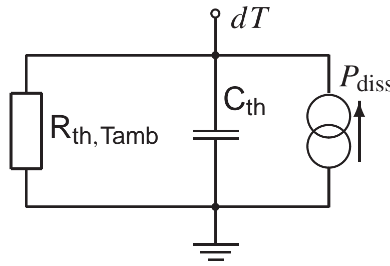

Figure 21: *The self-heating network. Note that for increased flexibility the node dT is made available to the user (see also Fig. 22). The thermal resistance $\mathsf{R}_{\mathsf{th,Tamb}}$ is the one after temperature scaling.*

the thermal resistance (in units K/W). We assume here that it does not matter *where* the power is actually dissipated. In reality, of course, a certain dissipation profile will also give a temperature profile over the transistor: not every part will be equally hot. We will not take this into account.

In non-stationary situations we have to take the finite heat capacity of the device into account [68]. So we must ask ourselves, what happens when a transistor is heated locally. The dissipated power creates a flow of energy, driven by a temperature gradient, from the transistor to some heat sink far away. The larger the gradient in the temperature, the larger the flow. This means that locally the temperature in the transistor will be larger than in the surrounding material. This increased temperature ΔT is directly related to the increase in the energy density ΔU via the heat-capacitance:

$$\Delta U = \mathsf{C}_{\mathsf{th}}\ \Delta T, \tag{8.3}$$

where C_{th} is the thermal capacitance (or effective heat capacitance) in units J/K. A part of the dissipated power will now flow away, and a part will be used to increase the local energy density if the situation is not yet stationary. Hence we can write

$$P_{\mathrm{diss}} = \frac{\Delta T}{\mathsf{R}_{\mathsf{th}}} + \mathsf{C}_{\mathsf{th}} \frac{\mathrm{d}\Delta T}{\mathrm{d}t}. \tag{8.4}$$

8.3 Implementation

For the implementation of self-heating an extra network is introduced, see Fig. 21. It contains the self-heating resistance R_{th} and capacitance C_{th}, both connected between ground and the temperature node dT. The value of the voltage $\mathcal{V}_{\mathrm{dT}}$ at the temperature node gives the increase in local temperature. The power dissipation as given above is implemented as a current source.

 ©Koninklijke Philips Electronics N.V. 2005

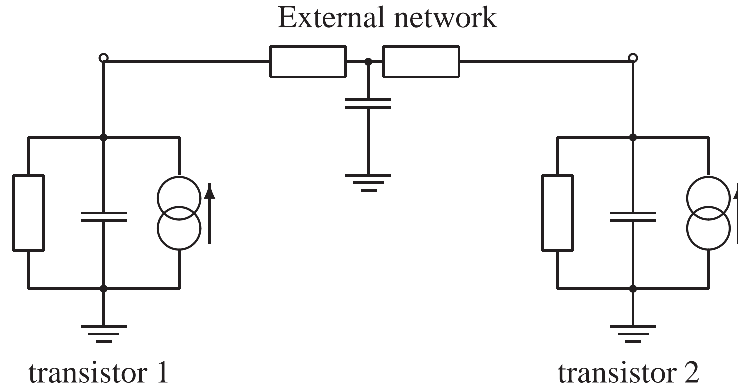

Figure 22: *An example of mutual self-heating of two transistors.*

8.4 Mutual heating

Apart from self-heating it is also possible to model mutual heating of two or more transistors close together. To do this the terminals dT of the transistors have to be coupled to each other with an external network. An example is given in Fig. 22. This external network is not an electrical network, but a network of heat-flow and heat-storage (just as the self-heating network within Mextram is not an electrical network). One has to be careful, therefore, not to connect any 'thermal' nodes with 'electrical' nodes. The external network can be made as complicated as one wishes, thermally connecting any number of transistors. For more information we refer literature, e.g. Refs. [69, 70, 71].

©Koninklijke Philips Electronics N.V. 2005

9 Noise model

9.1 Introduction

Apart from the DC and AC performance of the transistor model, we also have to consider noise sources. With noise we mean random fluctuations in the currents or voltages in the circuit. We refer to Refs. [72, 73, 74, 75] for an introduction into noise characterisation. For a discussion of the calculation of (white) noise in compact models we refer to Ref. [25]. Here we will give a basic introduction only.

Consider a resistor. Its current I can fluctuate, even when the applied voltage V is kept constant. Hence we can write $I(t) = I_0 + i(t)$, where $I_0 = V/R$. We cannot describe $i(t)$ in all detail. Instead we must look at its statistical properties. One of these properties must be that its average vanishes: $\overline{i(t)} = 0$. We can safely assume that the noise is a result of very many individual fluctuations. This means that the distribution of $i(t)$ is a Gaussian. We already calculated its mean. The distribution is then completely given by its second moment $\overline{i^2(t)}$. From elementary noise analysis it is known that we can write this average in terms of its spectral intensity S_i as

$$\overline{i^2(t)} = \int_0^\infty S_i(f)\, \mathrm{d}f, \tag{9.1}$$

where the integral is over all frequencies f. It is not necessary here to give the definition of the spectral intensity. Important is that within Mextram and other compact models the noise is not directly given in terms of this spectral intensity. Rather, we give the average of the current noise squared, in a certain frequency interval of width Δf. For a simple resistance, for instance, we write

$$\overline{i_R^2} = \frac{4kT}{R}\, \Delta f. \tag{9.2}$$

The total noise can then be calculated as a sum over different frequencies.

When looking at the equivalent circuit of this resistor we can add this current source parallel to the resistor, as in Fig. 23. Instead of a current noise term, one can also use

Figure 23: *Two equivalent ways of depicting the noise sources of a resistor. Left a current noise source (parallel to the resistor). Right a voltage noise source (in series with the resistor).*

 ©Koninklijke Philips Electronics N.V. 2005

a voltage noise term. From the intensity of the current noise term one can calculate the intensity of the voltage noise term. Suppose we have applied a voltage V over the resistor. We can then write for the current:

$$I + i = \frac{V}{R} + i = \frac{V - v}{R} \qquad \Longrightarrow \qquad v = -i\,R. \tag{9.3}$$

Again we see that the average of the voltage fluctuation vanishes: $\overline{v} = 0$. For the variance we have

$$\overline{v_R^2} = 4kT\,R\;\Delta f. \tag{9.4}$$

The thermal noise we have described here is normally given in terms of a voltage noise source. We can also note that its squared average, or its spectral intensity, is independent of the frequency. Hence it is called white noise.

9.2 Basic noise types

There are three basic types of noise that we will consider: thermal noise, shot noise and flicker noise.

9.2.1 Thermal noise

Thermal noise is the noise normally associated with resistances. We have already seen its normal behaviour above. It is a white noise, which means that its spectral density is frequency independent. It does not depend on the current through the resistance, or its potential.

9.2.2 Shot noise

The second basic type of noise is shot noise. This noise is a result from the fact that the current consists of particles moving around. When considering for instance the current over a pn-junction we know that either a carrier crossed the junction or it didn't. The fact that the carriers cross the barrier one by one gives a fluctuation given by

$$\overline{i_{\mathrm{shot}}^2} = 2qI\;\Delta f. \tag{9.5}$$

For a resistor the electrons can move about freely, and do not have to cross a barrier. Therefore no shot noise is present in resistors. Shot noise is present in the various base currents and in the main currents. Furthermore, Mextram also models the noise contributions due to impact ionisation or avalanche. This is discussed in detail in Ref. [76].

9.2.3 Thermal noise and shot noise as one concept

Although their origin seems to be very different, thermal noise and shot noise in semiconductor devices have the same background. Both can be found by considering the current equations and solving them while adding local fluctuations. These local fluctuations are based on thermal noise. We will see that shot noise in diodes can be derived from the same basic principle of local thermal noise. Although here it is a bit technical, we need the derivations for the noise in the main current and in the epilayer resistance. This also means that the simplified picture presented in the previous section for shot-noise is not quite true, although it is very good for getting quick results. We refer to the report [25] for more detail on calculating white noise in compact models.

Under quite general conditions the differential equation for the current-voltage relation can be given as $I = g\mathrm{d}V/\mathrm{d}x$, where the conductance is not necessarily a constant. For instance, the conductance can be directly dependent on the position: $g = g(x)$, like in a resistor where the resistance varies with the position along the current path. The current noise is then given by

$$\overline{i^2} = 4kT\ \Delta f \left(\int \frac{1}{g(x)}\,\mathrm{d}x\right)^{-1} = \frac{4kT}{R}\,\Delta f, \qquad \text{for } g = g(x), \tag{9.6}$$

where R is the total resistance.

In some other situations, like in a diode and in a MOSFET, the conductance does not directly depend on the position, but rather on the local voltage $V = \varphi_p - \varphi_n$, and we write $g = g(V)$. For instance, in a diode, we have from Eq. (1.5) $J = q\mu_n n(V)\,\mathrm{d}V/\mathrm{d}x$, where from Eq. (1.9) the minority concentration is given by $n(V) = n_i^2 e^{V/V_T}/N_A$. For these kind of conductivities the formula for the noise is [77]

$$\overline{i^2} = 4kT\ \Delta f\ \frac{1}{W^2}\int_0^W g[V(x)]\,\mathrm{d}x, \qquad \text{for } g = g(V). \tag{9.7}$$

It is important to realise the subtle difference between Eqs. (9.6) and (9.7). Especially when one realises that in the latter equation the conductivity is in an indirect way also a function of position. Here, however, this function will change with applied biases, whereas in the case of Eq. (9.6) the function which gives g as function of x is independent of voltage. For constant g both give the same result. For conductivities that depend both on position and voltage there is in general no simple expression that gives the current noise. These subtleties are discussed in more detail in Ref. [25].

In the case of short diode we have, as in the base of a bipolar (see Section 2.4.2), $n[V(x)] = n(0)(1 - x/W_B)$. The noise for this case is given by

$$\overline{i^2} = 2q\ \frac{Q_{\mathrm{tot}}}{W_B^2/2D_n}\ \Delta f \simeq 2qI\ \Delta f. \tag{9.8}$$

The total charge is given by $Q_{\mathrm{tot}} = qA_{\mathrm{em}}n(0)W_B$. Note that we basically used the charge control relation $Q_{\mathrm{tot}} = \tau\, I$, with $\tau = W_B^2/2D_n$ at low injection. It is important to realise

 ©Koninklijke Philips Electronics N.V. 2005

that the noise for a diode, as given above, is more general than just for the case we have derived above. It is well known that for a diode, independent of its doping profile or length[8], we have [72]

$$I = I_s \left(e^{V/V_T} - 1\right), \quad (9.9a)$$

$$\overline{i^2} = 2qI_s \left(e^{V/V_T} + 1\right) \Delta f. \quad (9.9b)$$

The difference between the $+1$ and the -1 explains the '$\simeq$'-sign in Eq. (9.8). Normally this difference is not important in compact modelling. Only in the case of the main current we will take the correct expression.

9.2.4 Flicker or $1/f$-noise

The last basic type of noise we will consider is called $1/f$ noise or flicker noise. The microscopic origin of $1/f$ noise can be various. We will not try to understand these mechanism. Rather, we use an empirical formula that gives the current noise as

$$\overline{i^2_{1/f}} = \mathsf{K_f}\ |I|^{\mathsf{A_f}}\ \frac{\Delta f}{f}, \quad (9.10)$$

where $\mathsf{A_f}$ and $\mathsf{K_f}$ are parameters. Flicker noise will be added for all base currents, but not for the main currents.

For flicker noise we have to be careful when modelling the noise over several transistors in parallel (i.e. when $\mathsf{MULT} \neq 1$). The variance of the noisy signal of multiple transistors is just the sum of the variances of the single transistors, since we assume independent noise sources. This means that we need to add the spectral intensities, or the $\overline{i^2}$. The current of a single transistor is the total current divided by the number of transistors. Hence we get

$$\overline{i^2_{1/f}} = \mathsf{MULT} \cdot \mathsf{K_f} \left|\frac{I}{\mathsf{MULT}}\right|^{\mathsf{A_f}} \frac{\Delta f}{f}. \quad (9.11)$$

For shot noise we should do the same. This does however not change the formula when $\mathsf{MULT} > 1$, since shot noise already scales linearly with the current. We will see the same kind of formulas whenever a base current is split into two or more parts.

9.3 Noise due to avalanche

The excess noise due to impact-ionisation and avalanche is described in Ref. [76]. There are two effects. First, the noise that is already present in the collector current is amplified just as the DC collector current. Second, the impact ionisation process itself leads to extra noise.

[8] We will neglect all high-injection noise effects [78, 79], which are due to the fact that hole current and electron current become dependent on each other.

©Koninklijke Philips Electronics N.V. 2005

In Ref. [76] we have shown the derivation. Here we just present the results and the actual implementation into Mextram. For the noise sources without avalanche one can write

$$\overline{i^2_{C0}} = 2q I_{C0}\,\Delta f, \tag{9.12a}$$
$$\overline{i^2_{B0}} = 2q I_{B0}\,\Delta f, \tag{9.12b}$$
$$\overline{i_{B0} i_{C0}} = 0. \tag{9.12c}$$

The subscript 0 stands for no avalanche. Including avalanche, the result for the noise at the terminals of the intrinsic transistor is then

$$\overline{i^2_{C}} = 2q I_{C0} M(2M-1)\,\Delta f, \tag{9.13a}$$
$$\overline{i^2_{B}} = 2q I_{B0}\,\Delta f + (M-1)(2M-1) 2q I_{C0}\,\Delta f, \tag{9.13b}$$
$$\overline{i_B i_C} = -2M(M-1) 2q I_{C0}\,\Delta f. \tag{9.13c}$$

The expressions are given in terms of the multiplication factor M. We want to present it in terms of the Mextram generation factor G_{EM} and the avalanche current I_{avl}. In Mextram the avalanche current given in Eq. (3.100) is defined in terms of the total collector current $I_{C_1C_2}$. Furthermore, it is limited in such a way that always $I_{\mathrm{avl}} < I_{C_1C_2}$ and $I_{\mathrm{avl}} < G_{\max} I_{C_1C_2}$. For the noise model we will neglect the influence of $G_{\max}$ (which means we assume it is infinite). We can then write

$$I_{\mathrm{avl}} = \frac{G_{\mathrm{EM}}}{1+G_{\mathrm{EM}}} I_{C_1C_2} = I_{C_1C_2} - I_N. \tag{9.14}$$

This allows us to write $I_{\mathrm{avl}} = G_{\mathrm{EM}} I_N$, which is now in terms of the main current I_N. This main current is equal to the current I_{C0} as used in the noise expressions above. Furthermore, we can now express the noise expression in terms of $G_{\mathrm{EM}} = M - 1$. The result is

$$\begin{aligned}\overline{i^2_{C}} &= 2q I_{C0}(1 + 3G_{\mathrm{EM}} + 2G^2_{\mathrm{EM}})\,\Delta f\\ &= 2q I_N\,\Delta f + 2q I_{\mathrm{avl}}(3 + 2G_{\mathrm{EM}})\,\Delta f,\end{aligned} \tag{9.15a}$$
$$\begin{aligned}\overline{i^2_{B}} &= 2q I_{B0}\,\Delta f + 2q I_{C0}(G_{\mathrm{EM}} + 2G^2_{\mathrm{EM}})\,\Delta f\\ &= 2q I_{B0}\,\Delta f + 2q I_{\mathrm{avl}}(1 + 2G_{\mathrm{EM}})\,\Delta f,\end{aligned} \tag{9.15b}$$
$$\begin{aligned}\overline{i_B i_C} &= -2q I_{C0}(2G_{\mathrm{EM}} + 2G^2_{\mathrm{EM}})\,\Delta f\\ &= -2q I_{\mathrm{avl}}(2 + 2G_{\mathrm{EM}})\,\Delta f.\end{aligned} \tag{9.15c}$$

The higher order contributions $4q I_{\mathrm{avl}} G_{\mathrm{EM}} \Delta f$ are not really relevant for the accuracy of the modelling. The avalanche current itself is not even accurate in that regime. However, the terms are needed to make sure that the model remains consistent, in the sense that no correlation coefficient larger than 1 (in absolute value) occurs.

Because of backward compatibility all noise contributions directly due to avalanche have an extra prefactor $\mathsf{K_{avl}}$.

 ©Koninklijke Philips Electronics N.V. 2005

9.4 Noise expressions in Mextram

For the three constant resistors in Mextram we can write (the 'iN' stands for 'noise current')

$$\overline{iN^2_{R_E}} = \frac{4kT}{\mathsf{R_E}}\,\Delta f, \tag{9.16a}$$
$$\overline{iN^2_{R_{Bc}}} = \frac{4kT}{\mathsf{R_{Bc}}}\,\Delta f, \tag{9.16b}$$
$$\overline{iN^2_{R_{Cc}}} = \frac{4kT}{\mathsf{R_{Cc}}}\,\Delta f. \tag{9.16c}$$

The value of the noise intensity in the variable base resistance must include current crowding. The derivation is discussed in detail in Refs [47, 25]. The result is

$$\overline{iN^2_{R_{Bv}}} = \frac{4kT}{R_{B_2}}\,\Delta f\,\frac{4\,e^{\mathcal{V}_{B_1B_2}/V_T}+5}{3}. \tag{9.17}$$

The expressions for the shot noise in the main currents of the intrinsic transistor and the parasitic PNP are now:

$$\overline{iN^2_C} = 2q\,\frac{I_f+I_r}{q_B}\,\Delta f + \mathsf{K_{avl}}\cdot 2q I_{\mathrm{avl}}(3+2G_{\mathrm{EM}})\,\Delta f, \tag{9.18a}$$
$$\overline{iN^2_{I_{\mathrm{sub}}}} = 2q\,|I_{\mathrm{sub}}|\,\Delta f, \tag{9.18b}$$
$$\overline{iN^2_{XI_{\mathrm{sub}}}} = 2q\,|XI_{\mathrm{sub}}|\,\Delta f. \tag{9.18c}$$

For the main current we added both the forward and reverse terms to make sure that it also works in reverse. Furthermore, the contribution due to avalanche is taken into account. Note that we do not model a reverse current of the parasitic PNP.

The shot noise and $1/f$-noise of the ideal forward base current and the non-ideal base currents are given by

$$\overline{iN^2_B} = \left\{2q\,\left(|I_{B_1}|+|I_{B_2}|\right) + \frac{\mathsf{K_f}}{f}\,(1-\mathsf{XI_{B_1}})\left(\frac{|I_{B_1}|}{1-\mathsf{XI_{B_1}}}\right)^{\mathsf{A_f}} + \frac{\mathsf{K_{fN}}}{f}\,\left|I_{B_2}\right|^{2(\mathsf{m_{Lf}}-1)+\mathsf{A_f}(2-\mathsf{m_{Lf}})}\right\}\Delta f + \mathsf{K_{avl}}\cdot 2qI_{\mathrm{avl}}(1+2G_{\mathrm{EM}})\,\Delta f, \tag{9.19a}$$
$$\overline{iN^2_{BS}} = \left\{2q\,|I^S_{B_1}| + \frac{\mathsf{K_f}}{f}\,\mathsf{XI_{B_1}}\left(\frac{|I^S_{B_1}|}{\mathsf{XI_{B_1}}}\right)^{\mathsf{A_f}}\right\}\Delta f, \tag{9.19b}$$
$$\overline{iN^2_{B_3}} = \left\{2q\,|I_{B_3}| + \frac{\mathsf{K_f}}{f}\,\left|I_{B_3}\right|^{\mathsf{A_f}}\right\}\Delta f. \tag{9.19c}$$

Note that the $1/f$ noise of the non-ideal base current has its own pre-factor and a fixed power ($A_f = 2$). This is a result from the work of Koolen and Aarts [80]. Also for the base current, the contribution due to avalanche is taken into account. For this contribution, also a correlation between base and collector current shot noise terms is needed [76]

$$\overline{iN_B\ iN_C^*} = -\mathsf{K_{avl}} \cdot 2q\, I_{\mathrm{avl}}(2 + 2G_{\mathrm{EM}})\ \Delta f \tag{9.20}$$

The parameter $\mathsf{K_{avl}}$ is just a pre-factor that was introduced for backward compatibility and should be set to its physical value of 1.

For the extrinsic reverse base current shot noise and $1/f$-noise we have to be careful. When $\mathsf{EXMOD} = 0$ we have

$$\overline{i N_{I_{\mathrm{ex}}}^2} = \left\{ 2q\ |I_{\mathrm{ex}}| + \frac{\mathsf{K_f}}{f}\ |I_{\mathrm{ex}}|^{\mathsf{A_f}} \right\}\ \Delta f. \tag{9.21}$$

When $\mathsf{EXMOD} = 1$ we have

$$\overline{i N_{I_{\mathrm{ex}}}^2} = \left\{ 2q\ |I_{\mathrm{ex}}| + \frac{\mathsf{K_f}}{f}\ (1{-}\mathsf{X_{ext}})\ \left(\frac{|I_{\mathrm{ex}}|}{1{-}\mathsf{X_{ext}}} \right)^{\mathsf{A_f}} \right\}\ \Delta f, \tag{9.22a}$$

$$\overline{i N_{XI_{\mathrm{ex}}}^2} = \left\{ 2q\ |XI_{\mathrm{ex}}| + \frac{\mathsf{K_f}}{f}\ \mathsf{X_{ext}}\ \left(\frac{|XI_{\mathrm{ex}}|}{\mathsf{X_{ext}}} \right)^{\mathsf{A_f}} \right\}\ \Delta f. \tag{9.22b}$$

 ©Koninklijke Philips Electronics N.V. 2005

10 Small-signal approximations in the operating-point

Operating point information is a feature of the circuit simulator that gives the user insight in the actual operating point of the transistor. This includes for instance the actual transconductance and actual capacitances. In the Pstar implementation all small-signal quantities are given, as well as many large signal quantities [1]. More important for the designer, however, are some compound small-signal quantities. One of them is the actual cut-off frequency f_T. Other quantities are those of the approximate small-signal circuit shown in Fig. 24.

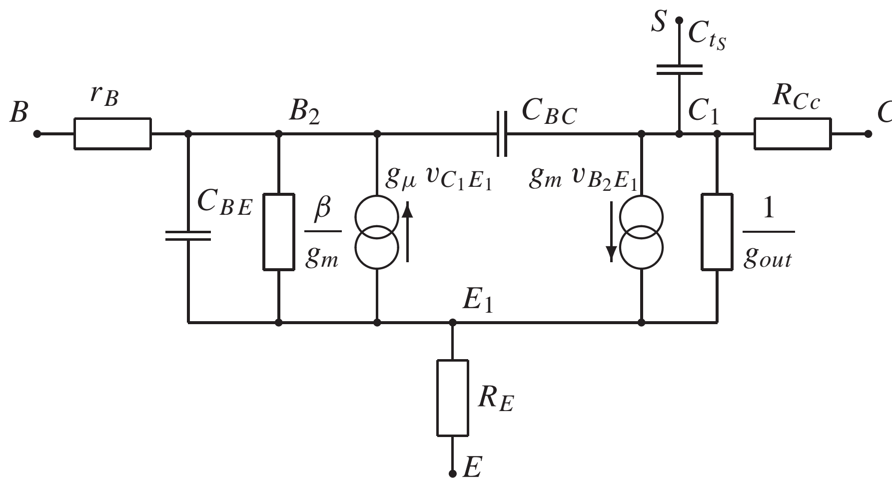

Figure 24: *Simplified small-signal circuit that approximates the full Mextram small-signal circuit. The names of the internal nodes correspond conceptually to the same nodes in the full Mextram circuit. However, the value of their node voltages will be slightly different, since it is an approximate circuit.*

10.1 Small-signal model

We start with the calculation of the approximate small-signal model. All the elements are calculated using the small-signal parameters of the full Mextram model. The external collector and emitter resistance are just the parameters themselves (after temperature scaling). The base resistance is simply given by

$$r_B = \mathsf{R_{Bc}} + r_{Bv}, \tag{10.1}$$

where the second term is already given in the operating point information. Also C_{tS} is already given.

For the calculation of the other terms we need some more work. This is similar to what we will need in the calculation of f_T later on. The part of the Mextram model located between the three nodes B_2, E_1 and C_1 contains four currents: I_N, $I_{C_1C_2}$, I_{BE} and I_{BC} (see Fig. 25). The latter two are (intrinsic) base currents. Mextram does not have a real

©Koninklijke Philips Electronics N.V. 2005

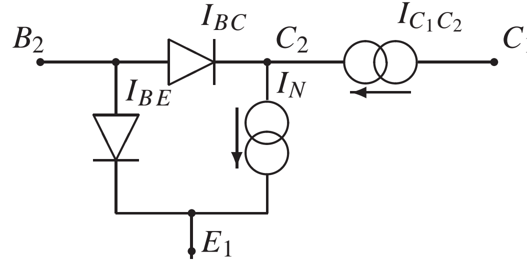

Figure 25: *Circuit that describes the four main currents in the intrinsic transistor.*

intrinsic base current that goes from base to collector. It does however have an avalanche current that goes from the collector (node C_2) to the base. Therefore: $I_{BC} = -I_{\rm avl}$.

The following derivatives are (or could be) present in the operating point information

$$\begin{aligned}
g_x &= \frac{\partial I_N}{\partial \mathcal{V}_{\rm B_2E_1}}; & g_y &= \frac{\partial I_N}{\partial \mathcal{V}_{\rm B_2C_2}}; & g_z &= \frac{\partial I_N}{\partial \mathcal{V}_{\rm B_2C_1}};\\
g_{Rcv,x} &= \frac{\partial I_{C_1C_2}}{\partial \mathcal{V}_{\rm B_2E_1}}; & g_{Rcv,y} &= \frac{\partial I_{C_1C_2}}{\partial \mathcal{V}_{\rm B_2C_2}}; & g_{Rcv,z} &= \frac{\partial I_{C_1C_2}}{\partial \mathcal{V}_{\rm B_2C_1}};\\
g_{\pi,x} &= \frac{\partial I_{BE}}{\partial \mathcal{V}_{\rm B_2E_1}}; & g_{\pi,y} &= \frac{\partial I_{BE}}{\partial \mathcal{V}_{\rm B_2C_2}}; & g_{\pi,z} &= \frac{\partial I_{BE}}{\partial \mathcal{V}_{\rm B_2C_1}};\\
g_{\mu,x} &= \frac{\partial I_{BC}}{\partial \mathcal{V}_{\rm B_2E_1}}; & g_{\mu,y} &= \frac{\partial I_{BC}}{\partial \mathcal{V}_{\rm B_2C_2}}; & g_{\mu,z} &= \frac{\partial I_{BC}}{\partial \mathcal{V}_{\rm B_2C_1}}.
\end{aligned} \tag{10.2}$$

Some of these terms are zero in Mextram (e.g. $g_{Rcv,x}$. The conductances $g_{\pi,y}$ and $g_{\pi,z}$ are non-zero only if base recombination is included). We include them here anyhow because the present derivation can also be used for other models (like Spice-Gummel-Poon).

First we need to look at the node C_2. It is not included in the small-signal model of Fig. 24. Hence we must calculate the variation of $\mathcal{V}_{\rm B_2C_2}$ as function of $\mathcal{V}_{\rm B_2E_1}$ and $\mathcal{V}_{\rm B_2C_1}$. To this end we use

$$I_N = I_{BC} + I_{C_1C_2}. \tag{10.3}$$

Taking the derivative we get

$$\begin{aligned}
&g_x\, {\rm d}\mathcal{V}_{\rm B_2E_1} + g_y\, {\rm d}\mathcal{V}_{\rm B_2C_2} + g_z\, {\rm d}\mathcal{V}_{\rm B_2C_1}\\
&\quad = (g_{Rcv,x}+g_{\mu,x})\, {\rm d}\mathcal{V}_{\rm B_2E_1} + (g_{Rcv,y}+g_{\mu,y})\, {\rm d}\mathcal{V}_{\rm B_2C_2} + (g_{Rcv,z}+g_{\mu,z})\, {\rm d}\mathcal{V}_{\rm B_2C_1}.
\end{aligned} \tag{10.4}$$

This directly leads to

$$\frac{{\rm d}y}{{\rm d}x} \equiv \left(\frac{\partial \mathcal{V}_{\rm B_2C_2}}{\partial \mathcal{V}_{\rm B_2E_1}}\right)_{\mathcal{V}_{\rm B_2C_1}} = \frac{g_x - g_{Rcv,x} - g_{\mu,x}}{g_{Rcv,y} + g_{\mu,y} - g_y}, \tag{10.5a}$$

$$\frac{{\rm d}y}{{\rm d}z} \equiv \left(\frac{\partial \mathcal{V}_{\rm B_2C_2}}{\partial \mathcal{V}_{\rm B_2C_1}}\right)_{\mathcal{V}_{\rm B_2E_1}} = \frac{g_z - g_{Rcv,z} - g_{\mu,z}}{g_{Rcv,y} + g_{\mu,y} - g_y}. \tag{10.5b}$$

 ©Koninklijke Philips Electronics N.V. 2005

We can now look at the small-signal circuit elements. We start with the collector current which is, at the end, only a function of two external biases, and given by either $I_{C_1C_2} = I_{C_1C_2}(\mathcal{V}_{\mathrm{B_2E_1}}, \mathcal{V}_{\mathrm{C_1E_1}})$ or $I_{C_1C_2} = I_{C_1C_2}(\mathcal{V}_{\mathrm{B_2E_1}}, \mathcal{V}_{\mathrm{B_2C_1}})$. We can use the equivalence of both to write for the transconductance

$$
\begin{aligned}
g_m &\equiv \left(\frac{\partial I_{C_1C_2}}{\partial \mathcal{V}_{\mathrm{B_2E_1}}}\right)_{\mathcal{V}_{\mathrm{C_1E_1}}} \\
&= \left(\frac{\partial I_{C_1C_2}}{\partial \mathcal{V}_{\mathrm{B_2E_1}}}\right)_{\mathcal{V}_{\mathrm{B_2C_1}}} \left(\frac{\partial \mathcal{V}_{\mathrm{B_2E_1}}}{\partial \mathcal{V}_{\mathrm{B_2E_1}}}\right)_{\mathcal{V}_{\mathrm{C_1E_1}}} + \left(\frac{\partial I_{C_1C_2}}{\partial \mathcal{V}_{\mathrm{B_2C_1}}}\right)_{\mathcal{V}_{\mathrm{B_2E_1}}} \left(\frac{\partial \mathcal{V}_{\mathrm{B_2C_1}}}{\partial \mathcal{V}_{\mathrm{B_2E_1}}}\right)_{\mathcal{V}_{\mathrm{C_1E_1}}} \\
&= \left(\frac{\partial I_{C_1C_2}}{\partial \mathcal{V}_{\mathrm{B_2E_1}}}\right)_{\mathcal{V}_{\mathrm{B_2C_1}}} + \left(\frac{\partial I_{C_1C_2}}{\partial \mathcal{V}_{\mathrm{B_2C_1}}}\right)_{\mathcal{V}_{\mathrm{B_2E_1}}} \qquad (10.6)
\end{aligned}
$$

The latter expression can then be rewritten in terms of the known Mextram quantities, using the fact that $\mathcal{V}_{\mathrm{B_2C_2}}$ is also a function of both $\mathcal{V}_{\mathrm{B_2E_1}}$ and $\mathcal{V}_{\mathrm{B_2C_1}}$. The transconductance then given by

$$
\begin{aligned}
g_m &= \left[g_{Rcv,x} + g_{Rcv,y}\frac{\mathrm{d}y}{\mathrm{d}x}\right] + \left[g_{Rcv,z} + g_{Rcv,y}\frac{\mathrm{d}y}{\mathrm{d}z}\right] \\
&= \frac{g_{Rcv,y}(g_x - g_{\mu,x} + g_z - g_{\mu,z}) - (g_{Rcv,x} + g_{Rcv,z})(g_y - g_{\mu,y})}{g_{Rcv,y} + g_{\mu,y} - g_y}. \qquad (10.7)
\end{aligned}
$$

Next we have the base conductance $g_\pi = g_m/\beta$ for which we use the same kind of techniques as above to go from its definition to the expression in terms of the full Mextram small-signal equivalent circuit:

$$
\begin{aligned}
g_\pi &\equiv \left(\frac{\partial(I_{BE} + I_{BC})}{\partial \mathcal{V}_{\mathrm{B_2E_1}}}\right)_{\mathcal{V}_{\mathrm{C_1E_1}}} = \left(\frac{\partial(I_{BE} + I_{BC})}{\partial \mathcal{V}_{\mathrm{B_2E_1}}}\right)_{\mathcal{V}_{\mathrm{B_2C_1}}} + \left(\frac{\partial(I_{BE} + I_{BC})}{\partial \mathcal{V}_{\mathrm{B_2C_1}}}\right)_{\mathcal{V}_{\mathrm{B_2E_1}}} \\
&= g_{\pi,x} + g_{\mu,x} + g_{\pi,z} + g_{\mu,z} + (g_{\pi,y} + g_{\mu,y})\left[\frac{\mathrm{d}y}{\mathrm{d}x} + \frac{\mathrm{d}y}{\mathrm{d}z}\right]. \qquad (10.8)
\end{aligned}
$$

It is not much use trying to simplify this last expression. The output conductance is

$$
\begin{aligned}
g_{\mathrm{out}} &\equiv \left(\frac{\partial I_{C_1C_2}}{\partial \mathcal{V}_{\mathrm{C_1E_1}}}\right)_{\mathcal{V}_{\mathrm{B_2E_1}}} = -\left(\frac{\partial I_{C_1C_2}}{\partial \mathcal{V}_{\mathrm{B_2C_1}}}\right)_{\mathcal{V}_{\mathrm{B_2E_1}}} \\
&= -g_{Rcv,z} - g_{Rcv,y}\frac{\mathrm{d}y}{\mathrm{d}z} \\
&= \frac{(g_y - g_{\mu,y})g_{Rcv,z} - (g_z - g_{\mu,z})g_{Rcv,y}}{g_{Rcv,y} + g_{\mu,y} - g_y}. \qquad (10.9)
\end{aligned}
$$

Note that for small currents $g_{Rcv,y} \simeq -g_{Rcv,z}$. This makes that the second expression in g_m and g_{out} are numerically unreliable since they contain a subtraction of two almost

©Koninklijke Philips Electronics N.V. 2005

equal numbers. At last we have the reverse transconductance

$$\begin{aligned} g_\mu &\equiv -\left(\frac{\partial(I_{BE}+I_{BC})}{\partial\mathcal{V}_{\mathrm{C_1E_1}}}\right)_{\mathcal{V}_{\mathrm{B_2E_1}}} = +\left(\frac{\partial(I_{BE}+I_{BC})}{\partial\mathcal{V}_{\mathrm{B_2C_1}}}\right)_{\mathcal{V}_{\mathrm{B_2E_1}}} \\ &= g_{\pi,z}+g_{\mu,z}+(g_{\pi,y}+g_{\mu,y})\frac{\mathrm{d}y}{\mathrm{d}z}. \end{aligned} \tag{10.10}$$

The reason for calling this term g_μ is that in the simple case where the BE-base current depends only on $\mathcal{V}_{\mathrm{B_2E_1}}$ we can write $g_\mu \simeq g_{\mu,z}+g_{\mu,y}$. Hence it is directly related to the conductance between base and collector. When we translate the circuit of Fig. 24 into the hybrid-pi model of Fig. 26 (see next section) we see that it is indeed between the nodes B_2 and C_1.

10.1.1 Mextram implementation

In the equations we derived above we made no assumptions for the currents. This means that the small-signal circuit is also correct when the transistor is used in reverse! However, we did not yet include the extrinsic regions. For the implementation in Mextram this is necessary. This also means that we need to approximate to keep the small-signal model simple. Furthermore, when including the charges it is also not possible to keep all of the Mextram structure intact.

The currents for the extrinsic regions can be added as follows

$$g_\pi \rightarrow g_\pi + g_\pi^S, \tag{10.11a}$$

$$g_\mu \rightarrow g_\mu + g_{\mu\mathrm{ex}} + Xg_{\mu\mathrm{ex}}, \tag{10.11b}$$

where g_π^S is the conductance of the base current $I_{B_1}^S$ through the sidewall. Note that the substrate current (which goes from the base node to the substrate node) is not modelled at all. This should not influence the collector and emitter currents.

For Mextram we have implemented:

$$g_m = \frac{g_{Rcv,y}(g_x-g_{\mu,x}+g_z-g_{\mu,z})-(g_{Rcv,x}+g_{Rcv,z})(g_y-g_{\mu,y})}{g_{Rcv,y}+g_{\mu,y}-g_y}, \tag{10.12a}$$

$$g_\pi = g_\pi^S+g_{\pi,x}+g_{\mu,x}+g_{\pi,z}+g_{\mu,z}+(g_{\pi,y}+g_{\mu,y})\left[\frac{\mathrm{d}y}{\mathrm{d}x}+\frac{\mathrm{d}y}{\mathrm{d}z}\right], \tag{10.12b}$$

$$\beta = g_m/g_\pi, \tag{10.12c}$$

$$g_{\mathrm{out}} = \frac{(g_y-g_{\mu,y})g_{Rcv,z}-(g_z-g_{\mu,z})g_{Rcv,y}}{g_{Rcv,y}+g_{\mu,y}-g_y}, \tag{10.12d}$$

$$g_\mu = g_{\pi,z}+g_{\mu,z}+(g_{\pi,y}+g_{\mu,y})\frac{\mathrm{d}y}{\mathrm{d}z}+g_{\mu\mathrm{ex}}+Xg_{\mu\mathrm{ex}}, \tag{10.12e}$$

$$C_{BE} = C_{BE,x}+C_{BE}^S+C_{BC,x}+(C_{BE,y}+C_{BC,y})\,\frac{\mathrm{d}y}{\mathrm{d}x}+\mathsf{C_{BEO}}, \tag{10.12f}$$

$$C_{BC} = (C_{BE,y}+C_{BC,y})\,\frac{\mathrm{d}y}{\mathrm{d}z}+C_{BC,z}+C_{BC\mathrm{ex}}+XC_{BC\mathrm{ex}}+\mathsf{C_{BCO}}. \tag{10.12g}$$

 ©Koninklijke Philips Electronics N.V. 2005

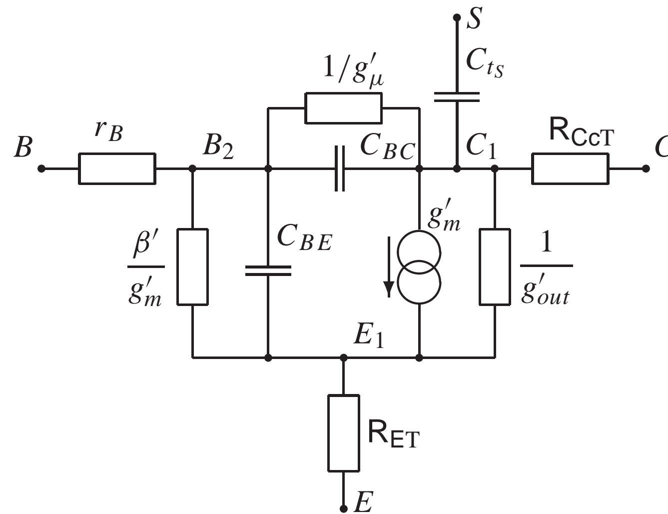

Figure 26: *Small-signal hybrid-pi circuit that also approximates the full Mextram small-signal circuit. It is equivalent to the circuit of Fig. 24.*

Note that in the implementation we will use $\beta = g_m/g_\pi$ instead of g_π directly. The base-emitter capacitance C_{BE} contains every term that is dependent on $v_{B_2E_1}$, even if it is in the complete circuit not between the nodes B_2 and E_1. The base-collector capacitance C_{BC} contains in a similar way all contributions that depend on $v_{B_2C_1}$.

10.1.2 The hybrid-pi model

Sometimes one would like to have the elements of the hybrid-pi small-signal circuit of Fig. 26, instead of the elements of the rather symmetric circuit of Fig. 24. All the elements in the figure now have an extra prime ($'$) to denote the difference with the original small circuit model.

To go from the circuit of Fig. 24 to that of Fig. 26 we have to move the current source $g_\mu\, v_{C_1E_1}$. This means also changing the other terms. The redistribution of the current source is shown in Fig. 27. From this we find the elements of the hybrid-pi model in terms of the symmetric model:

$$g'_m = g_m + g_\mu, \tag{10.13a}$$
$$g'_\pi = g_\pi - g_\mu, \tag{10.13b}$$
$$g'_{\text{out}} = g_{\text{out}} - g_\mu, \tag{10.13c}$$
$$g'_\mu = g_\mu, \tag{10.13d}$$
$$\beta' = g'_m/g'_\pi. \tag{10.13e}$$

Note that the conductance g'_μ is between different nodes than the term corresponding to g_μ.

©Koninklijke Philips Electronics N.V. 2005

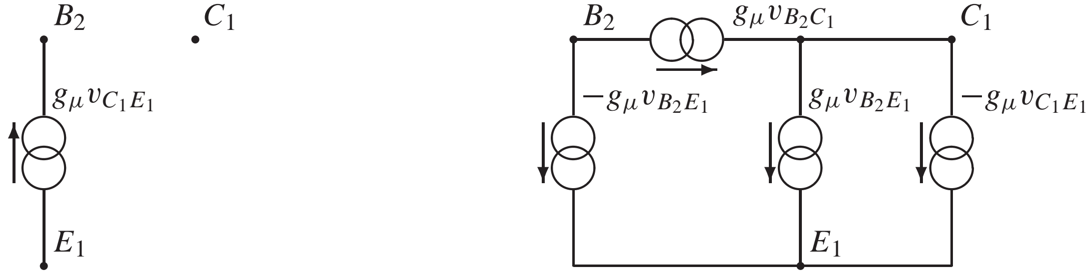

Figure 27: *The figure shows how to replace the current source $g_\mu\, v_{C_1E_1}$ that is present in the circuit of Fig. 24 and here shown on the left side, by the equivalent circuit of four currents here given on the right side. These equivalent four current sources, of which three can be replaced by resistances, are part of the circuit in Fig. 26.*

Using this transformation we now find for the complete hybrid-pi model:

$$g'_m = \frac{g_{Rcv,y}(g_x - g_{\mu,x} + g_z) + g_{\mu,y}(g_{Rcv,x} + g_z) - g_y(g_{\mu,z} + g_{Rcv,x} + g_{Rcv,z})}{g_{Rcv,y} + g_{\mu,y} - g_y} + g_{\pi,z} + g_{\pi,y}\frac{\mathrm{d}y}{\mathrm{d}z}, \tag{10.14a}$$

$$g'_\pi = g_{\pi,x} + g_{\mu,x} + (g_{\pi,y} + g_{\mu,y})\frac{\mathrm{d}y}{\mathrm{d}x}, \tag{10.14b}$$

$$g'_{\mathrm{out}} = \frac{g_y(g_{\mu,z} + g_{Rcv,z}) - g_z(g_{\mu,y} + g_{Rcv,y})}{g_{Rcv,y} + g_{\mu,y} - g_y} - g_{\pi,z} - g_{\pi,y}\frac{\mathrm{d}y}{\mathrm{d}z}, \tag{10.14c}$$

$$g'_\mu = g_{\pi,z} + g_{\mu,z} + (g_{\pi,y} + g_{\mu,y})\frac{\mathrm{d}y}{\mathrm{d}z}. \tag{10.14d}$$

These relations have been verified with Mathematica.

10.1.3 Simple case

Let us now consider what the equations above mean in a simple case. We take normal base and main currents that depend only on the nodes they are connected to. This means $g_{\pi,y} = g_{\pi,z} = g_{\mu,x} = g_{\mu,z} = g_z = 0$. We assume a negligible and constant collector epilayer resistance. This means $g_{Rcv,x} = 0$ and $g_{Rcv,y} = -g_{Rcv,z}$ is very large. We take the limit of $g_{Rcv,y} \to \infty$. This leads to

$$\frac{\mathrm{d}y}{\mathrm{d}x} = \left(\frac{\partial \mathcal{V}_{\mathrm{B_2C_2}}}{\partial \mathcal{V}_{\mathrm{B_2E_1}}}\right)_{\mathcal{V}_{\mathrm{B_2C_1}}} = 0, \tag{10.15a}$$

$$\frac{\mathrm{d}y}{\mathrm{d}z} = \left(\frac{\partial \mathcal{V}_{\mathrm{B_2C_2}}}{\partial \mathcal{V}_{\mathrm{B_2C_1}}}\right)_{\mathcal{V}_{\mathrm{B_2E_1}}} = 1. \tag{10.15b}$$

 ©Koninklijke Philips Electronics N.V. 2005

For the conductances we get

$$g_m = g_x + g_y - g_{\mu,y}, \quad (10.16a)$$
$$g_\pi = g_{\pi,x} + g_{\mu,y}, \quad (10.16b)$$
$$g_{\text{out}} = g_{\mu,y} - g_y, \quad (10.16c)$$
$$g_\mu = g_{\mu,y}. \quad (10.16d)$$

After the transformation to the hybrid-pi circuit we then have

$$g'_m = g_x + g_y, \quad (10.17a)$$
$$g'_\pi = g_{\pi,x}, \quad (10.17b)$$
$$g'_{\text{out}} = -g_y, \quad (10.17c)$$
$$g'_\mu = g_{\mu,y}. \quad (10.17d)$$

Note that since in general $g_y < 0$ the output conductance is positive. The result is as expected: the conductance at the base is indeed given by the derivative of the base current w.r.t. the base emitter voltage $g_{\pi,x}$, the output conductance is given by the derivative of the collector current w.r.t. the collector-base voltage $-g_y$, the feedback conductance due to the avalanche current is the derivative of this avalanche current w.r.t. the collector voltage $g_{\mu,y}$ and the transconductance is the derivative of the main current w.r.t. the base-voltage, which is a sum of the derivative w.r.t. the base-emitter voltage g_x and the derivative w.r.t. the base-collector voltage g_y, keeping the collector voltage constant.

10.1.4 The reverse hybrid-pi model

In very few cases it might be useful to have a hybrid-pi model for the reverse behaviour. We don't think it is useful to include in the operating point information. But here we show how one can very easily construct the model from the quantities we already have. We use the hybrid-pi model of Fig. 26 as a starting point.

We have already mentioned that in principle the given hybrid-pi model can also be used in reverse. We only need to add the substrate current, and we need to rewrite it such that not v_{BE} but rather v_{BC} is the controlling voltage. When we do this we find the circuit as given in Fig. 28. Note that some of the quantities will now be negative, like g'_m and β'. The reverse current amplification is not β', but it is $-g'_m/g'_\mu$. This does include the extrinsic reverse base currents. In reverse mode we must also take the substrate current into account, as has been done by adding an extra current source.

This reverse hybrid-pi model has not been tested very much.

10.2 Calculation of f_T

Now we want to calculate the cut-off frequency $f_T = 1/(2\pi\tau_T)$. We will do this in more detail and accuracy than in the previous section. The total transit time τ_T is the ratio of

©Koninklijke Philips Electronics N.V. 2005

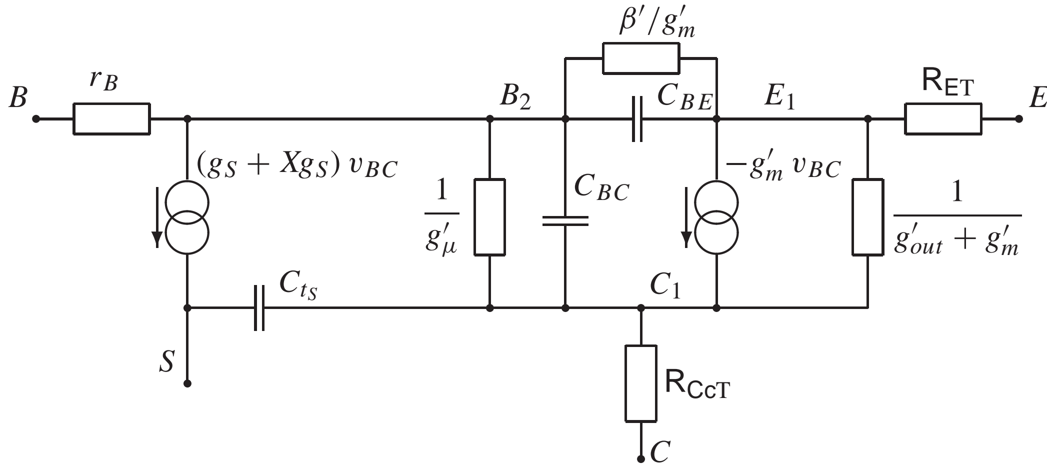

Figure 28: *Small-signal* reverse *hybrid-pi circuit that approximates the full Mextram small-signal circuit. Note the positions of the various external nodes. The value of* g'_m *will be negative, and therefore so will* β'.

the variation in the total charge connected to the base δQ and the variation in the current δI_C when keeping the collector-emitter bias constant $\delta \mathcal{V}_{\mathrm{CE}} = 0$:

$$\tau_T = \left.\frac{\delta Q}{\delta I_C}\right|_{\delta V_{CE}=0}. \tag{10.18}$$

To calculate the variation of the charges we first need to know what the variation of the internal biases is. This can be done in a similar way as above. Again we take the biases $\mathcal{V}_{\mathrm{B_2E_1}}$ and $\mathcal{V}_{\mathrm{B_2C_1}}$ as the independent quantities.

Variations of important quantities We start again with current conservation at the node C_2 which, as before, leads to

$$\frac{\mathrm{d}y}{\mathrm{d}x} \equiv \left(\frac{\partial \mathcal{V}_{\mathrm{B_2C_2}}}{\partial \mathcal{V}_{\mathrm{B_2E_1}}}\right)_{\mathcal{V}_{\mathrm{B_2C_1}}} = \frac{g_x - g_{Rcv,x} - g_{\mu,x}}{g_{Rcv,y} + g_{\mu,y} - g_y}, \tag{10.19a}$$

$$\frac{\mathrm{d}y}{\mathrm{d}z} \equiv \left(\frac{\partial \mathcal{V}_{\mathrm{B_2C_2}}}{\partial \mathcal{V}_{\mathrm{B_2C_1}}}\right)_{\mathcal{V}_{\mathrm{B_2E_1}}} = \frac{g_z - g_{Rcv,z} - g_{\mu,z}}{g_{Rcv,y} + g_{\mu,y} - g_y}. \tag{10.19b}$$

We can now look at the collector-emitter bias

$$\mathcal{V}_{\mathrm{CE}} = I_C\, \mathsf{R_{Cc}} - \mathcal{V}_{\mathrm{B_2C_1}} + \mathcal{V}_{\mathrm{B_2E_1}} + I_E\, \mathsf{R_E}. \tag{10.20}$$

We assume that there are no reverse base currents. Hence $I_C = I_{C_1C_2}$. The emitter current equals the sum of the main current I_N and the forward base current $I_{Bf} = I_{BE} + I^S_{B_1}$. When

 ©Koninklijke Philips Electronics N.V. 2005

we take the derivative of $\mathcal{V}_{\rm CE}$ to the two independent biases we get

$$\left(\frac{\partial \mathcal{V}_{\rm CE}}{\partial \mathcal{V}_{\rm B_2E_1}}\right)_{\mathcal{V}_{\rm B_2C_1}} = \left[g_{Rcv,x} + g_{Rcv,y}\frac{{\rm d}y}{{\rm d}x}\right] \mathsf{R_{Cc}} + 1 + \left[g_x + g_{Bf,x} + (g_y + g_{Bf,y})\frac{{\rm d}y}{{\rm d}x}\right] \mathsf{R_E}, \tag{10.21a}$$

$$\left(\frac{\partial \mathcal{V}_{\rm CE}}{\partial \mathcal{V}_{\rm B_2C_1}}\right)_{\mathcal{V}_{\rm B_2E_1}} = \left[g_{Rcv,z} + g_{Rcv,y}\frac{{\rm d}y}{{\rm d}z}\right] \mathsf{R_{Cc}} - 1 + \left[g_z + g_{Bf,z} + (g_y + g_{Bf,y})\frac{{\rm d}y}{{\rm d}z}\right] \mathsf{R_E}. \tag{10.21b}$$

We will calculate the various derivatives g_{Bf} of the base current later on. The variation of the collector-emitter bias can now be written as

$$\delta\mathcal{V}_{\rm CE} = \left(\frac{\partial \mathcal{V}_{\rm CE}}{\partial \mathcal{V}_{\rm B_2E_1}}\right)_{\mathcal{V}_{\rm B_2C_1}} \delta\mathcal{V}_{\rm B_2E_1} + \left(\frac{\partial \mathcal{V}_{\rm CE}}{\partial \mathcal{V}_{\rm B_2C_1}}\right)_{\mathcal{V}_{\rm B_2E_1}} \delta\mathcal{V}_{\rm B_2C_1}. \tag{10.22}$$

For the derivation of f_T we demand that

$$\delta\mathcal{V}_{\rm CE} = 0. \tag{10.23}$$

This leads to

$$\alpha \equiv \frac{\delta\mathcal{V}_{\rm B_2C_1}}{\delta\mathcal{V}_{\rm B_2E_1}} = -\left(\frac{\partial \mathcal{V}_{\rm CE}}{\partial \mathcal{V}_{\rm B_2E_1}}\right)_{\mathcal{V}_{\rm B_2C_1}} \Big/ \left(\frac{\partial \mathcal{V}_{\rm CE}}{\partial \mathcal{V}_{\rm B_2C_1}}\right)_{\mathcal{V}_{\rm B_2E_1}}. \tag{10.24}$$

We can now calculate the variations of all quantities under the condition that $\delta\mathcal{V}_{\rm CE} = 0$, in terms of $\delta\mathcal{V}_{\rm B_2E_1}$. For instance, we have

$$\delta I_C = \delta I_{C_1C_2} = \left[g_{Rcv,x} + g_{Rcv,y}\frac{{\rm d}y}{{\rm d}x} + \alpha\left(g_{Rcv,z} + g_{Rcv,y}\frac{{\rm d}y}{{\rm d}z}\right)\right]\delta\mathcal{V}_{\rm B_2E_1}. \tag{10.25}$$

Conductance of forward base current We still need to calculate the various conductances of the forward base current. We can write

$$I_{Bf} = I_{BE} + I^S_{B_1}(\mathcal{V}_{\rm B_2E_1} + \mathcal{V}_{\rm B_1B_2}), \tag{10.26}$$

using the fact that the sidewall base current is a function of $\mathcal{V}_{\rm B_1E_1}$. To calculate the conductance we first need the derivative of $\mathcal{V}_{\rm B_1B_2}$. To this end we write

$$I_{B_1B_2} = I_{BE} + I_{BC}. \tag{10.27}$$

©Koninklijke Philips Electronics N.V. 2005

The currents I_{BE} and I_{BC} are the same as used in the previous section. Taking for instance the derivative w.r.t. $\mathcal{V}_{\mathrm{B_2E_1}}$ we get

$$\frac{1}{r_{Bv}}\,\frac{\partial \mathcal{V}_{\mathrm{B_1B_2}}}{\partial \mathcal{V}_{\mathrm{B_2E_1}}} + g_{Rbv,x} = g_{\pi,x} + g_{\mu,x}. \tag{10.28}$$

where r_{Bv} is also present in the operating point information. This leads to the following definitions

$$\gamma_x \equiv \frac{\partial \mathcal{V}_{\mathrm{B_1B_2}}}{\partial \mathcal{V}_{\mathrm{B_2E_1}}} = (g_{\pi,x} + g_{\mu,x} - g_{Rbv,x})\, r_{Bv}, \tag{10.29a}$$

$$\gamma_y \equiv \frac{\partial \mathcal{V}_{\mathrm{B_1B_2}}}{\partial \mathcal{V}_{\mathrm{B_2C_2}}} = (g_{\pi,y} + g_{\mu,y} - g_{Rbv,y})\, r_{Bv}, \tag{10.29b}$$

$$\gamma_z \equiv \frac{\partial \mathcal{V}_{\mathrm{B_1B_2}}}{\partial \mathcal{V}_{\mathrm{B_2C_1}}} = (g_{\pi,z} + g_{\mu,z} - g_{Rbv,z})\, r_{Bv}. \tag{10.29c}$$

We now find for the derivatives of I_{Bf}

$$g_{Bf,x} = g_{\pi,x} + g_\pi^S\,(1+\gamma_x), \tag{10.30a}$$

$$g_{Bf,y} = g_{\pi,y} + g_\pi^S\,\gamma_y, \tag{10.30b}$$

$$g_{Bf,z} = g_{\pi,z} + g_\pi^S\,\gamma_z. \tag{10.30c}$$

Variation of biases We need to now the variation of various biases per unit variation of the collector current. For the three intrinsic biases we get

$$r_x \equiv \frac{\delta \mathcal{V}_{\mathrm{B_2E_1}}}{\delta I_C} = \left[g_{Rcv,x} + g_{Rcv,y}\frac{\mathrm{d}y}{\mathrm{d}x} + \alpha\left(g_{Rcv,z} + g_{Rcv,y}\frac{\mathrm{d}y}{\mathrm{d}z}\right)\right]^{-1}, \tag{10.31a}$$

$$r_y \equiv \frac{\delta \mathcal{V}_{\mathrm{B_2C_2}}}{\delta I_C} = \frac{1 - g_{Rcv,x}r_x - g_{Rcv,z}r_z}{g_{Rcv,y}}, \tag{10.31b}$$

$$r_z \equiv \frac{\delta \mathcal{V}_{\mathrm{B_2C_1}}}{\delta I_C} = \alpha r_x. \tag{10.31c}$$

For the calculation of r_y we used that

$$\delta I_C = g_{Rcv,x}r_x + g_{Rcv,y}r_y + g_{Rcv,z}r_z. \tag{10.32}$$

We can also calculate the variation of $\mathcal{V}_{\mathrm{B_1B_2}}$

$$r_{b1b2} \equiv \frac{\delta \mathcal{V}_{\mathrm{B_1B_2}}}{\delta I_C} = \gamma_x\, r_x + \gamma_y\, r_y + \gamma_z\, r_z, \tag{10.33}$$

where we used Eq. (10.29). For the base current we can write

$$I_B = I_{Bf} + I_{BC}. \tag{10.34}$$

 ©Koninklijke Philips Electronics N.V. 2005

The current amplification then is

$$h_{\text{fe}} \equiv \frac{\delta I_C}{\delta I_B} = [(g_{Bf,x} + g_{\mu,x})\ r_x + (g_{Bf,y} + g_{\mu,y})\ r_y + (g_{Bf,z} + g_{\mu,z})\ r_z)]^{-1}. \quad (10.35)$$

Using the current amplification we get the last two internal biases:

$$r_{\text{ex}} \equiv \frac{\delta \mathcal{V}_{\text{B}_1\text{C}_1}}{\delta I_C} = r_z + r_{b1b2}, \quad (10.36)$$

$$Xr_{\text{ex}} \equiv \frac{\delta \mathcal{V}_{\text{BC}_1}}{\delta I_C} = r_z + r_{b1b2} + \frac{\mathsf{R}_{\mathsf{Bc}}}{h_{\text{fe}}}. \quad (10.37)$$

For the overlap capacitances we also need the variation of the external base:

$$\frac{\delta \mathcal{V}_{\text{BC}}}{\delta I_C} = \frac{\delta \mathcal{V}_{\text{BE}}}{\delta I_C} = Xr_{\text{ex}} - \mathsf{R}_{\mathsf{Cc}}. \quad (10.38)$$

Total transit time The total transit time is now simple. It is given by

$$\begin{aligned} \tau_T &\equiv \frac{\delta Q_{\text{tot}}}{\delta I_C} = \sum_i \frac{\partial Q_{\text{tot}}}{\partial \mathcal{V}_{\text{i}}} \frac{\delta \mathcal{V}_{\text{i}}}{\delta I_C} \\ &= C_{BE}^S\ (r_x + r_{b1b2}) + (C_{BE,x} + C_{BE}^S + C_{BC,x})\ r_x + (C_{BE,y} + C_{BC,y})\ r_y \\ &\quad + (C_{BE,z} + C_{BC,z})\ r_z + C_{BC\text{ex}}\ r_{\text{ex}} + XC_{BC\text{ex}}\ Xr_{\text{ex}} \\ &\quad + (\mathsf{C}_{\mathsf{BEO}} + \mathsf{C}_{\mathsf{BCO}})(Xr_{\text{ex}} - \mathsf{R}_{\mathsf{Cc}}). \end{aligned} \quad (10.39)$$

We neglected the excess phase shift contribution which are present when $\mathsf{EXPHI} = 1$.

10.2.1 Mextram implementation

In this section we present the equations implemented in Mextram to calculate f_T. They are presented in an order such that each equation can be evaluated on basis of either existing operating point information or previously calculated results. We also use that in

Mextram $g_{Rcv,x} = 0$. The cut-off frequency can then be calculated as:

$$\frac{\mathrm{d}y}{\mathrm{d}x} = \frac{g_x - g_{\mu,x}}{g_{Rcv,y} + g_{\mu,y} - g_y}, \tag{10.40a}$$

$$\frac{\mathrm{d}y}{\mathrm{d}z} = \frac{g_z - g_{Rcv,z} - g_{\mu,z}}{g_{Rcv,y} + g_{\mu,y} - g_y}, \tag{10.40b}$$

$$\gamma_x = (g_{\pi,x} + g_{\mu,x} - g_{Rbv,x})\, r_{Bv}, \tag{10.40c}$$

$$\gamma_y = (g_{\pi,y} + g_{\mu,y} - g_{Rbv,y})\, r_{Bv}, \tag{10.40d}$$

$$\gamma_z = (g_{\pi,z} + g_{\mu,z} - g_{Rbv,z})\, r_{Bv}, \tag{10.40e}$$

$$g_{Bf,x} = g_{\pi,x} + g_\pi^S\,(1 + \gamma_x), \tag{10.40f}$$

$$g_{Bf,y} = g_{\pi,y} + g_\pi^S\,\gamma_y, \tag{10.40g}$$

$$g_{Bf,z} = g_{\pi,z} + g_\pi^S\,\gamma_z, \tag{10.40h}$$

$$\alpha = \frac{1 + \left[g_{Rcv,y}\frac{\mathrm{d}y}{\mathrm{d}x}\right]\mathsf{R_{Cc}} + \left[g_x + g_{Bf,x} + (g_y + g_{Bf,y})\frac{\mathrm{d}y}{\mathrm{d}x}\right]\mathsf{R_E}}{1 - \left[g_{Rcv,z} + g_{Rcv,y}\frac{\mathrm{d}y}{\mathrm{d}z}\right]\mathsf{R_{Cc}} - \left[g_z + g_{Bf,z} + (g_y + g_{Bf,y})\frac{\mathrm{d}y}{\mathrm{d}z}\right]\mathsf{R_E}}, \tag{10.40i}$$

$$r_x = \left[g_{Rcv,y}\frac{\mathrm{d}y}{\mathrm{d}x} + \alpha\,\left(g_{Rcv,z} + g_{Rcv,y}\frac{\mathrm{d}y}{\mathrm{d}z}\right)\right]^{-1}, \tag{10.40j}$$

$$r_z = \alpha\, r_x, \tag{10.40k}$$

$$r_y = \frac{1 - g_{Rcv,z} r_z}{g_{Rcv,y}}, \tag{10.40l}$$

$$r_{b1b2} = \gamma_x\, r_x + \gamma_y\, r_y + \gamma_z\, r_z, \tag{10.40m}$$

$$r_{\mathrm{ex}} = r_z + r_{b1b2}, \tag{10.40n}$$

$$Xr_{\mathrm{ex}} = r_{\mathrm{ex}} + \mathsf{R_{Bc}}[(g_{Bf,x} + g_{\mu,x})r_x + (g_{Bf,y} + g_{\mu,y})r_y + (g_{Bf,z} + g_{\mu,z})r_z], \tag{10.40o}$$

$$\begin{aligned}\tau_T = {} & C_{BE}^S\,(r_x + r_{b1b2}) + (C_{BE,x} + C_{BC,x})\, r_x + (C_{BE,y} + C_{BC,y})\, r_y \\ & + (C_{BE,z} + C_{BC,z})\, r_z + C_{BC\mathrm{ex}}\, r_{\mathrm{ex}} + XC_{BC\mathrm{ex}}\, Xr_{\mathrm{ex}} \\ & + (\mathsf{C_{BEO}} + \mathsf{C_{BCO}})(Xr_{\mathrm{ex}} - \mathsf{R_{Cc}}),\end{aligned} \tag{10.40p}$$

$$f_T = 1/(2\pi\,\tau_T). \tag{10.40q}$$

10.2.2 Possible simplified implementation

The calculation above is quite complicated, but very good. In practice one might not need it. To simplify matters, we neglect all g_μ terms and assume that $I_{B_1B_2}$ is only a function of

 ©Koninklijke Philips Electronics N.V. 2005

$\mathcal{V}_{\mathrm{B_1B_2}}$. We also assume that the forward base current only depends on $\mathcal{V}_{\mathrm{B_2E_1}}$. We then get

$$\frac{\mathrm{d}y}{\mathrm{d}x} = \frac{g_x}{g_{Rcv,y} - g_y}, \tag{10.41a}$$

$$\frac{\mathrm{d}y}{\mathrm{d}z} = \frac{g_z - g_{Rcv,z}}{g_{Rcv,y} - g_y}, \tag{10.41b}$$

$$g_{Bf,x} = g_{\pi,x} + g_\pi^S\,[1 + g_{\pi,x}\, r_{Bv}], \tag{10.41c}$$

$$\alpha = \frac{1 + \left[g_{Rcv,y}\frac{\mathrm{d}y}{\mathrm{d}x}\right]\ \mathsf{R_{Cc}} + \left[g_x + g_{Bf,x} + g_y\frac{\mathrm{d}y}{\mathrm{d}x}\right]\ \mathsf{R_E}}{1 - \left[g_{Rcv,z} + g_{Rcv,y}\frac{\mathrm{d}y}{\mathrm{d}z}\right]\ \mathsf{R_{Cc}} - \left[g_z + g_y\frac{\mathrm{d}y}{\mathrm{d}x}\right]\ \mathsf{R_E}}, \tag{10.41d}$$

$$r_x = \left[g_{Rcv,y}\frac{\mathrm{d}y}{\mathrm{d}x} + \alpha\ \left(g_{Rcv,z} + g_{Rcv,y}\frac{\mathrm{d}y}{\mathrm{d}z}\right)\right]^{-1}, \tag{10.41e}$$

$$r_z = \alpha\, r_x, \tag{10.41f}$$

$$r_y = (1 - g_{Rcv,z} r_z)/g_{Rcv,y}, \tag{10.41g}$$

$$r_{\mathrm{ex}} = r_z + r_{Bv}\, g_{\pi,x}\, r_x, \tag{10.41h}$$

$$Xr_{\mathrm{ex}} = r_{\mathrm{ex}} + \mathsf{R_{Bc}}\, g_{Bf,x}\, r_x, \tag{10.41i}$$

$$\begin{aligned}\tau_T = {} & (C_{BE,x} + C_{BE}^S + C_{BC,x})\ r_x + (C_{BE,y} + C_{BC,y})\ r_y \\ & + (C_{BE,z} + C_{BC,z})\ r_z + C_{BC\mathrm{ex}}\ r_{\mathrm{ex}} + XC_{BC\mathrm{ex}}\ Xr_{\mathrm{ex}} \\ & + (\mathsf{C_{BEO}} + \mathsf{C_{BCO}})(Xr_{\mathrm{ex}} - \mathsf{R_{Cc}}).\end{aligned} \tag{10.41j}$$

11 Geometric scaling

Geometric scaling rules are not incorporated into Mextram. The reason is that bipolar processes vary too much, already in possible layout structures, for one set of geometric scaling equations to be applicable in all cases. For that reason geometry scaling has to be tailored to the specific process, outside of the model.

Many geometry scaling equations have been presented in the report about parameter extraction [2], in some places even with some derivation. This chapter can therefore be very short. We will only discuss the scaling of the high-current parameters and those of the self-heating parameters. Appendix D discusses the scaling of the variable base resistance.

11.1 High current parameters

The scaling of the high-current parameters $\mathsf{R_{Cv}}$, $\mathsf{SCR_{Cv}}$, $\mathsf{I_{hc}}$, and $\mathsf{S_{fh}}$ has been discussed extensively in Ref. [33]. We will not repeat the derivation here, but only give the results. Note that these results are depending on the actual spreading model one assumes, and are therefore somewhat empirical.

The derivation starts with assuming that the collector current contains a bulk and a sidewall part, in the same way as does the saturation current [2]:

$$I_C = J_{\text{bulk}}(A_{\text{em}} + Y_c P_{\text{em}}), \tag{11.1}$$

where $P_{\text{em}} = 2(L_{\text{em}} + H_{\text{em}})$ is the perimeter of the emitter, and J_{bulk} is the bulk current density. The next assumption is that the spreading is such that the bulk current density can be written as $J_{\text{bulk}}(x) \propto 1/(1 + ax)$ as function of the depth x below the base-collector junction. The value of $a = \tan\alpha\, P_{\text{em}}/A_{\text{em}}$ depends on the spreading angle α. The effective parameters can now be expressed in terms of Y_c and the spreading angles α_l for low currents and α_h for high currents as

$$\mathsf{R_{Cv}} = \mathsf{R_{Cv,1d}} \frac{\theta}{1 + S_{fL}}, \tag{11.2a}$$

$$\mathsf{I_{hc}} = \mathsf{I_{hc,1d}} \frac{1 + S_{fL}}{\theta}, \tag{11.2b}$$

$$\mathsf{SCR_{Cv}} = \mathsf{SCR_{Cv,1d}} \frac{\theta}{1 + S_{fH}}, \tag{11.2c}$$

where

$$\theta = \left(1 + \frac{Y_c\, P_{\text{em}}}{2\, A_{\text{em}}}\right)^{-1}, \tag{11.2d}$$

$$S_{fL} = \tan\alpha_l \frac{W_{\text{epi}}\, P_{\text{em}}}{2\, A_{\text{em}}}, \tag{11.2e}$$

$$S_{fH} = \tan\alpha_h \frac{W_{\text{epi}}\, P_{\text{em}}}{3\, A_{\text{em}}}. \tag{11.2f}$$

 ©Koninklijke Philips Electronics N.V. 2005

Here it is assumed that the product $\mathsf{R_{Cv}I_{hc}}$ equals its low current value. The quantity θ is related to the ratio of the collector current that actually goes through the main part of the epilayer and the collector current that goes around (the sidewall part).

In the derivation of Ref. [33] already a few approximations are made. Furthermore, the basic assumptions are not necessarily valid. This makes the calculation of the spreading rather empirical. Since we do not need a very detailed spreading model (current dependent spreading was found to be of minor importance [33, 36]), but only a geometric scaling model, we can make some further simplifications. Since the scaling of θ is very similar to that of S_{fL} and S_{fH}, we can take the scaling of θ equal to that of either S_{fL} or S_{fH}. Assuming, furthermore, values of $\tan\alpha_l = 0.5$ and $\tan\alpha_h = 1$ we arrive at the scaling equations given in Ref. [2]:

$$\mathsf{R_{Cv}} = C_{\mathsf{R_{Cv}}} \frac{W_{\mathrm{epi}}}{q N_{\mathrm{epi}}\ \mu_0\ A_{\mathrm{em}}} \frac{1}{\left(1+S_{fL}\right)^2}, \tag{11.3a}$$

$$\mathsf{SCR_{Cv}} = C_{\mathsf{SCR_{Cv}}} \frac{W_{\mathrm{epi}}^2}{2\,\varepsilon\, v_{\mathrm{sat}}\, A_{\mathrm{em}}} \frac{1}{\left(1+S_{fH}\right)^2}, \tag{11.3b}$$

$$\mathsf{I_{hc}} = C_{\mathsf{I_{hc}}}\, q N_{\mathrm{epi}}\, A_{\mathrm{em}}\, v_{\mathrm{sat}} \left(1+S_{fL}\right)^2, \tag{11.3c}$$

$$S_{fL} = \frac{W_{\mathrm{epi}}\ P_{\mathrm{em}}}{4\,A_{\mathrm{em}}}; \qquad S_{fH} = \frac{W_{\mathrm{epi}}\ P_{\mathrm{em}}}{3\,A_{\mathrm{em}}}. \tag{11.3d}$$

Here each parameter has a pre-factor—which should be of the order of one—to give them effective values, rather than ideal values. When we look at these equations we see that the effect of the scaling is simply to make the area used for the calculation of the parameters an effective area, one that is larger than the emitter area. The increase in area depends on the size of the emitter area through S_{fL} and S_{fH}.

The parameter $\mathsf{S_{fh}}$, which is important for avalanche at high currents (but only if the extended avalanche model is used: $\mathsf{EXAVL} = 1$), is basically the same as the S_{fH} above, and therefore scales in the same way, although it might have a different pre-factor.

11.2 Self-heating

Self-heating in a transistor is a complex process. The source of dissipation is distributed over the transistor, and also the temperature varies, depending on the location within the transistor. Nevertheless, we model this with a simple self-heating network, containing a thermal resistance $\mathsf{R_{th}}$ [K/W] and a thermal capacitance $\mathsf{C_{th}}$ [J/K].

The thermal resistance is directly related to the thermal conductivity K [W/Km]. A dimensional analysis then tells us that the thermal resistance must be given as one over the thermal conductivity times some length scale ℓ. So, apart from a pre-factor, we can write

$$\mathsf{R_{TH}} \propto 1/(K\,\ell). \tag{11.4}$$

We can also give a derivation for the same effect, in the ideal case of a sphere of dissipation in an infinite substrate. We assume that the dissipation density inside this sphere of

radius R is uniform, and therefore given by $P_{\rm diss}/(\frac{4}{3}\pi R^3)$. The energy flux density $\boldsymbol{J}_u$ is related to the local temperature increase ΔT via the diffusion equation $\boldsymbol{J}_u = -K\,\nabla\Delta T$. Solution of this equation and the continuity equation $\nabla \boldsymbol{J}_u = 0$ in an infinite spherical symmetric medium gives

$$\Delta T(r) = \begin{cases} \dfrac{P_{\rm diss}}{4\pi K R}\left(\dfrac{3}{2} - \dfrac{r^2}{2R^2}\right), & \text{for } r < R, \\ \dfrac{P_{\rm diss}}{4\pi K r}, & \text{for } r > R. \end{cases} \tag{11.5}$$

The temperature in the region of interest, where the dissipation takes place, scales with one over the size of this region R.

In practice of course, the region of dissipation is not a sphere. It is more of a rectangular region. Nevertheless, the scaling is basically as given above. For a box with square surface and small constant thickness, for instance, the thermal resistance scales with the length of a side. For the reasons above, the geometric scaling of the thermal resistance can approximately be given as

$$\mathsf{R_{TH}} \propto \frac{1}{\sqrt{A_{\rm em}}}. \tag{11.6}$$

Some experimental evidence confirms this relation.

For small but long devices 3D effects become less important and the thermal resistance will scale with the length of the transistor

$$\mathsf{R_{TH}} \propto \frac{1}{L_{\rm em}}. \tag{11.7}$$

In practice the behaviour will be somewhere in between the square-root dependence on the emitter length and the linear dependence.

For the thermal capacitance there is a direct relation to the heat capacity per unit volume C_v [J/m^{3}K], which is proportional to the thermal conductivity $K = D\,C_v$, with D the diffusion constant (the same as for the electrical behaviour). Again, from a dimensional analysis, we find $\mathsf{C_{th}} = C_v\,\ell^3$. The thermal delay time is then given by $\tau = \mathsf{R_{th}}\,\mathsf{C_{th}} = \ell^2/D$. This is indeed a well known relation for a diffusive process: the time scales with the length squared.

For a transistor we therefore take the thermal capacitance proportional to the dissipating volume, which, for a fixed vertical structure, scales with the emitter area:

$$\mathsf{C_{TH}} \propto A_{\rm em}. \tag{11.8}$$

The reason that the delay time does no longer scale with the length of the emitter squared, but with the length itself, is due to the assumption of a small thickness of the dissipation region: the heat transport to the outside of this region can now go partially vertically, which makes it faster.

 ©Koninklijke Philips Electronics N.V. 2005

A General compact model formulations

A.1 Smooth minimum and maximum-like functions

Let us look at functions with the following properties

$$f(x) \simeq \begin{cases} 0, & \text{for } x < 0, \\ x, & \text{for } x > 0. \end{cases} \tag{A.1}$$

Basically this is the 'max' function: $f(x) = \max(x, 0)$. For compact modelling we need a smooth transition between the two asymptotes. In this section we present some possible formulations.

A.1.1 Hyperboles

Within Philips we mainly use the hyperbolic functions like

$$f(x) = \tfrac{1}{2}\left(x + \sqrt{x^2 + 4\varepsilon^2}\right). \tag{A.2}$$

It is shown if Fig. 29. Note that this function indeed describes a hyperbole. The disadvantage of this function is that it does not converge very fast to the asymptotes.

A.1.2 Exponents

An alternative function is

$$f(x) = \varepsilon\ \ln\left(1 + e^{x/\varepsilon}\right). \tag{A.3}$$

This function converges very rapidly to both asymptotes.

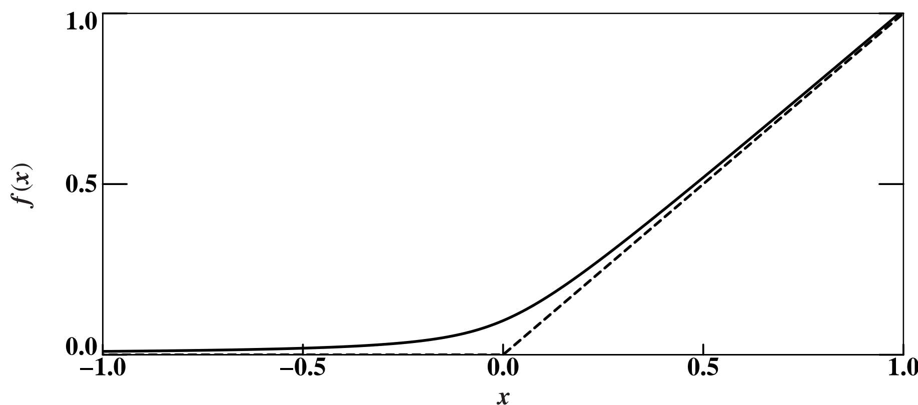

Figure 29: *The hyperbole $f(x)$ from Eq. (A.2) and its asymptotes ($\varepsilon = 0.1$).*

©Koninklijke Philips Electronics N.V. 2005

The disadvantage of this function is that it has a very abrupt transition between both asymptotes (as one would get by taking ε in the hyperboles very small). In that case even though the function is $\mathcal{C}^\infty$ (i.e. continuous in every order derivative), numerical routines may still experience problems around the transition to find a solution to the equations.

Another disadvantage is possibly the increase of computation time. Previously the time to calculate logarithms and exponents on a computer was much longer that that of square roots and simple multiplications. Due to the advances in modern compilers and IC design this difference has become much smaller. Given the complexity of the rest of the model, we don't consider the time constraints here as an issue anymore.

McAndrew [65] has made a slight improvement on the function above by writing

$$f(x) = \tfrac{1}{2}\left(x + \sqrt{x^2}\right) + \varepsilon\ \ln\left(1 + e^{-\sqrt{x^2}/\varepsilon}\right). \tag{A.4}$$

The advantage of this latter formulation is that, although it is mathematically equivalent to the previous one, numerically it is much more accurate for $x > 0$. The reason is that the argument of the exponential is always negative. Hence the argument of the logarithm is always between 1 and 2, and doesn't become exponentially large. Since the only advantage is from an implementation point of view, in our opinion the best way to implement the function is using

$$f(x) = \begin{cases} \varepsilon\ \ln\left(1 + e^{x/\varepsilon}\right), & \text{for } x \le 0, \\ x + \varepsilon\ \ln\left(1 + e^{-x/\varepsilon}\right), & \text{for } x > 0. \end{cases} \tag{A.5}$$

A.1.3 The linear function with a maximum

Sometimes a variation on the functions above is needed, one where $g(x) \simeq x$, up to a certain maximum, e.g.

$$g(x) = \begin{cases} x, & \text{for } x < 1, \\ 1, & \text{for } x > 1. \end{cases} \tag{A.6}$$

The function g is more or less a 'min'-function: $g(x) = \min(x, 1)$. One can make use of the functions above by writing $g(x) = 1 - f(1 - x)$. The results are

$$g(x) = \tfrac{1}{2}\left(x + 1 - \sqrt{(x-1)^2 + 4\varepsilon^2}\right), \tag{A.7}$$

$$\text{or} \quad 1 - \varepsilon \ln\left(1 + e^{(1-x)/\varepsilon}\right) = x - \varepsilon \ln\left(1 + e^{-(1-x)/\varepsilon}\right). \tag{A.8}$$

Often, as an extra demand on the function $g(x)$ one would like to have $g(0) = 0$ and $g'(0) = 1$. In other words, for small x one would like $g(x) \simeq x$. This is not easy to achieve. For the hyperbole, for instance, we have $g(0) \simeq -\varepsilon^2$, and this is not very small. The use of the function with exponents is better, since in that case $g(0) \simeq -\varepsilon\ e^{-1/\varepsilon}$,

 ©Koninklijke Philips Electronics N.V. 2005

which is very small for small ε, and hence in most practical cases already negligible. For instance, with $\varepsilon = 0.1$ it gives a value of $|g(0)| < 5 \cdot 10^{-6}$.

An alternative function for this special case is

$$g_m(x) = \frac{x}{\left(1 + x^{2m}\right)^{1/2m}}, \tag{A.9}$$

with, for small x,

$$g_m(x) \simeq x + \frac{x^{2m+1}}{2m} + \mathcal{O}(x^{2m+2}). \tag{A.10}$$

This equation fulfils all the properties we need for $x > 0$. However it is an odd function, which means that it has also a lower limit of -1 when $x \lesssim -1$.

If one really wants to have a function which approximates x for $x < 0$, one could use

$$g_m(x) = \frac{x}{\left(1 - \frac{1}{2}(x + |x|)\, x^{2m-1}\right)^{1/2m}}. \tag{A.11}$$

For this function Eq. (A.10) holds as long as x is positive. For negative x we have $g_m(x) = x$. This means that the function is no longer C^∞, but only $2m$ times differentiable.

A.2 Depletion capacitances

In the ideal case the depletion capacitance and the depletion charge have the form

$$C(V) = \frac{C_0}{(1 - V/V_d)^p}, \tag{A.12}$$

$$Q(V) = \frac{C_0 V_d}{1 - p}\left[1 - (1 - V/V_d)^{1-p}\right]. \tag{A.13}$$

This formulation however gives problems when $V \geq V_d$. Hence we need a continuation of the formulation. It is important to realise that it is not so important to have a physical description of depletion charge for $V \geq V_d$. The diffusion charge in that region is much more important. Hence we can choose a formulation that is best for compact modelling, i.e. a smooth formulation.

The formulations should be such that $Q(0) = 0$ (which is simple to achieve). But we also demand that $C(0) = C_0$, just as one would expect. This latter requirement is not fulfilled in all compact models, especially when looking at temperatures different than the reference temperature. We will show this below.

Various formulations of those discussed below are illustrated in Fig. 30.

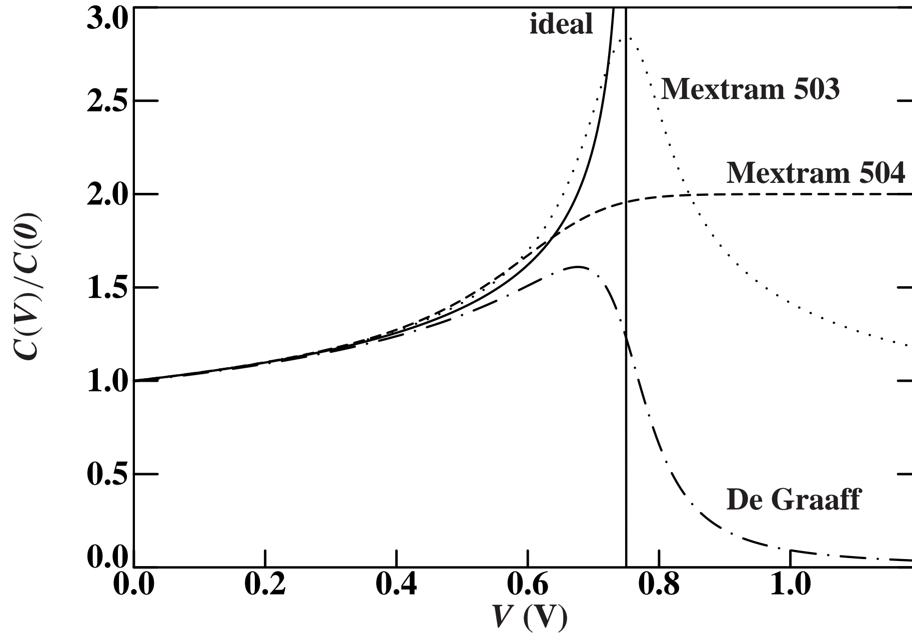

Figure 30: *The various formulas for the depletion capacitances, normalised to the zero bias value. Shown are the ideal curve (solid) from Eq. (A.13), the De Graaff expression (dashed-dotted) from Eq. (A.15), the expression used in Mextram 503 (dotted) from Eq. (A.17), and the expression used in Mextram 504 (dashed) from Eqs. (A.18) and (A.25).*

A.2.1 Spice-Gummel-Poon

In older compact models like the Spice-Gummel-Poon model the capacitance is ideal up to a the voltage $F_C\ V_d$, with F_C a parameter. From that voltage on a linear extrapolation is used for the capacitance. The clear disadvantage of this model is that higher order derivatives are not continuous. This gives kinks in for instance the output conductance and the cut-off frequency and discontinuities when looking at distortion.

A.2.2 De Graaff and Klaassen

In a formulation given by De Graaff [9] the charge is limited from above:

$$C(V) = \frac{C_0}{\sqrt{(1-V/V_d)^2+k}} \left[\frac{(1-V/V_d)+\sqrt{(1-V/V_d)^2+k}}{2}\right]^{1-p}, \quad \text{(A.14)}$$

$$Q(V) = \frac{C_0 V_d}{1-p} \left\{1-\left[\frac{(1-V/V_d)+\sqrt{(1-V/V_d)^2+k}}{2}\right]^{1-p}\right\}. \quad \text{(A.15)}$$

Here k is a constant of order 0.01. The capacitance decreases quite rapidly for biases beyond V_d. For $k \to 0$ one gets the ideal formulation up to $V = V_d$. After that the capacitance is 0.

 ©Koninklijke Philips Electronics N.V. 2005

A.2.3 Earlier versions of Mextram

The general Mextram formulation for levels up to and including 503 is the one given by Poon en Gummel [81]:

$$C = C_0 \frac{(1+k)^{p/2+1}}{1+k-p} \frac{(1-p)(1-V/V_d)^2+k}{[(1-V/V_d)^2+k]^{p/2+1}}, \tag{A.16}$$

$$Q = C_0 V_d \frac{1+k}{1+k-p} \left[1 - \frac{(1-V/V_d)\,(1+k)^{p/2}}{[(1-V/V_d)^2+k]^{p/2}} \right]. \tag{A.17}$$

Again k is a constant of order 0.01. This formulation is such that C is symmetric around V_d. This means that it will decrease again slowly when $V > V_d$. For $k \to 0$ we regain the ideal formulation (but still symmetric). The formulation is not very elegant. Furthermore the capacitance has a very small and high peak around $V = V_d$. Sometimes the effects of this peak can be seen in higher-order derivatives.

A.2.4 Modern compact models

All of the modern compact models use expressions similar to each other. The idea is to have the ideal capacitance curve for $V \lesssim V_d$ and a constant capacitance for $V \gtrsim V_d$. The capacitance can then be expressed as

$$C = \frac{C_0}{(1-V_j/V_d)^p} \frac{\mathrm{d}V_j}{\mathrm{d}V} + \frac{C_0}{(1-V_F/V_d)^p} \left(1 - \frac{\mathrm{d}V_j}{\mathrm{d}V}\right). \tag{A.18}$$

Here $V_j = V_j(V)$ is a function like the ones we discussed in Section A.1. For $V < V_F$ we have $V_j \simeq V$ and for $V > V_F$ we have $V_j \simeq V_F$. In this way the derivative $\mathrm{d}V_j/\mathrm{d}V$ is 1 for $V < V_F$. Only the first part of the expression is important. For $V > V_F$ the derivative goes to zero, and only the second part is important. The transition of this derivative from 1 to 0 happens around the switching voltage V_F. In other words, this derivative acts as a kind of switch between the ideal capacitance and a constant capacitance.

The corresponding equation for the charge is

$$Q = \frac{C_0 V_d}{1-p} \left[(1-V_{j0}/V_d)^{1-p} - (1-V_j/V_d)^{1-p} \right] + \frac{C_0}{(1-V_F/V_d)^p} \left(V - V_j + V_{j0}\right). \tag{A.19}$$

Here $V_{j0} = V_j(V{=}0)$, to make sure that the charge vanishes at zero bias. The value of V_F is calculated such that the constant capacitance equals a factor a (a model constant in Mextram, depending on the junction) times the zero bias capacitance.

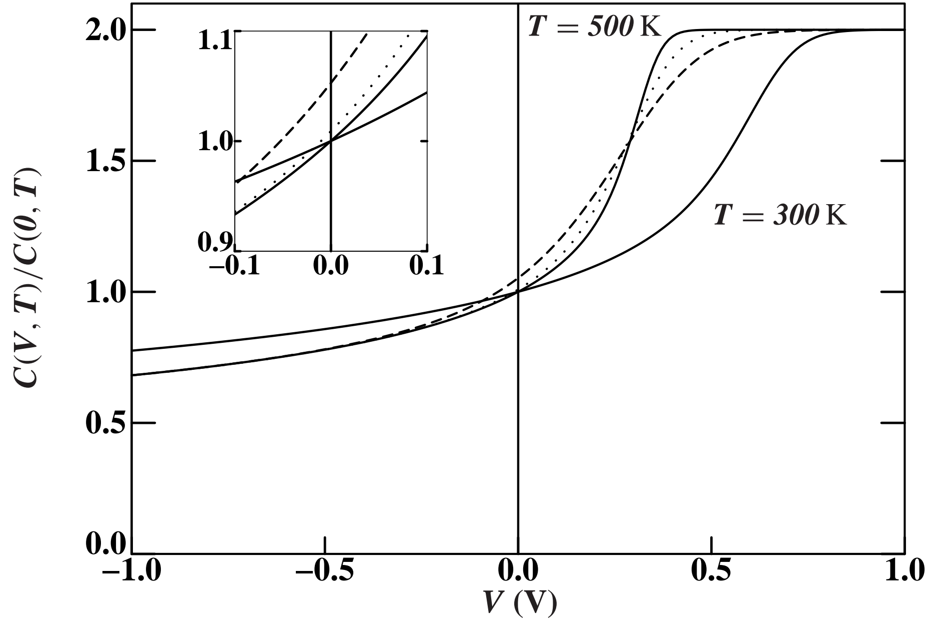

Figure 31: *The capacitance from Eqs. (A.18) and (A.24), normalised to its zero bias value, as function of bias for* $T = 300\,\mathrm{K}$ *and* $500\,\mathrm{K}$. *The different curves are for* $V_{ch} = 75\,\mathrm{mV}$ *(dotted),* $V_{ch} = 3V_T$ *(dashed), and* $V_{ch} = 0.1V_d$ *(solid). No difference can be seen at* $T = 300\,\mathrm{K}$. *The parameters are* $V_d = 0.75\,\mathrm{V}$, $p = 0.3$ *and* $a = 2$, *whereas the bandgap used for the temperature scaling of* V_d *is* $1.2\,\mathrm{V}$. *The inset shows a detail of the curves around* $V = 0\,\mathrm{V}$.

The difference between the various compact models lies in the formulation of $V_j(V)$. Hicum [10, 82] uses

$$V_j = V - V_T \ln\left(1 + \exp[(V - V_F)/V_T]\right), \tag{A.20}$$

$$\frac{\mathrm{d}V_j}{\mathrm{d}V} = \frac{1}{1 + \exp[(V - V_F)/V_T]}. \tag{A.21}$$

The advantage of using this function is that the zero-bias capacitance is to very high accuracy equal to C_0, and that we can take $V_{j0} = 0\,\mathrm{V}$. Vbic [10, 83, 84] uses

$$V_j = \tfrac{1}{2}\left(V + V_F - \sqrt{(V - V_F)^2 + k}\right), \tag{A.22}$$

$$\frac{\mathrm{d}V_j}{\mathrm{d}V} = \tfrac{1}{2}\left(1 - \frac{V - V_F}{\sqrt{(V - V_F)^2 + k}}\right). \tag{A.23}$$

Using this formulation means that a correction is needed to make sure that $C(V{=}0) = C_0$. In Mextram 504 we use an equation like Eq. (A.21):

$$V_j = V - V_{ch} \ln\left(1 + \exp[(V - V_F)/V_{ch}]\right). \tag{A.24}$$

To make the transition between the ideal capacitance and the constant capacitance less abrupt we choose for a higher value of V_{ch}, around 75 mV at room temperature. This can

 ©Koninklijke Philips Electronics N.V. 2005

be done in three ways: $V_{ch} = 75\,\text{mV}$, $V_{ch} = 3V_T$, or $V_{ch} = 0.1V_d$. At room temperature there is not much difference between the three expressions, as can be seen in Fig. 31. However, when we increase the temperature, we see the difference of the three possible expressions for V_{ch}. Only when we use $V_{ch} = 0.1V_d$ we are guaranteed that the zero bias capacitance is indeed the capacitance we expect from temperature scaling. Hence we use

$$V_j = V - 0.1\;V_d \ln\left(1 + \exp[(V - V_F)/0.1\;V_d]\right). \tag{A.25}$$

Together with this equation for V_j, and with $V_F = V_d(1 - a^{-1/p})$, we can now define the function used in the depletion capacitances:

$$V_{\text{depletion}}(V|V_d,\,p|a) = \frac{V_d}{1-p}\left[1 - (1 - V_j/V_d)^{1-p}\right] + a\,\left(V - V_j\right). \tag{A.26}$$

©Koninklijke Philips Electronics N.V. 2005

B Analytical calculation of the critical current

Under some assumptions it is possible to give an analytical relation between the current at the onset of quasi-saturation I_{qs} and the voltage $V_{qs} \simeq \mathsf{V}_{\mathsf{dC}} - \mathcal{V}_{\mathrm{B_2C_1}}$. For this we use the equations

$$\frac{\mathrm{d}E}{\mathrm{d}x} = \frac{qN_{\mathrm{epi}}}{\varepsilon}\left(1 - \frac{I_{\mathrm{epi}}}{qN_{\mathrm{epi}}A_{\mathrm{em}}v_{\mathrm{dr}}}\right), \tag{B.1a}$$

$$v_{\mathrm{dr}} = \frac{\mu_{n0}|E|}{1 + \mu_{n0}|E|/v_{\mathrm{sat}}}, \tag{B.1b}$$

$$V_{qs} = -\int_0^{W_{\mathrm{epi}}} E\,\mathrm{d}x, \tag{B.1c}$$

that have already been used in Chapter 3. Here, however, we do not assume that all electrons travel at the saturated velocity v_{sat}, but use the drift velocity v_{dr} to calculate the electron density. The boundary condition we use is $E(0) = 0$ for $I_{\mathrm{epi}} = I_{qs}$. This means that we assume that quasi-saturation starts once the electric field at the base-collector junction vanishes. In practice it will not really vanish, but keep a finite value. But we already mentioned before that in the injection region it is very small.

B.1 Derivation

We will start with writing all the equations in normalised quantities e, i, r, y and v:

$$E = e\,\mathsf{I}_{\mathsf{hc}}\,\mathsf{R}_{\mathsf{Cv}}/W_{\mathrm{epi}}, \tag{B.2a}$$

$$I_{qs} = i\,\mathsf{I}_{\mathsf{hc}}, \tag{B.2b}$$

$$\mathsf{R}_{\mathsf{Cv}} = r\,\mathsf{SCR}_{\mathsf{Cv}}, \tag{B.2c}$$

$$x = y\,W_{\mathrm{epi}}, \tag{B.2d}$$

$$V_{qs} = v\,\mathsf{I}_{\mathsf{hc}}\,\mathsf{R}_{\mathsf{Cv}}. \tag{B.2e}$$

We will see that it is then possible to express the normalised voltage v in terms of the normalised current i and only one parameter, r. The equations (B.1) above now become

$$\frac{\mathrm{d}e}{\mathrm{d}y} = \frac{2}{r}\,(1 - i + i/e), \tag{B.3a}$$

$$v = -\int_0^1 e\,\mathrm{d}y. \tag{B.3b}$$

In our derivation we will first calculate E_W, or rather its normalised variant, as function of the current. Then we will calculate V_{qs} using its expression given above.

 ©Koninklijke Philips Electronics N.V. 2005

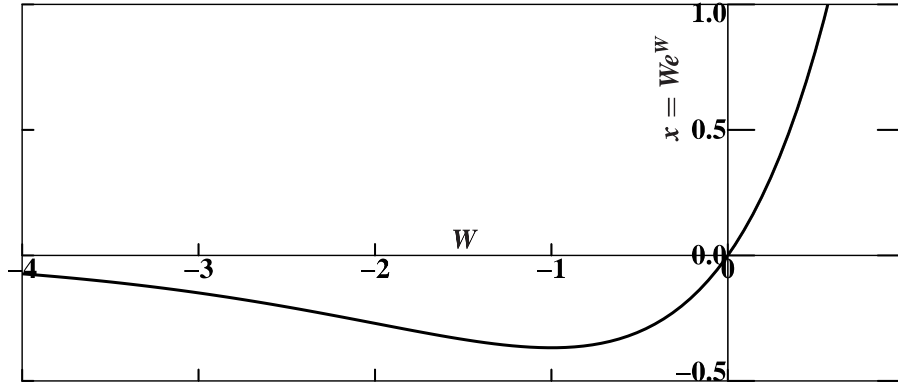

Figure 32: *The function* $x = We^W$*, which is the inverse of the two branches of the Lambert W-function:* $W_- < -1$ *and* $W_+ > -1$.

Calculating E_W For our derivation we start with finding the electric field at $x = W_{\text{epi}}$ (i.e. $y = 1$) by integrating the equation for $\mathrm{d}e/\mathrm{d}y$:

$$
\begin{aligned}
1 &= \int_0^1 \mathrm{d}y = \frac{r}{2}\int_0^{e_W} \frac{\mathrm{d}e}{1 - i + i/e} \\
&= \frac{ir}{2(1-i)^2}\left[e_W\frac{1-i}{i} - \ln\left(1 + e_W\frac{1-i}{i}\right)\right].
\end{aligned} \tag{B.4}
$$

From this equation we can solve e_W as function of normalised current i, given the resistance ratio r. To do so we introduce the help-variables

$$
\xi = e_W\frac{1-i}{i}, \qquad \text{and} \qquad f = \frac{2(1-i)^2}{ir}. \tag{B.5}
$$

We then need to solve

$$
f = \xi - \ln(1+\xi). \tag{B.6}
$$

The solution to this equation can be expressed in terms of the so-called Lambert-W function.

The Lambert-W function [85] is defined as

$$
W(x)\exp[W(x)] = x. \tag{B.7}
$$

The function is called ProductLog in programs like Mathematica and Maple. It can be used for instance to calculate the analytical solution of the current through an ideal diode in series with a resistor [86]. We have plotted the function We^W in Fig. 32. As one can see the inverse is not unique. The function has two branches. We define $W_+(x)$ as the function on the interval $[-1/e, \infty)$ giving a result $W_+(x) \geq -1$. We define $W_-(x)$ as the function on the interval $[-1/e, 0)$ giving a result $W_-(x) \leq -1$.

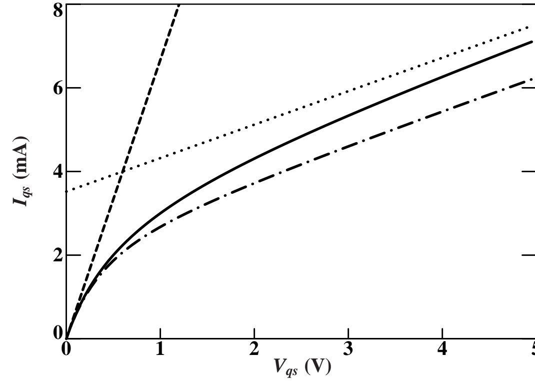

Figure 33: *The current I_{qs} at onset of injection as function of the applied voltage V_{qs} for the default parameter set [1], just as in Fig. 11. We have again shown the two limiting cases. The dash-dotted line is the exact result from Eq. (B.10)*

We must now realise that ξ can have two signs. Since E_W and hence e_W are negative, we have $\xi < 0$ for $i < 1$. For $i > 1$ we have $\xi > 0$. Hence we need the two branches of the Lambert-W function:

$$\xi = \begin{cases} -1 - W_+(-e^{-1-f}), & \text{for } i < 1 \text{ (i.e. } I_{qs} < \mathsf{I_{hc}}), \\ -1 - W_-(-e^{-1-f}), & \text{for } i > 1 \text{ (i.e. } I_{qs} > \mathsf{I_{hc}}). \end{cases} \tag{B.8}$$

Calculating V_{qs} The next step in our derivation is the calculation of V_{qs}, or rather v. The integral for v can be expressed as

$$\begin{aligned} -v &= \int_0^1 e\,\mathrm{d}y = \frac{r}{2}\int_0^{e_W} \frac{e\,\mathrm{d}e}{1-i+i/e} = \frac{r}{2}\int_0^{e_W} \frac{e(1-i+i/e)-i}{1-i}\,\frac{\mathrm{d}e}{1-i+i/e} \\ &= \frac{r}{2}\,\frac{1}{1-i}\int_0^{e_W} e\,\mathrm{d}e - \frac{r}{2}\,\frac{i}{1-i}\int_0^{e_W}\frac{\mathrm{d}e}{1-i+i/e} \\ &= \frac{r e_W^2}{4(1-i)} - \frac{i}{1-i}, \end{aligned} \tag{B.9}$$

where we used Eq. (B.4) for the second integral. Expressing v now in terms of the solution we found for e_W before (using ξ rather than e_W), we get

$$v = \frac{i}{1-i} - \frac{r i^2 \xi^2}{4(1-i)^3}. \tag{B.10}$$

B.2 The Mextram expression

In Mextram we have from Eq. (3.45) the normalised equation

$$i = \frac{v(1+rv)}{1+v}. \tag{B.11}$$

 ©Koninklijke Philips Electronics N.V. 2005

When we invert this we get

$$v = \frac{2i}{\sqrt{(1-i)^2 + 4ir} + 1 - i}. \tag{B.12}$$

We have shown the exact result for $V_{qs} = v\,\mathsf{I_{hc}}\,\mathsf{R_{Cv}}$ from Eq. (B.10) in Fig. 33, together with the Mextram result. One can see that the exact result and the Mextram expression are very similar, although the exact result is somewhat lower. This means that after parameter extraction the parameter $\mathsf{I_{hc}}$ will be somewhat smaller than the ideal value, which is not something to worry about.

B.3 The critical current in limiting cases

We can use the analytical solution to find various limits. We will consider $I_{qs} \ll \mathsf{I_{hc}}$, $I_{qs} = \mathsf{I_{hc}}$ and $I_{qs} \gg \mathsf{I_{hc}}$.

Small currents In the case of small currents f is very large and $\xi \simeq -1$. The error in ξ is exponentially small and can be neglected. We then find, both for the analytical expression derived here as for Mextram, to lowest order:

$$v \simeq i \qquad \text{or} \qquad V_{qs} \simeq I_{qs}\,\mathsf{R_{Cv}}. \tag{B.13}$$

The situation where $I_{qs} = \mathsf{I_{hc}}$ The case $I_{qs} = \mathsf{I_{hc}}$, or $i = 1$, is special in the sense that we can find an expression for v that does not use the Lambert-W function. We must expand around $i = 1$, and therefore write $i = 1 + \delta$. One can then find ξ to second order in δ as

$$\xi \simeq \frac{2\delta}{\sqrt{r}} + \frac{4 - \sqrt{r}}{3r}\delta^2. \tag{B.14}$$

Using this in the expression for v, and taking the limit $\delta \to 0$, we find

$$v = \frac{4}{3\sqrt{r}} \qquad \text{or} \qquad V_{qs} = \tfrac{4}{3}\sqrt{\mathsf{R_{Cv}}\,\mathsf{SCR_{Cv}}}\,\mathsf{I_{hc}}. \tag{B.15}$$

The Mextram equivalent is

$$v = \frac{1}{\sqrt{r}} \qquad \text{or} \qquad V_{qs} = \sqrt{\mathsf{R_{Cv}}\,\mathsf{SCR_{Cv}}}\,\mathsf{I_{hc}}. \tag{B.16}$$

©Koninklijke Philips Electronics N.V. 2005

Large currents In the case of large currents we have $f \gg 1$. We can then write $\xi \simeq f$. Using this first estimate, we can even give a better estimate by writing $\xi \simeq f + \ln f$. Using this in the expression for v, we find

$$v \simeq \frac{i-1}{r} - 1 + \ln \frac{2i}{r} \qquad \text{or}$$
$$V_{qs} \simeq \mathsf{SCR_{Cv}}\,(I_{qs} - \mathsf{I_{hc}}) + \mathsf{I_{hc}}\,\mathsf{R_{Cv}} \left(-1 + \ln \frac{2 I_{qs}\,\mathsf{SCR_{Cv}}}{\mathsf{I_{hc}}\,\mathsf{R_{Cv}}}\right). \tag{B.17}$$

For Mextram we find

$$v \simeq \frac{i-1}{r} + 1 \qquad \text{or} \qquad V_{qs} \simeq \mathsf{SCR_{Cv}}\,(I_{qs} - \mathsf{I_{hc}}) + \mathsf{I_{hc}}\,\mathsf{R_{Cv}}. \tag{B.18}$$

 ©Koninklijke Philips Electronics N.V. 2005

C The Kull-model around zero current

When the voltage over the epilayer $\mathcal{V}_{C_1C_2}$ is very small, the equations for the current $I_{C_1C_2}$ and for E_c, Eq. (3.26), and especially taht for the thickness of the injection region $x_i / W_{\rm epi}$, Eq. (3.47), can become numerical inaccurate [87]. For this reason here we study the Kull model [19] around $\mathcal{V}_{C_1C_2} = 0$ and discuss the numerical implications.

We assume that the bias $\mathcal{V}_{B_2C_1}$ is fixed and express the quantities in terms of $V = \mathcal{V}_{C_1C_2}$. We start with the expression and derivatives of K_0:

$$K_0(V) = \sqrt{1 + 4e^{(V+\mathcal{V}_{B_2C_1}-\mathsf{V_{d_C}})/V_T}}, \tag{C.1a}$$

$$\frac{dK_0}{dV} = \frac{K_0^2 - 1}{2K_0 V_T}, \tag{C.1b}$$

$$\frac{d^2K_0}{dV^2} = \frac{K_0^4 - 1}{4K_0^3 V_T^2}. \tag{C.1c}$$

From the definitions in Section 3.3.1, we also have $K_W = K_0(V{=}0)$. Next we consider the quantity E_c:

$$E_c = V_T \left(K_0 - K_W - \ln \frac{K_0 + 1}{K_W + 1} \right), \tag{C.2a}$$

$$\frac{dE_c}{dK_0} = \frac{V_T K_0}{K_0 + 1}, \tag{C.2b}$$

$$\frac{dE_c}{dV} = \frac{K_0 - 1}{2}, \tag{C.2c}$$

$$\frac{d^2E_c}{dV^2} = \frac{dK_0}{2\, dV}, \tag{C.2d}$$

$$\frac{d^3E_c}{dV^3} = \frac{d^2K_0}{2\, dV^2}. \tag{C.2e}$$

We can now give an expansion for E_c around $V = 0$:

$$\begin{aligned} E_c &\simeq E_c|_{V=0} + V \left.\frac{dE_c}{dV}\right|_{V=0} + \tfrac{1}{2}V^2 \left.\frac{d^2E_c}{dV^2}\right|_{V=0} + \tfrac{1}{6}V^3 \left.\frac{d^3E_c}{dV^3}\right|_{V=0} \\ &= \tfrac{1}{2}V \left(K_W - 1 + V \left.\frac{dK_0}{2\, dV}\right|_{V=0} + \tfrac{1}{3}V^2 \left.\frac{d^2K_0}{2\, dV^2}\right|_{V=0} \right) \\ &= \tfrac{1}{2}V \left(K_W - 1 + V \frac{K_W^2 - 1}{4K_W V_T} + \tfrac{1}{3}V^2 \frac{K_W^4 - 1}{8K_W^3 V_T^2} \right). \end{aligned} \tag{C.3}$$

Let us now consider the numerical accuracy of E_c. For the computer accuracy we write $\delta \simeq 10^{-15}$. Since E_c is calculated as the difference of two, possibly large, numbers, its numerical accuracy can be given by $\delta \cdot V_T K_W$. For small values of V it is better to

©Koninklijke Philips Electronics N.V. 2005

have an approximation for E_c that is numerically more accurate. Of course, the difference between the approximation and the exact result must be smaller than the typical numerical error of the exact expression. From Eq. (C.3) we find for the approximation

$$E_c \simeq \tfrac{1}{2} V \left(K_W - 1 + V \left. \frac{\mathrm{d}K_0}{2\,\mathrm{d}V} \right|_{V=0} \right) \simeq \tfrac{1}{2} V \left[K_W - 1 + (K_0 - K_W)/2 \right], \tag{C.4}$$

where we used $K_0 \simeq K_W + V \mathrm{d}K_0/\mathrm{d}V|_{V=0}$. This leads to

$$E_{c,\mathrm{appr}} = \tfrac{1}{4} V\,(K_0 + K_W - 2] = \tfrac{1}{2} V\,(p_0 + p_W) = V p_{\mathrm{av}}, \tag{C.5}$$

where p_{av} is used in the model documentation [1]. The error in this approximation is of the order of the last term in Eq. (C.3), i.e. of the order of or smaller than $V^3 K_W / V_T^2$. If this error is smaller than the numerical error in the exact result, $\delta \cdot V_T K_W$, it is better to take the approximation. Both errors are of the same order when

$$V \simeq \sqrt[3]{\delta} \cdot V_T \simeq 10^{-5} V_T. \tag{C.6}$$

So for $V_{C_1C_2} < 10^{-5} V_T$ it is better to use the approximation (C.5) instead of the exact result (C.2). Note that apart from the error made by the approximation, $E_{c,\mathrm{appr}}$ also has a numerical error. This error is of the order of $\delta \cdot E_{c,\mathrm{appr}}$ which is a factor V/V_T smaller than the numerical error in the exact result.

Within the Kull model also the thickness of the injection layer is defined:

$$\frac{x_i}{W_{\mathrm{epi}}} = \frac{E_c}{E_c + \mathcal{V}_{\mathrm{C_1C_2}}}, \tag{C.7}$$

which is already given in Eq. (3.47). Since in this expression we divide two small and possibly inaccurate numbers when $V = \mathcal{V}_{\mathrm{C_1C_2}}$ is small, it is very important that we approximate it, using Eq. (C.5), by

$$\frac{x_i}{W_{\mathrm{epi}}} \simeq \frac{p_{\mathrm{av}}}{p_{\mathrm{av}} + 1}. \tag{C.8}$$

 ©Koninklijke Philips Electronics N.V. 2005

D Current crowding at small currents

In Section 5.1.1 we have seen that the effective low current resistance of a distributed system like the pinched base can be given as a factor times the sheet resistance $\rho_\square$ of the pinched base. In this appendix we want to give a method to calculate this pre-factor for more general geometries [47]. The derivation is maybe not so important. So, after we have given the derivation, we will give a recipe to calculate the pre-factor. At the end we will present some examples.

D.1 Derivation

Our analysis is based on the analysis of Section 5.1. Here, however, we will only look at the small current limit, but we will allow for general non-linear currents from base to emitter. The derivation is therefore much more general than just for the pinched base.

We consider a two-dimensional pinched base, with sheet resistance $\rho_\square$. The geometry of this base is not yet fixed. Some parts of its outer boundary are connected to the external base. These will have a potential $\mathcal{V}_{\mathrm{B_1}}$. Where the base is connected current will flow into the pinched base. Other parts of the outer boundary are, possibly, not connected. The current that flows in this pinched base is given by $\boldsymbol{J}$, the base sheet current density (in units A/m). At every point of the pinched base a part of the current will go to the emitter (in our case). This amount of current is given by $I[V(x)]/A_{\mathrm{em}}$, and therefore depends on the local potential. When the sheet resistance of the base is zero, we have $I(0) = I_B$, a constant over the whole base. The equations we need to solve are very similar to those in Section 5.1

$$\nabla \cdot \boldsymbol{J} = -\frac{I(V)}{A_{\mathrm{em}}}, \tag{D.1a}$$

$$\nabla V = -\rho_\square \boldsymbol{J}. \tag{D.1b}$$

To solve these equations we need some boundary conditions. First of all, there is no current leaving or entering the base (under the emitter) where there is no connection. So at these places we have $\hat{\boldsymbol{n}} \cdot \boldsymbol{J} = 0$, where $\hat{\boldsymbol{n}}$ is a unit vector normal and outward to the boundary. This directly implies $\hat{\boldsymbol{n}} \cdot \nabla V = 0$. At the places where there *is* a connection, we have $V = \mathcal{V}_{\mathrm{B_1B_2}}$.

Let us now introduce a dimensionless quantity, defined by

$$f = \frac{R_{Bv}}{\rho_\square} - \frac{V}{I_B \rho_\square}. \tag{D.2}$$

Of course, $R_{Bv} = \mathcal{V}_{\mathrm{B_1B_2}}/I_B$ still needs to be determined. From the boundary conditions we see directly that $f = 0$ at connected boundaries. At non-connected boundaries we have $\hat{\boldsymbol{n}} \cdot \nabla f = 0$. The differential equation for f can be found from Eq. (D.1):

$$\nabla^2 f = -\frac{1}{A_{\mathrm{em}}} \frac{I(V)}{I_B}. \tag{D.3}$$

©Koninklijke Philips Electronics N.V. 2005

As mentioned before, we only consider small currents. This also means that $V \simeq 0$. We can therefore write

$$I(V) \simeq I_B + \frac{\mathrm{d}I}{\mathrm{d}V}\, V, \tag{D.4}$$

where the derivative is taken at $V = 0$. In the limit of small V the right-hand-side of Eq. (D.3) becomes simply $-1/A_{\mathrm{em}}$. The differential equation for f is now a very elementary one, which has no longer any link to the actual expression for $I(V)$. So f can be found. Next we need to find R_{Bv}. To this end we need the following integral over all points of the pinched base

$$\frac{\rho_\square}{A_{\mathrm{em}}} \int f \mathrm{d}A = R_{Bv} + \frac{1}{A_{\mathrm{em}} I_B} \int V \mathrm{d}A. \tag{D.5}$$

If the last term vanishes, we have a way of calculating R_{Bv}. To show that it does, we first consider the integral

$$\int I(V)\mathrm{d}A = -A_{\mathrm{em}} \int \boldsymbol{\nabla} \cdot \boldsymbol{J} \mathrm{d}A = -A_{\mathrm{em}} \int \boldsymbol{J} \cdot \mathrm{d}\hat{\boldsymbol{n}} = A_{\mathrm{em}} I_B. \tag{D.6}$$

The second step is by using a general theorem for rewriting a surface integral to a line integral over the boundary of this surface. The last step is an expression of the fact that all current must actually enter the pinched base through its boundary. Using Eq. (D.4) we can express the same integral also as

$$\int I(V)\mathrm{d}A = \int I_B \mathrm{d}A + \frac{\mathrm{d}I}{\mathrm{d}V} \int V \mathrm{d}A = A_{\mathrm{em}} I_B + \frac{\mathrm{d}I}{\mathrm{d}V} \int V \mathrm{d}A. \tag{D.7}$$

Combining two equations gives indeed $\int V \mathrm{d}A = 0$ (since $\mathrm{d}I/\mathrm{d}V \neq 0$).

D.2 Recipe

We are now ready to give the recipe to calculate R_{Bv}. First one needs to solve the differential equation

$$\nabla^2 f = -1/A_{\mathrm{em}}. \tag{D.8}$$

for a dimension-less quantity f. The boundary conditions are $f = 0$ everywhere where the base is connected to the external base, and $\hat{\boldsymbol{n}} \cdot \boldsymbol{\nabla} f = 0$ at the boundaries of the pinched base not connected to the external base. The low-current resistance is then given by an integral of f over the whole area of the pinched base.

$$R_{Bv} = \frac{\rho_\square}{A_{\mathrm{em}}} \int f \mathrm{d}A. \tag{D.9}$$

 ©Koninklijke Philips Electronics N.V. 2005

D.3 Examples

One-sided base contact For a rectangle connected at one side we have only one dimension to take into account. The differential equation is given by

$$\frac{\mathrm{d}^2 f}{\mathrm{d}x^2} = -1/H_{\mathrm{em}} L_{\mathrm{em}}. \tag{D.10}$$

The boundary conditions are $f(0) = 0$ and $\mathrm{d}f/\mathrm{d}x|_{H_{\mathrm{em}}} = 0$ which gives $f = (H_{\mathrm{em}}x - \frac{1}{2}x^2)/A_{\mathrm{em}}$. We thus find

$$R_{Bv} = \rho_{\square} A_{\mathrm{em}}^{-2} L_{\mathrm{em}} \int_0^{H_{\mathrm{em}}} (H_{\mathrm{em}}x - \tfrac{1}{2}x^2)\mathrm{d}x = \frac{1}{3}\rho_{\square}\frac{H_{\mathrm{em}}}{L_{\mathrm{em}}}. \tag{D.11}$$

For a square, contacted at one side, this means $R_{Bv} = \frac{1}{3}\rho_{\square}$.

Two-sided base contact Next we consider a rectangle connected at two sides, located at $x = \pm H_{\mathrm{em}}/2$. The boundary conditions read $f(\pm H_{\mathrm{em}}/2) = 0$, so we find $f = (H_{\mathrm{em}}^2 - 4x^2)/8A_{\mathrm{em}}$. This gives

$$R_{Bv} = \frac{1}{12}\rho_{\square}\frac{H_{\mathrm{em}}}{L_{\mathrm{em}}}. \tag{D.12}$$

For a square, contacted at two sides, we find $R_{Bv} = \frac{1}{12}\rho_{\square}$, just as we mentioned before.

Circular base As a third example we consider a disc, where all around the circular boundary a connection is made. The radius is R and the radial coordinate is r. The boundary condition is $f(r{=}R) = 0$. Furthermore we demand a non-singular solution to

$$\frac{1}{r}\frac{\mathrm{d}}{\mathrm{d}r}\, r\, \frac{\mathrm{d}}{\mathrm{d}r} f(r) = -\frac{1}{\pi R^2}. \tag{D.13}$$

The solution is $f = (1 - r^2/R^2)/4\pi$ which gives

$$R_{Bv} = \frac{1}{8\pi}\,\rho_{\square} \simeq \frac{1}{25.1}\,\rho_{\square}. \tag{D.14}$$

Rectangular base contacted on all sides As a last exact example we will consider a rectangle connected at all sides. A general expression for f in a rectangular geometry, such that the boundary conditions are obeyed, is given by

$$f = \sum_{m,n} a_{nm} \sin\frac{n\pi x}{H_{\mathrm{em}}}\, \sin\frac{m\pi y}{L_{\mathrm{em}}}, \tag{D.15}$$

©Koninklijke Philips Electronics N.V. 2005

where we take the rectangle to have the coordinates such that $0 \le x \le H_{\rm em}$ and $0 \le y \le L_{\rm em}$. Solving the differential equation gives

$$a_{nm} = \left(\frac{2}{\pi}\right)^4 \frac{1}{nm H_{\rm em} L_{\rm em} (n^2/H_{\rm em}^2 + m^2/L_{\rm em}^2)}, \qquad \text{when both } n, m \text{ odd}, \tag{D.16}$$

and $a_{nm} = 0$ otherwise. One then finds

$$\begin{aligned} \mathsf{R_{Bv}} &= \frac{\rho_\Box}{H_{\rm em} L_{\rm em}} \left(\frac{2}{\pi}\right)^6 \sum_{n,m \text{ odd}} \frac{1}{n^2 m^2 (n^2/H_{\rm em}^2 + m^2/L_{\rm em}^2)} \\ &= \frac{\rho_\Box H_{\rm em}}{L_{\rm em}} \sum_{m \text{ odd}} \frac{16}{a^3 m^5 \pi^5} \left(\frac{am\pi}{2} - \tanh \frac{am\pi}{2}\right), \end{aligned} \tag{D.17}$$

where $a = H_{\rm em}/L_{\rm em}$. In the limit for $H_{\rm em} \ll L_{\rm em}$ ($a \to 0$) we regain the case of a base contacted on two sides: $\mathsf{R_{Bv}} = \rho_\Box H_{\rm em}/12 L_{\rm em}$. For a square emitter we find

$$R_{Bv} = \rho_\Box \sum_{m \text{ odd}} \frac{16}{m^5 \pi^5} \left(\frac{m\pi}{2} - \tanh \frac{m\pi}{2}\right) \simeq \frac{\rho_\Box}{28.45}. \tag{D.18}$$

From numerical device simulations a value of $\rho_\Box/28.6$ was found in Ref. [53].

In the case of a rectangular base with a general value of $H_{\rm em}/L_{\rm em}$ it is not possible to give a simple expression. We therefore need a useful approximate formula. For a four-sided contacted square base the resistance is approximately $\rho_\Box/28$, as presented above. For non-square base it is assumed that we can apply the well know 1D relation to the middle region, which has length $L_{\rm em} - H_{\rm em}$. Then both resistances are placed in parallel. We then get

$$R_1 = \frac{\rho_\Box}{28.45}, \tag{D.19a}$$

$$R_2 = \frac{\rho_\Box H_{\rm em}}{12\,(L_{\rm em} - H_{\rm em})}, \tag{D.19b}$$

$$R_{Bv} = \frac{R_1\, R_2}{R_1 + R_2} = \frac{\rho_\Box H_{\rm em}}{12\, L_{\rm em} + 16.45\, H_{\rm em}}. \tag{D.19c}$$

Possibly a better expression [54], giving a result closer to Eq. (D.17) is given by

$$R_{Bv} = \frac{\rho_\Box H_{\rm em}}{L_{\rm em}} \left[\frac{1}{12} - \left(\frac{1}{12} - \frac{1}{28.45}\right) \frac{H_{\rm em}}{L_{\rm em}}\right]. \tag{D.20}$$

 ©Koninklijke Philips Electronics N.V. 2005

E Crosslinks of variables and parameters

The full equivalent circuit contains a number of current and charges. In Table 2 we have tabulated for each electrical model-parameter which currents and charges are functionally dependent on it. A same kind of cross-link is given between the temperature parameters and the electrical parameters in Table 3.

Table 2: *The relation between the parameters and the currents and charges of the equivalent circuit. When some I or Q is given, also the XI or XQ is meant if it exists. We disregarded the normally unimportant dependence of I_{avl} on G_{max}. We also disregarded the fact that I_{B_1} depends on many extra parameters when* $\mathsf{X}_{\mathsf{rec}} \neq 0$.

Parameter	Direct influence	Indirect influence	Very indirect influence
EXMOD	I_{ex}, I_{sub}, Q_{ex}		
EXPHI	Q_{BE}, Q_{BC}, $Q_{B_1B_2}$		
EXAVL	I_{avl}		
$\mathsf{I_s}$	I_N, I_{ex}, I_{sub}, I_{B_1}, $I^S_{B_1}$, Q_E, Q_{BE}, Q_{BC}	$I_{B_1B_2}$	
$\mathsf{I_k}$	I_N, Q_E, Q_{BE}, Q_{BC}, I_{ex}	$I_{B_1B_2}$	
$\mathsf{V_{er}}$	I_N, Q_{BE}, Q_{BC}	$I_{B_1B_2}$	
$\mathsf{V_{ef}}$	I_N, Q_{BE}, Q_{BC}	$I_{B_1B_2}$	
β_{f}	I_{B_1}, $I^S_{B_1}$		
$\mathsf{I_{Bf}}$	I_{B_2}		
$\mathsf{m_{Lf}}$	I_{B_2}		
$\mathsf{XI_{B_1}}$	I_{B_1}, $I^S_{B_1}$		
β_{ri}	I_{ex}	XI_{sub}	
$\mathsf{I_{Br}}$	I_{B_3}		
$\mathsf{V_{Lr}}$	I_{B_3}		
$\mathsf{X_{ext}}$	I_{ex}, I_{sub}, Q_{tex}, Q_{ex}		
$\mathsf{W_{avl}}$	I_{avl}		
$\mathsf{V_{avl}}$	I_{avl}		
$\mathsf{S_{fh}}$	I_{avl}		
$\mathsf{R_E}$	R_E		
$\mathsf{R_{Bc}}$	R_{Bc}		
$\mathsf{R_{Bv}}$	$I_{B_1B_2}$		
$\mathsf{R_{Cc}}$	R_{Cc}	XI_{ex}, XI_{sub}	
$\mathsf{R_{Cv}}$	$I_{C_1C_2}$, Q_{t_C}, Q_{epi}	I_N, Q_{BC}	I_{avl}, $I_{B_1B_2}$, Q_{BE}
$\mathsf{SCR_{Cv}}$	Q_{t_C}, Q_{epi}	I_N, Q_{BC}	I_{avl}, $I_{B_1B_2}$, Q_{BE}
$\mathsf{I_{hc}}$	Q_{t_C}, Q_{epi}	I_N, Q_{BC}	I_{avl}, $I_{B_1B_2}$, Q_{BE}
$\mathsf{a_{xi}}$	Q_{epi}	I_N, Q_{BC}, Q_{t_C}	I_{avl}, $I_{B_1B_2}$, Q_{BE}
$\mathsf{C_{jE}}$	Q_{t_E}, $Q^S_{t_E}$		
$\mathsf{V_{d_E}}$	Q_{t_E}, $Q^S_{t_E}$	I_N, Q_{BE}, Q_{BC}	$I_{B_1B_2}$
$\mathsf{p_E}$	Q_{t_E}, $Q^S_{t_E}$	I_N, Q_{BE}, Q_{BC}	$I_{B_1B_2}$

©Koninklijke Philips Electronics N.V. 2005

Parameter	Direct influence	Indirect influence	Very indirect influence
$\mathrm{XC_{j_E}}$	Q_{t_E}, $Q^S_{t_E}$		
$\mathrm{C_{BEO}}$	Q_{BEO}		
$\mathrm{C_{j_C}}$	Q_{t_C}, Q_{tex}		
$\mathrm{V_{d_C}}$	Q_{t_C}, Q_{tex}, Q_{epi}, $I_{C_1C_2}$, I_{avl}	I_N, Q_{BE}, Q_{BC}	$I_{B_1B_2}$
$\mathrm{p_C}$	Q_{t_C}, Q_{tex}	I_N, Q_{BE}, Q_{BC}	$I_{B_1B_2}$
$\mathrm{m_C}$	Q_{t_C}	I_N, Q_{BE}, Q_{BC}	$I_{B_1B_2}$
$\mathrm{X_p}$	Q_{t_C}, Q_{tex}	I_N, Q_{BE}, Q_{BC}	$I_{B_1B_2}$
$\mathrm{XC_{j_C}}$	Q_{t_C}, Q_{tex}		
$\mathrm{C_{BCO}}$	Q_{BCO}		
$\mathrm{m_\tau}$	Q_E		
τ_E	Q_E		
τ_B	Q_{BE}, Q_{BC}	Q_{ex}	
τ_epi	Q_{epi}	Q_{ex}	
τ_R	Q_{ex}		
$\mathrm{dE_g}$	I_N		
$\mathrm{X_{rec}}$	I_{B_1}		
$\mathrm{I_{Ss}}$	I_{sub}, I_{Sf}	I_{ex}	
$\mathrm{I_{ks}}$	I_{sub}	I_{ex}	
$\mathrm{C_{j_S}}$	Q_{t_S}		
$\mathrm{V_{d_S}}$	Q_{t_S}		
$\mathrm{p_S}$	Q_{t_S}		

Table 3: *The relation between the temperature parameters and the electrical parameters.*

Parameter	Direct influence	Indirect influence
$\mathrm{A_{Q_{B0}}}$	$\mathrm{R_{Bv}}$, β_f, $\mathrm{I_s}$, $\mathrm{V_{er}}$, $\mathrm{V_{ef}}$, τ_B	$\mathrm{I_{ks}}$
$\mathrm{A_E}$	$\mathrm{R_E}$, β_f	
$\mathrm{A_B}$	$\mathrm{R_{Bv}}$, β_f, $\mathrm{I_s}$, $\mathrm{I_k}$, τ_B	$\mathrm{I_{ks}}$
$\mathrm{A_{ex}}$	$\mathrm{R_{Bc}}$	
$\mathrm{A_C}$	$\mathrm{R_{Cc}}$	
$\mathrm{A_S}$	$\mathrm{I_{Ss}}$, $\mathrm{I_{ks}}$	
$\mathrm{dV_{g\beta f}}$	β_f	
$\mathrm{dV_{g\beta r}}$	β_ri	
$\mathrm{V_{g_B}}$	$\mathrm{V_{d_E}}$, $\mathrm{I_s}$, τ_E,	$\mathrm{C_{j_E}}$, $\mathrm{I_{ks}}$
$\mathrm{V_{g_C}}$	$\mathrm{V_{d_C}}$, $\mathrm{I_{Br}}$	$\mathrm{C_{j_C}}$
$\mathrm{V_{g_j}}$	$\mathrm{I_{Bf}}$	
$\mathrm{V_{g_t}}$	τ_E	
$\mathrm{V_{g_S}}$	$\mathrm{V_{d_S}}$, $\mathrm{I_{Ss}}$	$\mathrm{C_{j_S}}$, $\mathrm{I_{ks}}$

 ©Koninklijke Philips Electronics N.V. 2005

F Expression of parameters in physical quantities

In the derivation of several parameters we use a microscopic model. This gives us parameters in terms of microscopic quantities. Here we will summarise these expressions.

From the 1D main current (assuming a constant base doping profile)

$$\mathsf{I_s} = \frac{q\,D_n A_{\mathrm{em}} n_i^2}{W_B N_A}, \tag{F.1}$$

$$Q_{B0} = q\,A_{\mathrm{em}} W_B N_A, \tag{F.2}$$

$$Q_{B0}\,\mathsf{I_s} = q^2 D_n A_{\mathrm{em}}^2 n_i^2, \tag{F.3}$$

$$\mathsf{I_k} = \frac{4D_n}{W_B^2} Q_{B0} = \mathsf{I_s}\,\frac{4\,n_i^2}{N_A^2} = \frac{4\,q\,D_n A_{\mathrm{em}} N_A}{W_B}, \tag{F.4}$$

$$\tau_{\mathsf{B}} = \frac{W_B^2}{4\,D_n}. \tag{F.5}$$

From the 1D epilayer model:

$$e^{\mathsf{V_{d_C}}/V_T} = \frac{N_{\mathrm{epi}}^2}{n_i^2}, \tag{F.6}$$

$$\mathsf{R_{Cv}} = \frac{W_{\mathrm{epi}}}{q\,\mu_{n0} N_{\mathrm{epi}} A_{\mathrm{em}}}, \tag{F.7}$$

$$\mathsf{I_{hc}} = q\,N_{\mathrm{epi}} A_{\mathrm{em}} v_{\mathrm{sat}}, \tag{F.8}$$

$$\frac{\mathsf{R_{Cv}}\,\mathsf{I_{hc}}}{W_{\mathrm{epi}}} = \frac{v_{\mathrm{sat}}}{\mu_{n0}} = E_c, \tag{F.9}$$

$$\mathsf{SCR_{Cv}} = \frac{W_{\mathrm{epi}}^2}{2\varepsilon v_{\mathrm{sat}} A_{\mathrm{em}}} = \frac{q\,N_{\mathrm{epi}} W_{\mathrm{epi}}^2}{2\varepsilon}\,\frac{1}{\mathsf{I_{hc}}} = \frac{\mathsf{V_{d_C}}}{\mathsf{I_{hc}}}\,\frac{W_{\mathrm{epi}}^2}{x_{d0}^2}, \tag{F.10}$$

$$x_{d0} = \sqrt{\frac{2\varepsilon \mathsf{V_{d_C}}}{q\,N_{\mathrm{epi}}}}, \tag{F.11}$$

$$\mathsf{V_{avl}} = \mathsf{SCR_{Cv}}\,\mathsf{I_{hc}} = \frac{q\,N_{\mathrm{epi}} \mathsf{W_{avl}}^2}{2\varepsilon}, \tag{F.12}$$

$$\tau_{\mathsf{epi}} = \frac{W_{\mathrm{epi}}^2}{4\,D_n}, \tag{F.13}$$

$$Q_{\mathrm{epi0}} = q\,N_{\mathrm{epi}} A_{\mathrm{em}} W_{\mathrm{epi}} = \frac{4\,\tau_{\mathsf{epi}}\,V_T}{\mathsf{R_{Cv}}} = \frac{\mathsf{R_{Cv}}\,\mathsf{I_s}\,Q_{B0}}{V_T}\,e^{\mathsf{V_{d_C}}/V_T}. \tag{F.14}$$

Note that for the last expression we assume that the diffusion constants in the base and in the epilayer are equal. The expression for $\mathsf{V_{avl}}$ is in practice often not valid.

G Full equivalent circuit

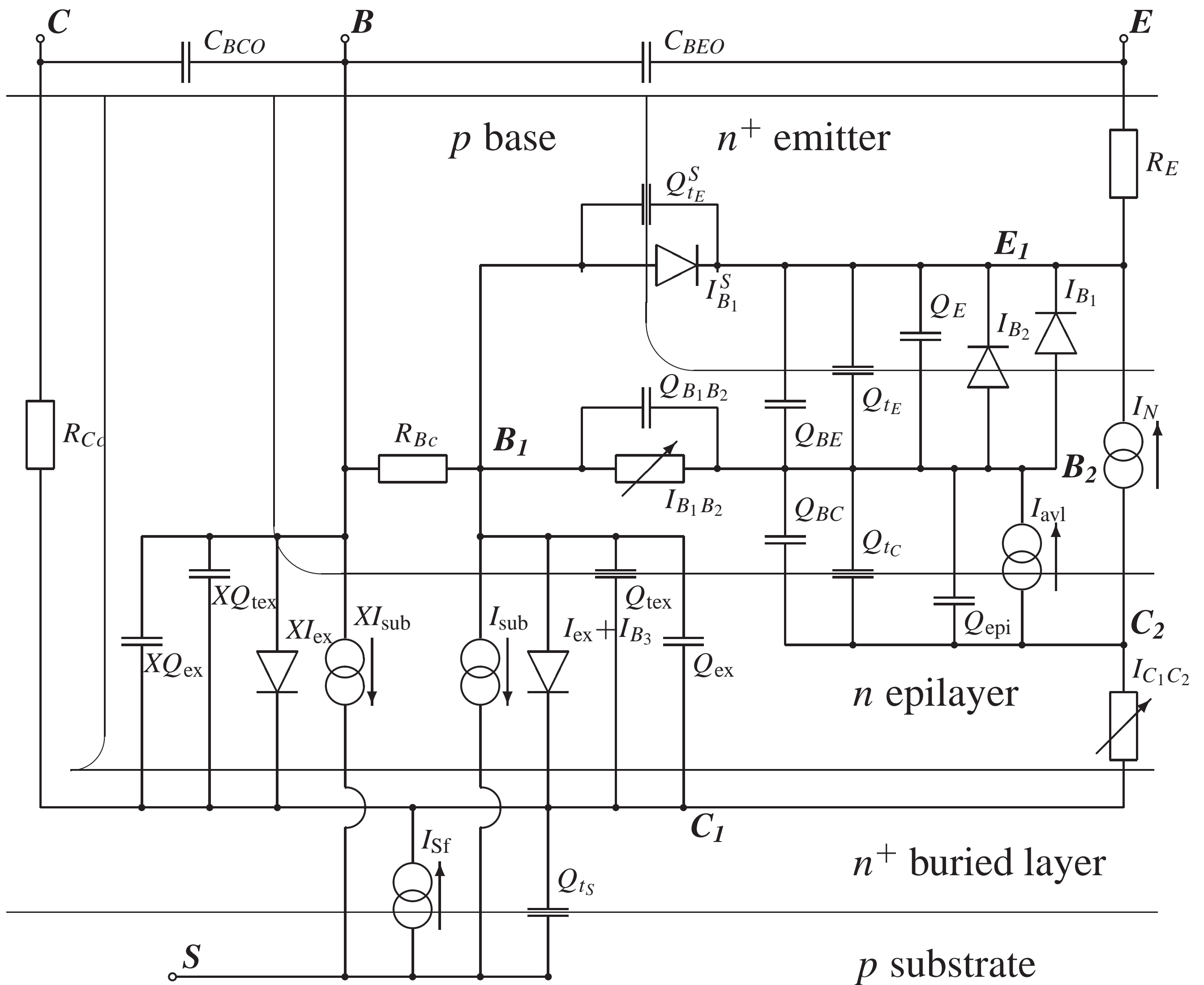

Figure 34: *The full Mextram equivalent circuit for the vertical NPN transistor. Schematically the different regions of the physical transistor are shown. The current $I_{B_1B_2}$ describes the variable base resistance and is therefore sometimes called R_{Bv}. The current $I_{C_1C_2}$ describes the variable collector resistance (or epilayer resistance) and is therefore sometimes called R_{Cv}. The extra circuit for self-heating is discussed in Chapter 8.*

 ©Koninklijke Philips Electronics N.V. 2005

References

[1] J. C. J. Paasschens and W. J. Kloosterman, "The Mextram bipolar transistor model, level 504," Unclassified Report NL-UR 2000/811, Philips Nat.Lab., 2000. See Ref. [3].

[2] J. C. J. Paasschens, W. J. Kloosterman, and R. J. Havens, "Parameter extraction for the bipolar transistor model Mextram, level 504," Unclassified Report NL-UR 2001/801, Philips Nat.Lab., 2001. See Ref. [3].

[3] For the most recent model descriptions, source code, and documentation, see the web-site http://www.semiconductors.philips.com/Philips_Models.

[4] J. J. Ebers and J. L. Moll, "Large signal behaviour of junction transistors," *Proc. IRE*, vol. 42, p. 1761, 1954.

[5] H. K. Gummel and H. C. Poon, "An integral charge control model of bipolar transistors," *Bell Sys. Techn. J.*, vol. May-June, pp. 827–852, 1970.

[6] R. S. Muller and T. I. Kamins, *Device electronics for integrated circuits*. Wiley, New York, 2nd ed., 1986.

[7] S. M. Sze, *Physics of Semiconductor Devices*. Wiley, New York, 2 ed., 1981.

[8] I. E. Getreu, *Modeling the bipolar transistor*. Elsevier Sc. Publ. Comp., Amsterdam, 1978.

[9] H. C. de Graaff and F. M. Klaassen, *Compact transistor modelling for circuit design*. Springer-Verlag, Wien, 1990.

[10] J. Berkner, *Kompaktmodelle für Bipolartransistoren. Praxis der Modellierung, Messung und Parameterbestimmung — SGP, VBIC, HICUM und MEXTRAM (Compact models for bipolar transistors. Practice of modelling, measurement and parameter extraction — SGP, VBIC, HICUM und MEXTRAM)*. Expert Verlag, Renningen, 2002. (In German).

[11] M. Reisch, *High-Frequency Bipolar Transistors*. Springer, Berlin, 2003.

[12] P. A. H. Hart, *Bipolar and bipolar-mos integration*. Elsevier, Amsterdam, 1994.

[13] H. C. de Graaff and W. J. Kloosterman, "The Mextram bipolar transistor model, level 503.2," Unclassified Report 006/94, Philips Nat.Lab., June 1995. See Ref. [3].

[14] J. C. J. Paasschens and W. J. Kloosterman, "Derivation of the model equations of Mextram, level 503," Unclassified Report NL-UR 2002/808, Philips Nat.Lab., 2002. See Ref. [3].

[15] W. J. Kloosterman and J. A. M. Geelen, "Parameter extraction methodology for the Mextram bipolar transistor model," Unclassified Report 003/96, Philips Nat.Lab., 1996. See Ref. [3].

©Koninklijke Philips Electronics N.V. 2005

[16] H. K. Gummel, "A charge control relation for bipolar transistors," *Bell Sys. Techn. J.*, vol. January, pp. 115–120, 1970.

[17] J. L. Moll and I. M. Ross, "The dependence of transistor parameters on the distribution of base layer resistivity," *Proc. IRE*, vol. 44, pp. 72–78, Jan. 1956.

[18] The term 'integral charge control model' was introduced by Gummel and Poon [5]. Their 'integral' means the combination of Gummel's new charge control relation [16] and conventional charge control theory, such "that parameters for the ac response also shape the dc characteristics" [5]. Unfortunately, nowadays the term 'integral charge control relation' (ICCR) is used to refer to Gummel's new charge control relation only, and not to the model by Gummel and Poon.

[19] G. M. Kull, L. W. Nagel, S. Lee, P. Lloyd, E. J. Prendergast, and H. Dirks, "A unified circuit model for bipolar transistors including quasi-saturation effects," *IEEE Trans. Elec. Dev.*, vol. ED-32, no. 6, pp. 1103–1113, 1985.

[20] M. Schröter, M. Friedrich, and H.-M. Rein, "A generalized integral charge-control relation and its application to compact models for silicon-based HBT's," *IEEE Trans. Elec. Dev.*, vol. ED-40, pp. 2036–2046, 1993.

[21] H. C. de Graaff and W. J. Kloosterman, "New formulation of the current and charge relations in bipolar transistor modeling for CACD purposes," *IEEE Trans. Elec. Dev.*, vol. ED-32, p. 2415, 1985.

[22] S.-Y. Oh, D. E. Ward, and R. W. Dutton, "Transient analysis of MOS transistors," *IEEE J. of Solid-State Circuits*, vol. 15, pp. 636–643, 1980.

[23] G. A. M. Hurkx, "A new approach to a.c. characterization of bipolar transistors," *Solid-State Elec.*, vol. 31, pp. 1269–1275, 1988.

[24] H. Klose and A. W. Wieder, "The transient integral charge control relation — a novel formulation of the currents in a bipolar transistor," *IEEE Trans. Elec. Dev.*, vol. ED-34, pp. 1090–1099, 1987.

[25] J. C. J. Paasschens and A. J. Scholten, "Some white noise calculations for compact modelling," Technical Note PR-TN 2004/00683, Philips Nat.Lab., 2004. In preparation.

[26] J. J. H. van den Biesen, "P-N junction capacitances part II: the neutral capacitance," *Philips J. Res.*, vol. 40, pp. 103–113, 1985.

[27] J. R. A. Beale and J. A. G. Slatter, "Equivalent circuit of a transistor with a lightly doped collector operating in saturation," *Solid-State Elec.*, vol. 11, pp. 241–252, 1968.

[28] D. L. Bowler and F. A. Lindholm, "High current regimes in transistor collector regions," *IEEE Trans. Elec. Dev.*, vol. ED-20, pp. 257–263, 1973.

 ©Koninklijke Philips Electronics N.V. 2005

[29] H. C. de Graaff, “Collector models for bipolar transistors,” *Solid-State Elec.*, vol. 16, pp. 587–600, 1973.

[30] H. C. de Graaff and R. J. van der Wal, “Measurement of the onset of quasi-saturation in bipolar transistors,” *Solid-State Elec.*, vol. 17, pp. 1187–1192, 1974.

[31] G. Rey, F. Dupuy, and J. P. Bailbe, “A unified approach to the base widening mechanism in bipolar transistors,” *Solid-State Elec.*, vol. 18, pp. 863–866, 1975.

[32] H. Jeong and J. G. Fossum, “A charge-based large-signal bipolar transistor model for device and circuit simulation,” *IEEE Trans. Elec. Dev.*, vol. ED-36, pp. 124–131, 1989.

[33] H. C. de Graaff and W. J. Kloosterman, “Modeling of the collector epilayer of a bipolar transistor in the Mextram model,” *IEEE Trans. Elec. Dev.*, vol. ED-42, pp. 274–282, Feb. 1995.

[34] M. M. S. Hassan, “Modelling of lightly doped collector of a bipolar transistor operating in quasi-saturation region,” *Int. J. Electronics*, vol. 86, pp. 1–14, 1999.

[35] M. Schröter and T.-Y. Lee, “Physics-based minority charge and transit time modeling for bipolar transistors,” *IEEE Trans. Elec. Dev.*, vol. ED-46, pp. 288–300, 1999.

[36] J. C. J. Paasschens, W. J. Kloosterman, R. J. Havens, and H. C. de Graaff, “Improved compact modeling of ouput conductance and cutoff frequency of bipolar transistors,” *IEEE J. of Solid-State Circuits*, vol. 36, pp. 1390–1398, 2001.

[37] W. J. Kloosterman, “The modelling of lightly doped collectors in bipolar transistors,” Report 6646, Philips Nat.Lab., 1992.

[38] J. C. J. Paasschens, W. J. Kloosterman, R. J. Havens, and H. C. de Graaff, “Improved modeling of ouput conductance and cut-off frequency of bipolar transistors,” in *Proc. of the Bipolar Circuits and Technology Meeting*, pp. 62–65, 2000.

[39] L. C. N. de Vreede, H. C. de Graaff, J. L. Tauritz, and R. G. F. Baets, “Extension of the collector charge description for compact bipolar epilayer models,” *IEEE Trans. Elec. Dev.*, vol. ED-42, pp. 277–285, 1998.

[40] J. C. J. Paasschens. Unpublished.

[41] W. J. Kloosterman, J. C. J. Paasschens, and R. J. Havens, “A comprehensive bipolar avalanche multiplication compact model for circuit simulation,” in *Proc. of the Bipolar Circuits and Technology Meeting*, pp. 172–175, 2000.

[42] A. G. Chynoweth, “Ionization rates for electrons and holes in silicon,” *Physical Review*, vol. 109, pp. 1537–1540, 1958.

[43] R. van Overstraeten and H. de Man, “Measurement of the ionization rates in diffused silicon *p-n* junctions,” *Solid-State Elec.*, vol. 13, pp. 583–608, 1970.

©Koninklijke Philips Electronics N.V. 2005

[44] W. J. Kloosterman and H. C. de Graaff, "Avalanche multiplication in a compact bipolar transistor model for circuit simulation," *IEEE Trans. Elec. Dev.*, vol. ED-36, pp. 1376–1380, 1989.

[45] P. Cullen, H. C. de Graaff, and W. J. Kloosterman, "A weak avalanche model to be incorporated into the compact transistor model Mextram," Technical Note 353/87, Philips Nat.Lab., 1987.

[46] H. C. Poon and J. C. Meckwood, "Modeling of avalanche effect in integral charge control model," *IEEE Trans. Elec. Dev.*, vol. ED-19, pp. 90–97, 1972. With comment by K. Gopal, *IEEE Trans. Elec. Dev.*, vol ED-23, p. 1112, 1976.

[47] J. C. J. Paasschens, "Compact modeling of the noise of a bipolar transistor under DC and AC current crowding conditions," *IEEE Trans. Elec. Dev.*, vol. 51, pp. 1483–1495, 2004.

[48] J. R. Hauser, "The effects of distributed base potential on emitter-current injection density and effective base resistance for stripe transistor geometries," *IEEE Trans. Elec. Dev.*, vol. May, pp. 238–242, 1964.

[49] H. Groendijk, "Modeling base crowding in a bipolar transistor," *IEEE Trans. Elec. Dev.*, vol. ED-20, pp. 329–330, 1973.

[50] H.-M. Rein, T. Schad, and R. Zühlke, "Der Einfluss des Basisbahnwiderstandes und der Ladungsträgermultiplikation auf das Ausgangskennlinienfeld von Planartransistoren (The influence of base resistance and carrier multiplication on the current-voltage characteristics of planar transistors)," *Solid-State Elec.*, vol. 15, pp. 481–500, 1972. (In German).

[51] M. Rickelt, H.-M. Rein, and E. Rose, "Influence of impact-ionization-induced instabilities on the maximum usable output voltage of Si-bipolar transistors," *IEEE Trans. Elec. Dev.*, vol. 48, pp. 774–783, 2001.

[52] E. S. Kohn, "Current crowding an a circular geometry," *J. Appl. Phys.*, vol. 42, pp. 2493–2497, 1971.

[53] H.-M. Rein and M. Schröter, "Base spreading resistance of square-emitter transistors and its dependence on current crowding," *IEEE Trans. Elec. Dev.*, vol. 36, pp. 770–773, 1989.

[54] M. Schröter, "Simulation and modeling of the low-frequency base resistance of bipolar transistors and its dependence on current and geometry," *IEEE Trans. Elec. Dev.*, vol. 38, pp. 538–544, 1991.

[55] R. L. Pritchard, "Two-dimensional current flow in junction transistors at high frequencies," *Proc. IRE*, vol. 26, pp. 1152–1160, 1958.

[56] J. C. J. Paasschens, W. J. Kloosterman, and R. J. Havens, "Modelling two SiGe HBT specific features for circuit simulation," in *Proc. of the Bipolar Circuits and Technology Meeting*, pp. 38–41, 2001.

 ©Koninklijke Philips Electronics N.V. 2005

[57] E. F. Crabbé, H. D. Cressler, G. L. Patton, J. M. C. Stork, J. H. Confort, and J. Y.-C. Sun, "Current gain rolloff in graded-base SiGe heterojunction bipolar transistors," *IEEE Elec. Dev. Lett.*, vol. 14, pp. 193–195, 1993.

[58] A. Neugroschel, G. Li, and C.-T. Sah, "Low frequency conductance voltage analysis of Si/Ge_xSi_{1-x}/Si heterojunction bipolar transistors," *IEEE Trans. Elec. Dev.*, vol. 47, pp. 187–196, 2000.

[59] S. L. Salmon, J. D. Cressler, R. C. Jaeger, and D. L. Harame, "The influence of Ge grading on the bias and temperature characteristics of SiGe HBT's for precision analog circuits," *IEEE Trans. Elec. Dev.*, vol. 47, pp. 292–298, 2000.

[60] H. Kroemer, "Two integral relations pertaining to the electron transport through a bipolar transistor with a non-uniform energy gap in the base region," *Solid-State Elec.*, vol. 28, pp. 1101–1103, 1985.

[61] A. J. Joseph, J. D. Cressler, D. M. Richey, R. C. Jaeger, and D. L. Harame, "Neutral base recombination and its influence on the temperature dependence of early voltage and current gain-early voltage product in UHV/CVD SiGe heterojunction bipolar transistors," *IEEE Trans. Elec. Dev.*, vol. 44, pp. 404–413, 1997.

[62] G.-B. Hong, J. G. Fossum, and M. Ugajin, "A physical SiGe-base HBT model for circuit simulation and design," in *IEDM Tech. Digest*, pp. 557–560, 1992.

[63] D. B. M. Klaassen, "A unified mobility model for device simulation—I. model equations and concentration dependence," *Solid-State Elec.*, vol. 35, no. 7, pp. 953–959, 1992.

[64] D. B. M. Klaassen, "A unified mobility model for device simulation—II. temperature dependence of carrier mobility and lifetime," *Solid-State Elec.*, vol. 35, no. 7, pp. 961–967, 1992.

[65] C. C. McAndrew, "Practical modeling for circuit simulation," *IEEE J. of Solid-State Circuits*, vol. 33, pp. 439–448, 1998.

[66] J. C. J. Paasschens, S. Harmsma, and R. van der Toorn, "Dependence of thermal resistance on ambient and actual temperature," in *Proc. of the Bipolar Circuits and Technology Meeting*, pp. 96–99, 2004.

[67] J. C. J. Paasschens, "Usage of thermal networks of compact models. Some tips for non-specialists," Technical Note PR-TN 2004/00528, Philips Nat.Lab., 2004.

[68] C. Kittel and H. Kroemer, *Thermal Physics*. Freeman & Co., second ed., 1980.

[69] J. S. Brodsky, R. M. Fox, and D. T. Zweidinger, "A physics-based dynamic thermal impedance model for vertical bipolar transistors on SOI substrates," *IEEE Trans. Elec. Dev.*, vol. 46, pp. 2333–2339, 1999.

[70] P. Palestri, A. Pacelli, and M. Mastrapasqua, "Thermal resistance in $Si_{1-x}Ge_x$ HBTs on bulk-Si and SOI substrates," in *Proc. of the Bipolar Circuits and Technology Meeting*, pp. 98–101, 2001.

[71] D. J. Walkey, T. J. Smy, R. G. Dickson, J. S. Brodsky, D. T. Zweidinger, and R. M. Fox, "A VCVS-based equivalent circuit model for static substrate thermal coupling," in *Proc. of the Bipolar Circuits and Technology Meeting*, pp. 102–105, 2001.

[72] A. van der Ziel, *Noise. Sources, characterization, measurement*. Prentice-Hall, Englewood Cliffs, 1970.

[73] M. J. Buckingham, *Noise in electronic devices and systems*. Ellis Horwood, Chichester, 1983.

[74] A. van der Ziel, *Noise in solid-state devices and circuits*. Wiley-Interscience, New York, 1986.

[75] F. Bonani and G. Ghione, *Noise in Semiconductor Devices*. Springer, Berlin, 2001.

[76] J. C. J. Paasschens and R. de Kort, "Modelling the excess noise due to avalanche multiplication in (heterojunction) bipolar transistors," in *Proc. of the Bipolar Circuits and Technology Meeting*, pp. 108–111, 2004.

[77] F. M. Klaassen and J. Prins, "Thermal noise of MOS transistors," *Philips Res. Repts.*, vol. 22, pp. 505–514, 1967.

[78] A. van der Ziel, "High-injection noise in transistors," *Solid-State Elec.*, vol. 20, pp. 715–720, 1977.

[79] A. van der Ziel and K. M. van Vliet, "Transmission line model of high injection noise in junction diodes," *Solid-State Elec.*, vol. 20, pp. 721–723, 1977.

[80] M. C. A. M. Koolen and J. C. J. Aerts, "The influence of non-ideal base current on $1/f$ noise behaviour of bipolar transistors," in *Proc. of the Bipolar Circuits and Technology Meeting*, pp. 232–235, 1990.

[81] H. C. Poon and H. K. Gummel, "Modeling of emitter capacitance," *Proc. IEEE*, vol. 57, pp. 2181–2182, 1969.

[82] For the model definition and more information about Hicum see http://www.iee.et.tu-dresden.de/iee/eb/comp_mod.html.

[83] C. C. McAndrew, J. A. Seitchik, D. F. Bowers, M. Dunn, M. Foisy, I. Getreu, M. McSwain, S. Moinian, J. Parker, D. J. Roulston, M. Schröter, P. van Wijnen, and L. F. Wagner, "Vbic95, the vertical bipolar inter-company model," *IEEE J. of Solid-State Circuits*, vol. 31, pp. 1476–1483, 1996.

[84] For the model definition and more information about Vbic see http://www.fht-esslingen.de/institute/iafgp/neu/VBIC/index.html.

 ©Koninklijke Philips Electronics N.V. 2005

[85] D. A. Barry, P. J. Culligan-Hensley, and S. J. Barry, “Real values of the W-function,” *ACM Trans. Math. Software*, vol. 21, pp. 161–171, 1995.

[86] T. C. Banwell, “Bipolar transistor circuit analysis using the Lambert W-function,” *IEEE Trans. Circuits and Systems*, vol. 47, pp. 1621–1633, 2000.

[87] J. J. Dohmen. Personal communication.

©Koninklijke Philips Electronics N.V. 2005

 ©Koninklijke Philips Electronics N.V. 2005

Index

parameter
- A, 86, 88, 89
- A_B, 9, 89–93, 140
- A_C, 9, 92, 140
- A_E, 9, 90, 91, 140
- A_S, 9, 91, 92, 140
- A_f, 9, 85, 101, 103, 104
- A_C, 89
- A_E, 89
- $A_{Q_{B0}}$, 9, 89, 90, 92, 94, 140
- A_{epi}, 9, 89, 92
- A_{ex}, 9, 89, 140
- A_{th}, 9, 94
- C_{BCO}, iv, 8, 66, 85, 108, 115–117, 140
- C_{BEO}, iv, 8, 66, 85, 108, 115–117, 140
- C_{TH}, 120
- C_{j_CT}, 56, 88
- C_{j_C}, 8, 20, 21, 56, 87, 88, 92, 140
- C_{j_ET}, 87
- C_{j_E}, 8, 19–21, 87, 92, 139, 140
- C_{j_ST}, 87
- C_{j_S}, 8, 18, 87, 140
- C_{th}, iv, 9, 85, 96, 119, 120
- DTA, 94
- EXAVL, 6, 60, 61, 63, 85, 119, 139
- EXMOD, 5, 6, 67, 85, 104, 139
- EXPHI, 5, 6, 29, 30, 78, 85, 115, 139
- I_k, 7, 22–24, 26–28, 30, 31, 33, 68, 91, 93, 139–141
- I_s, 6, 7, 17, 22–26, 30–33, 62, 68, 70–72, 85, 89–91, 93, 139–141
- I_{BfT}, 90, 91
- I_{Bf}, 7, 32, 90, 91, 139, 140
- I_{BrT}, 91
- I_{Br}, 7, 32, 91, 139, 140
- I_{SsT}, 91
- I_{Ss}, 7, 33, 68, 70, 91, 140
- $I_{hc,1d}$, 118
- I_{hc}, 8, 38, 47–51, 55, 56, 58, 60, 61, 64, 85, 118, 119, 128, 130–132, 139, 141
- I_{ksT}, 91
- I_{ks}, 7, 33, 68, 91, 140
- I_{kT}, 91
- I_k, 32, 68, 91
- I_{sT}, v, 6, 84, 85, 89–91
- I_s, 83, 91
- K_f, 9, 85, 101, 103, 104
- K_{avl}, v, 9, 102–104
- K_{fN}, 9, 85, 103
- LEVEL, 6, 85
- MULT, iv, 6, 85, 101
- R_E, 7, 9, 62, 63, 66, 103, 139, 140
- R_{BcT}, 89
- R_{Bc}, 7, 9, 62, 63, 66, 89, 95, 103, 105, 115–117, 139, 140
- R_{BvT}, 89
- R_{Bv}, 8, 9, 62, 72–76, 89, 138–140
- R_{CcT}, 89, 109, 112
- R_{Cc}, 8, 9, 36, 66, 69, 70, 89, 95, 103, 112, 113, 115–117, 139, 140
- $R_{Cv,1d}$, 118
- R_{CvT}, 89
- R_{Cv}, 8, 9, 38, 40, 44–58, 89, 118, 119, 128, 131, 132, 139, 141
- R_{ET}, 89, 109, 112
- R_E, 89, 95, 112, 113, 116, 117
- R_{TH}, 119, 120
- $R_{th,Tamb}$, 94, 96
- R_{th}, iv, 9, 85, 94–96, 119, 120
- $SCR_{Cv,1d}$, 118
- SCR_{Cv}, 8, 38, 40, 48–51, 57, 58, 60, 85, 118, 119, 128, 131, 132, 139, 141
- S_{fh}, 7, 64, 85, 118, 119, 139
- T_{ref}, iv, 9, 85, 94
- V_{Lr}, 7, 32, 85, 139
- V_{avl}, 7, 60, 61, 85, 139, 141
- V_{d_CT}, 56, 87, 88, 92
- V_{d_C}, 8, 20, 37, 40, 42–53, 55–58, 60, 61, 67–69, 87, 88, 92, 128, 133, 140, 141

©Koninklijke Philips Electronics N.V. 2005

$V_{d_{E}T}$, 87, 92
V_{d_E}, 8, 19–21, 87, 92, 93, 139, 140
$V_{d_{S}T}$, 87
V_{d_S}, 8, 18, 87, 140
V_{efT}, 84, 92
V_{ef}, 7, 21, 79, 81–84, 92, 139, 140
V_{erT}, 92
V_{er}, 7, 21, 79, 81–83, 92, 139, 140
V_{g_B}, 9, 87, 89, 90, 140
V_{g_C}, 9, 87, 91, 140
V_{g_S}, 9, 87, 91, 140
V_{g_j}, 9, 90, 91, 140
V_{g_t}, 140
W_{avl}, 7, 59, 60, 62–64, 85, 139, 141
XC_{j_C}, 7, 19–21, 56, 85, 92, 140
XC_{j_E}, 7, 19–21, 85, 92, 140
XI_{B_1}, 7, 31, 84, 85, 103, 139
X_p, 8, 20, 87, 88, 92, 140
X_{ext}, 7, 19, 20, 67, 68, 70, 85, 104, 139
X_{pT}, 56, 88
X_{rec}, 9, 83–85, 139, 140
ΔE_g, 81–83
β_f, 7, 31, 62, 63, 71, 72, 83, 90, 91, 139, 140
β_{fT}, 84, 90
β_{riT}, 90
β_{ri}, 7, 32, 33, 68, 70, 90, 139, 140
τ_B, 8, 22–24, 28, 67, 68, 92, 140, 141
τ_E, 8, 30, 31, 93, 140
τ_R, 8, 67, 68, 92, 140
τ_{BT}, 92
τ_{ET}, 93
τ_{RT}, 92
τ_{epiT}, 92
τ_{epi}, 8, 14, 28, 53, 67, 68, 92, 140, 141
a_{xi}, 8, 45, 46, 85, 139
dA_{I_s}, v, 90
dE_g, 9, 94, 140
dE_{gT}, 94
dT_a, 9, 85
$dV_{g\beta f}$, 9, 90, 140
$dV_{g\beta r}$, 9, 90, 140
$dV_{g\tau_E}$, 9, 93
m_C, 8, 56, 85, 140
m_{Lf}, 7, 32, 85, 90, 91, 103, 139
m_τ, 8, 30, 31, 85, 93, 140
p_C, 8, 20, 56, 85, 88, 92, 140
p_E, 8, 19–21, 85, 87, 92, 139
p_S, 8, 18, 85, 87, 140

 ©Koninklijke Philips Electronics N.V. 2005